MODELLING RAINY SEASON CHARACTERISTICS AND DROUGHT IN RELATION TO CROP PRODUCTION IN THE LUVUVHU RIVER CATCHMENT OF THE LIMPOPO PROVINCE

ME Moeletsi, TE Masupha, FP Tshililo, MP Thavhana, ZP Shabalala, KM Nape, SM Mazibuko, MI Tongwane & M Tsubo

WATER RESEARCH COMMISSION

TT 771/18

MODELLING RAINY SEASON CHARACTERISTICS AND DROUGHT IN RELATION TO CROP PRODUCTION IN THE LUVUVHU RIVER CATCHMENT OF THE LIMPOPO PROVINCE

Report to the

Water Research Commission

by

ME Moeletsi, TE Masupha, FP Tshililo, MP Thavhana, ZP Shabalala,
KM Nape, SM Mazibuko, MI Tongwane & M Tsubo

Agricultural Research Council – Institute for Soil, Climate and Water

WRC Report No. TT 771/18

October 2018

Obtainable from

Water Research Commission
Private Bag X03
Gezina, 0031

orders@wrc.org.za or download from www.wrc.org.za

This Project emanates from a project entitled *Modelling rainy season characteristics and drought in relation to crop production in the Luvuvhu River catchment of the Limpopo Province (WRC* Project No: K5/2403)

ISBN 978-0-6392-0052-1

Printed in the Republic of South Africa

ACKNOWLEDGEMENTS

The authors and project team would like to acknowledge the Water Research Commission of South Africa for funding this research project.

The staff of the Limpopo Provincial Department of Agriculture have been very helpful towards the implementation of the project. Special thanks to Mr Ramogondo, Mr Muthala, Mr Kwinda, Mr Sambo, Mr Mulelu, Mr Mudau, Mr Hlungwani and Mr Mashaku.

The authors would like to thank the following farmers who permitted the project to establish pilot sites on their farms:

Farm location	**Farmer**
1. Thononda	Mrs Alilali Mutshatshi
2. Elim (Mpheni)	Mr Selamulela and Mr Samson Muleya
3. Lamvi	Mr Heison Nemasisi
4. Malamulele	Mr Lovemore Masia
5. Mhinga	Mr Aron Ngobeni
6. Sanari	Mr Ndateni Reckson Maliehe

The project benefitted immensely from the participation of the Reference Group members: Dr E Archer, Dr S Mgquba and Dr G Backeberg, under the chairmanship of Prof. S Mpandeli.

Thanks to the staff of Agricultural Research Council – Institute for Soil, Climate and Water who assisted with the implementation of the project.

Editorial assistance from Dr T Fyfield is gratefully acknowledged.

EXECUTIVE SUMMARY

Weather and climate variability are the major factors that affect the inter-annual performance of crop production and yield in all environments. As a result, climate information has to be considered properly in the planning of agricultural activities and decision-making. In addition, many practices such as the use of irrigation, application of manure, improved cultivation and improved crop varieties have been developed over the years to enable agriculture to adapt to climate variability and climate change. Agricultural productivity can be improved further, costs of production can be reduced and crop failures can be avoided by using weather and climate information. The challenge that South Africa is currently facing is to use climate information for risk management strategies that increase preparedness and reduce vulnerability to climate variability. Planning and management of sustainable agricultural production systems require detailed agroclimatological information that is presented in a clear manner.

Agricultural production varies significantly from year to year mainly due to the climate risks that affect the country. The frequencies, means, extremes, deviations, exceedance of thresholds, spatial variability and trends of agroclimatological parameters are important for assessing and managing agricultural risk. Rainy season characteristics of importance to agriculture include onset, cessation and length of the growing season, rainfall amount, and the probability of a dry spell occurrence during the growing season. Delayed onset of the rainy season, especially in largely semi-arid southern Africa, extends the growing period of summer crops into winter.

Rainfall seasons in semi-arid environments are characterised by frequent drought incidences. Drought is one of the most disastrous climate-related hazards that has a significant impact on global agriculture, environment, infrastructure and socio-economic activities. In South Africa, recurring droughts have always been an endemic feature of climate, affecting all sectors of society. Agriculture is usually the first sector to be affected by drought in the country as it primarily depends on precipitation for crop growth and production. Long-term downward trends in South Africa's crop production are often associated with periods of meteorological droughts. Thus, better agricultural decisions can be made when determining drought incidences.

Climate variability and climate change have a direct impact on the productivity of many socio-economic activities. Due to its reliance on climate variables, it is projected that the agricultural sector in South Africa will be significantly affected by anticipated climate change. Drought risk is expected to increase in drought-prone areas, particularly in subtropical climates, which places stress on food security systems. Thus, high intra- and inter-seasonal climate variability, recurrent droughts and floods that affect both crops and livestock, and persistent poverty that limits the capacity to adapt to climate change, also contribute to increasing this vulnerability.

Rainfall variability poses a threat to farmers' livelihoods and agricultural production. The reliance of farmers on rainfall, which varies annually, makes them especially vulnerable to rainfall variability. Resource-poor farmers mostly conduct their agricultural activities without considering weather and climate information properly. These farmers are highly vulnerable to impacts of climate variability and climate change and thus the project assisted them in making informed choices on activities such as timing and planting as well as appropriate crop cultivars.

This study was necessitated by the common lack of useful packaging for the agroclimatological information to help farmers and decision makers. It particularly focuses on rainy season characteristics, drought and flood risk affecting crop production in the Luvuvhu River catchment in the Limpopo Province. The main aim of the project was to investigate rainfall characteristics, drought and floods with reference to crop production to assist the farmers to maximise productivity through utilisation of weather and climate knowledge. Rainy season characteristics of the study area were determined with reference to maize production in the catchment. The aims of the project were:

1. To identify and quantify the rainy season characteristics with reference to crop production in the Luvuvhu River catchment.
2. To calibrate crop models to suit the environmental and management conditions of the study area.
3. To investigate evolution of drought and rainy season characteristics in the Luvuvhu River catchment under climate change.
4. To investigate changes in crop productivity under climate change.
5. To develop a decision support tool for drought and rainy season characteristics for the Luvuvhu River catchment.

Climate, soil and hydrological data for the weather stations within the Luvuvhu River catchment was obtained from the Agricultural Research Council (ARC), the Department of Water and Sanitation and the South African Weather Service (SAWS). Other parameters such as evapotranspiration, which are also important for agroclimatological risk, were estimated using the Hargreaves method.

All daily climate data was subjected to quality checks. The stations that had more than 30 years of data since 1970 were selected. The ARC stand-alone patching tool was developed to patch missing climate data. This tool patches missing values of daily minimum and maximum temperatures, rainfall, solar radiation, water vapour pressure and wind speed. The tool employs commonly used techniques including arithmetic averaging, normal ratio, inverse distance weighted (IDW), correlation coefficient, multiple linear regression (MLR) and UK traditional method (UK). It compares the best method of estimating the daily data by using mean absolute error, root mean square error (RMSE) and correlation coefficient (r). For the Luvuvhu River catchment, the IDW and MLR methods provided better results for temperature than other methods.

Simulated daily climate change data (solar radiation, rainfall, minimum and maximum temperature) for the period 1980/1981 to 2099/2100 were obtained from the Climate Change, Agriculture and Food Security climate data portal. The data was the output of the high resolution projections of the Conformal-Cubic Atmospheric Model (CCAM), which is a regional model that is downscaled from the coupled global climate model CSIRO Mark3.6.0.

The Instat+ v 3.36 statistical program was used to calculate onset, cessation and length of the rainy season, and dry spells characteristics. Statistica software was used to generate descriptive statistics as well as to calculate probability of exceedance and non-exceedance for the rainy season characteristics. The Anderson–Darling goodness-of-fit test was performed to determine the distribution model that best represents the data. The resultant probabilities of exceedance were then computed from the distribution models that best fit the data. A non-parametric Spearman rank correlation coefficient test was used to analyse data for trends in rainy season characteristics as well as monthly rainfall.

Two drought indices – the Standardised Precipitation Evapotranspiration Index (SPEI) and the Water Requirement Satisfaction Index (WRSI) – were used to assess drought in the catchment. A 120-day maturing maize crop was considered and three consecutive planting dates were staggered based on the average start of the rainy season. Frequencies and probabilities during each growing stage of maize were calculated based on the results of the two indices. Temporal variations of drought severity from 1975 to 2015 were evaluated and trends analysed using the non-parametric Spearman's rank correlation test at significance level, α of 0.05. For assessing climate change impact on drought, SPEI and WRSI were computed using an output from downscaled future projections of climate change. The frequency of drought was calculated and the difference in SPEI and WRSI means between future climate periods and the base period was assessed using the independent *t*-test at α (0.05) significance level in Statistica software.

The Soil and Water Assessment Tool (SWAT) was used to simulate streamflows (run-off) in the Luvuvhu River catchment. The model was executed through an interface between SWAT and QGIS desktop 2.6.1 software, namely, QSWAT 1.3 2016. The model was run for a 33-year period from 1983 to 2015. The model produced 17 sub-catchments of which four were used for analysis. Sensitivity analysis, calibration and validation were conducted using the SUFI-2 algorithm through its interface with SWAT calibration and uncertainty procedure (SWAT-CUP). Data from 1983-1985 was used to prepare/initialise the model; the calibration process was conducted for the period 1986-2005 and the validation process used data from 2006-2015. A minimum of 300 simulations were performed for each run. The model performance to simulate run-off was based on four objective functions: coefficient of determination , Nash–Sutcliffe efficiency (NSE) index, RMSE observations standard deviation ratio and percent bias, and two performance indices: P-factor and R-factor.

The results of the study revealed that the Luvuvhu River catchment can be divided into different agroclimatic zones with different rainfall characteristics, namely, arid, semi-arid, sub-humid and humid. Seasonal rainfall ranges from 315 mm in the northern and eastern plains to more than 1500 mm in the elevated south-western parts of the catchment. Early onset in October occurs in areas situated in mountainous areas that receive more than 700 mm of annual rainfall, while onset occurs later in November in the low-lying areas of the catchment receiving less than 500 mm of annual rainfall.

The study shows that planting a 120-day maturing maize crop in December poses a high risk of frequent severe to extreme droughts during flowering to grain-filling stages at Levubu, Lwamondo, Thohoyandou, and Tshiombo; while planting in October places crops at a lower risk of reduced yield and even total crop failure. In contrast, stations located in the low-lying plains of the catchment (Punda Maria, Sigonde and Pafuri) are exposed to frequent moderate droughts following planting in October, with favourable conditions noted following the December planting date. This shows that there is a high probability of crop failure if planting occurs following the first onset in the dry areas of the catchment. Therefore, based on rainfall, areas in the upper part of the catchment are favourable to maize production while the northern and eastern plains are not suitable for maize production.

Results by SPEI show that 40-54% of the agricultural seasons during the base period experienced mild drought conditions (SPEI 0 to −0.99), which correspond to a recurrence of drought once in two seasons. However, WRSI results clearly indicated that stations in the drier regions (annual rainfall < 600 mm) of the catchment experienced mild drought (WRSI 70-79) corresponding to satisfactory crop performance every season. Results further showed overall mild to moderate droughts in the beginning of the near-future climate period (2020/21-2036/37) with SPEI values not decreasing below −1.5. These conditions are expected to change during the far-future climate period (2055/56-2089/90), whereby results on the expected crop performance predicted significantly drier conditions ($p < 0.05$).

The SWAT simulation results were satisfactory for run-off simulation in the Luvuvhu River catchment. The use of SUFI-2 in SWAT-CUP quantified the calibration and validation results well. Flood frequency analyses indicate increasing floods at greater probability of exceedance for all return periods. Following the above-mentioned model analysis, sub-catchment 17 being the Luvuvhu catchment outlet, 50-, 100- and 200-year floods revealed flood magnitudes of 960.70 $m^3 \cdot s^{-1}$, 1121.02 $m^3 \cdot s^{-1}$ and 1281.35 $m^3 \cdot s^{-1}$ respectively. The log-normal distribution model shows high peak events that can be used as estimating limiting values for design purposes and can be considered as a distribution of choice in terms of flood frequency analysis and planning in the Luvuvhu River catchment.

The project developed a web-based decision support tool, the Luvuvhu Agroclimatological Risk Tool (LART), which will be used to provide agroclimatological risk information important to the production of rain-fed maize in the catchment. The LART has two main components: climatological risk and forecasting crop yield. The climatological risk component consists of all the algorithms for rainy season characteristics, drought risk indices and flood frequencies, utilising the methodologies developed within this project. This will enable the user to obtain agroclimatological risks for different maize crop varieties for a planting window starting in October to January. Another important feature of this tool is the functionality of using climate forecasts obtained from the national forecasting centres. Drought indices can be predicted for different planting dates to provide farmers with valuable information prior, during and after each agricultural season.

Stakeholder involvement was conducted in a form of various workshops where project team members visited various sites in the Luvuvhu River catchment. The workshops were held in November 2015, 2016 and 2017. The main aim of the visits was to present the seasonal forecast released in November by SAWS in preparation for the agricultural season ahead. Farmers were made aware of the weather conditions to be expected for the upcoming season. The presentations focused on providing potential benefits as well as the possible negative effects provided by the forecast. Recommendations and preplanting training were then given accordingly.

Recommendations based on this research are as follows:

- Information on rainy season characteristics of different areas should be communicated to extension officers and farmers during workshops.
- Farmers are advised to use seasonal forecasts as a guide when planning for the upcoming season.
- In early onset seasons, late maturing varieties should be planted; in seasons with late onset, early-maturing and drought-tolerant maturities should be planted.
- Farmers in wet areas of the catchment are advised to plant both long, medium and early-maturing varieties, whereas farmers in dry areas of the catchment are advised to plant early-maturing varieties.
- Analysis on previous droughts led to a recommendation of using the October to November period as the optimum planting date in the catchment.
- For minimising the risk of damaging drought conditions on maize, planting in October can be recommended for high to moderate rainfall regions. However, planting too early (1st dekad of October) might place crops grown in these areas under drought stress.
- Farmers located in the drier areas of the catchment are also advised to plant in November.
- Farmers located in vulnerable areas can be advised to supplement rain-fed farming with irrigation should they be located near rivers.
- Due to many assumptions and uncertainties, it is recommended that the SWAT model be used in conjunction with other hydrological models as a conceptual model.
- The results obtained from the frequency analysis would assist in the planning purposes of the catchment to mitigate and adapt to flooding seasons.
- There are many future research areas involving the SWAT model that need attention.
- It is recommended that there is proper dissemination of flood information from disaster management agencies to the farmers so that they can be prepared properly for the future.
- Sustainable water management measures (such as conservation agriculture) should be planned to mitigate the possible effects of climate variability and extremes under climate change.
- For the improvement of agricultural productivity, the government needs to ensure that proper support such as effective early warning systems and input provision is provided.
- Essential communication between scientists, decision makers and the farmers can help in planning and decision-making ahead of and during the occurrence of droughts.

TABLE OF CONTENTS

LIST OF FIGURES

LIST OF TABLES

ABBREVIATIONS

AA	Arithmetic Averaging
ARC	Agricultural Research Council
ARC-ISCW	Agricultural Research Council – Agroclimate Information System
CC	Correlation Coefficient
CCAM	Conformal-Cubic Atmospheric Model
CMIP5	Coupled Model Intercomparison Project Phase 5
CV	Coefficient of Variation
DEM	Digital Elevation Model
DSS	Decision Support System
DST	Decision Support Tools
DWS	Department Of Water And Sanitation
ENSO	El Niño Southern Oscillation
GIS	Geographical Information System
HRU	Hydrological Response Unit
IDW	Inverse Distance Weighted
IPCC	Intergovernmental Panel On Climate Change
LART	Luvuvhu Agroclimatological Risk Tool
MAE	Mean Absolute Error
MBE	Mean Bias Error
MLR	Multiple Linear Regression
NR	Normal Ratio
NSE	Nash–Sutcliffe Efficiency
R	Correlation Coefficient
R^2	Coefficient of Determination
RCP	Representative Concentration Pathway
Revap	Re-evaporation
RMSE	Root Mean Square Error
RSR	RMSE Observations Standard Deviation Ratio
SAWS	South African Weather Service
SBE	Single Best Estimator

SCS	Soil Conservation Service
SPEI	Standardised Precipitation Evapotranspiration Index
STD	Standard Deviation
STRM	Shuttle Radar Topography Mission
SUFI	Sequential Uncertainty Fitting
SWAT	Soil and Water Assessment Tool
SWAT-CUP	SWAT Calibration and Uncertainty Procedure
SWHC	Soil Water-Holding Capacity
UNEP	United Nations Environment Programme
UTM	Universal Transverse Mercator
WMA	Water Management Area
WMO	World Meteorological Organization
WMU	Water Management Unit
WRSI	Water Requirement Satisfaction Index

CHAPTER 1:INTRODUCTION

1.1 General Background

Weather and environmental conditions during the growing period have a direct bearing on plant growth and development, and ultimately affect the crop yield. Thus, the most important way of ensuring that crop production remains sustainable is to ensure that crops and cropping systems match the climate of the location. Moreover, analyses of agrometeorological information can help the farming community to plan better, and improve preparedness and adaptive capacity – especially for farmers such as those in the Luvuvhu River catchment as they rely solely on maize as a staple food and are considered economically poor according to South African standards (DWAF, 2004; Friesland & Lopmeier, 2006).

South Africa is a semi-arid country. The provinces that are highly vulnerable to rainfall variability are the Eastern Cape, KwaZulu-Natal, North West and Limpopo (Zuma et al., 2012; Hart et al., 2013). High intra-seasonal and inter-annual rainfall variability has led to extreme events such as floods occurring more frequently in the country (Davis & Joubert, 2011). There have been several natural disaster events in South Africa between 1980 and 2014, and within this period, flooding has occurred many times including during the years 1981, 1987, 1994, 2000 and 2013 (Moodley, 2014).

Numerous studies have been conducted to identify the connection between rainfall anomalies that could lead to flooding in South Africa (Tennant & Hewitson, 2002; Kane, 2009). South African rainfall is not equally distributed spatially and temporally (Hart et al., 2013). According to Moeletsi et al. (2011), there are extreme rainfall events during La Niña years that may lead to flooding. A study done by Warburton et al. (2010) revealed that climate variability has a significant impact on hydrological responses of a catchment. This was further confirmed by a study done by Gaur (2013) where even small changes in climate variables showed results of significant impact on hydrological characteristics of a catchment. According to such findings, it can be ascertained that climate change continues to be one of the greatest challenges in terms of hydrological responses with an annual risk of flooding of 83.3% in South Africa (Zuma et al., 2012).

1.2 Motivation

Water is among the most important elements affecting agriculture as it is one of the limiting resources for crop growth in semi-arid regions such as southern Africa. This limiting factor is mostly caused by unreliable seasonal rainfall, and high variability of onset of rains and cessation of rains (Barron et al., 2003). Delays in planting due to the late onset of the rains may result in reduced yield while planting too early risks a false onset of the rainy season, which may lead to insufficient soil moisture for proper germination of crops (Wetterhall et al., 2015). Crop yield may also be significantly affected by damaging dry spells during the season (Ati et al., 2002; Mugulavai et al., 2008). Moreover, heavy rainfall at the end of the rainy season can cause crops to spoil or prevent ripening and harvesting (Stern & Coe, 1984). This raises major concerns, particularly for vulnerable small-scale farmers who rely on rain for crop production.

In semi-arid regions such as the Limpopo Province of South Africa, high intra- and inter-seasonal climate variability as well as climate hazards have the most detrimental effects on crop production. The most affected people are resource-poor farmers whose productivity is highly threatened. This study was therefore conducted to improve agricultural productivity and thus help to develop measures to secure livelihoods of the vulnerable small-scale farmers in the Luvuvhu River catchment.

1.3 Aims of the Study

The main aim of the project was to investigate rainfall characteristics and drought, and further estimate flood peaks in the Luvuvhu River catchment. The specific objectives were to:

1. Identify and quantify the rainy season characteristics with reference to crop production in the Luvuvhu River catchment.
2. Calibrate crop models to suit the environmental and management conditions of the study area.
3. Investigate evolution of drought and rainy season characteristics in the Luvuvhu River catchment under climate change.
4. Estimate design flood peaks and conduct flood frequency analysis in the Luvuvhu River catchment.
5. Investigate changes in crop productivity under climate change.

1.4 Study Area

Figure 1 shows the location of the Luvuvhu River catchment, which is within the Vhembe District in the north-eastern corner of the Limpopo Province of South Africa. The catchment covers an area of 5941 km^2. Along with the Letaba River catchment, the Luvuvhu River catchment forms part of the Luvuvhu/Letaba water management area (WMA). This WMA is one of the 19 WMAs in South Africa, which are delineated and acknowledged by the Department of Water and Sanitation (DWS) (Jewitt et al., 2004; Masereka et al., 2015). The catchment consists of 14 water management units (WMUs), which are demarcated according to quaternary catchments and have been adjusted to account for streamflow gauging stations (Warburton et al., 2010). The Luvuvhu River catchment is subdivided into 14 DWS quaternary catchments as depicted by Figure 1 (Jewitt et al., 2004; Nkuna & Odiyo, 2011).

The Luvuvhu River catchment has a humid subtropical climate that is fairly warm to hot during summer, and dry in winter (FAO, 2005). Precipitation varies greatly (Figure 2) and it is mostly determined by orographic patterns with the topography in the catchment ranging from 200 m to 1300 m. The highest rainfall occurs in the south-western area of the catchment where the Soutpansberg Mountains are located. Meanwhile, the north-east is regarded as the driest area and is sparsely populated. The mean annual temperature ranges from < 18°C in the mountainous regions to > 24°C in the north-eastern plains of the catchment (Figure 2). The catchment is characterised by a wide spectrum of soils with sandy loam soils being the most prevalent and the soil water-holding capacity ranging from 21 mm to 80 mm (DWAF, 2004; ARC-ISCW, 2016).

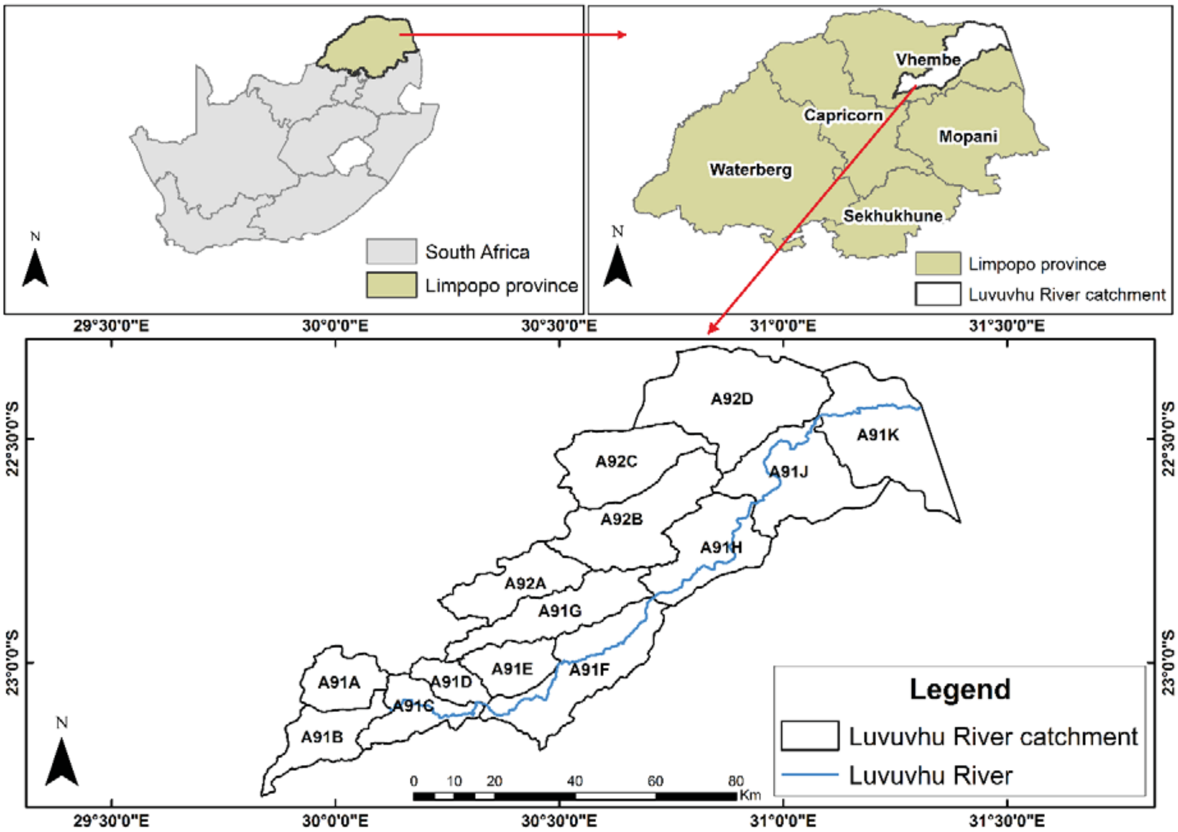

Figure 1: Location of the Luvuvhu River catchment, Luvuvhu River and quaternaries

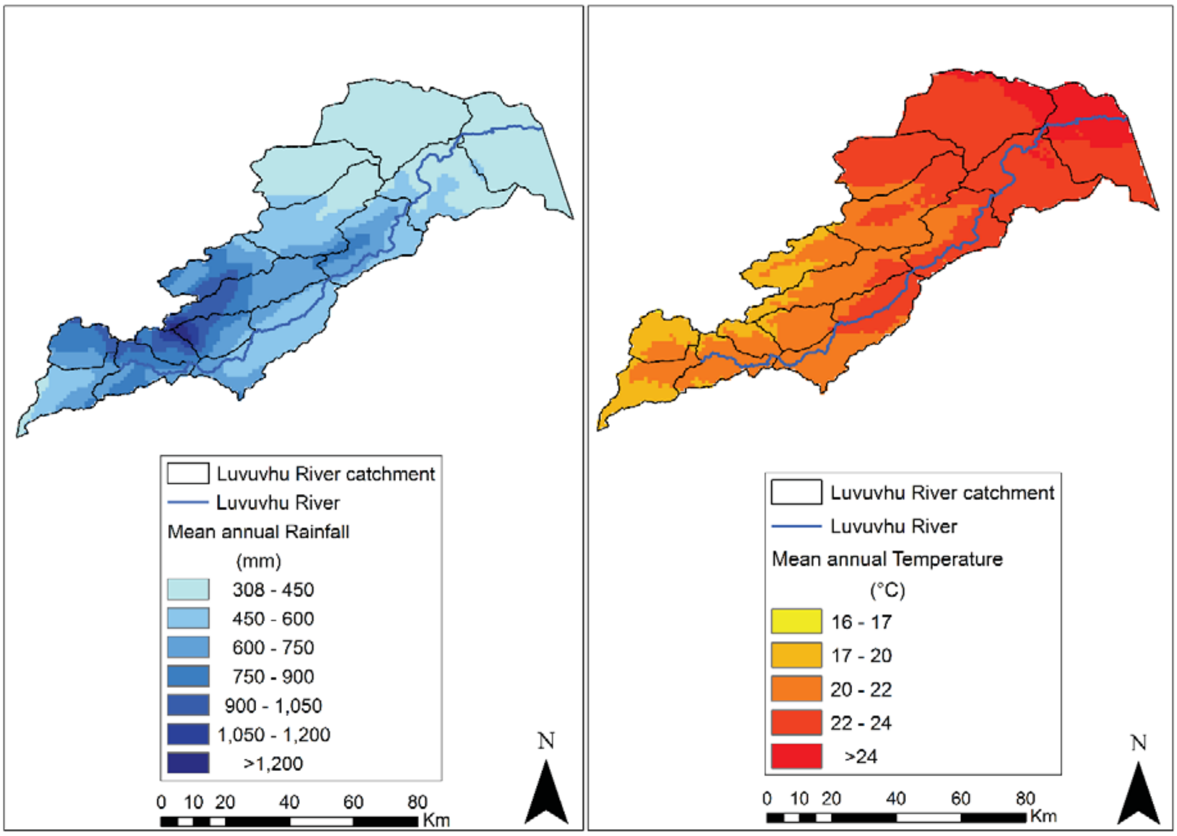

Figure 2: Long-term mean annual rainfall and mean annual temperature of Luvuvhu River catchment

Large-scale commercial forests, fruits, and vegetable farms are dominant in the high rainfall regions of the catchment; however, small-scale and subsistence livestock and rain-fed maize farming, which are controlled by regional Venda and Tsonga Chiefs, play a crucial role in the improvement of livelihoods and food security in most parts of the catchment (Griscom et al., 2009; DWAF, 2012). Many people in the catchment acquire their income from remittances, livestock and rain-fed maize farming (DWAF, 2004). State and privately owned forest plantations (pine, eucalyptus and wattle) are located to the south of the Soutpansberg Mountains (Jewitt et al., 2004). Moreover, a change in land cover caused by clearing of forests and shrubs for the provision of fuelwood, maize fields, and pasture has been noted since 1978 (WRC, 2001; DWAF, 2004; Jewitt et al., 2004).

2 CLIMATE STATION NETWORK IMPROVEMENT AND DATA QUALITY CONTROL

2.1 Introduction

Climate data is collected using meteorological or climatological station networks. Climate monitoring is a crucial exercise embarked on by national meteorological services, government agencies and international bodies (WMO, 2015). Rainfall is the common meteorological parameter measured by almost all observational networks. Most of the uses for climate data cannot be foreseen during the planning of the establishment of the network. New applications surface frequently long after the information is acquired.

Initially, the primary use of the weather data in most countries was to support weather forecasting and to improve safety of the aviation industry. However, weather and climate information is currently used by researchers, industries and decision makers for different purposes. In agriculture, weather and climate data can be used to delineate a portion of land that is suitable for planting a particular crop, the optimal timing of planting and harvesting, and crop yield estimation among other applications (Moeletsi & Walker, 2012). In sustainable water management practices, climate data can be used in run-off modelling, modelling of groundwater levels, and assistance in the design of drainage systems (Srikanthan & MacMahon, 2001; Prucha et al. 2016).

For proper analyses to be performed, it is imperative to have appropriate climate data in the format required by the investigator or researcher. The climate variables considered important for this study are rainfall, minimum temperature, maximum temperature and evapotranspiration. Daily climate data in South Africa dates back to the 1800s with rainfall being the most common element measured. There are a few stations around the country that recorded temperature, humidity and wind in the early 1900s but the number increased significantly from 1950 onwards. With the improvement in technology, automatic weather stations that record climate data at shorter time scales (hourly or less) were introduced in South Africa in the 1990s. Increased frequency of measurements means better climate monitoring and an understanding of weather occurrences with a life cycle shorter than one day.

2.2 Improvement of the Weather Station Network

Weather station monitoring systems have to be erected at suitable and representative areas to enable archiving of this valuable information. To install weather stations at any location, a thorough investigation of the site needs to occur. The main determining factors for the stations are availability of a network signal, identification of a safe and secure area, adherence to World Meteorological Organization (WMO) standards, and accessibility of the area.

2.2.1 Improvement of the station network by the project

Before the project, there were six operational Agricultural Research Council (ARC) weather stations in the Luvuvhu River catchment and another six stations close to the catchment (Figure 3). Most stations were in the upper parts of the catchment while the lower parts, including the Kruger National Park, were underserviced. The southern/south-western side of the Luvuvhu River catchment also had no stations.

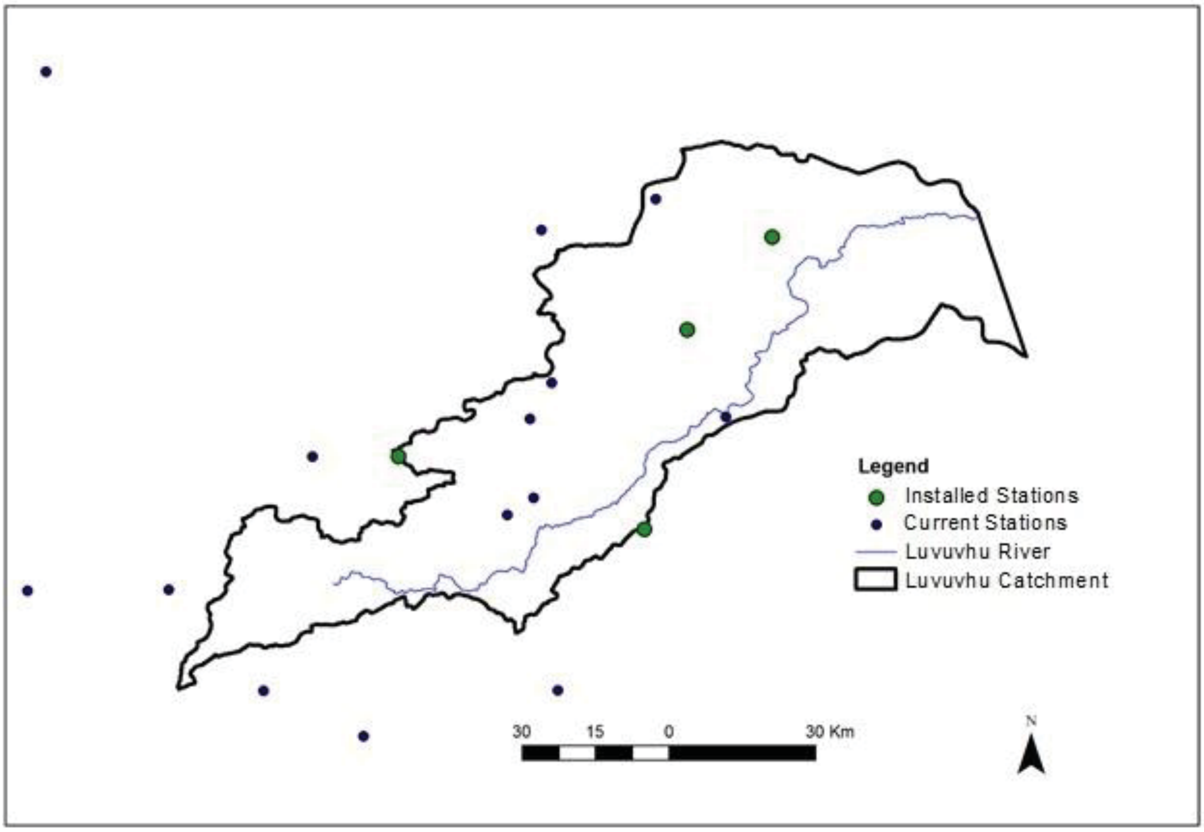

Figure 3: Weather station network in the Luvuvhu River catchment

Four new sites were identified and stations installed (Figure 4 to Figure 7), namely:

- Malamulele (to serve areas on the southern side of the Luvuvhu River catchment).
- Lamvi and Mutele (to serve areas in the upper parts of the catchment).
- Thononda (to serve areas at the source of Mutele River – a tributary of the Luvuvhu River).

The stations have the following sensors: rainfall gauge, wind vane, cup anemometer, temperature sensor, humidity sensor and solar radiation sensor.

Figure 4: Installed weather station at Malamulele agricultural offices

Figure 5: Installed weather station at Sumbana Secondary School (Lamvi)

Figure 6: Installed weather station at Sanari

Figure 7: Installed weather station at Ndweleni Secondary School (Thononda)

2.3 Patching of Weather Data

Climate data records that were collected over a long period of time can contain gaps. The number of gaps in the records usually increases with an increase in the length of the data set. The frequency of gaps in the climate data in most cases makes it difficult to make sound studies since some of the important climatological events would not covered by the records (Tang et al., 1996; Moeletsi et al., 2016). In some instances there might have been recordings of poor quality that may further increase the uncertainty of archived climate data. Several circumstances contribute to the prevalence of missing data, for example, loss of records, equipment vandalism, instrument malfunction, poor observation techniques or observer negligence (Tang et al., 1996; Makhuvha et al., 1997; Vilazón & Willems, 2010).

Three common approaches often used in treating the missing climate data gaps are:

1. To only use continuous records and ignore the prior events.
2. To ignore the missing gaps based on the assumption that the data is one continuous series of records (Tang et al., 1996).
3. To patch the data (Moeletsi et al., 2016).

The main disadvantage to the first approach is wasting valuable and previous information, and the true statistical inferences cannot be made. On the other hand, the second approach shrinks the period of recorded events available for analysis, thus over- or underestimating the likelihood of major events occurring (Tang et al., 1996). The recommended method is that of patching the data, but it has to be approached in a manner that eliminates bias and conforms to the climatological variation in the target region (Moeletsi et al., 2016).

2.3.1 Development of the patching tool

There are several techniques used to patch missing or defective climatological data. The most common techniques are (Tang et al., 1996; De Silva et al., 2007; Radi et al., 2015):

- Arithmetic averaging method (AA).
- Single best estimator (SBE).
- Normal ratio method (NR).

- Inverse distance weighted method (IDW).
- Correlation coefficient method (CC).
- Multiple linear regression (MLR).

The best method differs from region to region based on variances in climate. The method also depends on the weather element to be estimated (De Silva et al., 2007). Two versions of the patching programs (tools) were developed, namely, a climate database and a stand-alone program. These programs had the same functionality, but the report concentrates on the stand-alone program version (Figure 8) of the data patching tool, which provides the functionality to patch climate data. The program was developed using Java as the development language. The patching process flow chart and function workflow of this tool are depicted from Figure 8 to Figure 15, and Table 1.

2.3.1.1 *User interface*

A basic user interface is given in Figure 8.

Figure 8: User interface of the ARC climate data patching tool

2.3.1.2 *Tool input*

The tool reads from two or more workbooks that are compatible with at least Microsoft Office Excel™ 1997-2003. The first workbook is called *station.xls* and contains information of all the stations (total being 65 535) available for the tool to use. The tool also has a directory called *stations*, which contain multiple workbooks, i.e. *input_0.xls*, *input_1.xls*, *input_2.xls*, etc. Each of the input workbooks can have a maximum of 252 stations and can contain approximately 179 years of data.

The main inputs to the tool are the following parameters (Figure 8 and Figure 9):

- ***Target***: The unique number of the station of interest.
- ***No. of Neighbours***: Number of surrounding stations to be used.
- ***Date From* and *Date To***: Start and end date.
- ***Method***: Name of infilling techniques.
- ***Distance/Correlation***: Using either closest or best correlation stations.

The settings inputs have the following parameters (Figure 10):

- ***No. of Workbooks***: The number of input workbooks.
- ***No. of Filtered Stations***: The number of all stations to be considered based on some radius.
- ***No. of Decimals***: The number of decimals for rounding off.
- ***Write to File***: Writing the output result to either text or Excel™ file.
- ***Show Observed/Estimated Values***: Include observed/estimated values in the output file.

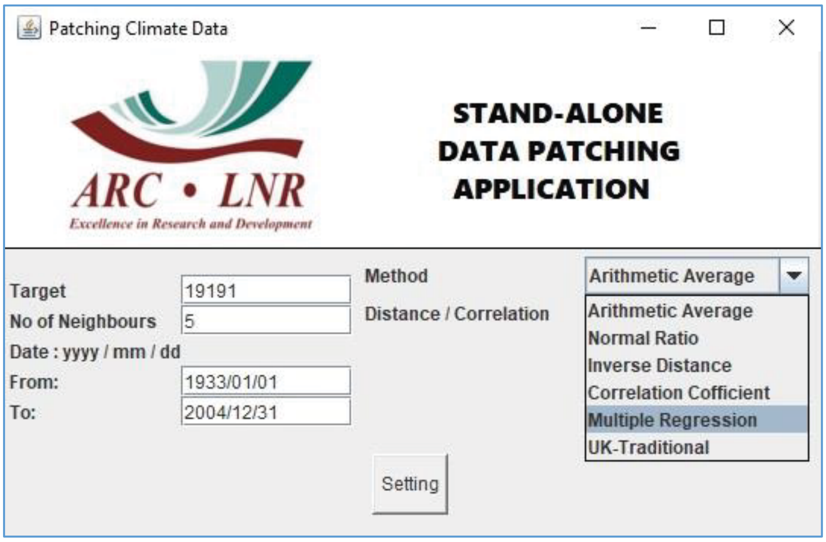

Figure 9: Selection of method in the ARC climate data patching tool

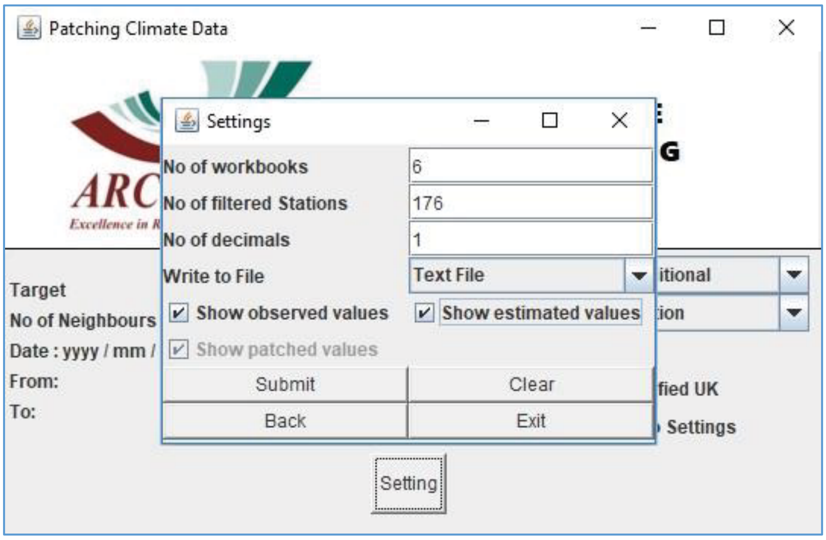

Figure 10: Settings of the ARC climate data patching tool

2.3.1.3 Preparing of data

Figure 11 and Figure 12 show how the data set was prepared. A description of each of the columns in the workbooks is given below.

The description of columns in the workbook station.xls:

- ***Column A***: Unique number for each station.
- ***Column B***: Station name.

- ***Column C***: Latitude.
- ***Column D***: Longitude.
- ***Column E***: Altitude (optional).

The description of columns in the input(s) workbooks:

- ***Columns A to C***: For the dates.
- ***Column D***: Heading for the station unique number.
- ***Rest of the columns***: Contains station data sets, where −999 represent a missing value.

A	B	C	D	E
19068	GOOLDVILLE - HOSP	-22.8833	30.48333	762
19069	THOHOYANDOU	-22.9667	30.5	600
19070	TSHANDAMA	-22.7667	30.53333	600
19073	PUNDA MARIA	-22.6833	31.01667	462
19179	PONTDRIFT - POL	-22.2167	29.15	580
19191	MACUVILLE - AGR	-22.2667	29.9	522
19921	HOEDSPRT GLENCOE	-24.3167	30.9	457
19934	LETSITELE LETABA	-23.9667	30.18333	722
19935	LETABA LETSITELE	-23.8667	30.31667	623
19936	MESSINA PROEFPLAAS	-22.2333	29.91667	505
19937	L.TRICHARD:LEVUBU (S)	-23.0833	30.28333	610
19938	DUPLEX:TZANEEN.	-23.75	30.3	550

Figure 11: Station information required by the ARC climate data patching tool

A	B	C	D	E	F	G	H
			CompNO	17914	17958	18701	19191
nYear	nMonth	nDay					
1960	1	1		31.3	30.2	-999	30.8
1960	1	2		32.6	33	-999	35.3
1960	1	3		33.9	34.4	-999	39.3
1960	1	4		33.6	33.3	-999	35.6
1960	1	5		29.5	29.7	-999	30.6
1960	1	6		27.6	27.4	-999	26.7
1960	1	7		30.4	29	-999	27.7
1960	1	8		33.2	33.2	-999	33.5
1960	1	9		35.3	33.8	-999	35.2

Figure 12: Preparation of data set for patching using ARC climate data patching tool

2.3.1.4 Tool output

The tool will display a progress bar after all the inputs have been submitted. When it finishes computing the estimates, it will display a message box showing the results of the error measures (Figure 13). The tool will also create a file called *Distances.txt* or *Correlation.txt*, which contains the distances or correlation of the target station and the neighbouring stations. Thereafter, a file will be created that contains the user results or estimates. It will be named with a unique computer number (Figure 14).

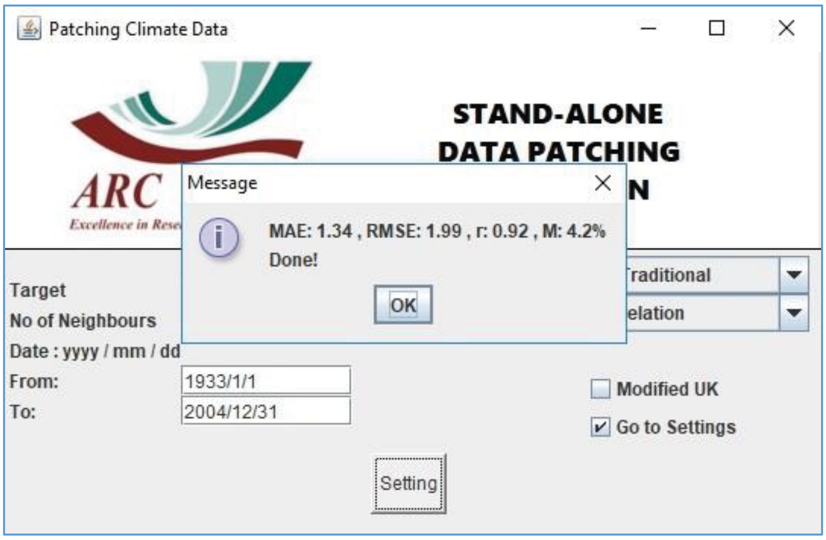

Figure 13: The results showing the performance of the ARC climate data patching tool

A	B	C	D	E	F
1960	1	1	30.8	30.2	30.8
1960	1	2	35.3	34.9	35.3
1960	1	3	39.3	38.7	39.3
1960	1	4	35.6	33.7	35.6
1960	1	5	30.6	32.3	30.6
1960	1	6	26.7	28.1	26.7
1960	1	7	27.7	27.4	27.7
1960	1	8	33.5	33.5	33.5
1960	1	9	35.2	34.5	35.2

Figure 14: The results of the ARC climate data patching tool showing observed (Column D), estimated (Column E) and output (Column F) data

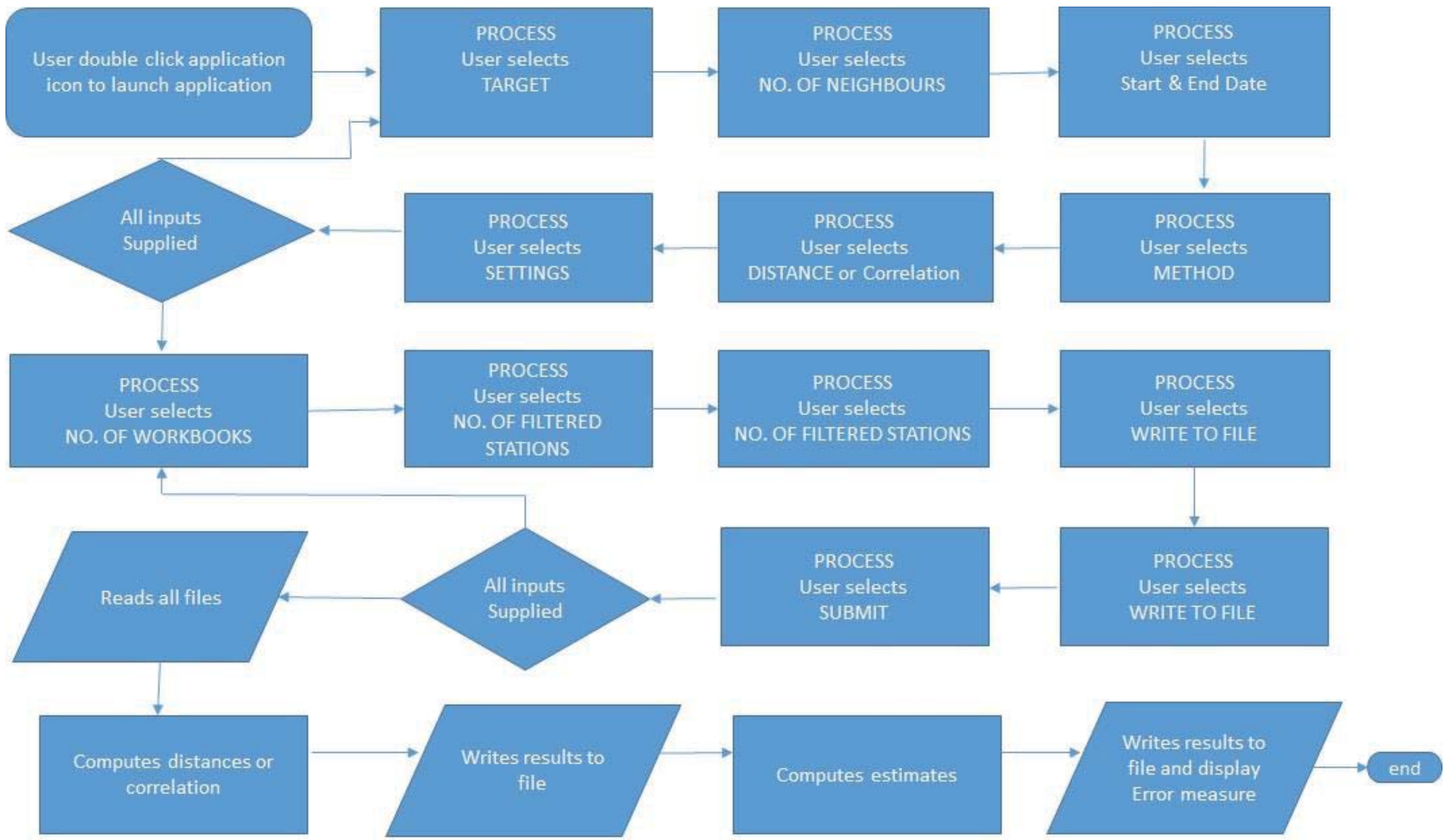

Figure 15: Process flow diagram of the data patching program

Table 1: Patching function workflow

Step	Role Name	Description of Action
1	User (Researcher/ Technician)	Launches the application by double-clicking the application icon.
2	User	Supplies the ***Target*** station number.
3	User	Supplies the ***no. of neighbours***.
4	User	Supplies the start date (***From***).
5	User	Supplies the end date (***To***).
6	User	Selects a ***Method*** of choice.
7	User	Selects ***Distance*** or ***Correlation***.
8	User	Selects ***Setting*** button.
9	System: Stand-alone Patch Function	Checks if all inputs have been supplied by the user.
10	User	Supplies the ***No. of Workbooks***.
11	User	Supplies the ***No. of filtered stations***.
12	User	Supplies the ***No. of Decimals*** (1 is a default value).
13	User	Selects ***Write to File***.
14	User	Starts the patching process by clicking: ***Submit***.
15	System: Stand-alone Patch Function	Displays a progress bar.
16	System: Stand-alone Patch Function	• Checks if all inputs have been supplied by the user. • Checks if *station.xls* file exists and meets system requirements. • Checks if *inputs.xls* file exist and meets system requirements.
17	System: Stand-alone Patch Function	• Checks if target station exists. • Computes the distances or correlation. • Writes the outputs to a file named *Distances.txt* or *Correlation.txt.*
18	System: Stand-alone Patch Function	• Selects the method of choice. • Computes the estimate values using the method of choice by using either the closest or best correlated neighbouring stations. • Outputs the data to either a text or Excel™ file. • Computes and outputs mean absolute error (MAE), RMSE, r and M values on screen (message box).

2.3.2 Validation of patching methods

The data used in this study was downloaded from the ARC's Agroclimate Information System (ARC-ISCW, 2016). Eight target stations with daily temperature for both minimum temperature (Tmin) and maximum temperature (Tmax) were used. Figure 16 shows the distribution over the province. Table 2 gives the geographical and data recording information. Stations selected had a missing data percentage of less than 40% and more than 20 years of data. A total of 176 neighbouring stations distributed all over the Limpopo Province were used to estimate both minimum and maximum temperatures (Figure 17).

Table 2: Geographical and data information of eight target stations used to evaluate methods of patching temperature data in the Limpopo Province

Station no.	Station name	Latitude	Longitude	Altitude (m)	Start date	End date	No. of years	Missing%
19935	LETABA LETSITELE	−23,87	30,32	623	1974-01	2008-02	34	10.2
19970	PIETERSBURG	−23,84	29,69	1226	1984-07	2010-08	26	18.3
18743	MARA: AGR	−23,15	29,57	894	1949-0	2004-03	55	22.7
17958	TOWOOMBA	−24,9	28,33	1143	1937-01	2004-03	67	22.7
19191	MACUVILLE – AGR	−22,27	29,9	522	1933-10	2004-01	70	24.3
19982	VENDA: TSHIOMBO	−22,80	30,48	650	1983-01	2006-03	23	28.4
19994	ELANDSKLOOF	−24,28	28,05	1215	1979-03	2001-09	23	33.6
19961	HOEDSPRUIT	−24,41	30,78	573	1985-07	2005-01	20	38.0

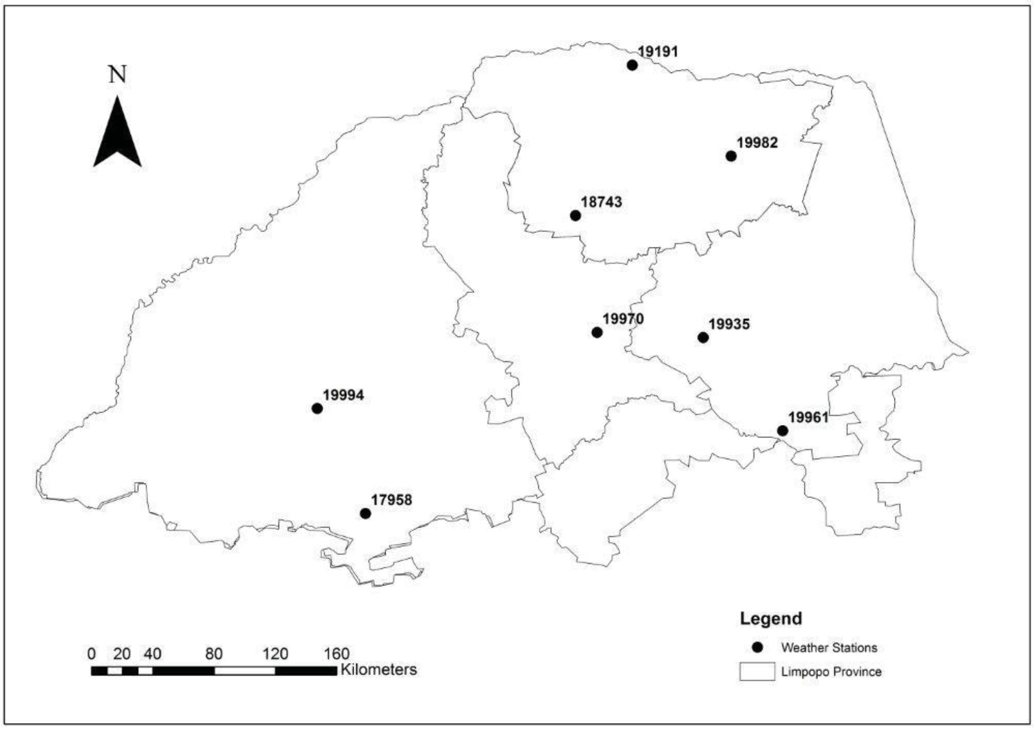

Figure 16: Spatial distribution of target stations used to evaluate methods of patching temperature data in Limpopo Province

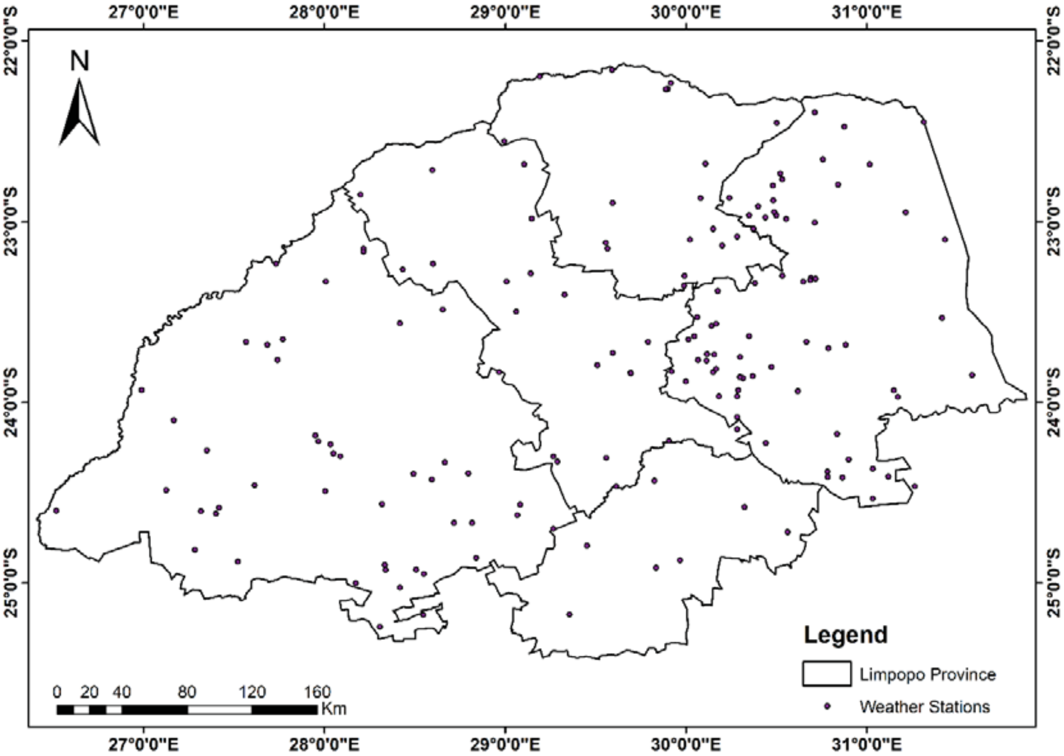

Figure 17: Spatial distribution of all the temperature stations across Limpopo Province

There are many methods that can be employed to estimate missing temperature data; however, this study focused only on the arithmetic averaging, normal ratio, IDW, correlation coefficient, MLR and UK approaches. These methods either consider the closest and/or the best correlated neighbouring stations to estimate the missing data. The numbers of neighbouring stations used for each method are three, five and eight stations.

2.3.2.1 Arithmetic averaging method

The missing data is obtained by arithmetically averaging data from the neighbouring stations. The equation for estimating by the arithmetic averaging method is given below:

$$\mathbf{Px} = \frac{\mathbf{1}}{\mathbf{n}}\sum_{\mathbf{i=1}}^{\mathbf{i=n}} \mathbf{Pi} \quad (\mathbf{1})$$

Where

Px is the estimated value,

$p1, p2, p3, \ldots, pn$ are temperature values of the neighbouring stations, and

n is the number of neighbouring stations.

There are two sub-categories of this method:

i. ***Nearest stations (AA_D)***

The estimation is based on averaging the closest stations to the target station (Xia et al., 1999). Neighbouring stations are ranked based on their distance to the target stations.

ii. ***Best correlated stations***

The estimation is based on averaging the values of the best correlated stations. Neighbouring stations are ranked based on their data correlation with the target station.

2.3.2.2 Normal ratio method

Missing data is estimated as the weighted average of the closest neighbouring station. The neighbouring station's data is weighted by the ratio of the average target station data and the average of the neighbouring station data (Radi et al., 2015). The equation for estimation is as follows:

$$\mathbf{Px} = \frac{\mathbf{1}}{\mathbf{n}} \sum_{\mathbf{i=1}}^{\mathbf{i=n}} \frac{\mathbf{Nx}}{\mathbf{Ni}} \mathbf{Pi} \quad (2)$$

Where

Px is the estimated value,

$p1, p2, p3, \dots, pn$ is temperature values of the neighbouring station,

$N1, N2, N3 \dots, Ni$ is annual average temperature of the neighbouring station,

Nx is annual average temperature of the target station, and

n is the number of neighbouring stations.

2.3.2.3 IDW method

The missing data is obtained by assuming that the target station data could be influenced mostly by the nearest station and less by further distance stations (Xia et al., 1999; Radi et al., 2015; De Silva, 2007). The equation of estimation is as follows:

$$\mathbf{Px} = \frac{\sum_{\mathbf{i=1}}^{\mathbf{i=n}} \frac{\mathbf{1}}{\mathbf{d^q}} \mathbf{Pi}}{\sum_{\mathbf{i=1}}^{\mathbf{i=n}} \frac{\mathbf{1}}{\mathbf{d^q}}} \quad (3)$$

Where

Px is the estimated value,

$p1, p2, p3, \dots, pn$ are temperature values of the neighbouring station,

d is the distance between the target station and the neighbouring station,

q is a natural number, usually $q = 2$, and

n is the number of neighbouring stations.

2.3.2.4 Correlation coefficient weighted method

The missing data is obtained by finding the correlation coefficient between the target station and neighbouring stations, and replacing the weighted value of IDW with the correlation coefficient. The target station value is influenced more by how alike the target station data is compared with each neighbouring station's data (Teegavarapu, 2009; Radi et al., 2015). The equation of estimation is as follows:

$$\mathbf{Px} = \frac{\sum_{i=1}^{i=n} \mathbf{rPi}}{\sum_{i=1}^{i=n} \mathbf{r}} \quad (4)$$

Where

Px is the estimated value,

$p1, p2, p3, \dots, pn$ are temperature values of the neighbouring station,

r is the correlation coefficient between target station and neighbouring station, and

n is the number of neighbouring stations.

2.3.2.5 MLR method

The missing data is estimated by calculating the regression coefficient between the target station and the best correlated neighbouring station (Xia et al., 1999).

$$\mathbf{Px} = \mathbf{b_0} + \sum_{i=1}^{i=n} \mathbf{biPi} \quad (5)$$

Where

Px is the estimated value,

$p1, p2, p3, \dots, pn$ are temperature values of the neighbouring station,

$b0, b1, b2, \dots, bn$ are regression coefficients, and

n is the number of neighbouring stations.

2.3.2.6 The UK traditional methods

The estimation of missing data involves assuming a constant difference between the long-term data from the target station and the neighbouring stations (Xia et al., 1999). For each month of the year, long-term data for each neighbouring station is compared with data of the target station. Suppose that the monthly neighbour's temperature is a *y* value more than the monthly target station data, the value *y* will be subtracted from the daily neighbouring station value. In contrast, if the monthly neighbour's temperature is a *y* value less than the monthly target station data, the value *y* must be added to the daily neighbouring station value. The method can be approached using either correlation or distances between the target and neighbouring stations. The following are ways of estimating missing values under the UK method:

i. Averaging the best correlated stations (UK_AA_C)

Calculating an arithmetic average of the individual estimations of the best correlated stations.

ii. Blending of UK and correlation coefficient (UK_CC_C)

Correlation coefficient method used in estimating value at the target station based on the individual neighbour UK estimations.

iii. Averaging of the closest station estimates (UK_AA_D)

Calculating of an arithmetic averaging of the UK estimations of the closest stations.

iv. Blending of UK and IDW (UK_ID_D)

The IDW equation is used to estimate values at the target station based on individual neighbour UK estimations.

Statistical analysis

To determine the best method of estimating temperature records, the MAE, root mean squared error (RMSE), correlation coefficient (R) and accuracy rate were used to measure the accuracy between estimated values and observed values (De Silva et al., 2007; Teegavarapu, 2009; Vilazón & Willems, 2010).

All the patching methods were tested to patch the data for the entire data set at each of the target stations using either three, five or eight neighbouring stations. The following are the equations of the statistical parameters:

Correlation coefficient (R)

$$\mathbf{R} = \frac{\sum_{i=1}^{i=n} (\mathbf{P} - \bar{\mathbf{P}}\mathbf{i})(\hat{\mathbf{P}}\mathbf{ı} - \bar{\mathbf{P}}\mathbf{i})}{\sqrt{\sum_{i=1}^{i=n} (\mathbf{P} - \bar{\mathbf{P}}\mathbf{i})^2 (\hat{\mathbf{P}}\mathbf{ı} - \bar{\mathbf{P}}\mathbf{i})^2}} \quad (6)$$

Where

Pi is the actual value,

$\widehat{P\imath}$ is the estimated value, and

$\bar{P}i$ is the mean.

MAE

$$\mathbf{MAE} = \frac{1}{n}\sum_{i=1}^{i=n} \left|\hat{\mathbf{P}}\mathbf{ı} - \mathbf{Pi}\right| \quad (7)$$

Where

Pi is the actual value, and

$\widehat{P\imath}$ is the estimated value.

RMSE

$$\mathbf{RMSE} = \sqrt{\frac{1}{n}\sum_{i=1}^{i=n} (\hat{\mathbf{P}}\mathbf{ı} - \mathbf{Pi})^2} \quad (8)$$

Where

Pi is the actual value, and

$\widehat{Pi}$ is the estimated value.

Accuracy rate

Accuracy rate is the percentage that each method had the lowest MAE.

2.4 Results and Discussion

This sections shows the result of the analyses for all the methods per station and highlight some important points from the analyses.

2.4.1 Minimum temperature

The correlation coefficient (R) for the estimated daily minimum temperatures as compared with observed values showed consistency across all the stations (Table 3).

Table 3: Correlation coefficient (R) for each method for all target stations

Station no.	AA_D			AA_C			IDW			Correlation coefficient			UK_AA_D		
	3	5	8	3	5	8	3	5	8	3	5	8	3	5	8
17958	0.946	0.949	0.945	0.946	0.950	0.949	0.940	0.944	0.945	0.946	0.950	0.949	0.947	0.951	0.950
18743	0.925	0.928	0.940	0.955	0.961	0.966	0.918	0.925	0.937	0.955	0.961	0.966	0.937	0.943	0.948
19191	0.942	0.944	0.940	0.965	0.955	0.957	0.956	0.955	0.953	0.965	0.956	0.957	0.949	0.950	0.946
19935	0.925	0.937	0.950	0.954	0.958	0.959	0.938	0.945	0.950	0.954	0.958	0.959	0.945	0.951	0.959
19961	0.945	0.951	0.951	0.939	0.944	0.949	0.944	0.945	0.946	0.940	0.944	0.949	0.945	0.951	0.954
19970	0.901	0.917	0.927	0.921	0.932	0.943	0.860	0.872	0.881	0.921	0.932	0.943	0.934	0.941	0.940
19982	0.939	0.952	0.959	0.959	0.961	0.962	0.899	0.912	0.920	0.959	0.961	0.963	0.947	0.956	0.962
19994	0.950	0.957	0.961	0.951	0.957	0.960	0.948	0.955	0.958	0.951	0.957	0.960	0.949	0.959	0.963
Average	**0.934**	**0.942**	**0.946**	**0.949**	**0.952**	**0.956**	**0.925**	**0.932**	**0.936**	**0.949**	**0.952**	**0.956**	**0.944**	**0.950**	**0.953**
	UK_ID_D			**UK_AA_C**			**UK_CC_C**			**Normal ratio**			**MR**		
	3	5	8	3	5	8	3	5	8	3	5	8	3	5	8
17958	0.941	0.945	0.947	0.949	0.954	0.952	0.949	0.954	0.953	0.947	0.950	0.948	0.953	0.960	0.943
18743	0.935	0.941	0.946	0.963	0.967	0.967	0.963	0.967	0.967	0.927	0.935	0.948	0.965	0.971	0.964
19191	0.957	0.957	0.957	0.967	0.964	0.960	0.967	0.964	0.961	0.942	0.943	0.940	0.972	0.976	0.973
19935	0.952	0.955	0.958	0.962	0.965	0.965	0.962	0.965	0.965	0.934	0.942	0.956	0.969	0.972	0.968
19961	0.942	0.943	0.945	0.952	0.953	0.955	0.952	0.953	0.955	0.945	0.951	0.953	0.958	0.962	0.949
19970	0.932	0.938	0.940	0.952	0.953	0.956	0.952	0.954	0.956	0.905	0.922	0.928	0.955	0.959	0.955
19982	0.925	0.934	0.939	0.961	0.963	0.964	0.961	0.963	0.964	0.940	0.953	0.960	0.963	0.966	0.965
19994	0.948	0.955	0.958	0.955	0.960	0.963	0.955	0.960	0.963	0.950	0.959	0.962	0.963	0.968	0.965
Average	**0.941**	**0.946**	**0.949**	**0.958**	**0.960**	**0.960**	**0.958**	**0.960**	**0.961**	**0.936**	**0.944**	**0.949**	**0.962**	**0.967**	**0.960**

The correlation is very good with values exceeding 0.93 in all stations and for all the different patching methods. The results also depict that an increase in the number of stations used to estimate daily values gave rise to a slight increase of the correlation coefficient in most stations. Even though the increase is not significant, it is an indication that estimating climate data should be done with more than three neighbouring stations and increasing the number of contributing stations improves the relationship of the observed versus the estimated.

The MAE for the comparison of estimated daily minimum temperatures and observed temperatures mostly ranged from 0.8°C to 3.8°C (Table 4).

Table 4: MAE for each method for all target stations

Station no.	AA_D			AA_C			IDW			Correlation coefficient			UK_AA_D		
	3	*5*	*8*	*3*	*5*	*8*	*3*	*5*	*8*	*3*	*5*	*8*	*3*	*5*	*8*
17958	1.322	1.296	1.516	1.355	1.380	1.558	1.409	1.334	1.306	1.354	1.377	1.548	1.307	1.251	1.272
18743	2.575	2.419	2.316	2.905	2.453	2.486	2.596	2.444	2.348	2.909	2.457	2.489	1.473	1.413	1.361
19191	1.576	1.691	1.954	1.583	1.797	1.782	1.162	1.177	1.193	1.583	1.789	1.776	1.321	1.348	1.442
19935	1.691	1.609	1.467	1.226	1.282	1.248	1.542	1.505	1.451	1.226	1.279	1.246	1.215	1.162	1.069
19961	1.225	1.181	1.246	1.330	1.303	1.402	1.337	1.321	1.310	1.331	1.303	1.400	1.121	1.063	1.042
19970	3.635	3.725	3.676	3.279	3.542	3.574	3.358	3.386	3.307	3.278	3.538	3.570	1.617	1.545	1.565
19982	1.089	1.013	0.934	1.009	0.940	0.932	1.445	1.334	1.263	1.009	0.940	0.931	0.996	0.945	0.872
19994	1.649	1.508	1.551	1.501	1.472	1.458	1.666	1.537	1.493	1.498	1.469	1.454	1.280	1.163	1.103
Average	**1.845**	**1.805**	**1.832**	**1.774**	**1.771**	**1.805**	**1.814**	**1.755**	**1.709**	**1.773**	**1.769**	**1.802**	**1.291**	**1.236**	**1.216**
	UK_ID_D			**UK_AA_C**			**UK_CC_C**			**Normal ratio**			**MR**		
	3	*5*	*8*	*3*	*5*	*8*	*3*	*5*	*8*	*3*	*5*	*8*	*3*	*5*	*8*
17958	1.382	1.324	1.298	1.289	1.228	1.253	1.289	1.227	1.250	1.352	1.271	1.317	1.213	1.117	1.178
18743	1.500	1.440	1.386	1.138	1.075	1.055	1.138	1.075	1.054	2.212	2.071	1.972	1.113	1.008	1.150
19191	1.154	1.156	1.154	1.115	1.200	1.259	1.112	1.195	1.254	1.459	1.532	1.778	0.977	0.898	0.947
19935	1.113	1.085	1.053	1.005	0.960	0.970	1.004	0.959	0.969	1.371	1.287	1.109	0.881	0.840	0.910
19961	1.155	1.142	1.130	1.054	1.046	1.032	1.054	1.045	1.031	1.257	1.171	1.137	0.963	0.917	1.091
19970	1.616	1.550	1.536	1.343	1.329	1.313	1.343	1.328	1.313	2.524	2.464	2.516	1.282	1.239	1.300
19982	1.177	1.089	1.041	0.846	0.841	0.834	0.846	0.841	0.833	1.062	0.987	0.899	0.824	0.796	0.811
19994	1.309	1.219	1.173	1.205	1.133	1.097	1.204	1.133	1.096	1.295	1.184	1.124	1.071	1.003	1.065
Average	**1.301**	**1.251**	**1.221**	**1.124**	**1.101**	**1.102**	**1.124**	**1.100**	**1.100**	**1.566**	**1.496**	**1.481**	**1.040**	**0.977**	**1.057**

Even though using a high number of stations resulted in relatively higher correlation, the MAE did not show the same trend. Using three stations resulted in a relatively higher MAE than using five and eight neighbouring stations. For all patching methods employed, using five neighbouring stations had the tendency of obtaining lower MAE than eight stations. Thus, there is a higher accuracy of estimating daily minimum temperatures when deploying five neighbouring stations.

The best performing method was still the MLR method with the lowest average MAE of less than 1°C when using data from 1933 to 2010. Using UK_CC_C also yielded a low MAE when compared with the other methods, indicating the relatively high accuracy of the method. The arithmetic averaging using distance as the weight (AA_D) was the worst performing method with the MAE exceeding 1.8°C. It can be noted that Pietersburg (station no. 19970) had the highest MAE with values in excess of 3°C, showing a very poor accuracy level. Since the density of the stations in that region is relatively good, this low accuracy can be attributed to local microclimate at the target station, which makes estimating the parameter a challenge.

The RMSE values for estimated minimum temperatures ranged from 1.1°C to 4.4°C. The MLR method followed by blended UK_CC_C and the UK_AA_C have the lowest RMSE values not exceeding 1.56°C. In general for all the patching methods, using five neighbouring stations resulted in slightly lower RMSE values than when using three and eight stations. The AA_D and the IDW methods can be the worst performing ones for estimating daily minimum temperatures in the Limpopo Province.

Table 5: RMSE for each method for all target stations

Station no.	AA_D			AA_C			IDW			Correlation coefficient			UK_AA_D		
	3	*5*	*8*	*3*	*5*	*8*	*3*	*5*	*8*	*3*	*5*	*8*	*3*	*5*	*8*
17958	1.948	1.870	2.060	1.944	1.914	2.063	2.095	2.000	1.954	1.943	1.911	2.052	1.893	1.827	1.845
18743	3.325	3.176	3.000	3.284	2.819	2.833	3.359	3.215	3.056	3.286	2.822	2.835	2.014	1.921	1.837
19191	2.139	2.226	2.471	2.011	2.255	2.236	1.837	1.851	1.871	2.010	2.245	2.228	1.903	1.899	1.967
19935	2.136	1.980	1.815	1.693	1.712	1.651	1.980	1.891	1.819	1.692	1.710	1.649	1.658	1.572	1.439
19961	1.669	1.575	1.624	1.832	1.752	1.825	1.856	1.834	1.821	1.833	1.753	1.823	1.529	1.421	1.376
19970	4.388	4.388	4.329	3.816	4.016	3.984	4.268	4.229	4.127	3.815	4.012	3.980	2.114	2.001	2.023
19982	1.573	1.416	1.311	1.413	1.343	1.355	2.119	1.957	1.865	1.412	1.342	1.353	1.465	1.345	1.251
19994	2.108	1.925	1.929	1.923	1.870	1.843	2.132	1.974	1.903	1.920	1.867	1.837	1.712	1.545	1.459
Average	**2.411**	**2.319**	**2.318**	**2.240**	**2.210**	**2.224**	**2.456**	**2.369**	**2.302**	**2.239**	**2.208**	**2.220**	**1.786**	**1.691**	**1.650**
	UK_ID_D			**UK_AA_C**			**UK_CC_C**			**Normal ratio**			**MR**		
	3	*5*	*8*	*3*	*5*	*8*	*3*	*5*	*8*	*3*	*5*	*8*	*3*	*5*	*8*
17958	2.014	1.946	1.911	1.863	1.784	1.804	1.862	1.783	1.800	1.934	1.845	1.896	1.800	1.653	1.984
18743	2.054	1.961	1.872	1.559	1.481	1.469	1.559	1.480	1.468	2.755	2.604	2.459	1.509	1.378	1.554
19191	1.776	1.770	1.767	1.548	1.622	1.690	1.545	1.616	1.684	2.061	2.109	2.322	1.437	1.326	1.410
19935	1.558	1.506	1.457	1.392	1.328	1.327	1.391	1.327	1.326	1.826	1.707	1.483	1.244	1.190	1.280
19961	1.591	1.570	1.552	1.420	1.395	1.364	1.419	1.394	1.363	1.670	1.537	1.487	1.317	1.249	1.456
19970	2.140	2.040	2.015	1.817	1.781	1.737	1.817	1.780	1.736	3.077	2.978	3.020	1.750	1.681	1.757
19982	1.780	1.653	1.585	1.258	1.230	1.219	1.258	1.230	1.218	1.556	1.397	1.279	1.228	1.180	1.195
19994	1.743	1.617	1.550	1.605	1.506	1.450	1.605	1.505	1.449	1.731	1.572	1.474	1.451	1.351	1.418
Average	**1.832**	**1.758**	**1.714**	**1.558**	**1.516**	**1.508**	**1.557**	**1.514**	**1.506**	**2.076**	**1.969**	**1.928**	**1.467**	**1.376**	**1.507**

The accuracy rate values ranged from less than 1% to up to 15% (Table 6). The accuracy rate is highest for the MLR method with averages of around 6%, 7% and 8.2% when using three, five and eight neighbouring stations, respectively, and collectively being 21% of the time closest estimate to observed value in all the stations. Furthermore, for station no. 19191, the collective accuracy rate for MLR exceeds 33%, which shows that the method is best in estimating daily minimum temperatures in the region.

The normal ratio method is the second highest accurate method. The correlation coefficient and UK_CC_C methods have the lowest accuracy rate. It has to be noted that, even though the frequency of these methods has been the closest to daily, the observed is lower than the rest of the methods; the RMSE and MAE of some of these methods had been lower than the most methods. It is recommended that RMSE and MAE be used as the main measure of accuracy and these methods can be complemented by accuracy rate approach.

Table 6: Accuracy rate for each method for all target stations

Station no.	AA_D			AA_C			IDW			Correlation coefficient			UK_AA_D		
	3	*5*	*8*	*3*	*5*	*8*	*3*	*5*	*8*	*3*	*5*	*8*	*3*	*5*	*8*
17958	5.219	2.849	5.413	4.604	1.972	4.513	8.376	2.906	2.678	2.177	1.504	1.994	3.259	2.313	3.362
18743	2.415	3.084	3.277	1.043	1.531	1.191	2.234	2.200	2.427	0.941	1.055	0.930	3.969	3.390	4.354
19191	2.271	2.376	2.853	2.399	2.085	1.863	5.590	0.850	1.304	1.770	1.735	1.724	3.761	3.191	4.414
19935	2.494	2.799	3.250	3.908	3.731	3.054	2.975	1.591	1.728	1.895	2.425	2.249	4.271	4.183	3.888
19961	4.051	3.710	5.572	2.416	2.075	4.208	4.364	1.421	2.303	1.791	1.379	1.791	4.648	4.051	4.705
19970	1.826	1.890	2.387	1.188	0.767	0.864	3.068	1.145	1.545	1.091	0.637	0.519	4.148	4.634	5.639
19982	4.464	3.189	3.826	4.820	4.268	5.016	3.814	1.962	2.624	2.845	2.404	2.637	3.974	3.140	3.642
19994	3.590	3.029	4.857	3.082	2.082	2.722	3.042	1.708	2.896	2.095	1.655	1.468	3.443	3.029	3.990
Average	**3.291**	**2.866**	**3.930**	**2.933**	**2.314**	**2.929**	**4.183**	**1.723**	**2.188**	**1.826**	**1.599**	**1.664**	**3.934**	**3.491**	**4.249**
	UK_ID_D			**UK_AA_C**			**UK_CC_C**			**Normal ratio**			**MR**		
	3	*5*	*8*	*3*	*5*	*8*	*3*	*5*	*8*	*3*	*5*	*8*	*3*	*5*	*8*
17958	4.114	1.812	2.177	2.416	1.048	2.895	1.687	1.368	1.504	3.430	2.838	4.946	4.604	5.174	6.849
18743	3.946	2.835	2.608	3.935	3.300	4.116	4.343	2.801	2.517	4.195	3.651	4.490	6.872	6.645	9.706
19191	3.203	0.862	1.840	2.189	2.620	2.515	1.922	1.514	1.397	2.946	3.191	4.542	6.836	15.081	11.156
19935	4.144	2.514	2.622	3.162	3.083	3.751	2.818	2.190	2.052	3.388	4.134	3.869	6.353	5.577	5.901
19961	4.065	1.052	1.805	2.388	2.331	3.085	1.891	1.606	1.734	4.165	3.454	4.662	5.487	5.913	7.875
19970	5.228	2.366	2.593	3.630	3.500	4.613	3.468	2.312	2.593	3.803	3.867	4.094	7.832	7.918	10.835
19982	3.753	2.073	2.490	2.416	3.213	4.207	2.441	2.109	2.526	4.182	2.674	3.078	4.231	3.434	4.550
19994	2.816	2.028	2.322	3.136	1.882	2.989	2.455	1.748	1.681	5.404	3.870	5.004	7.099	6.325	8.554
Average	**3.909**	**1.943**	**2.307**	**2.909**	**2.622**	**3.521**	**2.628**	**1.956**	**2.001**	**3.939**	**3.460**	**4.336**	**6.164**	**7.008**	**8.178**

2.4.2 Maximum temperature

The MAE when comparing observed daily maximum temperature with estimated maximum temperatures ranged from 0.55°C to over 2.8°C for all patching methods (Table 7). Conversely, the average MAE for all the patching methods and using three, five or eight neighbouring stations resulted in an average MAE of less than 1.5°C. The MLR method yielded a relatively low average MAE for all the stations used with the lowest of 0.74°C when estimating daily maximum temperature with five neighbouring stations.

The other best methods of estimating daily maximum temperatures were UK_CC_C and UK_AA_C. The UK_AA_D and UK_ID_D methods also produced estimates close to observed for all stations with an average MAE of less than 1°C for all the validation stations. The arithmetic averaging method was the worst among all the tested approaches with both AA_D (closest station) and AA_C (highly correlated) resulting in an average MAE across all the stations exceeding 1.2°C. The lowest average MAE was mostly attained when using five neighbouring stations to estimate the daily maximum temperature at the target stations followed by the use of three nearby stations.

Table 7: MAE for each method for all target stations

Station no.	**AA_D**			**AA_C**			**IDW**			**Correlation coefficient**			**UK_AA_D**		
	3	*5*	*8*	*3*	*5*	*8*	*3*	*5*	*8*	*3*	*5*	*8*	*3*	*5*	*8*
17958	1.094	0.991	1.119	1.167	1.138	1.178	1.083	0.977	0.964	1.167	1.136	1.167	0.996	0.923	1.018
18743	1.539	1.360	1.400	1.158	1.046	1.112	1.619	1.453	1.442	1.157	1.045	1.110	1.158	1.089	1.038
19191	1.928	2.162	2.789	1.235	1.540	1.730	0.754	0.825	0.877	1.223	1.526	1.716	0.949	0.997	1.084
19935	1.470	1.404	1.172	1.062	0.966	0.991	1.371	1.347	1.271	1.061	0.964	0.989	0.928	0.864	0.820
19961	0.908	1.051	1.278	0.904	1.073	1.364	0.832	0.826	0.821	0.904	1.069	1.353	0.889	0.879	0.906
19970	1.790	2.023	2.009	2.306	2.677	2.767	1.638	1.739	1.734	2.302	2.672	2.763	1.300	1.225	1.148
19982	1.043	0.953	0.902	0.835	0.931	0.930	1.166	1.042	0.974	0.835	0.929	0.928	0.836	0.769	0.734
19994	1.366	1.434	1.331	1.642	1.439	1.393	1.347	1.385	1.316	1.643	1.441	1.389	0.943	0.882	0.883
Average	**1.392**	**1.422**	**1.500**	**1.289**	**1.351**	**1.433**	**1.226**	**1.199**	**1.175**	**1.286**	**1.348**	**1.427**	**1.000**	**0.953**	**0.954**
	UK_ID_D			**UK_AA_C**			**UK_CC_C**			**Normal ratio**			**MR**		
	3	*5*	*8*	*3*	*5*	*8*	*3*	*5*	*8*	*3*	*5*	*8*	*3*	*5*	*8*
17958	0.984	0.924	0.907	0.840	0.866	0.980	0.838	0.862	0.967	1.035	0.947	1.052	0.770	0.730	0.752
18743	1.177	1.110	1.058	1.075	1.001	0.994	1.075	1.001	0.994	1.223	1.139	1.079	1.069	0.945	1.044
19191	0.630	0.622	0.613	0.781	0.878	0.899	0.775	0.872	0.894	1.064	1.134	1.261	0.573	0.547	0.555
19935	0.869	0.832	0.807	0.790	0.780	0.805	0.789	0.779	0.803	0.956	0.899	0.854	0.720	0.712	0.725
19961	0.838	0.831	0.825	0.894	0.874	0.928	0.894	0.873	0.926	0.877	0.893	0.943	0.727	0.626	0.636
19970	1.301	1.255	1.194	1.105	1.087	1.062	1.104	1.086	1.061	1.299	1.234	1.160	0.936	0.877	0.928
19982	0.888	0.837	0.806	0.782	0.750	0.743	0.781	0.750	0.742	0.821	0.764	0.735	0.749	0.693	0.731
19994	0.939	0.877	0.855	0.914	0.868	0.875	0.913	0.868	0.871	0.951	0.895	0.885	0.867	0.810	0.848
Average	**0.953**	**0.911**	**0.883**	**0.898**	**0.888**	**0.911**	**0.896**	**0.886**	**0.907**	**1.028**	**0.988**	**0.996**	**0.801**	**0.743**	**0.777**

As shown in Table 8, the RMSE results of the daily estimated maximum versus observed maximum temperatures also revealed MLR as the best performing method with values around 1.2°C for all the three approaches (three, five or eight neighbouring stations). The other methods that resulted in low RMSE are UK_CC_C and UK_AA_C. AA_D, IDW and AA_C were the worst performing methods for estimating daily maximum temperatures. In most cases, the average RMSE was the lowest when using five and eight neighbouring stations.

Table 8: RMSE for each method for all target stations

Station no.	AA_D			AA_C			IDW			Correlation coefficient			UK_AA_D		
	3	*5*	*8*	*3*	*5*	*8*	*3*	*5*	*8*	*3*	*5*	*8*	*3*	*5*	*8*
17958	1.579	1.395	1.657	1.526	1.500	1.586	1.628	1.460	1.432	1.526	1.496	1.568	1.505	1.358	1.575
18743	2.664	2.091	1.942	1.574	1.422	1.483	3.310	2.687	2.390	1.572	1.422	1.480	2.386	1.855	1.592
19191	2.361	2.625	3.196	1.605	1.953	2.150	1.447	1.577	1.657	1.591	1.936	2.133	1.438	1.440	1.516
19935	2.012	1.806	1.546	1.435	1.337	1.362	2.416	2.299	2.192	1.434	1.335	1.359	1.516	1.333	1.246
19961	1.364	1.461	1.679	1.292	1.463	1.741	1.368	1.355	1.348	1.292	1.458	1.728	1.307	1.238	1.261
19970	2.214	2.621	2.456	2.725	3.032	3.077	2.113	2.196	2.169	2.721	3.027	3.073	1.764	1.963	1.690
19982	1.625	1.454	1.361	1.364	1.389	1.387	1.779	1.634	1.540	1.364	1.387	1.385	1.450	1.324	1.250
19994	1.765	1.810	1.704	2.034	1.810	1.763	1.757	1.771	1.691	2.035	1.812	1.757	1.362	1.264	1.264
Average	**1.948**	**1.908**	**1.943**	**1.694**	**1.738**	**1.819**	**1.977**	**1.872**	**1.802**	**1.692**	**1.734**	**1.810**	**1.591**	**1.472**	**1.424**
	UK_ID_D			**UK_AA_C**			**UK_CC_C**			**Normal ratio**			**MR**		
	3	*5*	*8*	*3*	*5*	*8*	*3*	*5*	*8*	*3*	*5*	*8*	*3*	*5*	*8*
17958	1.548	1.437	1.406	1.233	1.248	1.392	1.231	1.243	1.374	1.556	1.388	1.604	1.153	1.094	1.109
18743	3.046	2.450	2.094	1.473	1.374	1.371	1.472	1.374	1.370	2.437	1.900	1.633	1.457	1.319	1.426
19191	1.192	1.149	1.118	1.140	1.258	1.288	1.132	1.250	1.280	1.568	1.600	1.728	0.950	0.924	0.929
19935	2.066	1.975	1.905	1.181	1.173	1.187	1.180	1.171	1.184	1.545	1.361	1.268	1.122	1.110	1.108
19961	1.380	1.363	1.351	1.266	1.231	1.269	1.266	1.229	1.267	1.316	1.255	1.297	1.102	0.976	0.969
19970	1.782	1.731	1.653	1.510	1.475	1.445	1.508	1.474	1.445	1.761	1.914	1.672	1.334	1.256	1.307
19982	1.570	1.477	1.420	1.322	1.261	1.250	1.322	1.261	1.249	1.446	1.326	1.253	1.294	1.212	1.245
19994	1.367	1.268	1.234	1.319	1.249	1.255	1.318	1.248	1.250	1.372	1.279	1.270	1.276	1.198	1.233
Average	**1.744**	**1.606**	**1.523**	**1.305**	**1.284**	**1.307**	**1.304**	**1.281**	**1.302**	**1.625**	**1.503**	**1.465**	**1.211**	**1.136**	**1.166**

Correlation between estimated daily maximum temperatures and observed maximum temperatures was high for the MLR, UK_CC_C and the UK_AA_C methods with values around 0.97, 0.96 and 0.96 respectively (Table 9). Relatively weak association was obtained when using the IDW and UK_ID_D methods with values of 0.93 and 0.94 respectively. Using eight neighbouring stations tended to yield relatively higher correlation coefficients followed by five stations.

Table 9: Correlation coefficient for each method for all target stations

Station no.	AA_D			AA_C			IDW			Correlation coefficient			UK_AA_D		
	3	*5*	*8*	*3*	*5*	*8*	*3*	*5*	*8*	*3*	*5*	*8*	*3*	*5*	*8*
17958	0.940	0.955	0.938	0.962	0.962	0.952	0.938	0.950	0.953	0.962	0.962	0.954	0.945	0.956	0.940
18743	0.882	0.924	0.939	0.948	0.959	0.956	0.827	0.877	0.904	0.948	0.959	0.957	0.893	0.930	0.947
19191	0.951	0.944	0.942	0.968	0.957	0.955	0.960	0.954	0.950	0.968	0.958	0.956	0.959	0.959	0.954
19935	0.935	0.949	0.959	0.961	0.964	0.963	0.897	0.908	0.915	0.961	0.964	0.963	0.946	0.958	0.963
19961	0.955	0.956	0.952	0.959	0.952	0.946	0.955	0.956	0.957	0.959	0.953	0.947	0.957	0.962	0.960
19970	0.919	0.905	0.924	0.935	0.941	0.946	0.920	0.924	0.929	0.935	0.941	0.946	0.927	0.912	0.932
19982	0.948	0.961	0.961	0.961	0.965	0.965	0.935	0.945	0.951	0.961	0.965	0.965	0.956	0.963	0.968
19994	0.944	0.953	0.955	0.950	0.956	0.957	0.944	0.952	0.956	0.950	0.956	0.957	0.952	0.958	0.958
Average	**0.934**	**0.943**	**0.946**	**0.955**	**0.957**	**0.955**	**0.922**	**0.933**	**0.939**	**0.956**	**0.957**	**0.956**	**0.942**	**0.950**	**0.953**
	UK_ID_D			**UK_AA_C**			**UK_CC_C**			**Normal ratio**			**MR**		
	3	*5*	*8*	*3*	*5*	*8*	*3*	*5*	*8*	*3*	*5*	*8*	*3*	*5*	*8*
17958	0.943	0.950	0.952	0.964	0.963	0.953	0.964	0.963	0.955	0.942	0.954	0.938	0.968	0.971	0.971
18743	0.840	0.886	0.912	0.955	0.961	0.961	0.955	0.961	0.961	0.889	0.928	0.946	0.956	0.964	0.958
19191	0.971	0.973	0.974	0.973	0.968	0.966	0.974	0.968	0.966	0.952	0.951	0.944	0.981	0.982	0.982
19935	0.906	0.913	0.918	0.967	0.967	0.967	0.967	0.968	0.967	0.947	0.958	0.963	0.970	0.971	0.971
19961	0.953	0.954	0.955	0.961	0.963	0.960	0.961	0.963	0.961	0.957	0.962	0.960	0.970	0.976	0.977
19970	0.926	0.929	0.935	0.944	0.946	0.948	0.944	0.946	0.948	0.920	0.906	0.927	0.954	0.959	0.956
19982	0.948	0.954	0.958	0.963	0.967	0.968	0.963	0.967	0.968	0.956	0.963	0.967	0.965	0.969	0.968
19994	0.952	0.958	0.960	0.955	0.959	0.959	0.955	0.959	0.959	0.951	0.958	0.958	0.957	0.962	0.960
Average	**0.930**	**0.940**	**0.946**	**0.960**	**0.962**	**0.960**	**0.960**	**0.962**	**0.961**	**0.939**	**0.947**	**0.950**	**0.965**	**0.970**	**0.968**

The MLR method has the highest accuracy rate with 20% (Table 10). This indicates that the MLR estimates were the closest to the observed values compared with all the methods. The maximum combined accuracy rate of 28% was obtained in Macuville (station no. 19191) in northern Limpopo. The second and third methods with the highest accuracy rate were normal ratio and UK_CC_C with 12.5% and 10.7% respectively. The correlation coefficient and the UK_CC_C methods had the lowest combined average accuracy rate of 5% and 6.2% respectively. It can be noted that using three neighbouring stations had more hits than using five and eight stations with combined accuracy rates across the methods of 37.2%, 29.6% and 33.2% respectively.

Table 10: Accuracy rate for each method for all target stations estimating maximum temperature

Station no.	AA_D			AA_C			IDW			Correlation coefficient			UK_AA_D		
	3	*5*	*8*	*3*	*5*	*8*	*3*	*5*	*8*	*3*	*5*	*8*	*3*	*5*	*8*
17958	3.903	3.435	2.591	2.751	2.785	2.614	5.193	2.956	2.751	2.568	2.146	2.283	2.967	3.127	2.910
18743	3.228	3.559	6.400	5.419	3.833	7.529	3.491	2.624	2.852	1.894	1.745	2.567	3.034	2.932	3.491
19191	1.910	1.712	1.479	2.073	1.153	1.223	7.417	0.803	2.271	1.851	1.164	1.036	3.819	2.993	3.144
19935	2.828	2.799	3.083	2.848	2.249	2.524	3.339	2.042	2.425	1.610	1.875	1.650	3.987	3.731	4.684
19961	5.955	4.107	5.131	2.260	2.061	2.572	4.505	2.359	2.786	1.052	1.251	1.507	4.704	3.539	3.084
19970	2.710	2.440	2.505	1.835	1.080	1.274	2.753	2.116	2.289	1.436	0.864	0.659	3.477	3.822	4.189
19982	4.691	4.765	5.738	3.127	3.435	4.371	4.420	2.302	2.696	1.477	2.487	2.241	3.792	3.041	3.743
19994	3.757	2.496	3.532	2.071	1.660	1.965	3.691	1.620	2.390	1.938	1.155	1.726	3.133	3.253	4.660
Average	**3.623**	**3.164**	**3.807**	**2.798**	**2.282**	**3.009**	**4.351**	**2.103**	**2.557**	**1.728**	**1.586**	**1.708**	**3.614**	**3.305**	**3.738**
	UK_ID_D			**UK_AA_C**			**UK_CC_C**			**Normal ratio**			**MR**		
	3	*5*	*8*	*3*	*5*	*8*	*3*	*5*	*8*	*3*	*5*	*8*	*3*	*5*	*8*
17958	5.581	2.522	2.602	3.184	2.340	2.362	3.059	2.123	1.883	4.348	4.063	4.211	5.798	4.976	5.969
18743	3.183	2.122	2.304	1.814	1.905	2.761	1.529	1.186	1.859	3.194	2.795	3.331	4.529	5.829	7.061
19191	7.382	1.351	3.237	3.843	2.771	3.307	3.214	2.108	1.735	3.354	2.538	2.946	9.234	12.145	6.789
19935	5.725	2.671	3.123	2.681	2.514	2.504	2.366	2.072	1.915	4.792	3.820	4.262	5.116	7.669	7.099
19961	5.259	1.478	2.430	1.720	1.691	2.658	1.976	1.450	1.450	4.377	3.695	4.704	6.410	6.694	7.135
19970	4.016	2.213	2.613	3.498	2.926	3.390	3.055	2.289	1.749	5.798	4.815	4.610	8.864	9.274	7.439
19982	4.075	2.253	2.204	1.884	2.327	2.807	1.835	1.650	1.859	5.147	3.607	3.866	4.309	4.432	5.417
19994	4.288	2.443	2.961	3.452	2.390	3.478	3.425	2.071	1.899	5.550	4.381	6.121	5.868	5.470	7.156
Average	**4.939**	**2.132**	**2.684**	**2.759**	**2.358**	**2.908**	**2.557**	**1.869**	**1.794**	**4.570**	**3.714**	**4.256**	**6.266**	**7.061**	**6.758**

2.5 Conclusions

A major obstacle facing research is the absence of a complete and continuous data record: the data is either incomplete or not reliable. This becomes a limitation since observed climatic data records are not readily available or are insufficient for conducting a good study. Due to limited historical data (less than 30 years), a researcher has limited knowledge to conduct a study and to further determine the magnitude of risk involved in the event of any future changes. This chapter highlighted the importance of installing automatic weather stations across the different study areas as most studies require observed long-term daily climatic data such as daily rainfall, maximum and minimum air temperature, relative humidity, solar radiation and wind speed. The chapter highlighted the importance of data patching and introduced the different patching methods.

Different techniques for estimating missing daily temperature values were investigated. The MLR method performed the best. The MLR method calculated using five neighbouring stations had slightly smaller errors than using three and eight neighbouring stations. The second best method was the UK method, which produced lower deviations when using best correlated neighbouring stations than when using closest neighbouring stations. Generally, a comparison of UK_AA_C and UK_CC_C showed better estimates than UK_CC_C. The normal ratio method was another method that yielded smaller errors. The IDW method estimated temperature better than other techniques. The arithmetic averaging and correlation coefficient methods were the worst for estimating temperature using a neighbouring station. On average, MLR estimates were approximately twofold closer to measured values than estimates calculated using normal ratio, UK_AA_D, AA_D, UK_ID_D, IDW, UK_AA_C, and AA_C; approximately threefold closer than estimates calculated using UK_CC_C; and approximately fourfold closer than estimates calculated using correlation coefficient.

3 RAINY SEASON CHARACTERISTICS

3.1 Introduction

Most socio-economic activities in South Africa, especially agriculture, depend on climate and specifically rainfall (FAO, 2004). Rainfall variability and patterns of extremely high or low rainfall are very important for agriculture as well as the economy of those depending on rain-fed agriculture (Igwenagu, 2015). There were significant decreasing trends of annual precipitation in the northern parts of Limpopo, southern Mpumalanga, north-eastern Free State and western KwaZulu-Natal for the period 1910-2004 (Kruger, 2006). There have also been changes in monthly rainfall over the past years (Hewitson et al., 2005). Across the globe, rain-fed agriculture is practised in 80% of agricultural areas. In sub-Saharan Africa, 93% of cultivated land is rain-fed. Therefore, rain-fed agriculture plays a significant role in food security (Maponya, 2010; Chikodzi et al., 2012). It has been projected that by 2020, between 75 and 250 million people in Africa will be exposed to increased water scarcity and production from rain-fed agriculture could decrease by 50% (IPCC, 2007a).

Regardless of the increase in fertiliser use and improvement in planting technologies, the climate within the growing period still plays a significant role in agricultural production (Ayoade, 2004). Other factors that affect crop production include soil and farm management practices (Munodowafa, 2011). However, fertiliser application is critically dependent on rainfall, making it the most important factor affecting crop production as water availability is essential in sustaining crop productivity in rain-fed agriculture (Munodowafa, 2011). Even if drought-tolerant cultivars are planted, water will not be available to crops when there is no water in the soil as variations in rainfall from season to season affect soil water availability to crops, which then poses crop production risks (Harvest Choice, 2010). Irrigation is said to be an important approach to deal with the current climatic conditions in semi-arid areas as rain-fed agriculture is still dominant in most developing countries (Tilahun, 2006).

A rainy season is defined as that period when a significant amount of rainfall occurs; this can vary from place to place (Smith et al., 2008). Rainy season characteristics of importance to agriculture are onset, cessation and length of the growing season, rainfall amount and the probability of dry spell occurrence during the growing season (Hassan & Stern, 1988). Information regarding the onset of the rainy season assists farmers to prepare land, seeds, manpower and equipment (Omotosho et al., 2000). A delayed onset of the rainy season, especially in semi-arid regions of southern Africa, extends the growing period of summer crops into winter (Mubvuma, 2013). However, planting after a false early onset may result in crop failure, which leads to expensive replanting (Ayoade, 2004).

Similarly, if cessation occurs early, the crops might experience low cob development, which results in poor harvest (Stern & Coe, 1984). Information on the cessation of the rainy season also helps in assessing the possible length of the rain-fed cropping season and provides information on optimal harvesting and storage of crops (Hachigonta et al., 2008). Heavy rainfall at the end of the rainy season can cause crops to spoil or prevent ripening and harvesting (Stern & Coe, 1984). The yield may be significantly affected by a late onset or early cessation of the season as well as damaging dry spells during the season (Ati et al., 2002; Mugulavai et al., 2008).

Farmers' main concerns are for rainfall to be consistent throughout the season so there is guaranteed sufficient soil water at planting and that those conditions are maintained throughout the season (Walter, 1967). If farmers are given information on the seasonal distribution of rainfall, they can choose to plant either more drought-tolerant crops or longer maturing varieties (Tadross et al., 2003).

3.2 Data

Daily historical rainfall data of 25 years or more were obtained from the ARC-Institute for Soil, Climate and Water (ARC-ISCW) and the South African Weather Service (SAWS) for 12 stations (Table 11). The IDW method (Chen & Lui, 2012) was used to patch missing data using neighbouring stations within a radius of 50 km.

Table 11: Geographic information of meteorological stations used in the study

Station	Latitude (°)	Longitude (°)	Elevation (m)	Data period
Elim	−23.17	30.05	808	1945-2004
Entabeni	−23.00	30.27	1376	1923-2012
Folovhodwe	−22.53	30.48	610	1954-2004
Levubu	−23.04	30.15	877	1986-2015
Lwamondo	−23.04	30.37	650	1978-2015
Mampakuil	−23.17	29.00	945	1945-2004
Pafuri	−22.42	31.22	201	1970-2004
Punda Maria	−22.68	31.02	462	1945-2004
Sigonde	−22.40	30.71	416	1983-2015
Thathe	−22.88	30.32	1250	1963-2004
Tshiombo	−22.80	30.48	650	1983-2009
Vreemedeling	−22.96	30.01	1421	1945-2004

3.3 Determination of the Rainy Season Characteristics

3.3.1 Dry and rainy days

Meteorologically, a rainy day is defined as any one day with a total cumulative rainfall of at least 0.85 mm (Mupangwa et al., 2011). However, definitions of the rainy season characteristics in relation to any application are region specific (Ambrosino et al., 2014). A study by Woltering (2005) showed that the Mzinyathini catchment in neighbouring Zimbabwe experienced a pan evaporation rate of 4-8 mm per day. Hence, rainfall of 0.85 mm might not have a significant influence on the crop growth in the Luvuvhu River catchment. Different authors use different thresholds for dry and rainy days, e.g. Tadross et al. (2007) use a threshold of 2 mm, Mupangwa et al. (2011) use 5 mm and Reason et al. (2005) use 1 mm. This study adopted a threshold of 5 mm. Therefore, the definitions are:

- Rainy day: any day with a total rainfall of 5 mm or more.
- Dry day: any day with a total rainfall of less than 5 mm.

3.3.2 Onset, cessation and the length of the rainy season

Onset, cessation, and length of the rainy season are regarded as the most important indices affecting maize production (Tadross et al., 2007). These indices should influence the choice of cultivars. The study defined onset as the first day after 1 October when at least 25 mm rainfall has accumulated in 10 days (Tadross et al., 2007).

Ambrosino et al. (2014) argued that the criteria for avoiding false onset such as those used by Reason et al. (2005), Moeletsi & Walker (2011), Mupangwa et al. (2011), Tongwane & Moeletsi (2014) and Masupha et al. (2016) are useful for retrospective analysis only. The criteria are of no use to farmers as they plant after the first significant rainfall irrespective of what might occur in the following days. Not all farmers plant after the first rainfall for a number of reasons such as the unavailability of tractors, manpower and inputs (Masupha et al., 2016), as well as oversaturated soil, which makes it difficult for tractors to plough.

Therefore, three onset dates were generated for each station. The second onset was calculated 7 days after the first onset, while the third onset was calculated 7 days after the second onset. Cessation was defined as three consecutive dekads (10-day periods) of less than 20 mm each occurring after 1 February (Tadross et al., 2007). The length of the rainy season was calculated by subtracting the first onset date from the cessation date.

3.3.3 False onset

In order to calculate the risk of the first onset date being a false onset, a further criterion was introduced to account for a false onset. Thus, the second definition of onset was defined as the first day after which 25 mm or more, and 20 mm of rainfall accumulate in the first and second dekads respectively. The rainfall in the second dekad guarantees that the maize has enough soil water to sustain crop growth in the first 30 days (Moeletsi & Walker, 2011). Results obtained using the two definitions were then compared.

The study assumed that planting would have failed in that year if the amount of rainfall was less than 20 mm in the following two dekads after planting. For example, if the results generated by the two definitions were different, then planting would have failed in that particular year. The percentage of failure was determined for all stations within the catchment.

3.3.4 Monthly rainfall

Rainfall data analysis depends on its distribution pattern (Sharma & Singh, 2010). The most commonly used probability distributions include normal, log-normal, gamma, Weibull and Gumbell. Probability distributions are widely used to understand the rainfall pattern and calculate probabilities as it is thought that rainfall events follow a particular type of distribution (Abdullah & Al-Mazroui, 1998).

A goodness-of-fit test based on the Anderson–Darling at a 0.05 significance level was used to determine the best probabilistic distribution model that fit the monthly rainfall data. The Anderson–Darling statistic (A^2) is given by (Stephens, 1974):

$$A^2 = -n\frac{1}{n}\sum_{i=1}^{n}(2i-1).\left[lnF(X_i) + ln\left(1 - F(X_{n-i+1})\right)\right] \quad (9)$$

Where

n is the sample size,

F is cumulative distribution function of probability distribution, and

X_i is the ordered observations.

The Anderson–Darling statistic measures how well the data follows a particular distribution. The corresponding p-value was used to test whether the data comes from a chosen distribution. If the p-value is less than 0.05, the null hypothesis that the data comes from that distribution is rejected (Mzezewa et al., 2010). The p-value with the greatest magnitude was considered to be the best fit. Monthly rainfall data was fitted into four probability distributions, namely, normal, log-normal, Weibull and generalised extreme value (Table 12).

Table 12: Probability distribution models used in the study

Distributions	Probability density function	Parameter description
Normal	$F(x) = n(x;\mu,\sigma) = \frac{1}{\sigma\sqrt{2\pi}}\exp\left[-0.5\left(\frac{x-\mu}{\sigma}\right)^2\right]$ $-\infty \le x \le \infty$	μ = mean of population σ = standard deviation of the population x
Log-normal	$Y = \frac{1}{\sigma_y\sqrt{2\pi}}\exp\left[0.5\left(\frac{y-\mu}{\sigma}\right)^2\right]$ $0 \le x \le \infty$	$Y = lnx$ σ_y = is the standard deviation of lnx μ = is the mean of lnx

Distributions	Probability density function	Parameter description
Weibull	$F(\mathrm{x}) = \frac{\propto}{\beta}\left(\frac{x}{\beta}\right)^{\alpha-1} \exp\left(-\left[\frac{x}{\beta}\right]^{\alpha}\right)$ for $0 \leq x \leq \infty$	α = is the scale parameter β = is the shape parameter of the distribution
Generalised extreme value	$\mathrm{F}(x; \mu, \sigma, \varepsilon) = \exp\left\{-\left[1 + \varepsilon\left(\frac{x-\mu}{\sigma}\right)^{\frac{-1}{\varepsilon}}\right]\right\}$	ε=extreme value shape parameter μ = Location parameter σ = Scale parameter

3.3.5 Aridity index

The agroclimatic zonation for the catchment was calculated using the United Nations Environment Programme (UNEP) (1992) aridity index (*AI*) equation represented by:

$$AI = \frac{P}{ET_o} \quad (10)$$

Where

P is the mean annual rainfall, and

ET_o is the mean annual potential evapotranspiration.

According to the UNEP classification, $AI < 0.05$ represents a hyper-arid zone, 0.05-0.20 represents an arid zone, 0.20-0.50 represents a semi-arid zone, 0.50-0.65 is a sub-humid zone and greater than 0.65 represents a humid zone.

The mean annual rainfall was calculated from daily rainfall data. Daily ET_o was calculated using the Hargreaves and Samani (1982) equation given by:

$$ET_o = 0.0135\,(KT)(R_a)(TD)^{0.5}(TC + 17.8) \quad (11)$$

Where

$TD = T_{max} - T_{min}$ (°C) is the decimal air temperature range,

TC is the average daily temperature (°C),

R_a is the extra-terrestrial radiation (mm/day), and

KT is an empirical coefficient.

Hargreaves (1994) recommended using $KT = 0.162$ for interior regions and $KT = 0.19$ for coastal regions. Although the Hargreaves and Samani (1982) method may overestimate ET_o (Sheffield et al., 2012), the equation has been used successfully in some locations for estimating ET_o where sufficient data was not available to use other methods (Orang et al., 1995).

3.4 Data Analysis

3.4.1 Statistical analysis

Instat+ V 3.36 was used to analyse daily rainfall data for onset, cessation and length of the rainy season, false onset, total seasonal rainfall and number of rainy days. Years in which onset of rains occurred after 31 January were regarded as years in which rainfall did not meet the onset criterion and were therefore not included in the analysis. Descriptive statistics such as mean, coefficient of variation (CV), standard deviation (STD), skewness coefficient (C_s) and kurtosis coefficient (C_k) were calculated for monthly rainfall data from October to April using Statistica software.

3.4.2 Probabilities of exceedance and non-exceedance

Probabilities of non-exceedance for onset, length of the season, the number of rainy days, seasonal rainfall and monthly rainfall were calculated using Statistica software. For onset, 20%, 50% and 80% were used to indicate early, normal and late onset and cessation of the rainy season respectively. A 20% probability of non-exceedance was used as an indicator for short season, while 50% and 80% were used to represent a normal season and long season in that order. For seasonal rainfall, the probabilities of non-exceedance were used to represent the dry, normal and rainy seasons. Monthly probabilities of non-exceedance at 80%, 50%, and 20% were determined and represented wet years, normal years and dry years respectively. The return period (T) is the period expressed in a number of years in which the annual observation is expected to return. It is calculated according to the following equation:

$$T = \frac{1}{P} \quad (12)$$

Where

P is the exceedance probability (i.e. the probability that a given monthly rainfall is equalled or exceeded).

3.4.3 Trends

Spearman's rank correlation test was conducted to detect trends in rainy season characteristics over the years. The Spearman rank correlation coefficient is a non-parametric test used to evaluate the relationship between two independent variables (Gauthier, 2001). It is similar to the Pearson Product Moment. The only difference is that the Spearman test operates on the ranks of data rather than raw data (Gauthier, 2001). The Spearman rank was used as it is a non-parametric technique unaffected by the distribution of the data. The Spearman rank correlation was calculated using the following equation:

$$r_s = 1 - \frac{6 \sum d_i^2}{n^3 - n} \quad (13)$$

Where

d_i is the difference between ranks for each x_i, y_i data pair, and

n is the number of data pairs.

The value of r_s can be any value between −1 and 1. When the value of r_s is equal to 1, the data pairs have a perfect positive correlation ($d_i = 0$); when it is −1, there is a perfect negative correlation (Gauthier, 2001). A negative value indicates a decreasing trend and a positive value an increasing trend. For this study, r_s values will be interpreted as follows:

- 0.0-0.2 very weak.
- 0.2-0.4 weak.
- 0.4-0.6 moderate.
- 0.6-0.8 strong.
- 0.8-1.0 very strong.

3.5 Results and Discussion

3.5.1 Onset of the rainy season

Three generated onset dates at 20%, 50% and 80% probability of non-exceedance are shown in Table 13. The first significant rainfall for the rainy season was observed to occur early in the first week of October at Entabeni, Levubu and Lwamondo, and later in the second week of December at Sigonde, Folovhodwe, Pafuri and Elim. At a 20% probability of non-exceedance, onset can be expected from the first week of October to the third week of November depending on the location within the catchment. At a 50% probability of non-exceedance, onset can be expected to occur from the second week of October at Entabeni, Thathe and Levubu to the second week of November at Folovhodwe. Late first onset corresponding to an 80% probability of non-exceedance can be expected from the last week of October to the second week of December (Table 13).

Due to unavailability of tractors, shortage of seeds, personal reasons and for variation purposes, farmers might not plant immediately after the first rains of the season, indicating that these farmers will delay a few more days before they plant. Hence, the second onset was calculated. The second rains at 20%, 50% and 80% probability of non-exceedance of the season can be expected from the third week of October to the last week of December depending on the location (Table 13). At a 20% probability of non-exceedance, second onset occurs from the third week of October to the second week of November. At a 50% probability of non-exceedance, second rains for the season can be expected from the last week of October to the first week of December. Late onset can be expected from the second week of November to the last week of December. The third onset of rains for the season can be expected from the last week of October to the third week of January depending on the location. In one out of five years, the third onset can be expected from the last week of October to the first week of December at the catchment. In one out of two years, the third rains for the season can be expected from the second week of November to the last week of December. In four out of five years, the third rains of the season can be expected from the last week of December to the second week of January.

Table 13: Early (20%) probability of non-exceedance, normal (50%) and late (80%) onset dates for 12 meteorological stations in the Luvuvhu River catchment

	First onset				Second onset				Third onset			
Stations	**Early**	**Normal**	**Late**	**STD (days)**	**Early**	**Normal**	**Late**	**STD (days)**	**Early**	**Normal**	**Late**	**STD (days)**
Elim	11/10	19/11	09/12	16	29/10	15/11	01/12	16	13/11	02/12	15/12	12
Entabeni	06/10	13/10	22/10	11	18/10	30/10	12/11	12	03/11	13/11	26/11	11
Folovhodwe	18/11	11/11	09/12	21	08/11	05/12	28/ 12	16	01/12	28/12	18/01	13
Levubu	06/10	13/10	24/10	11	19/10	28/10	14/11	11	31/10	11/11	27/11	10
Lwamondo	06/10	19/10	09/11	18	19/10	11/11	28/11	16	31/10	22/11	12/12	15
Mampakuil	16/10	03/11	21/11	16	06/11	24/11	14/12	14	24/11	10/12	28/12	12
Pafuri	13/10	04/11	08/12	21	12/11	03/12	01/01	18	29/11	25/12	17/01	13
Punda Maria	19/10	03/11	25/11	16	11/11	24/11	18/12	12	28/11	20/12	15/01	14
Sigonde	20/10	14/11	07/12	18	07/11	03/12	08/12	17	28/11	13/12	16/01	13
Thathe	08/10	15/10	30/10	17	20/10	04/11	16/11	14	02/11	15/11	03/01	14
Tshiombo	12/10	24/10	14/11	15	26/10	11/11	25/11	14	13/11	27/11	19/12	11
Vreemedeling	12/10	21/10	09/11	13	03/11	17/11	02/12	13	18/11	03/12	19/12	12

The results from this study show that stations situated in high rainfall areas experience an earlier onset than those situated in the dry low-lying areas of the catchment. This was also demonstrated in a study by Sithole (2010) where an early onset occurred in wet areas, and late onset in dry areas in Zimbabwe, implying that onset of the rainy season is influenced by rainfall distribution, which is influenced by topography. For example, an early onset occurs at Entabeni, which is situated along the Soutpansberg mountain range that receives more than 1735 mm of annual rainfall. Late onset occurs at Sigonde, Pafuri and Folovhodwe, which are situated in the dry low-lying areas of the catchment that receive less than 500 mm of annual rainfall. These results are also consistent with those of Aviad et al. (2004) and Mupangwa et al. (2011), which indicated that onset of the rainy season starts later as aridity increases. Onset dates varied by between three and six weeks depending on the location within the catchment.

It has been demonstrated that planting on the date corresponding to 20% probability of non-exceedance has a high probability of a false onset as there might not be enough rainfall to sustain maize until vegetative stages, which might lead to crop failure (Moeletsi et al*.,* 2013). Farmers are advised not to plant on dates corresponding to 20% probability of non-exceedance.

Raes et al. (2004) stated that planting later in the season on dates corresponding to an 80% probability of non-exceedance reduced the risk of crop failure and shortened the season. But early-maturing varieties are recommended as late planting shortens the season and crops might not reach maturity if late varieties are planted. However, farmers who intend to sell their maize for high profit can plant on this date, provided that they have alternative sources of water such as rainwater harvesting technologies and irrigation systems (Moeletsi & Walker, 2012).

Farmers can obtain high profits before maize is readily available but these will decrease once it is more readily available in the markets (Raes et al., 2004). Onset varied by nearly a month between wet and dry areas of the catchment, demonstrating that farmers in wet areas should plant maize a month earlier than farmers in arid areas of the catchment. A study by Masupha et al. (2016) investigating probabilities of dry spells indicated that when planting is done after the second and third onset, there is a low probability of medium and dry spells in the Luvuvhu River catchment. Farmers are therefore advised to plant following the second onset of rains and use the first onset for planning purposes, and gathering of tools, seeds and manpower.

3.5.2 Trends in onset

The Spearman's rank correlation coefficient test results indicated that there was no significant change in all three onset dates at the Luvuvhu River catchment except for Pafuri. Therefore, the onset of the rainy season has not changed over the years in most areas of the catchment (Table 14). An increasing trend is also notable at Pafuri ($r_s = 0.34$) for the third onset, indicating that for this area, onset of rains has shifted forward by a few days. Therefore, the onset of the rainy season has not changed over the years (Table 14). Although not significant statistically, there is a decreasing trend notable at Sigonde ($r_s = -0.29$) for the second onset. This indicates that the second rains of the season over the years have been occurring earlier than before and therefore lengthening the rainy season.

Table 14: Spearman's rank correlation coefficient test results for first, second and third onsets within the Luvuvhu River catchment

Stations	First onset			Second onset			Third onset		
Spearman rank	*t*-stat	*p*-value	r_s	*t*-stat	*p*-value	r_s	*t*-stat	*p*-value	r_s
Elim	−0.64	0.52	−0.08	−1.03	0.30	−0.13	0.05	0.95	0.00
Entabeni	0.25	0.79	0.02	1.07	0.28	0.11	0.75	0.45	0.08
Folovhodwe	−1.40	1.60	−0.18	−0.69	0.49	−0.10	0.40	0.68	0.07
Levubu	1.12	0.26	0.19	0.95	0.34	0.16	−0.08	0.93	−0.01
Lwamondo	1.17	0.24	0.19	1.22	0.22	0.20	1.09	0.28	0.18
Mampakuil	−0.13	0.89	0.01	0.55	0.57	0.07	1.17	0.24	0.16
Pafuri	−0.20	0.84	−0.03	0.96	0.34	0.18	1.77	0.08	0.34*
Punda Maria	−1.70	0.08	−0.23	0.05	0.95	0.00	0.56	0.57	0.08
Sigonde	−0.88	0.38	−0.16	−1.08	0.28	−0.29	−0.05	0.95	−0.01
Thathe	1.13	0.26	0.18	0.23	0.81	0.03	0.93	0.35	0.15
Tshiombo	0.59	0.55	0.11	1.00	0.32	0.19	0.30	0.76	0.06
Vreemedeling	−0.59	0.55	−0.07	−0.18	0.85	−0.02	−0.12	0.90	−0.01

*Significant at $P < 0.05$

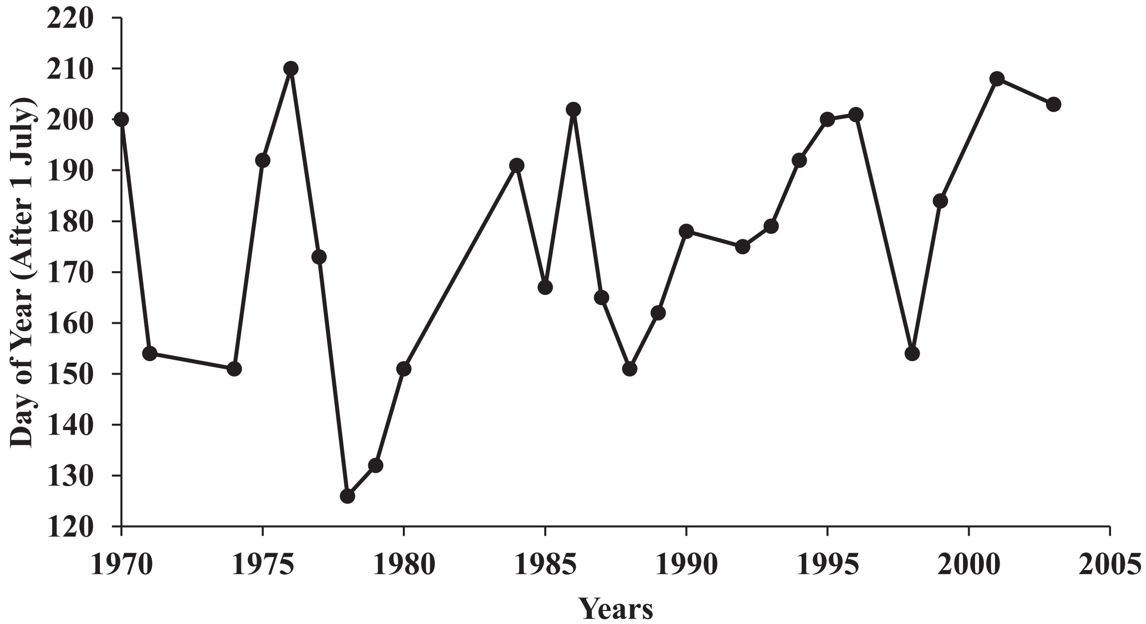

Figure 18: Temporal variation in the third onset dates at Pafuri

3.5.3 False onset

The number of years with false onsets are shown in Table 15. The years with false onsets increase as one moves from stations situated in high rainfall areas to arid areas. Levubu had no risk of false onset occurrence; therefore, maize planted at Levubu is less prone to a shortage of soil water. Pafuri had the highest number of years with false onsets while Entabeni had relatively low chances (4%).

For years analysed, planting failed in four out of 90 years at Entabeni. A farmer can only wait for seven days before planting after the first onset. At Pafuri, planting failed in 18 out of 34 years; therefore, the risk of a false onset is estimated to be 55%. The area has a high risk of crop failure if planting is done after the first onset. For other years in which planting would have failed, farmers had to wait between 33 and 71 days for successful planting. At Sigonde, Lwamondo and Tshiombo, farmers had to wait about 29-64 days before successful planting, which implies high vulnerability at these areas.

During the 1970/71 rainy season, farmers would have waited for seven days before they could have replanted if they had planted after the first onset. If farmers had planted in the years with false onsets, it would have resulted in total crop failure, which would have needed expensive replanting. Therefore, farmers at Pafuri and Sigonde are advised not to plant after the first onset as there is a high risk of crop failure. However, if farmers in these areas want to plant after the first onset, they should explore other options such as rainwater harvesting so that they have supplementary water for the plants during dry spells.

Table 15: Number of years with false onsets at stations within the Luvuvhu River catchment

Stations	No. of years with false onsets	No. of years analysed	Percentage (%)
Entabeni	4	90	4
Levubu	0	34	0
Lwamondo	9	38	23
Tshiombo	7	27	26
Pafuri	18	34	55
Sigonde	10	32	31
Mampakuil	15	59	25
Elim	16	59	27
Thathe	5	40	13
Punda Maria	20	59	34
Folovhodwe	19	59	32
Vreemedeling	20	59	28

3.5.4 Cessation of the rainy season

Calculated early, normal and late cessation dates are presented in Table 16. Cessation of the rainy season can be expected from the first week of February to the first week of May depending on the location at the catchment. At an 80% level of probability of exceedance, cessation can be expected on or after the first week of February at Pafuri, Sigonde, Punda Maria, Folovhodwe and Mampakuil.

Early cessation of rains can subject the maize to a high risk of water stress as maize planted might not reach maturity (Moeletsi & Walker, 2012) – especially if rains end in the first week of February. A 120-day maize crop planted in November will not have reached maturity by the first week of February, indicating that in four out of five years it will not reach maturity if late maturing varieties are planted.

The normal cessation of the rainy season can be expected from after the third week of February at Folovhodwe, Punda Maria, Sigonde, Mampakuil and Pafuri to the second week of April at Entabeni (Table 16). At Levubu, cessation can be expected after the first week of April. Late cessation (20th percentile) is likely to occur after the last week of February at Folovhodwe and the first week of May at Entabeni and Levubu.

The probability of crops experiencing water stress due to early cessation is said to be lower when the season ends on the dates corresponding to a 20% probability of exceedance (Moeletsi & Walker, 2011). Therefore, in one out of five years, crops will have a low probability of experiencing water stress due to early cessation of rains. At an 80%, 50% and 20% probability of exceedance, cessation of the season is delayed by between 20 and 50 days when comparing dry and wet areas of the catchment as wet areas of the catchment receive the last rains of the season later than the dry areas.

Cessation of the rainy season indicates a high variability on a yearly basis when compared with onset. Studies of rainy season characteristics in the Free State showed high variability for the onset as compared with cessation of rain (Moeletsi & Walker, 2012). The standard deviations are the highest at Entabeni (33) followed by Levubu (31), Thathe (29), Lwamondo (28), Tshiombo (28), Elim (27), Vreemedeling (26), Punda Maria (22), Mampakuil (21), Pafuri (20), Folovhodwe (19) and lowest for Sigonde (17) (Table 16). The standard deviations are higher in wet areas than in dry areas of the catchment, indicating that cessation can easily be predicted more accurately in dry areas than in wet areas.

Table 16: Early (80%) probability of exceedance, normal (50%) and late (20%) cessation dates and standard deviations for 12 meteorological stations in the Luvuvhu River catchment

Station	Early	Normal	Late	STD (days)
Entabeni	06/03	08/04	03/05	33
Levubu	26/02	01/04	02/05	31
Lwamondo	11/02	16/03	15/04	28
Tshiombo	07/02	02/02	30/03	28

Station	Early	Normal	Late	STD (days)
Pafuri	01/02	18/02	07/03	20
Sigonde	01/02	21/02	11/03	17
Mampakuil	03/02	24/02	12/03	21
Elim	17/02	06/03	02/04	27
Thathe	28/02	23/03	16/04	29
Punda Maria	01/02	20/02	16/03	22
Folovhodwe	01/02	17/02	28/02	19
Vreemedeling	20/02	11/03	07/04	26

3.5.5 Trends in cessation

The Spearman's rank correlation coefficient test at the 5% and 10% level of significance revealed that there was no significant trend in cessation dates at any stations of the catchment except for Entabeni and Tshiombo (Table 17). At Entabeni, a weak decreasing trend ($r_s = -0.24$) is evident, indicating that the rainy season has been ending earlier by a few days over the years; therefore, decreasing the length of the rainy season (Figure 19). At Tshiombo, an increasing trend ($r_s = 0.36$) is notable, implying that the rainy season has been ending later over the years.

Table 17: Spearman's rank correlation coefficient test results for the cessation of the rainy season for the various stations within the Luvuvhu River catchment

Station	*t*-stat	*p*-value	r_s
Elim	0.45	0.64	0.06
Entabeni	−2.34	0.02	−0.24*
Folovhodwe	0.25	0.79	0.03
Levubu	1.40	0.16	0.24
Lwamondo	0.11	0.91	0.01
Mampakuil	−0.56	0.57	−0.07
Pafuri	−0.44	0.65	−0.07
Punda Maria	0.67	0.50	0.08
Sigonde	0.51	0.60	0.09
Thathe	0.13	0.89	−0.02
Tshiombo	1.95	0.06	0.36**
Vreemedeling	0.87	0.38	0.11

* Significant at 5%; ** Significant at 10%

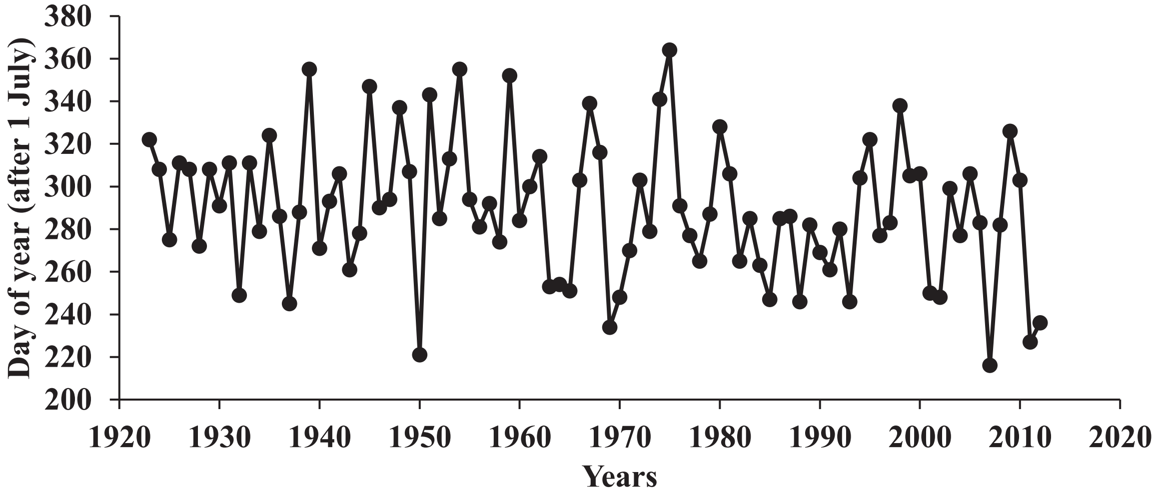

Figure 19: Temporal variation in the cessation of the rainy season at Entabeni

3.5.6 Length of the rainy season

At a 20%, 50% and 80% probability of non-exceedance, the length of the rainy season ranges from 67 days at Folovhodwe to 203 days at Entabeni (Table 18). In one out of five years, the length of the rainy season ranges from 67 days at Folovhodwe to 149 days at Entabeni. Depending on the cultivar, maize generally requires an average rainy season of 120 days from planting until harvesting (Hachigonta et al., 2008). The length of rainy season was less than 120 days for five out of the 12 stations. Medium maturing maize should not be planted during the years of drought (shortened length of rains) as the maize will suffer from a shortage of water due to the early cessation of rains. Therefore, farmers are advised not to plant maize unless they have an alternative source of water to supplement the maize crop until it reaches full maturity.

In normal years (50th percentile), all areas of the catchment will have a rainy season greater than 120 days except for Pafuri, Sigonde, Punda Maria, Folovhodwe and Mampakuil. Wet areas of the catchment experience a longer growing season than dry areas. At Thathe, Levubu and Entabeni, farmers can plant early to late maturating varieties depending on the date of planting. At Folovhodwe, Pafuri, Mampakuil and Sigonde, farmers are advised to only plant early-maturing varieties. At Lwamondo, Tshiombo, Elim and Vreemedeling, farmers should plant both very early, medium and late maturing maize varieties. At Sigonde, Folovhodwe, Pafuri and Punda Maria, the length of the rainy season differs by more than 70 days when comparing these stations to Entabeni, which has a long rainy season. The length of the rainy season at the Luvuvhu River catchment deviates by more than 25 days at all stations, indicating high variability.

Table 18: Short (20% probability of non-exceedance), normal (50%) and long (80%) length of the rainy season and standard deviation

Stations	Short	Normal	Long	STD (days)
Elim	112	135	169	34
Entabeni	149	177	203	35

Stations	Short	Normal	Long	STD (days)
Folovhodwe	67	92	132	38
Levubu	133	163	200	32
Lwamondo	114	146	175	37
Mampakuil	89	113	140	31
Pafuri	72	103	136	38
Punda Maria	82	108	143	26
Sigonde	77	104	125	31
Thathe	127	153	186	38
Tshiombo	102	131	168	34
Vreemedeling	114	139	169	32

3.5.7 Trends in length of the rainy season

The Spearman rank correlation coefficient test at 5% level of significance showed that the relationship between time and duration of the rainy season was not significant at all stations except for Thathe, Entabeni and Punda Maria (Table 19). There is a weak decreasing trend at Thathe and Entabeni, which means that the rainy season has been shortening slowly over the years (Figure 20 and Figure 21). Punda Maria shows a decreasing trend in the length of the rainy season, but which is significant at a 10% level.

Table 19: Spearman's rank correlation coefficient test results for the duration of the rainy season

Station	*t*-stat	*p*-value	r_s
Elim	10.16	0.24	0.15
Entabeni	−2.20	0.02	-0.22^{*}
Folovhodwe	1.36	0.17	0.18
Levubu	0.80	0.42	0.14
Lwamondo	−0.47	0.63	−0.07
Mampakuil	−0.67	0.50	−0.08
Pafuri	−0.06	0.94	−0.00
Punda Maria	1.82	0.07	0.23^{**}
Sigonde	1.15	0.25	0.22
Thathe	−2.19	0.03	-0.33^{*}
Tshiombo	0.78	0.13	0.15
Vreemedeling	0.90	0.37	0.11

**Significant at 0.05;* ***Significant at 0.1*

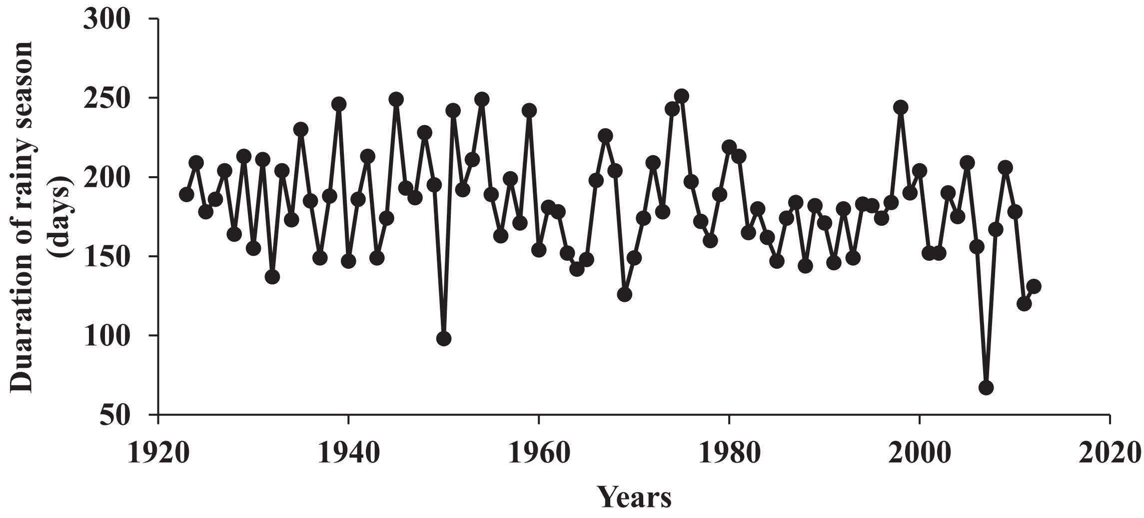

Figure 20: Temporal variation in the duration of the rainy season at Entabeni

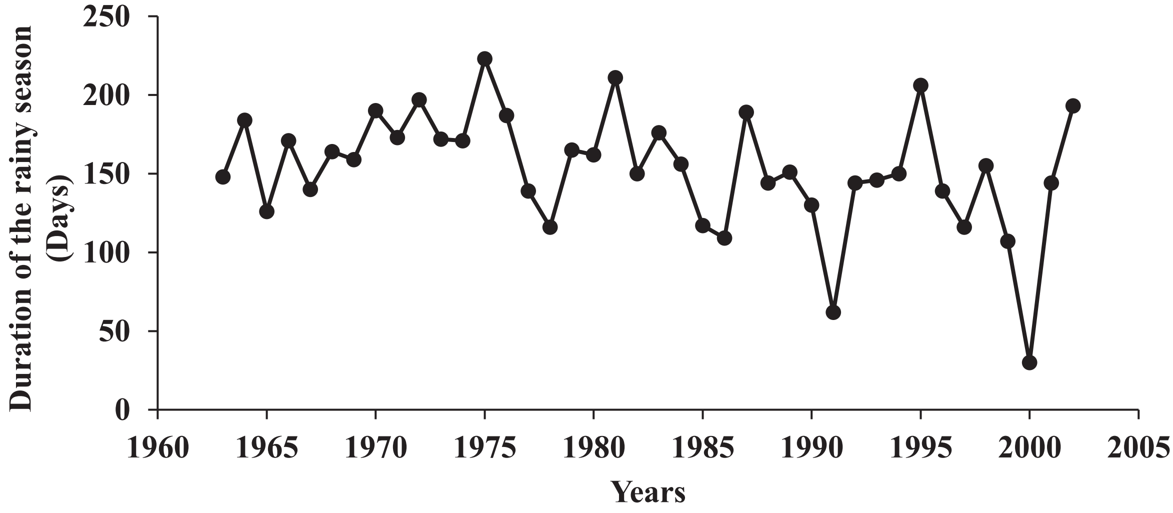

Figure 21: Temporal variation in the length of the rainy season at Thathe

3.5.8 Monthly rainfall during the rainy season

Table 20 and Table 21 show the descriptive statistics for monthly rainfall from October to April for 12 stations located within the Luvuvhu River catchment. In October, rainfall at the catchment ranged from 20 mm at Sigonde to 98 mm at Thathe. For November and December, all the stations had greater than 50 mm of rainfall. The Luvuvhu River catchment received peak rainfall in January and February with all stations receiving more than 100 mm of rainfall except for Mampakuil, Folovhodwe and Sigonde (Figure 22). In March, rainfall ranged from 39 mm at Sigonde to 180 mm at Levubu.

The results of this study show high rainfall variability of monthly rainfall on a yearly basis with the coefficient of variation and standard deviation ranging from 52-131% and 20-231 mm respectively. As a result, it is difficult to predict monthly rainfall totals within the catchment from historical data due to the high variability in monthly rainfall.

Table 20: Descriptive statistics for monthly rainfall from October to January

	October					November					December					January				
	Mean (mm)	STD (mm)	CV (%)	C_s	C_k	Mean (mm)	STD (mm)	CV (%)	C_s	C_k	Mean (mm)	STD (mm)	CV (%)	C_s	C_k	Mean (mm)	STD (mm)	CV (%)	C_s	C_k
Elim	49	34	69	0.70	0.06	77	45	58	0.40	−0.60	108	64	59	0.81	−0.21	148	121	82	1.60	3.70
Entabeni	100	71	71	1.30	2.17	166	91	55	0.90	0.90	249	142	57	1.03	0.79	341	197	57	0.85	0.34
Folovhodwe	28	29	106	1.38	4.26	45	54	119	2.45	7.58	58	60	103	1.57	2.55	60	79	119	2.53	7.79
Levubu	82	64	86	0.57	−0.39	146	81	55	1.49	3.53	196	100	52	0.62	0.30	262	231	88	1.82	2.30
Lwamondo	74	60	81	1.38	1.79	112	81	73	0.70	−0.26	119	66	55	1.30	2.45	167	161	93	2.90	11.00
Mampakuil	32	26	84	1.73	3.57	62	40	64	0.76	−0.23	77	43	56	0.64	0.19	98	81	83	0.99	0.30
Pafuri	28	27	95	1.10	0.77	59	51	87	0.95	0.20	66	53	81	1.05	0.86	102	100	98	1.63	3.07
Punda Maria	33	30	93	1.84	4.26	70	51	73	0.80	0.09	90	61	67	0.88	0.27	103	103	100	2.36	7.17
Sigonde	20	20	101	0.91	−0.37	55	49	89	0.99	0.26	73	53	73	1.26	1.49	92	112	121	2.95	11.29
Thathe	74	53	71	1.81	4.94	110	74	67	0.61	−0.15	162	125	77	1.92	1.14	213	186	87	2.21	7.85
Tshiombo	57	42	74	1.38	2.00	121	84	69	0.57	−0.08	140	85	60	0.82	−0.25	183	145	79	1.27	1.55
Vreemedeling	49	34	69	1.08	1.22	89	55	62	0.89	0.01	118	62	52	0.60	−0.86	161	140	87	2.47	9.45

Table 21: Descriptive statistics for monthly rainfall from February to April

	February					March					April				
	Mean (mm)	STD (mm)	CV (%)	C_s	C_k	Mean (mm)	STD (mm)	CV (%)	C_s	C_k	Mean (mm)	STD (mm)	CV (%)	C_s	C_k
Elim	152	164	107	4.30	25.50	90	97	108	3.50	15.80	44	74	106	2.90	13.40
Entabeni	344	288	84	2.10	7.70	253	206	82	1.90	5.20	107	71	71	1.34	2.17
Folovhodwe	72	71	98	1.46	2.82	42	56	131	2.01	4.04	24	32	133	2.38	7.79
Levubu	223	281	126	3.50	15.80	74	64	86	1.64	2.70	74	64	86	1.64	2.75
Lwamondo	123	156	127	5.27	30.20	97	67	69	1.48	2.10	57	59	104	2.22	5.78
Mampakuil	97	124	128	3.82	16.61	61	53	86	1.44	1.81	27	31	114	1.63	2.99
Pafuri	100	107	107	1.92	4.83	51	50	97	1.47	2.84	18	29	161	3.26	13.61
Punda Maria	104	102	98	1.79	4.25	54	65	119	2.46	8.42	27	31	111	1.88	4.07
Sigonde	79	103	121	3.34	14.45	39	34	89	0.82	−0.42	21	30	142	1.69	1.56
Thathe	251	253	101	1.94	4.26	143	136	95	1.59	2.34	77	126	164	5.10	29.48
Tshiombo	192	221	115	2.49	7.30	153	146	95	2.09	5.23	38	37	97	2.15	6.89

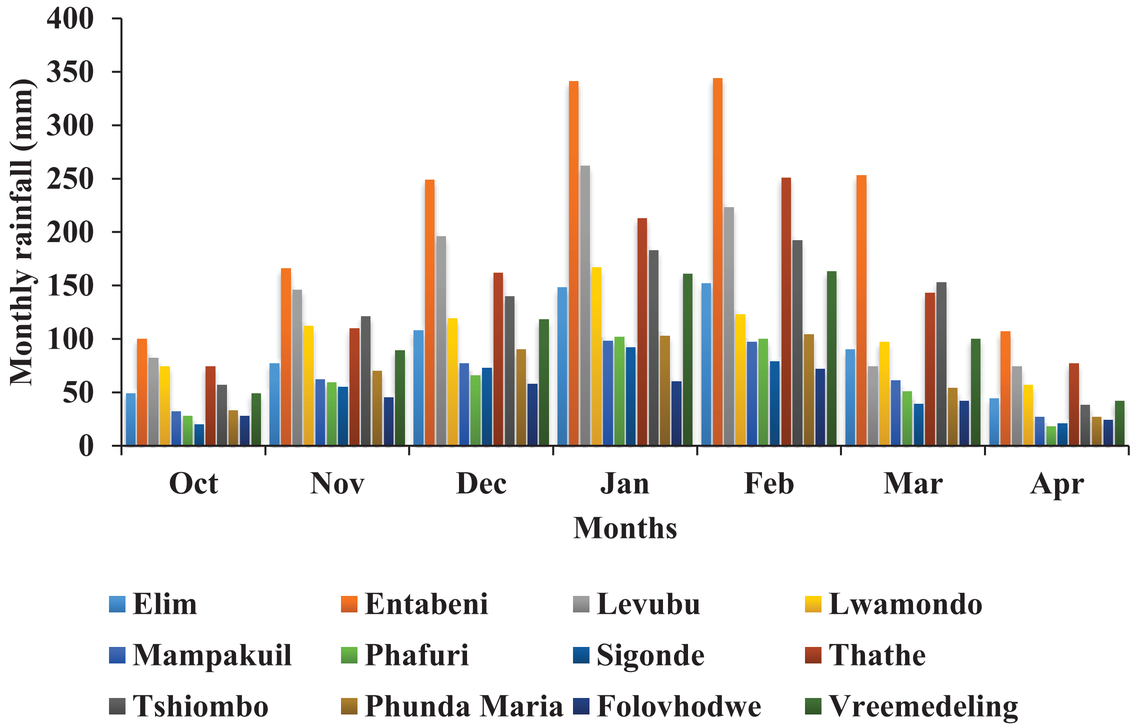

Figure 22: Monthly rainfall from October to April in the Luvuvhu River catchment

3.5.9 Aridity index and implications for crop production

Table 22 shows the mean annual rainfall, evapotranspiration and aridity index for selected stations within the Luvuvhu River catchment. The resultant agroclimatic zones based on UNEP (1992) are also included. The average annual rainfall in the catchment ranges from 356 mm for Folovhodwe to 1735 mm for Entabeni. The annual evapotranspiration ranges from 1450 mm for Levubu to 1804 mm for Elim. Comparable to the results by Mzezewa et al. (2010), the ET_0 is higher than the rainfall, which means that rainfall is not effective within the catchment. A study by Jalota & Prihar (1990) showed that 50-70% of annual rainfall evaporates to the atmosphere without any benefit to crop production. As a result, necessary steps such as dry-planting, conservation agriculture, intercropping, wind breaks, agroforestry and mulching are required to utilise the rainfall effectively and to reduce evapotranspiration from the soil surface (Rockstrom et al., 2010).

Aridity index values show that Entabeni is a humid zone; Levubu, Lwamondo, Tshiombo and Thathe are sub-humid zones; Sigonde, Elim, Punda Maria, Mampakuil and Pafuri are semi-arid zones; and Folovhodwe is an arid zone. In arid zones, crop water requirements frequently exceed the total rainfall received. As a result, no rain-fed agriculture can be practised without plans for alternative water sources (Wani et al., 2003).

Rainfall is not the only limiting factor in agricultural production in semi-arid and dry sub-humid zones, but extreme rainfall variability coupled with high rainfall intensity, few rainfall events, and poor spatial and temporal rainfall distribution also play a crucial role (Rockstrom et al., 2010). Dry spells are said to occur almost every season in semi-arid and sub-humid zones

(Wani et al., 2003). As a result, irrigation is said to be crucial for good and reliable harvests as semi-arid areas carry a high risk of unreliable rainfall, which might lead to crop failure (Brouwer & Heibloem, 1986).

Farmers in the semi-arid and sub-humid areas of the Luvuvhu River catchment are advised to adopt rainwater management and other conservation agriculture strategies to improve their yield. Rainwater management strategies include external water harvesting systems, in situ water harvesting systems, evaporation management, and integrated soil and crop management. These strategies help to improve yields and water productivity (Rockstrom et al., 2010). For example, at Patancheru in India, the sorghum/pigeon pea intercropping yield increased from 1.1 ton·ha^{-1} with normal practices to 5.1 ton·ha^{-1} with improved rainwater management practices, which indicates that rainwater management strategies indeed do improve yield (Rockstrom et al., 2010).

Table 22: Agroclimatic zones of the 12 selected stations at the Luvuvhu River catchment

Station	Annual precipitation (mm)	Annual evapo-transpiration (mm)	Aridity index	Zones
Elim	732	1804	0.40	Semi-arid
Entabeni	1735			Humid*
Folovhodwe	356			Arid*
Levubu	1356	1450	0.93	Sub-humid
Lwamondo	865	1580	0.54	Sub-humid
Mampakuil	497			Semi-arid*
Pafuri	464	1789	0.25	Semi-arid
Punda Maria	526			Semi-arid*
Sigonde	421	1750	0.24	Semi-arid
Thathe	1172			Sub-humid*
Tshiombo	986	1558	0.63	Sub-humid
Vreemedeling	801			Sub-humid*

*Brouwer & Heibloem (1986) climate classification

3.6 Conclusions

The study investigated rainy season characteristics (onset, cessation and length of the rainy season, seasonal rainfall, dry spells, number of rainy days per season, monthly rainfall and seasonal rainfall). Twelve meteorological stations were selected based on the location and length of the data set. Stations chosen were representative of different rainfall regions within the Luvuvhu River catchment. The findings of this chapter can be summarised as follows:

- Rainfall from October to April indicates high variability on a yearly basis with a coefficient of variation ranging from 52% to 131%. Peak rainfall in the catchment is experienced in January and February.
- Rainy season characteristics of the catchment are influenced by rainfall distribution and topography. Therefore, early onset in October occurs in areas situated in mountainous areas that receive more than 700 mm of annual rainfall such as Entabeni, Levubu, Thathe, Lwamondo, Vreemedeling, and Tshiombo. Onset occurs later in November in the low-lying areas of the catchment that receive less than 500 mm of annual rainfall such as Sigonde, Pafuri, Punda Maria, Folovhodwe and Mampakuil.
- Wet areas of the catchment experience earlier onset than other areas from mid-October and late cessation from mid-March to early April; therefore, leading to a longer rainy season than the remainder of the catchment. Dry areas (north and north-eastern) of the catchment, with less than 600 mm of annual rainfall, experience onset later in November and early cessation in February; therefore, making the season shorter than that for wet areas (south-western parts).
- There is a delay in receiving the first rainfall of the season by nearly a month compared with wet areas (Entabeni, Levubu and Thathe) for dry areas (Folovhodwe, Mampakuil, Pafuri, Punda Maria and Sigonde) of the catchment.
- There is a high probability of crop failure if planting is done following the first onset for dry areas of the catchment (Folovhodwe, Mampakuil, Punda Maria, Pafuri and Sigonde).
- Seasonal rainfall ranges from 315 mm for Folovhodwe to more than 1500 mm for Entabeni.
- Areas favourable to maize production at the catchment are Entabeni, Lwamondo, Levubu, Thathe, Tshiombo and Vreemedeling. Areas not suitable for maize production are Folovhodwe, Mampakuil, Pafuri, Punda Maria and Sigonde. Other crops such as sorghum, beans, and cow peas should be considered.
- For dry years (20% percentile), rainfall is not sufficient to permit planting for the following areas: Folovhodwe, Mampakuil, Pafuri, Punda Maria and Sigonde. For Entabeni, Levubu, Lwamondo, Thathe and Vreemedeling, planting can start in October in dry years. For wet years (80% percentile), the season starts in October and ends in April in all areas of the catchments.
- No changes in the onset of the rainy season for the catchment were noted for period 1923-2015. However, changes were noted in cessation, the length of the season, the number of rainy days, monthly rainfall and seasonal rainfall for the catchment.

4 DROUGHT ANALYSIS WITH REFERENCE TO MAIZE CROP PERFORMANCE

4.1 Introduction

The recurrence of drought is considered to be one of the most common climate disasters that affect most economic sectors (Sonmez et al., 2005; Li et al., 2009). Drought occurs in virtually most parts of the world, even in different climate regimes such as high and low rainfall areas (Mniki, 2009). This is because generally, drought is considered a prolonged lack of precipitation, which is relative to a region's long-term average (Dai, 2011). It is important not to confuse drought with related concepts such as aridity or desertification where low rainfall is a permanent climatic feature of the region; drought is merely a temporary phenomenon (Das, 2012).

Droughts are distinguished by intensity, temporal and special coverage. Thus, each drought year is unique in its climatic characteristics and impacts (Wilhite & Svoboda, 2000). Intensity refers to the degree of precipitation deficit and/or the severity of impacts associated with the shortfall (Dlamini, 2013). However, Das (2012) mentioned that the formation and intensity of drought are gradual and cumulative processes that occur slowly and are not easily detected, making drought a complex phenomenon. Another eminent feature of drought is duration, which is related to the timing and the effectiveness of the rains. It is closely linked to intensity as it is essential in determining the impact of drought (Dlamini, 2013). This refers to the primary season of occurrence, delays in the onset of the rainy season, occurrence of rains in relation to crop growth stages, rainfall intensity, etc. (Wilhite & Svoboda, 2000). Droughts commonly require a minimum of two to three months to become established and can then continue for months or years (Wilhite & Svoboda, 2000).

Droughts also differ regarding their spatial characteristics. It is very common for one area to suffer dry conditions while neighbouring areas experience normal or even above-normal rainfall conditions (Vicente-Serrano, 2006). Droughts can occur over vast areas covering a few hundred square kilometres but with different intensities and durations (Das, 2012). Such variation is often caused by complex atmospheric circulation patterns; hence, droughts cannot be associated with a single type of atmospheric condition (Vicente-Serrano, 2006). Therefore, this makes it rare to determine areas over which drought evolution is homogeneous.

In South Africa, one of the main causes of drought is the El Niño Southern Oscillation (ENSO) phenomenon (Tyson & Preston-Whyte, 2000). This refers to the interaction of the global atmosphere with the eastern and central Pacific Ocean, which results in variable ocean and climate patterns (Holloway et al., 2012). During an El Niño event, the atmospheric convergence of cloud bands, usually the source of high rainfall, moves offshore and thus results in warm and drought conditions over the south-eastern parts of the subcontinent (Austin, 2008; Tyson & Preston-Whyte, 2000). Contrary to El Niño, a La Niña event is associated with above-normal rainfall, often resulting in floods (Nicholson & Selato, 2000).

Although there is a correlation between ENSO events and drought, not all drought events in South Africa can be explained by this phenomenon (Tyson & Preston-Whyte, 2000; Vogel et al., 2000). According to Wright et al. (2015), the frequent drought occurrences over South

Africa can also be linked to regular climate variability and global warming due to climate change. Intra- and inter-annual climate variability and droughts are part of the earth's natural climate dynamics and partially caused by oscillations and complex configurations of global and regional climate systems (Wright et al., 2015).

4.2 Data

The geographical description of the weather stations that were selected with data sets of ≥ 30 years is given in Table 23.

Table 23: Details of the eight weather stations used in the study

Station name	Latitude	Longitude	Altitude (m)	Time frame (Rainfall)	Time frame (Temperature)	SWHC (mm)
1. Mampakuil	−23.167	29.900	945	1945-2004	–	21-40
2. Levubu	−23.042	30.151	880	1945-2014	1983-2014	61-80
3. Lwamondo	−23.044	30.374	648	1954-2014	1983-2014	61-80
4. Thohoyandou	−22.967	30.500	600	1982-2014	1983-2014	41-60
5. Tshiombo	−22.801	30.481	653	1954-2014	1983-2014	41-60
6. Punda Maria	−22.683	31.017	457	1945-2004	1975-2004	41-60
7. Sigonde	−22.397	30.713	428	1983-2014	1983-2014	21-40
8. Pafuri	−22.450	31.317	305	1945-2004	1975-2004	21-40

4.2.1 Historical climate data

Climatological data (rainfall and temperature) and soil water-holding capacity (SWHC) data were obtained from the ARC (ARC-ISCW, 2016). To assure data quality, climate data was inspected and the ARC stand-alone patching tool, which applies the IDW and the MLR method using neighbouring stations, was used to fill in missing values (Shabalala & Moeletsi, 2015; Moeletsi et al., 2016). Daily data was then aggregated into dekads, i.e. a sum of 10-day values resulting in three values per month:

- 1^{st} dekad (day 1-10).
- 2^{nd} dekad (day 11-20).
- 3^{rd} dekad (day 21-31).

4.2.2 Future projected data

Projected climate data of daily rainfall and temperature at a resolution of 5 × 5 km for the period 2020-2090 was obtained from the Climate Change, Agriculture and Food Security climate data portal (http://www.ccafs-climate.org/). The data is an output of detailed projections of a coupled global climate model called the CSIRO-Mk3.6.0. The output was downscaled and calibrated (bias-corrected) to a high resolution over southern Africa. Simulations were forced by the RCP 4.5 (intermediate emissions) scenario, which is part of the recently developed representative concentration pathways (RCPs). This RCP assumes a future of relatively ambitious emissions reductions, with a stabilised radiative forcing after 2100 (Bjørnæs, 2013). These projections formed part of the Coupled Model Intercomparison Project Phase 5 (CMIP5) and contributed to Assessment Report Four (AR5) of the Intergovernmental Panel on Climate Change (IPCC, 2007b).

4.2.3 Estimating evapotranspiration

Temperature data was used to calculate the evapotranspiration (ET_o) needed in the formulation of the selected drought indices. For the present study, the reference ET_o was calculated based on the Hargreaves method (Hargreaves & Samani, 1985) from an input data file containing geographic coordinates of the station, minimum and maximum air temperature.

This method was selected as it is the best alternative for quantifying ET_o in large-scale studies where data (relative humidity, vapour pressure deficit, wind speed or solar radiation) is missing (see e.g. Droogers & Allen, 2002; Moeletsi et al., 2013; Trambauer et al., 2014). Moreover, Hargreaves & Allen (2003) indicated that this method leads to a notably smaller sensitivity to error in climatic inputs as it calculates ET_o as a function of the minimum and maximum air temperature and extra-terrestrial radiation. The Hargreaves method is given by Hargreaves & Samani (1985) (see Section 3.3.5, Equation 11).

4.3 Methods: Determination of Drought

4.3.1 Drought indices

Agricultural drought is a complex phenomenon as it links meteorological drought and soil moisture deficits with impacts on crop growth and production (Wilhite & Glantz, 1987). As a result, an assessment of agricultural drought requires joint analyses of rainfall, temperature and soil moisture conditions (Hao & Aghakouchak, 2013). For the purpose of this study, various meteorological and agricultural drought indices were reviewed and the two drought indices, the Standardised Precipitation Evapotranspiration Index (SPEI) and the Water Requirement Satisfaction Index (WRSI), were selected based on the following criteria:

1. Quantify precipitation deficit at multiple time scales (Gocic & Trajkovic, 2014).
2. Account for the role played by the soil in regulating moisture in the crop root zone (Jayanthi & Husak, 2013).
3. Integrate crop factors such as potential evapotranspiration (Meyer et al., 1993).
4. Be applied in most areas of the Luvuvhu River catchment where there is limited weather and yield data (Wu et al., 2004).
5. Be computed in order to match a crop's phenological cycle (Wu et al., 2004).

Each index provides a different measure of drought; therefore, a single drought index is often inadequate for completely representing this complex phenomenon (Heim, 2002). Studies that employ multiple drought indices for drought risk assessment are meaningful, and may provide a more comprehensive assessment of drought conditions (Heim, 2002).

4.3.1.1 Standardised Precipitation Evapotranspiration Index

For calculating SPEI, the algorithm developed by Vicente-Serrano et al. (2010) was applied using the R package SPEI version 1.6 (http://cran.r-project.org/web/packages/SPEI) developed by Bergueria & Vicente-Serrano (2013). The package calculates the potential (*PET*) or reference ET_o using the Thornthwaite, Penman–Monteith, or Hargreaves method (Vicente-Serrano et al., 2015).

The first step was to compute the climatic water balance (D), i.e. the difference between precipitation (P) and ET_o for a given month:

$$D = P - ET_o \quad (14)$$

Where

D = Climatic water balance

P = Precipitation

ET_o = Reference evapotranspiration

A log-logistic probability function was then fitted to the data series of D, where the log-logistic is the distribution of a random variable whose logarithm follows a logistic distribution. The probability density function $F(x)$ of a log-logistic distribution is given by (Vicente-Serrano et al., 2015):

$$F(x) = \frac{\beta}{\alpha}\left(\frac{x-\gamma}{\alpha}\right)^{\beta-1}\left[1+\left(\frac{x-\gamma}{\alpha}\right)^{\beta}\right]^{-2}, \text{with } \gamma \leq x < \infty, \alpha < 0, \beta < 0 \text{ and } \gamma < 0 \quad (15)$$

Where

α = Scale parameter

β = Shape parameter

γ = Location parameter

The function $F(x)$ was then transformed to a normal variable following the classical approximation of (Abramowitz & Stegun, 1965):

$$Z = U - \frac{c_{0+} c_1 U + c_2 U^2}{1 + d_1 U + d_2 U^2 + d_3 U^3} \quad (16)$$

Where

$U = \sqrt{2\ln(H(x))}$ for $0 < H(x) \leq 0.5$ with $H(x) = 1 - G(x)$ being the probability of exceeding a D value.

The constants are: $c_0 = 2.515517$; $c_1 = 0.802853$; $c_2 = 0.010328$; $d_1 = 1.432788$; $d_2 = 0.189269$ and $d_3 = 0.001308$.

The SPEI is the obtained variable *Z*, which it ranges from ≥ +2 (extremely wet) and ≤ −2 (extremely dry). Negative SPEI values specify drought conditions (Table 24). The larger the negative value, the more intense the drought.

Table 24: Classification of drought by SPEI values (McKee et al., 1993)

SPEI	Drought category
> 0	No drought
0 to −0.99	Mild drought
−1.0 to −1.49	Moderate drought
−1.5 to −1.99	Severe drought
≤ −2.0	Extreme drought

4.3.1.2 Water requirement satisfaction index

The WRSI was generated by a crop water balance model in Instat+ software. In this model, the WRSI for a season was calculated as the ratio of seasonal actual evapotranspiration (AET) to the seasonal crop water requirement (WR), expressed by (Senay & Verdin, 2002):

$$WRSI = \frac{AET}{WR} \times 100 \ (17)$$

The water requirement was determined by multiplying the ET_o by the crop coefficient (Kc) given by Allen et al. (1998):

$$WR = ET0 \ \times Kc \ (18)$$

The reference ET_o was estimated using the Hargreaves method (Hargreaves & Samani, 1985) from an input data file containing geographic coordinates of the station, and minimum and maximum air temperature (see Section 4.2.3). The crop coefficient was calculated using the single Kc approach developed by Allen et al. (1998). The approach for calculating the Kc values was based on the four growing stages of the maize crop, i.e. initial stage; development stage; mid-season stage; and late season stage. The Kc values for initial and end were obtained from Allen et al. (1998) and adjusted according to the area's climatic conditions. Thereafter, intermediate Kc values were linearly interpolated to obtain the crop coefficients during the whole growing period (Figure 23).

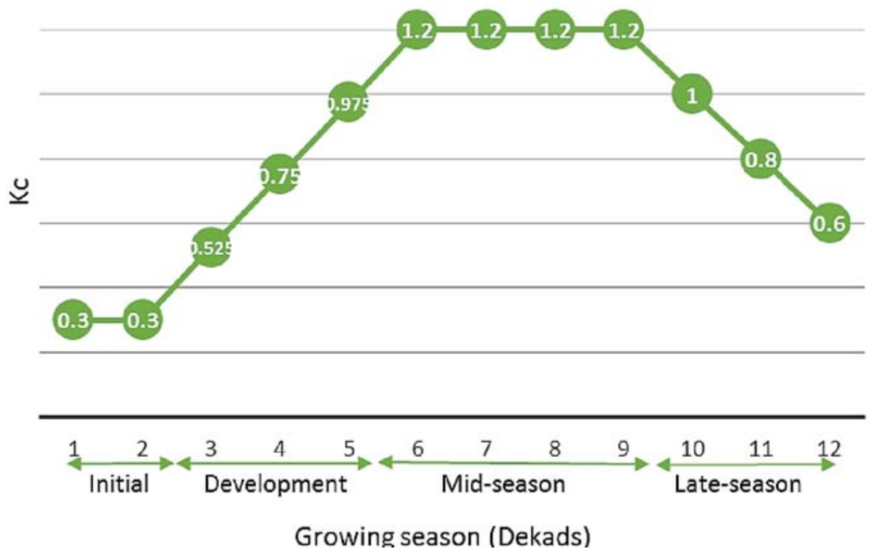

Figure 23: Dekad crop coefficient (Kc) curve during each growing phase of maize

After calculating the water requirement, the AET, which represents the actual amount of water withdrawn from the soil water reservoir, was estimated using the soil water balance method incorporated within the model. In order to determine AET for the maize crop, the dekadal rainfall (PPT) was added to the soil water content to produce a plant-available-water (PAW) value:

$$PAW_i = SW_{i-1} + PPT \quad (19)$$

Where

SW_{i-1} = soil water content at the end of the previous i^{th} time interval (mm/dekad)

Depending on the PAW in the soil reservoir, the value of AET was estimated using the following equations (Senay & Verdin, 2002):

$$AET = WR \text{ when } PAW \geq SWC \quad (20)$$

$$AET = \frac{WR}{SWC} \times PAW \text{ when } PAW < SWC \quad (21)$$

$$AET = PAW \text{ when } AET > PAW \quad (22)$$

Where

SWC = critical soil water level in the soil reservoir

The WRSI is recorded at the end of each dekad up to the end of the crop growth cycle. The value at the end of the growth cycle reflects the cumulative stress experienced by the crop after the dekad (FAO, 1986). The index starts with a value of 100 and is reduced when the crop undergoes water stress in a form of water deficit and if the water surplus is greater than 100 mm (Allen et al., 1998). A case of no deficit will result in a WRSI value of 100, which corresponds to the absence of yield reduction related to water deficit. A seasonal WRSI value less than 50 is regarded as a total crop failure condition as illustrated in Table 25 (FAO, 1986).

Table 25: Classification of WRSI for drought conditions and crop performance (FAO, 1986; Legesse, 2010)

WRSI	Drought classification	Crop performance description
80-100	No drought	Good
70-79	Mild	Satisfactory
60-69	Moderate	Average
50-59	Severe	Poor
< 50	Extreme	Total crop failure

4.3.2 Analysis of drought under historical and future climates

To assess the possible impact of climate change on drought characteristics in relation to maize, a medium maturing (120-day) maize crop was considered. Three consecutive planting dates were staggered based on three consecutive onsets of the rainy season. Drought was categorised according to the definition of each index and the output series were arranged in accordance with the rainfall season, i.e. starting from 1 July to 30 June.

Assessment of drought was conducted during the whole growing period of maize as well as for each phenological stage. The outputs were analysed using the following statistical methods: frequency analysis, probability distributions, non-parametric Spearman's rank correlation test and independent *t*-test. For future drought projections, drought indices were computed using outputs from the CGCMs and time series variations were evaluated. These steps are elaborated in the subsequent sections.

4.3.3 Temporal variability and trends analysis

Outputs from the drought indices were analysed to investigate the evolution of drought occurrences and severity during the whole study period. Thereafter, the non-parametric Spearman's rank correlation test was conducted at α (0.05) significance level to determine trends in droughts. This correlation test is based on the coefficient ρ that ranges from −1 to 1. A negative value implies a decreasing trend while a positive value represents an increasing trend. The absolute value of the coefficient indicates its strength, which means that larger values specify stronger linear relationships (Gitau, 2011). The method of calculating the coefficient ρ to determine the trend is given by (Gitau, 2011):

$$\rho = -6\sum_{i-1}^{n}\left(\frac{d_i}{n(n^2-1)}\right)^2 \quad (23)$$

Where

d_i = the difference between each rank of corresponding values of x and y

n = the number of data pairs

4.3.4 Analysis of extreme widespread dry and wet agricultural seasons

Three stations (Lwamondo, Tshiombo and Sigonde), which represent the different rainfall regions in the catchment from high to low, were randomly selected and analysed using the December results as this was identified as the period in which the drought was more intense than other planting dates.

Notable agricultural seasons subjected to extreme widespread drought given by SPEI (< −2) were assessed by studying the actual rainfall and evapotranspiration during the summer rainfall season in the catchment, i.e. from October to April (ARC-ISCW, 2016). Subsequently, seasons reflecting WRSI values corresponding to extreme drought (< 50) were evaluated to measure the extent to which the water requirement of the crop had been met during each stage of the growing season. On further analysis, the seasons in which there was no drought (wet seasons) and whereby there was mild to moderate drought at low rainfall regions (due to high risk of recurrent drought occurrence) were also evaluated to inspect the intra-seasonal variability of rainfall throughout the growing season.

4.3.5 Assessment of drought conditions under future climate

To assess the possible impact of climate change on drought characteristics in relation to maize, a medium maturing (120-day) maize crop was considered. The two drought indices were analysed based on the average start of significant rains in the area (November) as indicated by Masupha et al. (2016). Drought was then calculated with reference to the whole growing period of maize. Calculations for the SPEI were conducted at a four-month time scale, whereby the value at the end of February represented the accumulated water stress for that particular period. Formulation for WRSI was conducted for the three dekads of November and the median of the resultant values at the end of the growing cycle were used for analysis.

Future drought events in the catchment were generated from time series of SPEI and WRSI, for three periods, namely, base period 1980/81-2014/15, near-future 2020/21-2054/55 and far-future 2055/56-2089/90. Drought frequencies were obtained by calculating the ratio of the number of drought events (by SPEI and WRSI) corresponding to each drought category to the total number of agricultural seasons analysed. To test whether the frequency and severity of drought are projected to significantly increase or decrease relative to the base period, a z-test was conducted at α (0.05) significance level in Statistica software. The test was run based on the following hypothesis:

- H0: $(\mu_1 = \mu_2)$ – the means of the drought indices for future climate periods are equal to the base period.
- H1: $(\mu_1 \neq \mu_2)$ – the means of the drought indices for future climate periods are different from the base period.

Test statistic from normally distributed populations with population variances known (Daniel, 1999):

$$z = \frac{(\bar{X}_1 - \bar{X}_2) - (\mu_1 - \mu_2)}{\sqrt{\sigma_1^2/N_1 + \sigma_2^2/N_2}} \quad (24)$$

Where

$\bar{X}_1$ *and* $\bar{X}_2$	= sample means
μ_1*and* μ_2	= hypothesised means
N_1 *and* N_2	= sizes of the samples
σ_1^2 *and* σ_2^2	= sample standard deviation

Rejection or failure to reject the null hypothesis would then be on the basis that the corresponding p-value is less or greater than the significance level of 0.05, respectively.

4.4 Results and Discussion

4.4.1 Relative frequency of drought by SPEI for each growth stage of maize

Figure 24 shows that mild droughts occur most frequently (100%) during all growth stages following the three planting dates (October, November and December). During the first stage of the crop, considering the first planting date, it can be noted that the highest frequency was at Tshiombo (47%), while other stations revealed a frequency of ≤ 30%.

Severe drought conditions were observed at six of the seven stations, with Tshiombo being the only station revealing no occurrence at this stage. Extreme drought was observed only at Sigonde, giving a frequency of 6%. Relative to planting in November, it can be seen that moderate droughts were most frequent at Punda Maria (44%), followed by Levubu (40%). Severe drought frequency was the highest at Levubu and Sigonde (13%), while Lwamondo and Punda Maria revealed no occurrences. Similarly, planting in November resulted in extreme drought conditions only at Sigonde.

When looking at December planting date, results indicate that moderate drought conditions were most frequent at Sigonde (53%) and Tshiombo (47%), giving a return period of once in two drought events. The highest frequency of severe droughts was observed at Levubu (16%), with Tshiombo revealing no occurrence; while extreme droughts were identified only at Thohoyandou, with a 6% frequency.

During the vegetative stage (stage 2), moderate drought conditions were most frequent at Punda Maria (44%), while the lowest frequency was observed at Pafuri (27%), following planting in October. Severe droughts were observed at five of the seven stations, while extreme drought was noted only at Sigonde. For planting in November, Sigonde revealed the highest frequency (53%) of moderate drought conditions, with the least frequency (22%) observed at Lwamondo.

Severe droughts during this stage were detected most frequently at Levubu, while an occurrence of extreme drought was noted only at Thohoyandou. Relative to planting in December, high frequencies of moderate drought conditions were observed at Lwamondo (54%), Thohoyandou (67%), Tshiombo (44%) and Sigonde (47%). Frequencies of severe drought during this stage ranged from 6% at Tshiombo to 20% at Punda Maria, while there was no occurrence of extreme droughts observed at all stations following this planting date.

When considering planting in October for stage 3, it can be observed that moderate drought was most frequent at Sigonde (53%), followed by Tshiombo and Pafuri with 44% and 43%, respectively. Severe drought conditions were most frequent at Levubu (16%), with Tshiombo revealing no occurrence of drought during this stage. Extreme drought conditions were noted only at Thohoyandou, giving a frequency of 3%.

Relative to the second planting date, high frequencies of moderate drought conditions were observed at Lwamondo (54%), Thohoyandou (67%), Tshiombo (50%) and Sigonde (47%), implying that moderate drought was observed once in two drought events during this stage. Severe drought conditions were most frequent at Punda Maria (20%), while a non-occurrence of extreme drought during this stage was observed. When looking at planting in December during this stage, the highest frequency of moderate drought conditions was observed at

Thohoyandou (40%), with Punda Maria revealing the least (21%). For severe droughts, Tshiombo indicated the highest frequency (15%), with extreme droughts observed only at Levubu (6%) and Punda Maria (11%) during this stage.

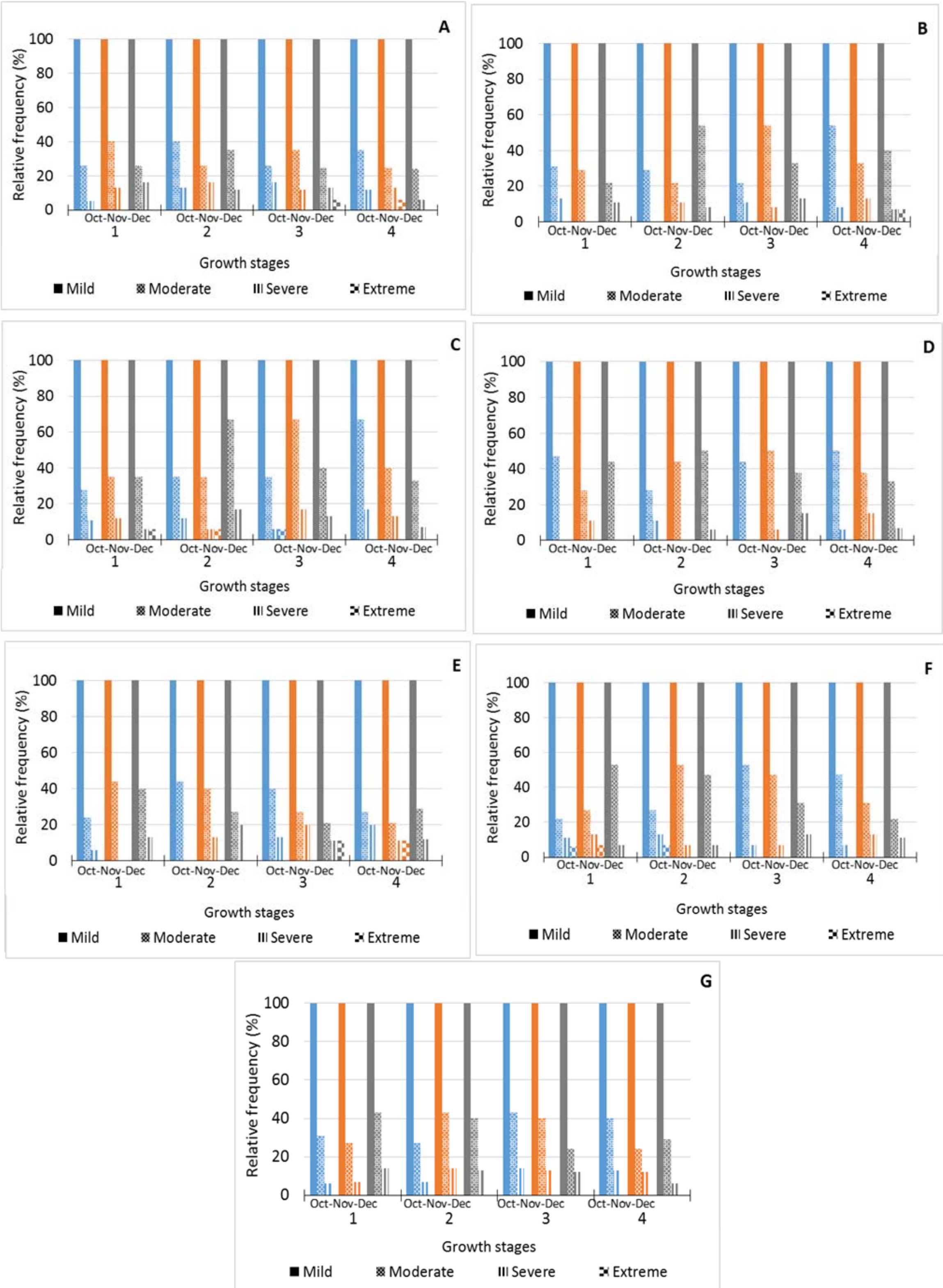

Figure 24: Relative frequency of SPEI drought categories during each growing stage of the maize crop relative to planting in October, November and December for stations Levubu (A), Lwamondo (B), Thohoyandou (C), Tshiombo (D), Punda Maria (E), Sigonde (F) and Pafu

During stage 4, moderate drought (≥ 50%) conditions were noted at three stations (Lwamondo, Thohoyandou and Tshiombo) following the October planting date. Severe drought conditions were most frequent at Punda Maria (20%), with no occurrence of extreme drought during this stage. Following the second planting date, Thohoyandou recorded the highest frequency (40%) of moderate droughts with severe drought conditions noted to be most frequent (15%) at Tshiombo, followed by Levubu, Lwamondo, Thohoyandou and Sigonde with a frequency of 13%. Furthermore, extreme drought was noted only at Levubu and Punda Maria, while the December planting date revealed the highest frequency (40%) of moderate drought during stage 4 at Lwamondo, with Sigonde being the least at 22%. Severe drought conditions were most frequent at Punda Maria (12%) as compared with other stations, while extreme drought conditions were observed only at Lwamondo.

Relative frequencies varied among stations for all the planting dates. It was noted that mild drought conditions revealed a 100% frequency for all the growing stages as expected. This is due to the comparable classification of mild drought to the definition of drought as presented in Table 24. For the first stage of the crop, high frequencies of moderate drought were recorded following the first planting date at Lwamondo and Tshiombo, while other stations indicated a higher risk relative to planting in November to December. At this stage, drought delays imbibition and can thus lead to decreased germination rates and total germination percentage (Prasad et al., 2008). Results during the vegetative stage indicate that stations located in regions receiving annual precipitation of 600-900 mm (Lwamondo, Thohoyandou and Tshiombo) are at higher risk of moderate drought conditions following planting in December, while the other stations indicated a higher risk following October-November planting.

Results during the third stage of maize showed that stations located in the middle-lower catchment are at a higher risk of moderate drought during stage 3 relative to planting in November. Additionally, these areas were more frequent to severe-extreme droughts following December planting date, implying that planting in October at Levubu, Lwamondo, Thohoyandou and Tshiombo could place crops at a lower risk of reduced yield and even total crop failure. Furthermore, a return period of one extreme drought (SPEI < 2) in 17 drought events was noted for Thohoyandou relative to planting in October. In contrast, stations located in the low-lying plains of the upper catchment (Punda Maria, Sigonde and Pafuri) were exposed to frequent moderate droughts following planting in October, with favourable conditions noted following December planting date.

For a maize crop, flowering to grain-filling (stage 3) is considered the most sensitive phase of reproductive growth as drought during this stage can result in abortion of ovules, kernels and ears (Aslam et al., 2013). This can have serious implications on the yield. Therefore, it is crucial for farmers to adapt to planting at proper times in environments where drought stress is observed to be more frequent during late vegetative, flowering and grain-filling stages.

4.4.2 Temporal evolution of drought and trends based on SPEI

Noticeable seasons subjected to drought conditions were noted as (Figure 25):

- 1983/84,
- 1986/87,
- 1988/89,
- 1991/92,
- 1994/95,
- 1997/98,
- 2000/01,
- 2002/03,
- 2004/05,
- 2006/07,
- 2009/10,
- 2011/12, and
- 2014/15.

This corresponds to an average frequency of once every two to three seasons. The 1983/84 drought reached severe conditions at five of the seven stations, while the worst drought was detected during the 1991/92 season, reaching severe to extreme conditions at all the stations. When considering this drought season, extreme conditions were identified following planting in November at four of the seven stations.

Resulting implications could cause reduced yields as the maize crop is sensitive to the occurrence of drought (Wetterhall et al., 2015). This would then lead to food shortages and an increase in vulnerability to disease across the affected areas (Nyabeze, 2004). Adaptation methods such as shifting planting dates are relatively inexpensive and easy to implement, therefore, they should be applied in order to cope with inter-annual droughts in rain-fed systems (Thomas, 2008).

The Spearman's rank correlation test for drought trends (Figure 25) show that at Levubu and Lwamondo, noticeable upward trends (ρ values of 0.4) occurred relative to planting in November and October, respectively. The same trend was observed at Thohoyandou for all the planting dates. This implies a slight decrease in the severity of drought during the growing period of maize in the regions that receive ≥ 750 mm of annual precipitation. It can also be noted that there was no significant change in the severity of drought at other stations (Tshiombo, Punda Maria, Sigonde and Pafuri). A similar study on simulating the characteristics of droughts in southern Africa showed a slight significant downward trend, implying an increase in the intensity of drought over the area (Ujeneza, 2014). However, the study was conducted at a country level, using monthly gridded climatic data for the period 1940-2004.

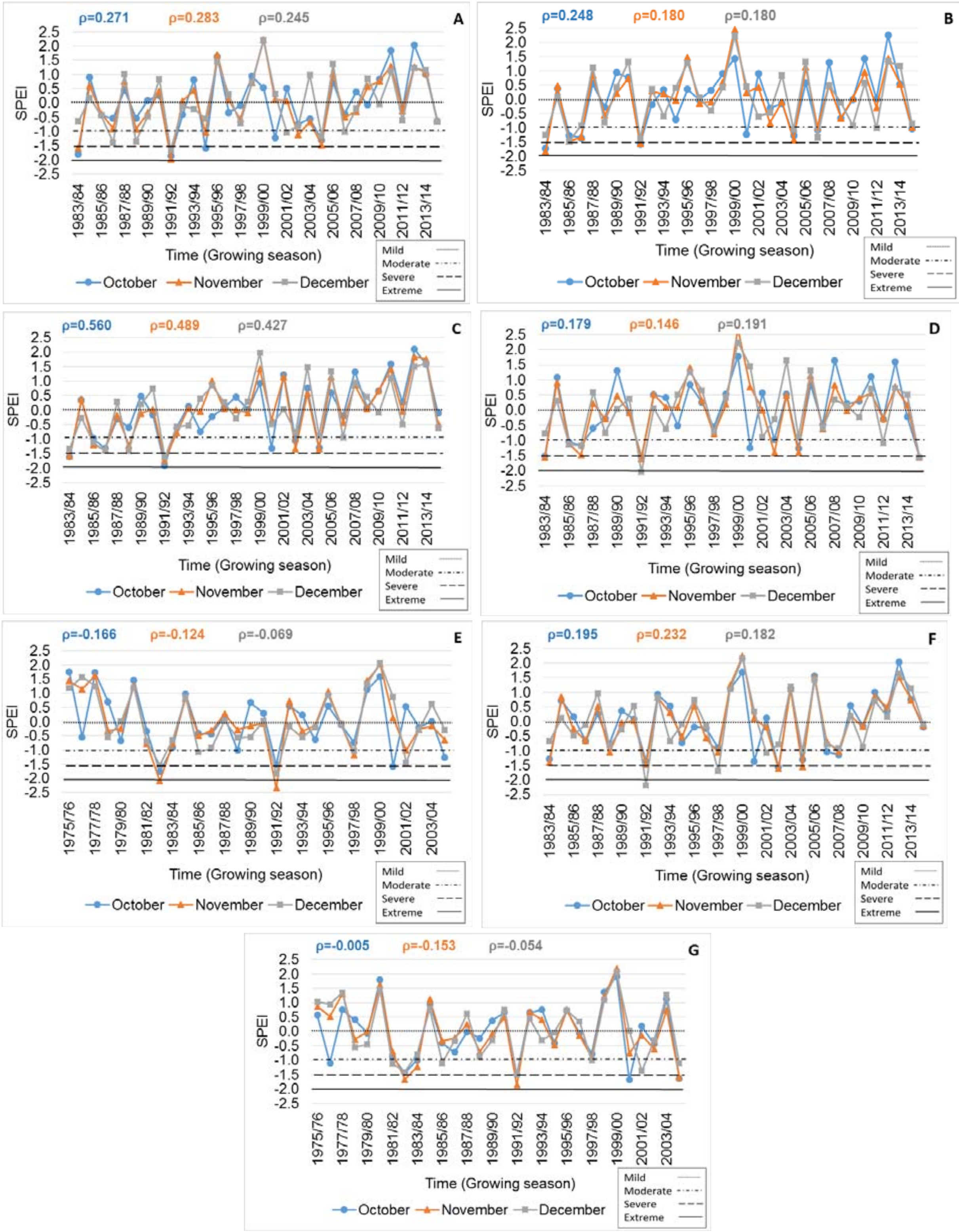

Figure 25: Observed SPEI time series and trends per growing season relative to the three planting dates for stations Levubu (A), Lwamondo (B), Thohoyandou (C), Tshiombo (D), Punda Maria (E), Sigonde (F) and Pafuri (G)

4.4.3 Observed extreme widespread dry and wet agricultural seasons using SPEI

As per the SPEI results, notable seasons subjected to extreme widespread drought were identified as 1983/84 and 1991/92. The monthly distribution of rainfall and evapotranspiration during these seasons indicates that during the 1983/84 drought, evapotranspiration reached a peak of about 200 mm in January at all stations, while accumulated rainfall was recorded as < 100 mm at Tshiombo and < 50 mm at Lwamondo and Sigonde (Figure 26). This indicates that satisfactory rain was not available for crop use due to an imbalance between crop water demand and supply. Furthermore, these conditions improved by March, whereby at the high and moderate rainfall regions, amounts of rain were recorded to be higher than the accumulated evapotranspiration rates. It can also be noted that at Sigonde (low rainfall region), the highest rainfall amount during this rainfall season was also recorded in March; however, due to the region experiencing fairly high temperatures as compared with other regions in the catchment, the evapotranspiration remained higher.

Drought conditions during the 1991/92 agricultural season can clearly be described by the low rainfall amounts together with high evapotranspiration rates throughout the rainfall season. Similar to the 1983/84 season, the month of January experienced the highest accumulated evapotranspiration as compared with the other months of the season. At Sigonde, there was no rainfall during October, January and February, with the highest amount recorded as 75 mm in November, suggesting that rainfall was not enough to meet evapotranspiration demands, thus the prevalence of water deficit during this season. This shows that even though the catchment was struck by widespread droughts, conditions in the low rainfall regions seemed to be more severe than other parts that receive fairly good rains in summer.

In order to minimise additional water losses due to increased evaporative demand, various mulching techniques can be employed (Thomas, 2008). Seasonal forecasts during drought seasons would also be beneficial for local rain-fed maize growers especially in regions where moisture is available for a short period during the growing season. Moreover, these farmers should consider planting short maturing crop varieties in order to increase the probability of meeting crop water requirements during the sensitive stages of crop growth (Das, 2012).

Results further revealed 1999/00 and 2012/13 as being the extreme wet seasons in the area for the analysis period. The potential water balance presented in Figure 27 shows that, in general, there was a marginal difference between the actual amount of rainfall received and evapotranspiration rates as compared with the drought seasons. It is also evident that in January 2000, the area received considerably high rainfall, which continued to increase in February, recording values of about 1000 mm at the high and moderate rainfall regions.

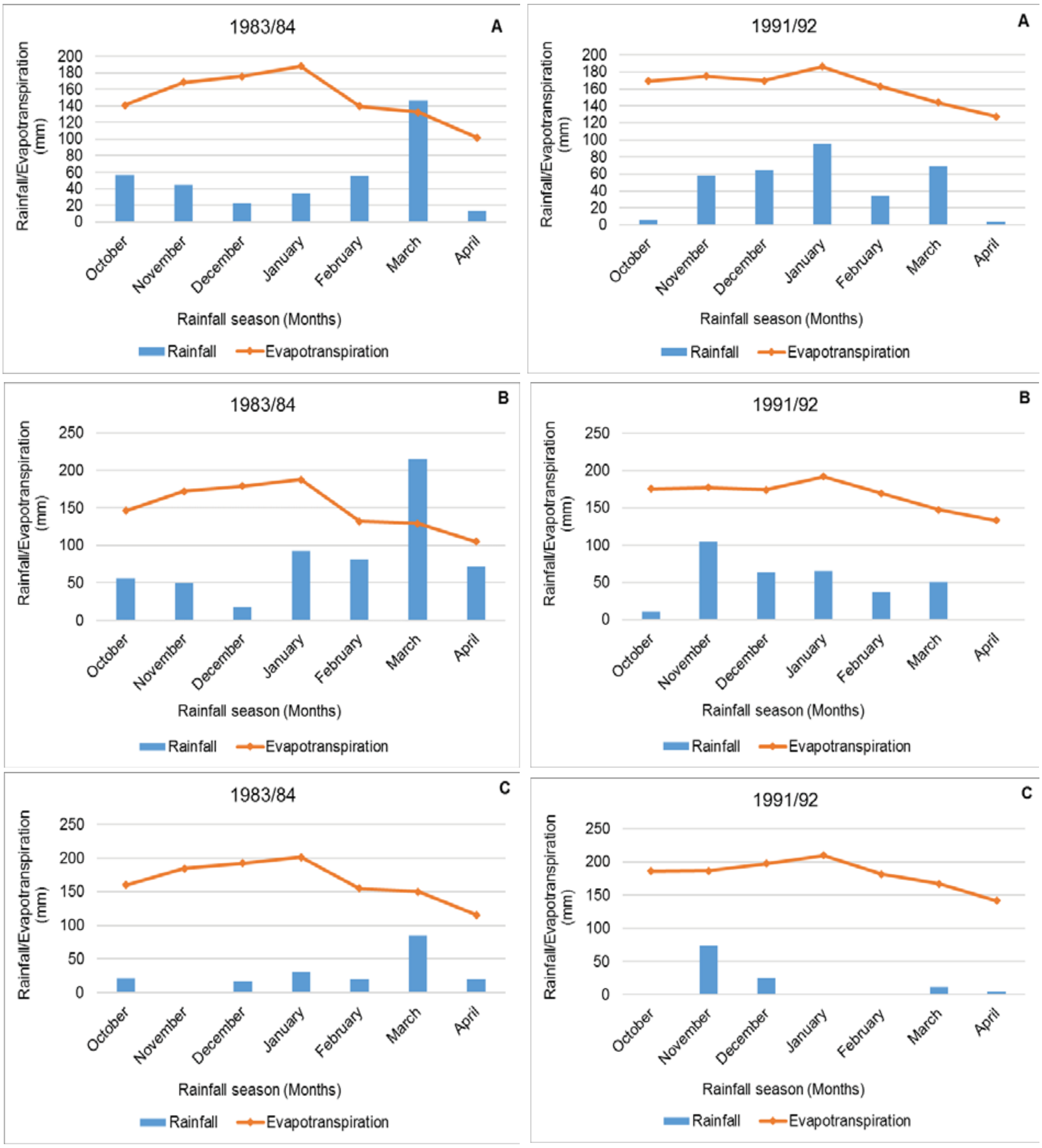

Figure 26: Monthly distribution of rainfall and evapotranspiration during 1983/84 and 1991/92 extreme widespread droughts, for stations Lwamondo (A), Tshiombo (B) and Sigonde (C)

At Sigonde, the weather station recorded 550 mm of rain in February, which is substantially high considering that the area is situated in a region that receives a mean annual rainfall of < 450 mm. These heavy rains resulted in flooding across the Limpopo Province, filling the channels of the Luvuvhu River catchment and basins (DWAF, 2004). The strength of the water removed soil, vegetation and rocks, which led to crop failure in several regions of the catchment (Khandlhela & May, 2006). Reason & Keibel (2004) explained that the main cause of these floods was due to the occurrence of a tropical cyclone, which was the longest lasting tropical storm observed to date in southern Africa.

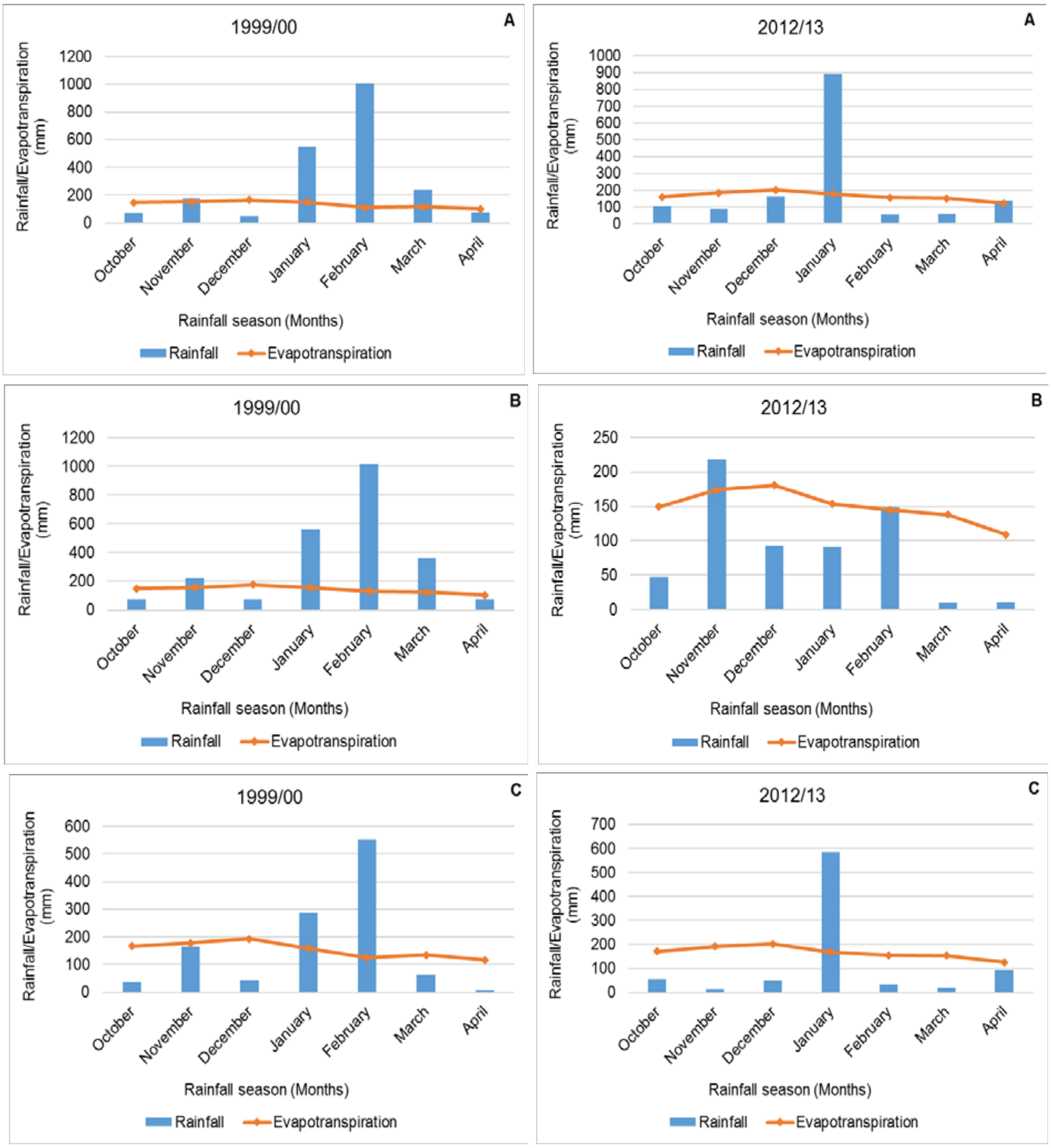

Figure 27: Monthly distribution of rainfall and evapotranspiration during 1999/2000 and 2012/13 extreme widespread wet seasons, for stations Lwamondo (A), Tshiombo (B) and Sigonde (C)

For the 2012/13 season, rainfall amounts of up to 900 mm at Lwamondo and 590 mm at Sigonde were observed in January, while at Lwamondo rainfall amounts of between 90 and 210 mm were experienced from November to February. This implies that crops that were planted in November were at an advantage of receiving significant amounts of rain during the most critical stages of growth and development. Furthermore, the distribution of rainfall and evapotranspiration amounts noted during the four months at Lwamondo showed a good water balance. Hence, the resulting SPEI indicated values corresponding to no-drought conditions, suggesting the probability of good agricultural productivity during that season.

4.4.4 Predicted future drought in relation to the growing period of maize using SPEI

Figure 28 shows the projected changes in drought conditions given by SPEI under the RCP 4.5 scenario, while the expected frequencies are clearly depicted in Table 26. Results show that 40-54% of the agricultural seasons during the base period experienced mild drought conditions (SPEI 0 to −0.99), corresponding to a recurrence of once in two seasons. These conditions are then expected to change during the future climate periods. Mild drought can be expected to increase by up to 26% at Levubu, followed by 23% and 20% at Tshiombo and Lwamondo, respectively, during the far-future period. Mild drought frequency at Sigonde and Punda Maria can be expected to decrease from the base period during the near-future climate period by 8% and 5%, respectively, and then increase during the far-future climate period.

The highest increase in the frequency of moderate drought (SPEI from −1 to −1.49) from the base period can be expected during the far-future as compared with the near-future period. This reflects a frequency of 29% at Levubu, Lwamondo, Tshiombo and Mhinga, while at the other stations 26% of the far-future period can be expected to be under moderate drought conditions. However, comparing these frequencies to the base period shows that the highest increase will be experienced at Levubu. This is also the only station that revealed a statistically different mean in SPEI ($p = 0.04$) as compared with the base period, with a decrease in SPEI values during the near-future period.

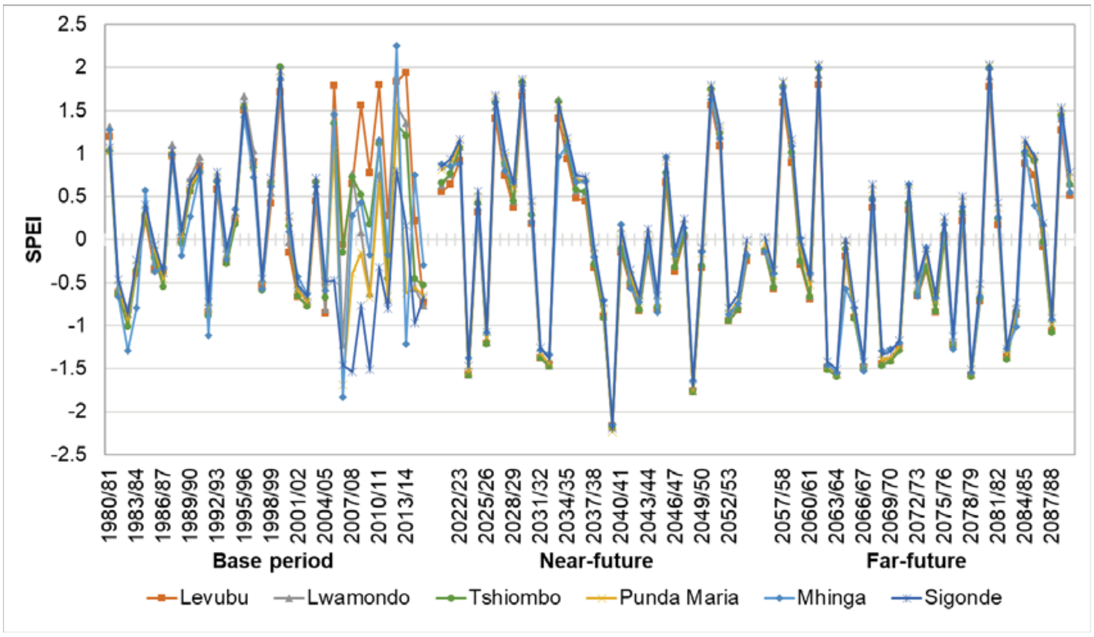

Figure 28: Simulated SPEI time series per growing season of the base period and future climate periods

Table 26: Frequency (%) of the different levels of drought (by SPEI) during future climates, relative to the base period, in the Luvuvhu River catchment

Station	Drought category	Climate period		
		Base period	Near future	Far future
Levubu	Mild	40	51	66
	Moderate	0	17	29
	Severe	0	9	9
	Extreme	0	3	0
Lwamondo	Mild	46	51	66
	Moderate	3	17	29
	Severe	0	9	6
	Extreme	0	3	0
Tshiombo	Mild	43	51	66
	Moderate	3	17	29
	Severe	0	9	9
	Extreme	0	3	0
Punda Maria	Mild	51	46	63
	Moderate	3	17	26
	Severe	3	9	6
	Extreme	0	3	0
Mhinga	Mild	46	49	60
	Moderate	11	17	29
	Severe	3	6	9
	Extreme	0	3	0
Sigonde	Mild	54	46	60
	Moderate	9	17	26
	Severe	6	6	6
	Extreme	0	3	0

Table 27 shows that droughts are likely to intensify at Levubu and Tshiombo during the far-future period, whereby the means were significantly different (p < 5%) from the base period. Projections also showed expected widespread occurrences of severe to extreme droughts during the 2039/40 and 2048/50 agricultural seasons during the near-future, whereby the far-future will be expected to reach this severity level during the 2063/64, 2066/67 and 2078/79 seasons. This could be beneficial if crops are at a mature stage when the water demand is lower, but could also be harmful if water is unavailable during the reproductive stages (Kraemer, 2015). These drought conditions can be explained by the expected increases in temperature in the Limpopo Province by 2040-2060; and along with projected decreases in precipitation, given by Lobell & Gourdji (2012), this could lead to significant drying of the soil and a higher risk of experiencing agricultural drought.

Table 27: Z-test between SPEI means of the future climates, relative to the base period, in the Luvuvhu River catchment. Values highlighted in italics differ statistically at α (0.05)

Station	Statistics parameters	Base	Near future	Far future
Levubu	Mean	0.37	−0.09	−0.28
	Known variance	0.77	1.01	1.02
	z	0.00	2.01	2.82
	p (Z ≤ z) two-tail	1.00	*0.04*	*0.00*
	z-critical two-tail	0.00	1.96	1.96
Lwamondo	Mean	0.21	−0.01	−0.21
	Known variance	0.74	1.11	1.10
	z	0.00	0.94	1.78
	p (Z ≤ z) two-tail	1.00	0.35	0.07
	z-critical two-tail	0.00	1.96	1.96
Tshiombo	Mean	0.24	−0.02	−0.22
	Known variance	0.63	1.15	1.16
	z	0.00	1.13	2.01
	p (Z ≤ z) two-tail	1.00	0.26	*0.04*
	z-critical two-tail	0.00	1.96	1.96
Punda Maria	Mean	0.07	0.06	−0.14
	Known variance	0.69	1.16	1.17
	z	0.00	0.04	0.90
	p (Z ≤ z) two-tail	1.00	0.97	0.37
	z-critical two-tail	0.00	1.96	1.96

Station	Statistics parameters	Base	Near future	Far future
Mhinga	Mean	0.14	0.02	−0.18
	Known variance	0.87	1.02	1.09
	z	0.00	0.52	1.34
	p (Z ≤ z) two-tail	1.00	0.60	0.18
	z-critical two-tail	0.00	1.96	1.96
Sigonde	Mean	−0.05	0.12	−0.08
	Known variance	0.74	1.14	1.14
	z	0.00	−0.69	0.16
	p (Z ≤ z) two-tail	1.00	0.49	0.87
	z-critical two-tail	0.00	1.96	1.96

4.4.5 Probabilities of WRSI during the growing season of maize

The WRSI probability plots showing drought-proneness relative to planting in October, November and December are presented in Figure 29 to Figure 31. At the 20th percentile mark, results show that mild conditions (WRSI 70-79) can be expected at Levubu, following October and November planting dates, while December planting reflected WRSI values corresponding to moderate-severe droughts. At Lwamondo and Tshiombo, probabilities of severe droughts (WRSI < 60) were observed relative to planting during the 2nd dekad of October to the 1st dekad of November, with the drought intensifying to extreme conditions (WRSI < 50) in December. Moreover, at Thohoyandou, the least risk can be expected during the 1st dekad of October, while at Punda Maria, Sigonde and Pafuri, extreme droughts can be expected once in five seasons, regardless of the planting date.

When observing at the 50% probability of non-exceedance, it was evident that at Levubu, WRSI reflected values of ≥ 80 during all planting dates. This implies that once in two seasons, the farmers in this region can expect no-drought conditions, resulting in good crop performance. At Lwamondo, it can be seen that planting in the 1st dekad of October could results in severe drought while the risk may possibly be reduced if planting occurs during the 3rd dekad of October to the 3rd dekad of December, with WRSI values ranging from 70-79 during this period. At Tshiombo and Thohoyandou, planting during the 1st dekad and 2nd to 3rd dekad of December, respectively, gave a risk of severe droughts, while planting in October to November could result in better crop produce at both stations. Similar to the 20th percentile, it can also be seen at 50% probability (with a return period of once every two seasons), that Punda Maria, Sigonde and Pafuri can expect to receive extreme drought conditions following all the planting dates. This implies an imbalance between the distribution of rainy days and the amount of rainfall as compared with the crop requirements (Yengoh et al., 2010).

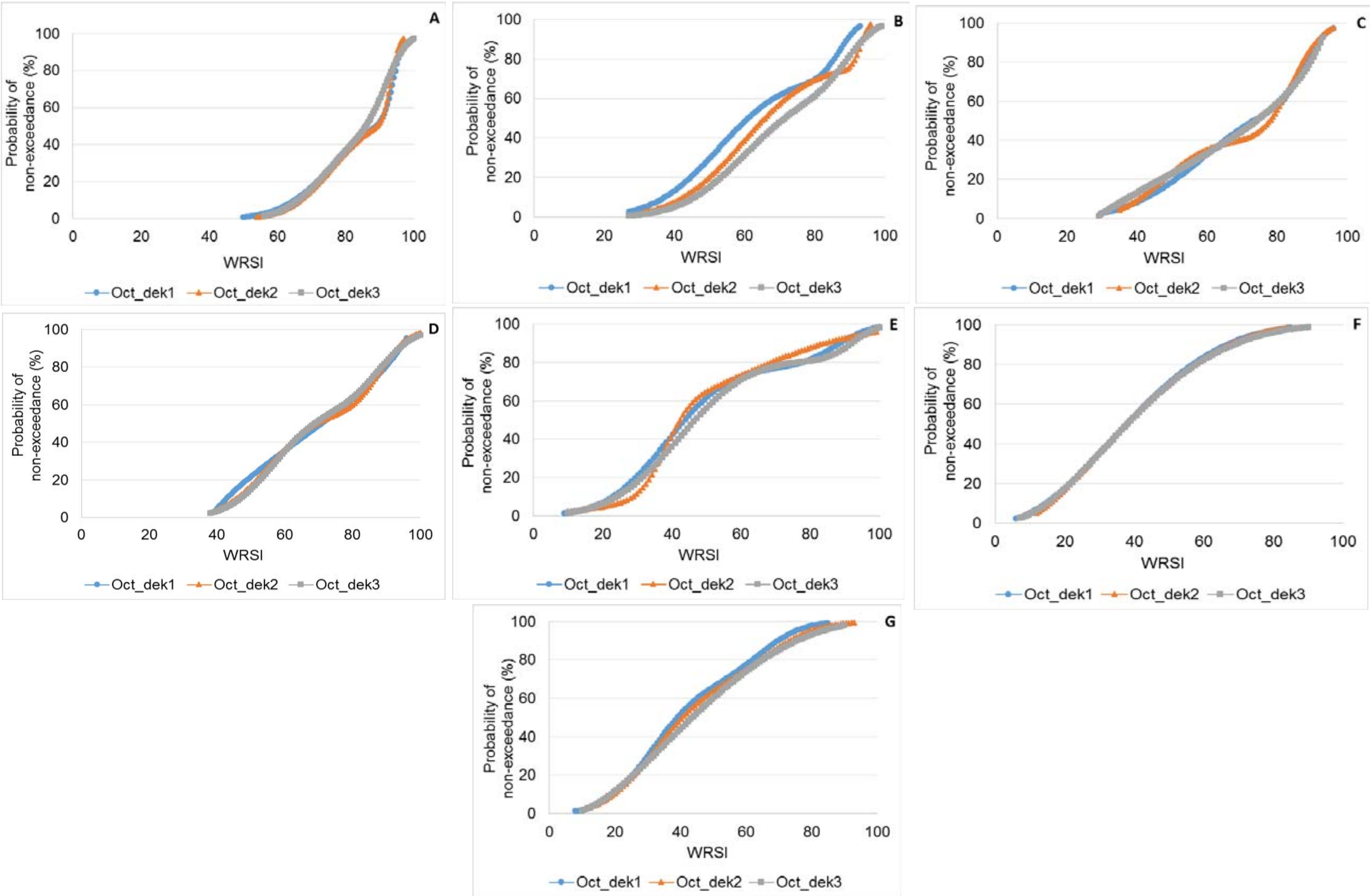

Figure 29: Cumulative distribution function of WRSI during the growing season of maize relative to planting in October for stations Levubu (A), Lwamondo (B), Thohoyandou (C), Tshiombo (D), Punda Maria (E), Sigonde (F) and Pafuri (G)

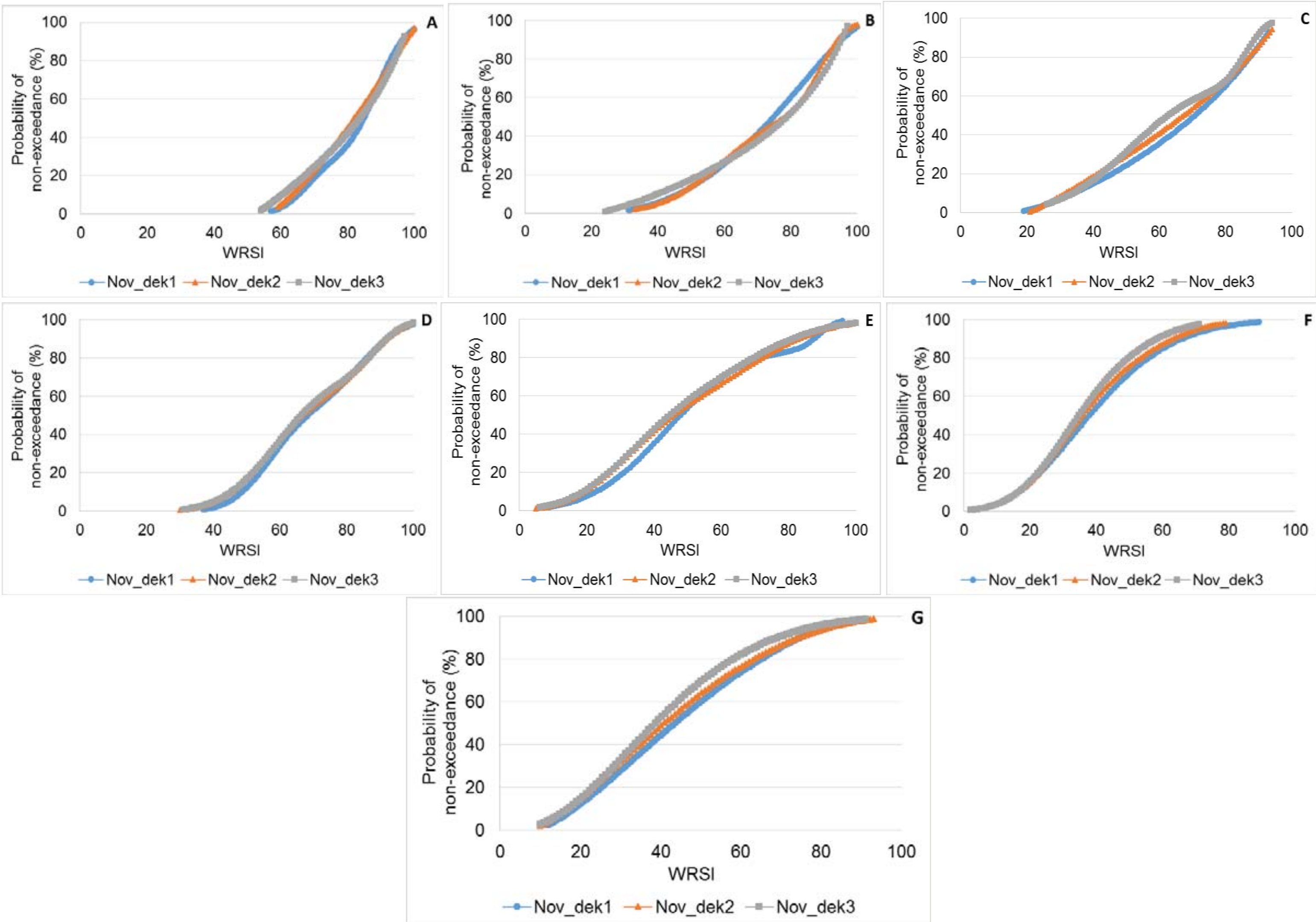

Figure 30: Cumulative distribution function of WRSI during the growing season of maize relative to planting in November for stations Levubu (A), Lwamondo (B), Thohoyandou (C), Tshiombo (D), Punda Maria (E), Sigonde (F) and Pafuri (G)

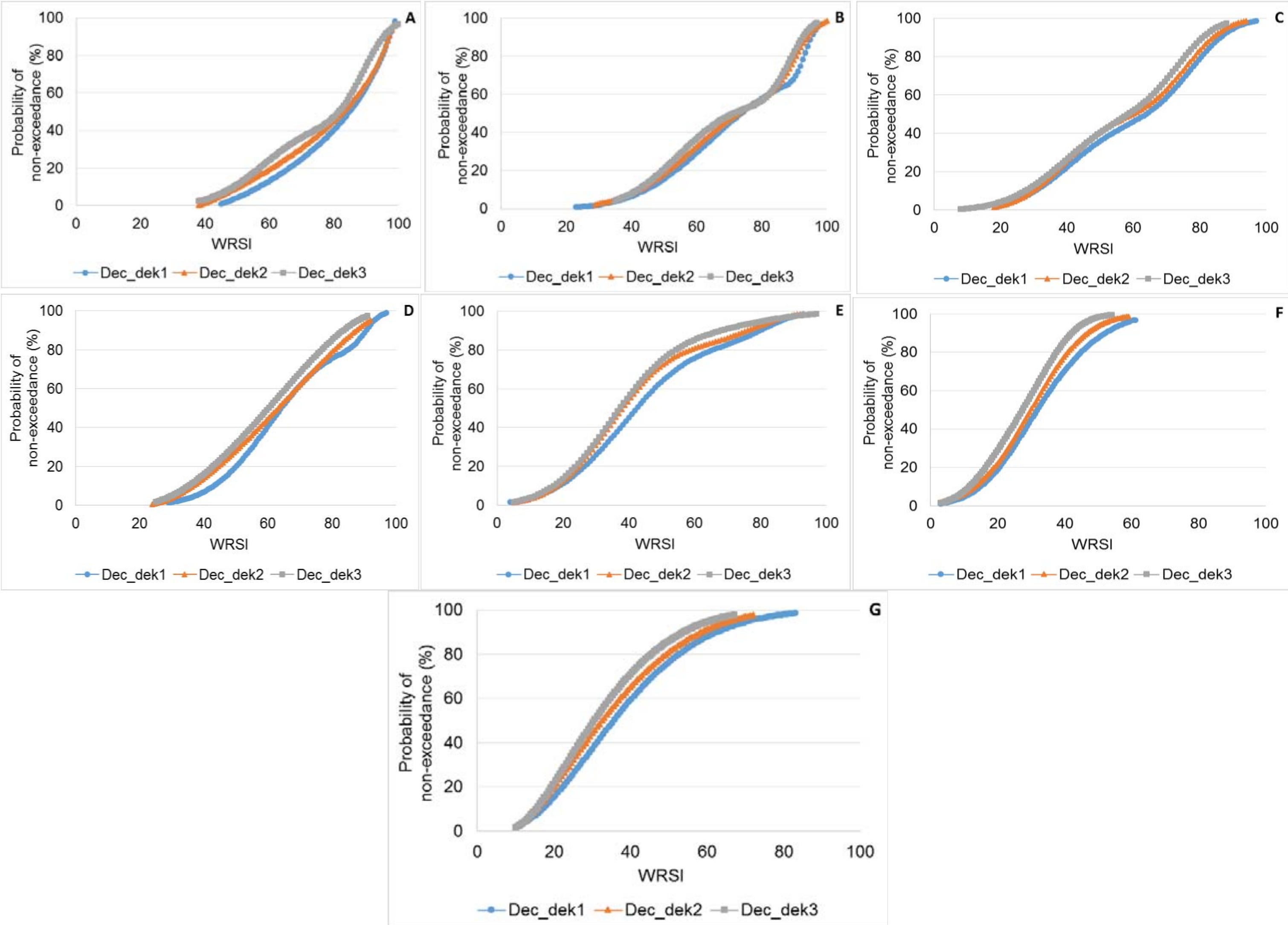

Figure 31: Cumulative distribution function of WRSI during the growing season of maize relative to planting in December for stations Levubu (A), Lwamondo (B), Thohoyandou (C), Tshiombo (D), Punda Maria (E), Sigonde (F) and Pafuri (G)

At an 80% probability of non-exceedance, conditions of no drought can be expected at Levubu and Lwamondo following all planting dates. Similar pattern can be observed at Thohoyandou and Tshiombo; however, cases of mild drought were observed following planting in December. This shows that the risk of experiencing drought every season in these areas is very low. On the contrary, given the same return period, drought conditions can be expected at stations that are located in the upper catchment (Punda Maria, Sigonde and Pafuri). At Punda Maria, planting in the first dekad of October to the first dekad of December could result in mild to moderate drought, while planting later (second dekad onwards) in December suggests probability of severe droughts (WRSI <60). Results further indicate that delay in planting at Sigonde and Pafuri could place the maize crop at higher risk of total crop failure as compared with the other planting dates.

The WRSI results indicate that the optimal planting date for rain-fed maize crop in the Luvuvhu River catchment area is during October to November, with WRSI values relatively higher than other growing periods. Although early planting can be advised, it is important to note that at Thohoyandou, planting too early (first dekad of October) might place crops grown in this area under drought stress. This indicates that there is a risk that water requirements of the crop will be met only slightly during critical periods of the growing season, following this planting date. Dryland farmers can be advised to change their cropping patterns and rotations, and switch to crop varieties that are more tolerant to drought (Thomas, 2008).

4.4.6 Temporal evolution of drought and trends based on WRSI

The temporal patterns of WRSI (Figure 32 to Figure 34) reveal that the catchment encountered notable drought conditions at different severities during the analysed agricultural seasons. WRSI values corresponding to mild and moderate droughts showed to be more frequent at Levubu, Lwamondo, Thohoyandou and Tshiombo. This was commonly observed once every two to three seasons.

There have also been notable widespread extreme droughts in the past, including 1983/84, 1988/89, 1991/92, 1993/94, 2001/02, 2002/03, 2004/05 and 2014/15. These historical droughts were recorded at all stations except Levubu, where the drought was observed to be less intense. Previous findings recorded by the Agricultural Disaster Management Policy (2011) stated that the 1991/92 drought was the most severe across the whole country. Moreover, a report conducted by Pretorius & Smal (1992) indicated estimates of a decline in the gross value added by the agricultural sector based on summer crop estimates for 1991/92 as compared with previous agricultural seasons.

Austin (2008) reported that in 2001, maize prices had dramatically increased within five months in the season. This increase could have been due to different influential factors such as world price of maize, the exchange rate, or the availability of maize in the other southern African countries (Chabane, 2002). By 2002, the average farming output of the country was recorded to have decreased by 75% of the previous output. These reductions resulted in reduced economic growth and loss of the much-needed foreign exchange normally derived from agricultural exports (FAO, 2004).

Planting in December resulted in more seasons being exposed to the occurrence of extreme droughts compared with planting in October and November. This is evident for all stations analysed. A previous study conducted by Mzezewa et al. (2010), using a station in Thohoyandou, indicated that the probability of receiving high rainfall (> 100 mm) was greatest in December (58%) and lowest in October (20%). It is worth noting that these findings do not imply December as being the optimum planting date and can therefore suggest that planting prior this month can place crops at a good probability of receiving considerable amounts of rainfall as the crop develops.

Furthermore, the least potential risk of crop damage was observed at Levubu with no occurrences of extreme droughts (WRSI <50) following planting during the second dekad of October to the third dekad of November, while December planting date revealed three extreme drought events during the third dekad of December. When looking at the occurrence of severe drought, it was seen that only two cases were observed relative to planting in October, followed by four and nine cases should planting occur in November and December, respectively. This implies that late planting could increase the risk of possible total crop failure in the region. Another evident observation is that at Punda Maria, Sigonde and Pafuri, extreme drought episodes (WRSI < 50) were generally predominant during the growing period irrespective of the different planting dates. This implies a high risk of total crop failure, making the upper regions of the catchment unsuitable for rain-fed maize production.

WRSI time series trends provided by the Spearman's rank correlation test did not show any significant increase or decrease. This implies that although the Luvuvhu River catchment has experienced several drought events in the past, the area has not become drier since the 1980s. Earlier findings have reported significant decreases in annual precipitation as well as a strong warming trend in the northern parts of Limpopo Province (Kruger & Shongwe, 2004; Kruger, 2006). However, these studies were carried out over long periods (1910-2004 for rainfall and 1960-2003 for temperature) over the whole province. Contrary to these findings, weak increasing trends were noted at Lwamondo following the December planting date, whereas at Thohoyandou the trend (ρ values of 0.5) was observed following planting in the first dekad of October. This increase in WRSI suggests that there has been a gradual decrease in drought severity following the respective planting dates, implying improved precipitation patterns in those regions.

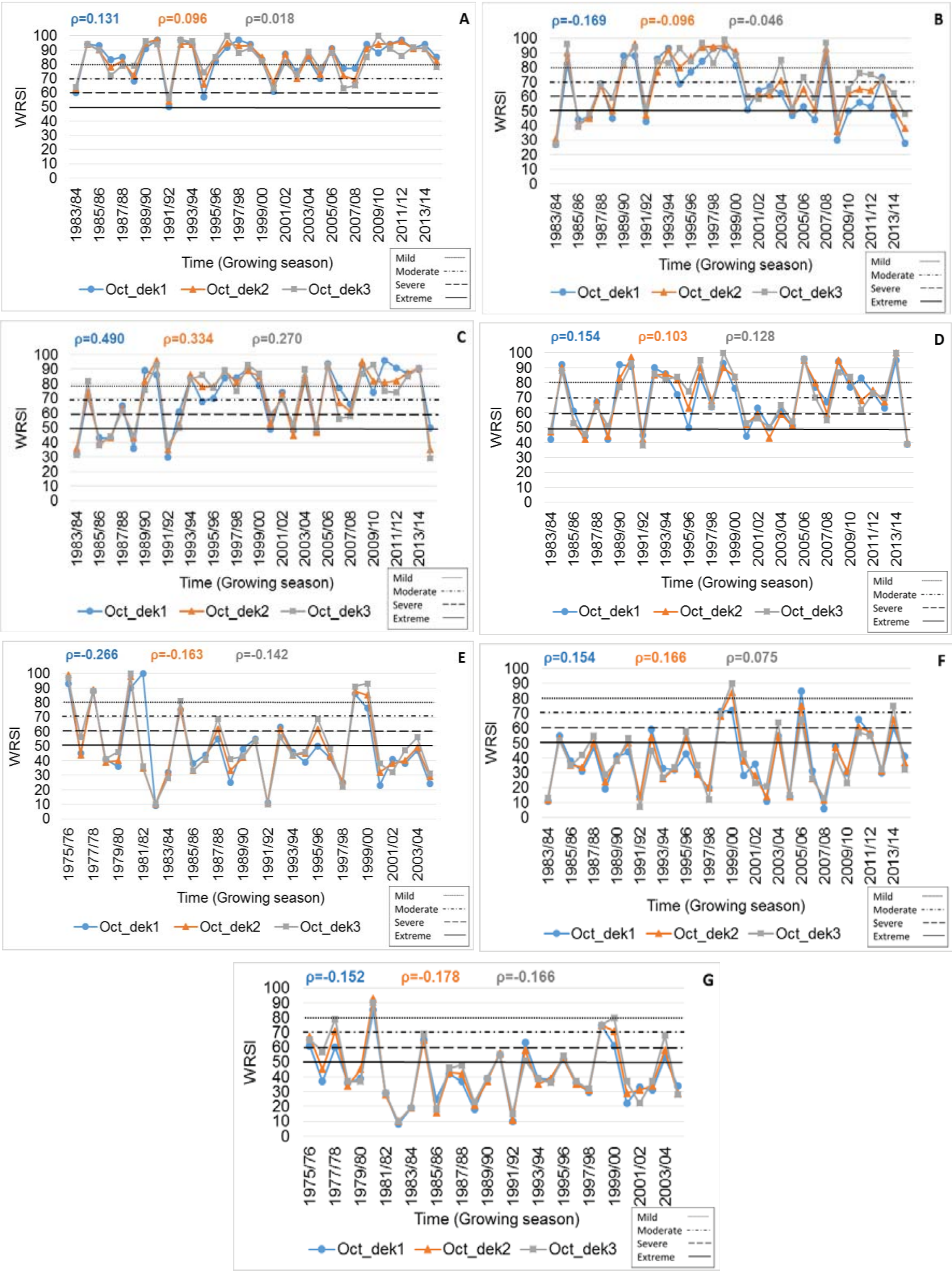

Figure 32: Observed WRSI time series and trends per growing season relative to planting in October for stations Levubu (A), Lwamondo (B), Thohoyandou (C), Tshiombo (D), Punda Maria (E), Sigonde (F) and Pafuri (G)

Figure 33: Observed WRSI time series and trends per growing season relative to planting in November for stations Levubu (A), Lwamondo (B), Thohoyandou (C), Tshiombo (D), Punda Maria (E), Sigonde (F) and Pafuri (G)

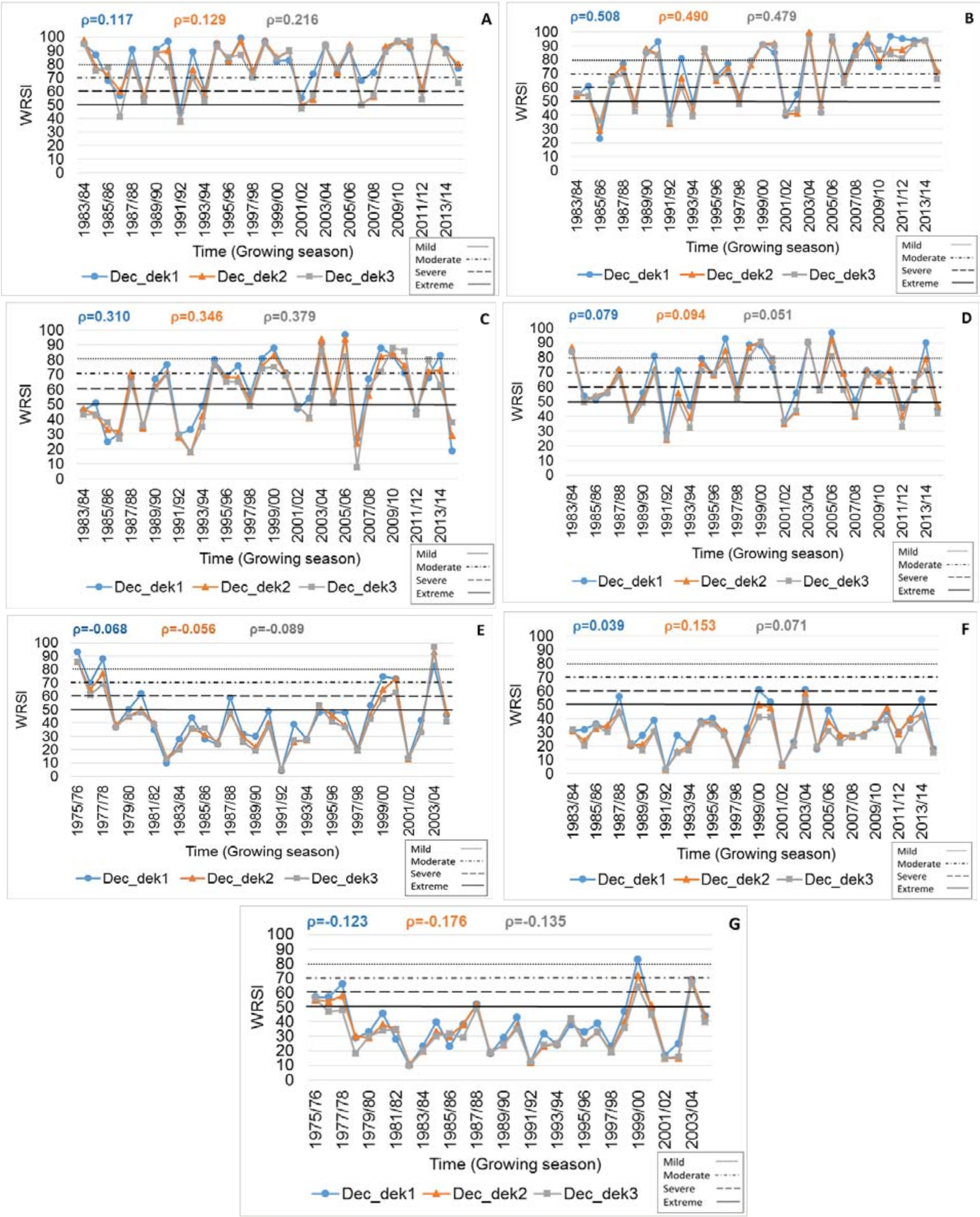

Figure 34: Observed WRSI time series and trends per growing season relative to planting in December for stations Levubu (A), Lwamondo (B), Thohoyandou (C), Tshiombo (D), Punda Maria (E), Sigonde (F) and Pafuri (G)

4.4.7 Observed extreme widespread dry and wet agricultural seasons using WRSI

The widespread drought events and wet seasons were evaluated to measure the extent to which the water requirements of the crop had been met during each stage of the growing season. It appears (Figure 35 to Figure 37) that the droughts were due to a deficit of water starting from the 5th dekad to the 12th dekad of the growing period. This means that the rainfall experienced during that period did not meet the crop water requirements and therefore crops did not get sufficient water during the most critical stages (7th to 9th dekad), explaining the decline of WRSI line. This is consistent with literature, as it has been revealed that the maize crop is unable to resume growth and development after a severe drought at tasselling to silking stage (Whitmore, 2000). Another interesting finding is that at Sigonde, the extreme drought of 1991/92 was caused by lack of water throughout the growing season, with only four dekads receiving rainfall of less than 10 mm per dekad. The resulting WRSI during that season was zero.

During the 1993/94 season, it is interesting to note that despite the good start to the season, with fairly good rainfall occurring during the 1st to 4th dekad, conditions at the end of the season resulted in WRSI values of < 50. A similar study has shown that the 1991/92 drought effects worsened until the end of 1993, correspondingly affecting the hydrological water supply (Trambauer et al., 2014). This prolonged drought was widely experienced throughout the country and in other parts of southern Africa, including Botswana, Zimbabwe and Mozambique, causing widespread crop failure and livestock mortalities (FAO, 2004). After the year 2000, the area experienced extreme drought for two consecutive seasons (2001/02 and 2002/03), and again during 2004/05 at Lwamondo and Sigonde. Thereafter, the area was again struck by extreme drought after a decade (2014/15) at the moderate and low rainfall regions.

In contrast, results showed extreme wet seasons as being 1987/88, 1999/00, 2003/04 and 2013/14. Figure 37 shows that during the course of these seasons, rainfall was equal or more than the corresponding water requirements for a considerable number of dekads including the critical stage of the crop. It was further noted that for some dekads the index was reduced despite the high rainfall amounts that were received. According to Allen et al. (1998), this is because the index is not only reduced when the crop undergoes water stress, but also when the water surplus is > 100 mm. However, the WRSI value at the end of these seasons reflected good crop performance at the high and moderate rainfall regions and average crop performance at the low rainfall regions.

The total crop failure during the notable seasons could be explained by the lack of rainfall during the growing season at the low rainfall regions as well as during the sensitive stages at the high and moderate rainfall regions. This intra-seasonal variability of rainfall could result in deficient uptake of the required water by crops due to a reduction of moisture in the root zone (Das, 2012). However, during the wet seasons it was observed that the rainfall was evenly distributed, thus resulting in WRSI values corresponding to good crop performance, implying satisfactory yields.

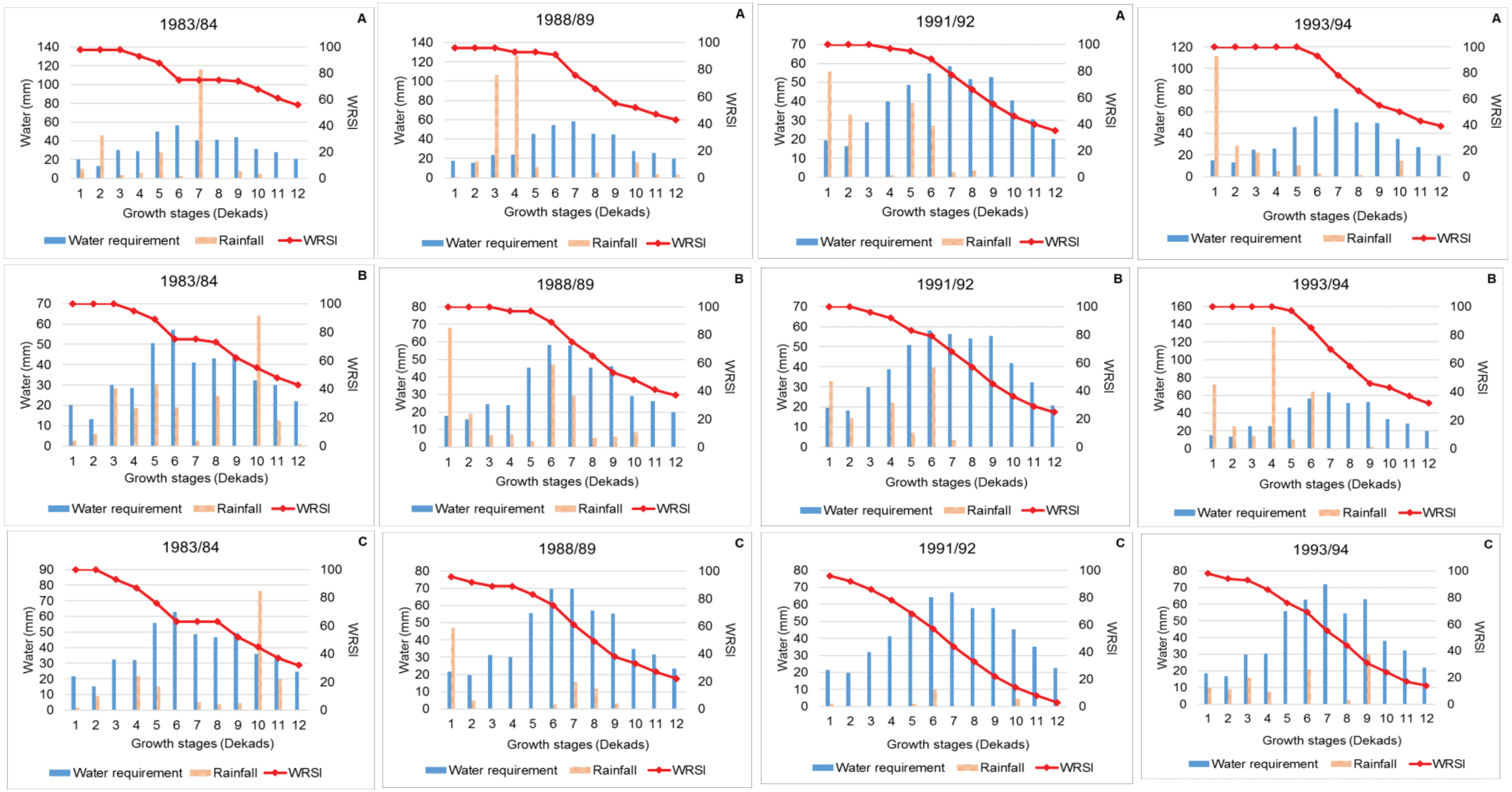

Figure 35: Crop water balance and WRSI for each dekad of the growing period, during notable widespread drought seasons (1983/84, 1988/99, 1991/92 and 1993/94), for stations Lwamondo (A), Tshiombo (B) and Sigonde (C)

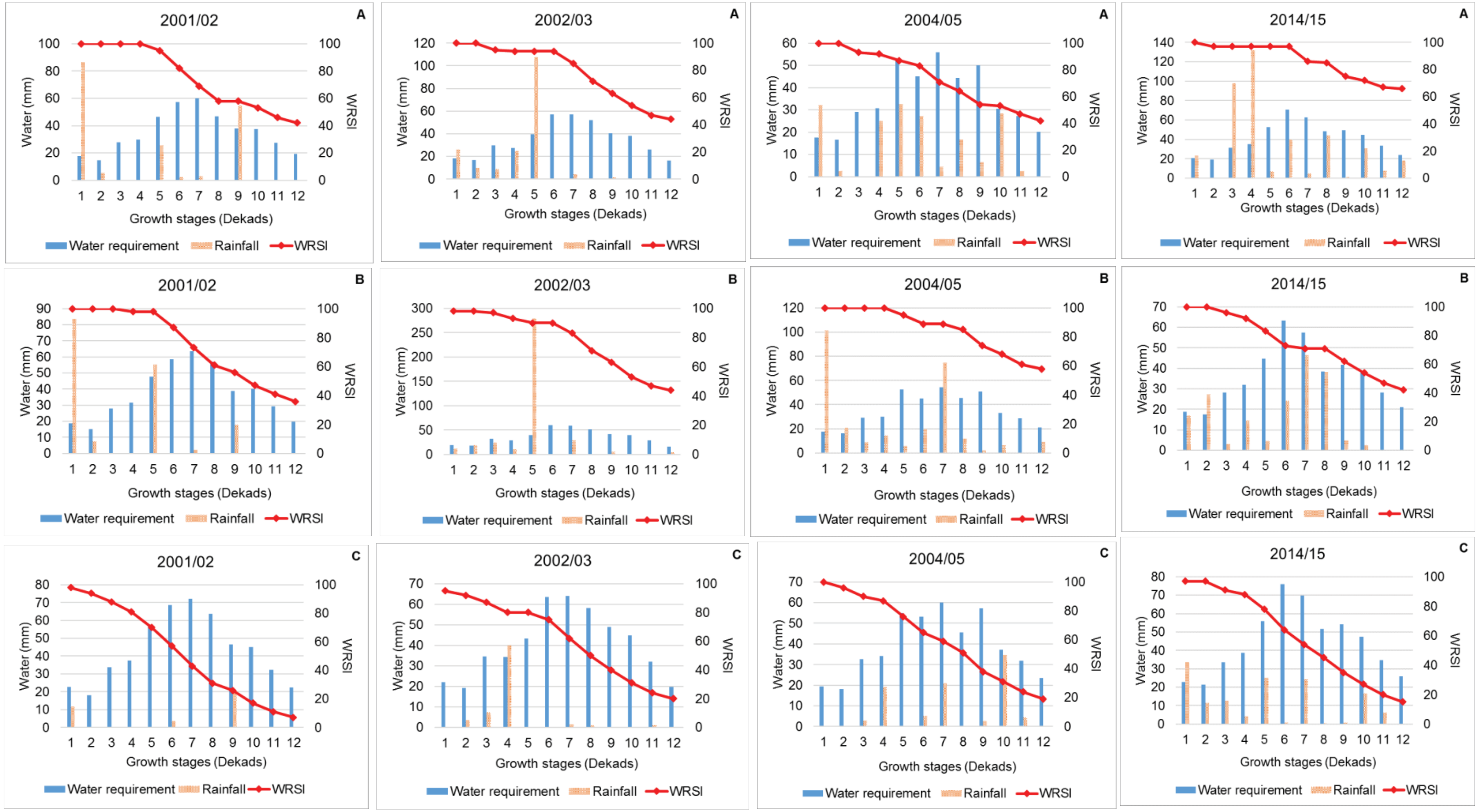

Figure 36: Crop water balance and WRSI for each dekad of the growing period, during notable widespread drought seasons (2001/02, 2002/03, 2004/05 and 2014/15), for stations Lwamondo (A), Tshiombo (B) and Sigonde (C)

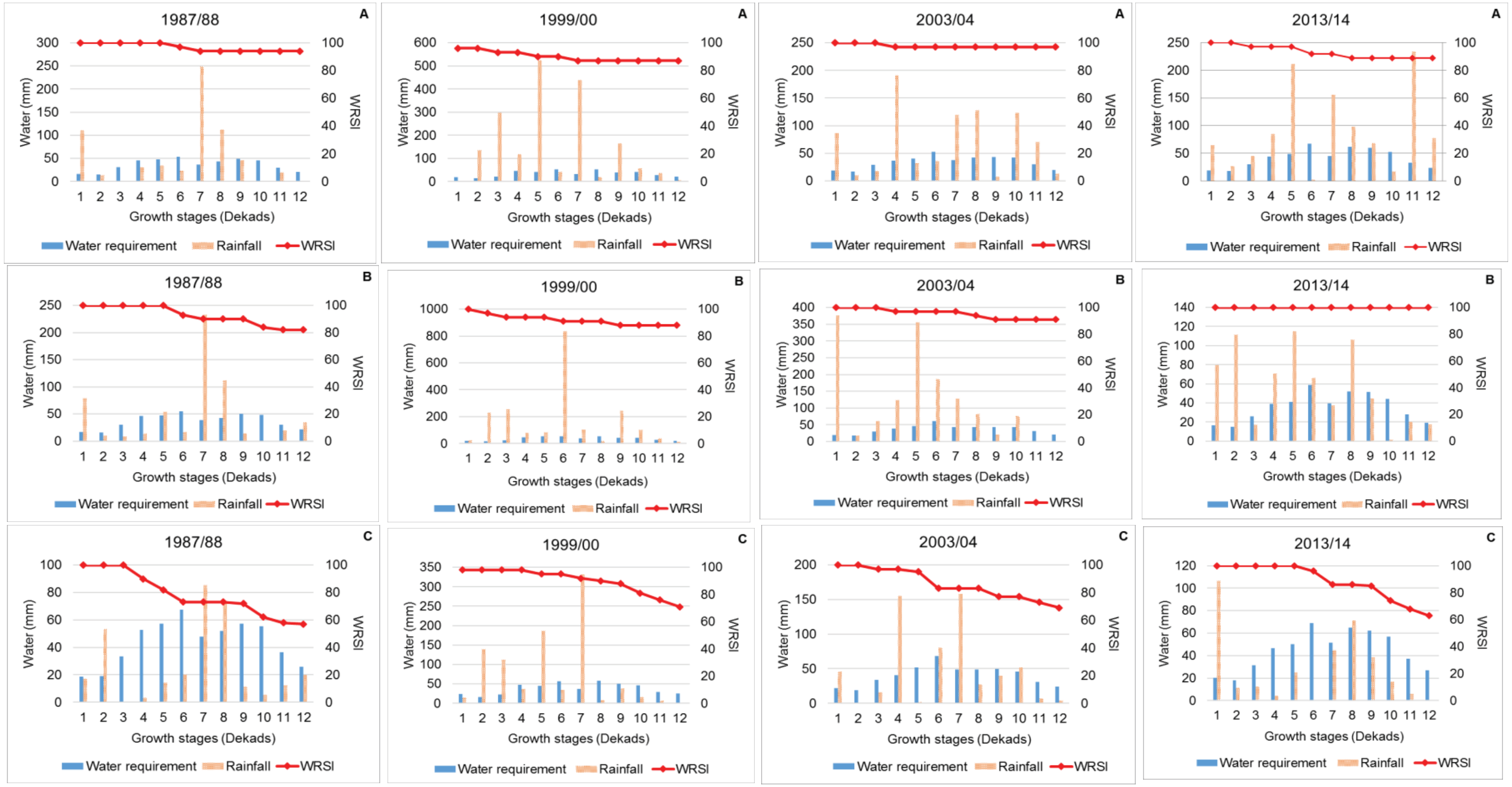

Figure 37: Crop water balance and WRSI during widespread wet seasons, for stations Lwamondo (A), Tshiombo (B) and Sigonde (C)

4.4.8 Maize crop performance for future climates simulated by WRSI

Figure 38 presents the results regarding projected drought conditions corresponding to maize crop performance, by means of the WRSI, with the frequency between the future climates clearly seen in Figure 39. Generally, mild drought conditions showed to be more frequent than other drought categories, as expected. Results also showed that stations receiving a mean annual rainfall of < 600 mm (Punda Maria, Mhinga and Sigonde) are drier than the high and moderate rainfall regions (Figure 39).

Mild droughts are expected to occur once in every agricultural season at Tshiombo, Punda Maria, Mhinga and Sigonde, with a frequency of >80% during the near-future to the far-future period. However, at Levubu and Lwamondo, these conditions can only be noted during the far-future period. The average frequency of observed moderate drought conditions during the base period was 50%, with the highest (74%) noted at Mhinga, while a low of 23% was seen at Levubu. The frequency of this level of drought corresponding to average crop performance at Sigonde is expected to remain the same during the near-future climate period, with an increase of 18% seen for the far-future climate.

Results indicated severe drought conditions (WRSI < 60) that often lead to poor crop performance to increase during the near-future and far-future climate period, as compared with the base period. The highest increase in frequency (40%) can be noted at Tshiombo and Mhinga during the far-future. Figure 38 further shows that widespread conditions relating to total crop failure were predicted during the following agricultural seasons of the near-future period: 2023/24, 2025/26, 2031/32, 2032/33, 2038/39, 2039/40, 2042/43, 2044/45, 2048/49 and 2052/53. Meanwhile, these conditions can be expected in the far-future, during the following agricultural seasons: 2057/58, 2063/64/65/66, 2067/68, 2069/70, 2071/72, 2076/77, 2079/80, 2083/84/85/86.

It can be noted that the severity of drought is likely to intensify during the far-future period, with the two predicted extreme droughts (2063 and 2083) predicted to prolong for three consecutive seasons. This indicates a high risk of crop failure caused by drought, suggesting that most regions of the catchment could not be suitable for growing the maize crop during those seasons. Furthermore, it appears that the WRSI mean during the near-future to the far-future period (Table 28) can be expected to be lower than the base period, suggesting more intense drought events. This is evident at all stations, with a resultant p-value < 5%, agreeing on a statistically significant shift towards drier conditions during these respective climate periods. However, at Sigonde, these conditions were noted only for the far-future, and the near-future is not expected to significantly decrease from the base.

Findings reported by Engelbrecht et al. (2015) projected significant reduction in rainfall over the subtropics, as well as a temperature increase of 4-7°C towards the end of the 21st century relative to present-day climate under the SRES[1] A2 (a low mitigation) scenario. However, it is interesting to note that the expected conditions resulting in total crop failure by the end of the

[1] Special Report on Emissions Scenarios

century might be due to the projected high evapotranspiration rates, which may also intensify the drought more quickly during the growing period regardless of the high precipitation rates experienced in the previous seasons (Törnros & Menzel, 2014). This will plausibly have an adverse impact on rain-fed maize farmers in the Luvuvhu catchment since they rely solely on maize and are considered economically poor by South African standards (DWAF, 2004).

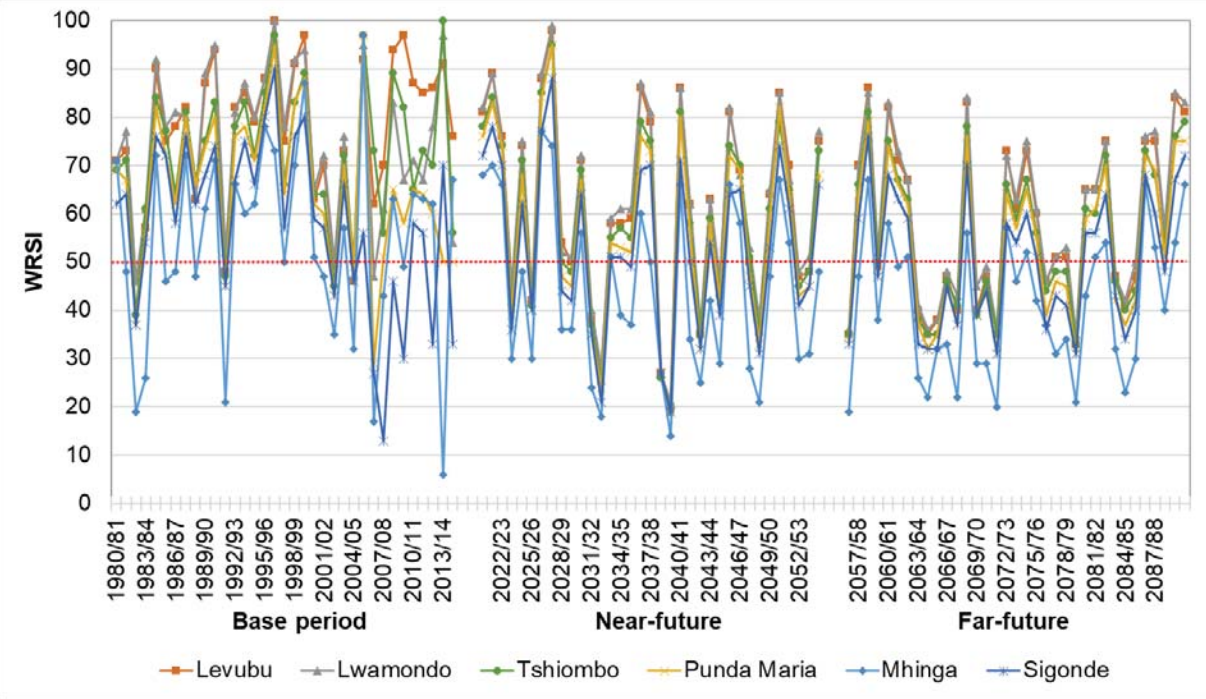

Figure 38: Simulated WRSI time series per growing season of the base period and future climate periods. The red dotted line represents the threshold for total crop failure

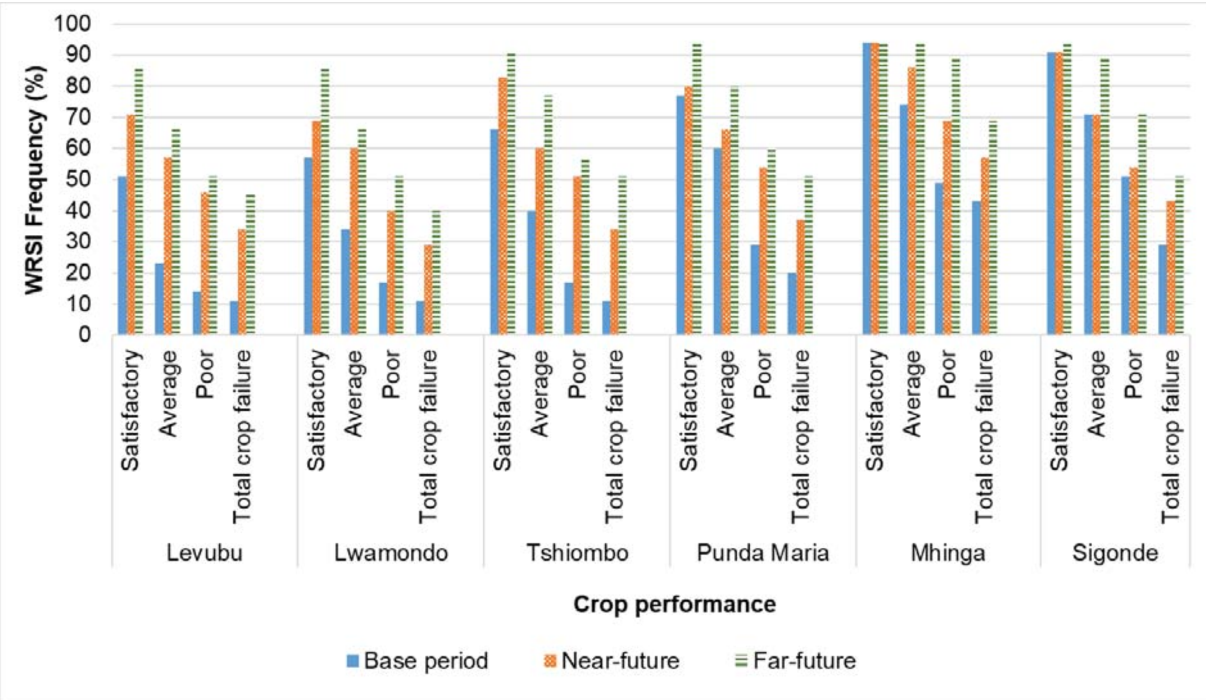

Figure 39: Frequency (%) of the different levels of drought representing the maize crop performance during future climates, relative to the base period, in the Luvuvhu River catchment

Table 28: Z-test between WRSI means of the future climates, relative to the base period, in the Luvuvhu River catchment. Values highlighted in italics differ statistically at α (0.05)

Station	Stats parameters	Base	Near future	Far future
Levubu	Mean	77	61	58
	Known variance	236	415	262
	z	0.00	3.85	5.07
	p (Z ≤ z) two-tail	1.00	*0.00*	*0.00*
	z-critical two-tail	0.00	1.96	1.96
Lwamondo	Mean	75	61	59
	Known variance	247	409	250
	z	0.00	3.09	4.12
	p (Z ≤ z) two-tail	1.00	*0.00*	*0.00*
	z-critical two-tail	0.00	1.96	1.96
Tshiombo	Mean	72	58	55
	Known variance	218	373	208
	z	0.00	3.49	4.90
	p (Z ≤ z) two-tail	1.00	*0.00*	*0.00*
	z-critical two-tail	0.00	1.96	1.96
Punda Maria	Mean	66	56	59
	Known variance	246	381	250
	z	0.00	2.23	4.12
	p (Z ≤ z) two-tail	1.00	*0.03*	*0.00*
	z-critical two-tail	0.00	1.96	1.96
Mhinga	Mean	54	44	41
	Known variance	417	325	193
	z	0.00	2.15	3.07
	p (Z ≤ z) two-tail	1.00	*0.03*	*0.00*
	z-critical two-tail	0.00	1.96	1.96
Sigonde	Mean	58	52	50
	Known variance	306	308	175
	z	0.00	1.29	2.14
	p (Z ≤ z) two-tail	1.00	0.20	*0.03*
	z-critical two-tail	0.00	1.96	1.96

4.5 Conclusions

The main objective of this chapter was to assess past and future occurrences of drought in relation to its effects on the development of maize in the Luvuvhu River catchment area of South Africa. The study used SPEI and WRSI to detect the onset, severity and temporal variations of drought. Variations were observed in how these two indices were able to identify drought occurrences. The SPEI was used to account for the influence of evapotranspiration in determining the possible effects of drought for each stage of the crop, while the WRSI captured the crop's vulnerability to the occurrence of droughts by indicating the extent to which the crop water requirements have been satisfied during the growing season. Results given by the two drought indices (SPEI and the WRSI) are summarised as follows:

- The frequency analysis of drought given by the SPEI revealed that for the emergence and early vegetative stage, a high risk of frequent droughts was observed following planting in November-December at five of the seven stations. For stage 2 (vegetative), the risk was noted for the October-November planting. Furthermore, results for stage 3 (flowering to grain-filling) showed that severe to extreme droughts were mostly observed at Levubu, Lwamondo, Thohoyandou and Tshiombo relative to planting in December, while this planting period gave lower risks for stations in the low-lying plains of the upper catchment (Punda Maria, Sigonde and Pafuri).
- WRSI values corresponding to more intense drought conditions were reflected during the December planting date for all stations. Extreme droughts occurred once in five seasons, regardless of the planting date, at Punda Maria, Sigonde and Pafuri.
- SPEI results identifies notable seasons subjected to extreme widespread drought as 1983/84 and 1991/92; while WRSI reflected 1983/84, 1988/89, 1991/92, 1993/94, 2001/02, 2002/03, 2004/05 and 2014/15 as having experienced extreme widespread droughts.
- Generally, there were no significant trends noted with the exception of some stations revealing weak decreasing drought trends (ρ = of 0.5 for WRSI at Thohoyandou; Levubu and Lwamondo with ρ = of 0.4 for SPEI).
- Analysis of water balance during the widespread droughts given by SPEI showed that the occurrence and the severity of drought were aggravated by the low rainfall amounts together with high evapotranspiration rates throughout the rainfall season.
- WRSI results also showed the 1991/92 drought as being the worst; however, unlike the SPEI, it was noted that the drought effects of this drought worsened until the end of 1993.
- SPEI results further revealed 1999/00 and 2012/13 as being the extreme wet seasons in the area for the analysis period; WRSI results showed the extreme wet seasons as being 1987/88, 1999/00, 2003/04 and 2013/14.
- Future climates analysis by SPEI showed expected widespread occurrences of severe to extreme droughts (SPEI values of -1.5 to -2) during the 2039/40, 2048/50, 2063/64, 2066/67 and 2078/79 agricultural seasons.
- Projections given by WRSI showed a tendency to significantly intensify during the far-future relative to the base at all stations. A frequency increase of severe to extreme drought conditions (WRSI < 60), which often lead to poor crop performance and failure during the near-future to the far-future period, was projected.

5 HYDROLOGICAL MODELLING

5.1 Introduction

Flooding has often been identified as a natural, climatic and recurring event, during which an area of land is covered with an extensive amount of water over a short period of time (Gichere et al., 2013). This occurs depending on the parameters that govern the flood phenomena such as rainfall amount, catchment area and soil antecedent moisture content (Alexakis et al., 2012; Gichere et al., 2013).

In some cases, this type of event is not natural in its cause, but rather, anthropogenic (Tshikolomo et al., 2013). For example, a dam wall or a water pipeline bursting in an impervious area may also lead to flooding (Kozlovac, 1995; Etuonovbe, 2011). In most cases, flooding is caused by an event whereby heavy and continuous rainfall occurs for an extended period of time, which then exceeds the infiltration capacity of soil or flow capacity of rivers, streams and coastal areas, thus resulting in run-off (Hirschboeck et al., 2000; Ezemonye & Emeribe, 2011; Singo et al., 2012; Tshikolomo et al., 2013). The run-off produced from this climatic condition (heavy rainfall) may then cause the catchment to respond in a manner that results in flooding (O'Connell et al., 2007; Warburton et al., 2010).

The geographical distribution of river floodplains may also have an influence on flood occurrence (Smith, 2001). According to Hart et al. (2013) and Wetterhall et al. (2015), South Africa's rainfall distribution varies considerably both spatially and temporally, which has led to more floods across the country (Kane, 2009). The frequency and distribution of floods are usually defined by the cycle of ENSO events where ENSO is an irregular phenomenon that recurs every two to seven years (Kane, 2009; Trenberth, 2011). The phenomenon accounts for the extreme variability of climate in the global climate system (Allan, 2000). ENSO is often associated with rainfall in most parts of the southern African region, interchanging between two extreme events known as El Niño (drought) and La Niña (floods) (Allan, 2000; Moeletsi et al., 2011). These two events differ in magnitude, area of impact, onset, duration and cessation (Davis & Joubert, 2011).

Although some floods may be accounted for by climate change, documentation and classification of the different types of flood exists, including among others river floods, flash floods, structural failure, urban drainage and coastal flooding (Table 29) (DePue, 2010; Sauer, 2011). According to the SAWS, examples of floods that have occurred throughout South Africa over the past few decades, which display some characteristics mentioned in Table 29, include those that occurred in the years 1980, 1984, 1987, 1995, 2000, 2007 and 2010/11 (Dyson, 2009; Zuma et al., 2012).

Table 29: Different types of flooding and their characteristics (DePue, 2010)

Flood type	Cause	Impact	Duration
River floods	Inability of the river system to carry certain number of flows due to heavy rains or prolonged rains.	Floodplain areas along the riverbanks.	Slow onset and may last for a short or long period depending on rainfall characteristics.

Flood type	Cause	Impact	Duration
Flash floods	Heavy and localised rainfall over a short period of time in a steep or impervious catchment. Closely linked with structural failure.	Destruction of infrastructure such as bridges and roads.	Quick onset and lasts over a short period of time, but impacts are severe.
Structural failure	Structural failure after periods of heavy rainfall in a catchment due to inadequate structure design, or the dam design structure capacity has been exceeded.	Area along the structure and downstream residence if it is a dam.	Quick onset, occurring without warning and over a short period of time.
Urban drainage	The drainage is unable to handle the floods due to heavy and localised rainfall, or the design has been exceeded.	Urban areas and residence.	Bursting of pipes, without warning over a short period of time.
Coastal flood	Hurricanes and tropical cyclones along the coastal lines.	Impacts along the coastal area and may extend inland.	Quick onset and flooding may last for a long period.

Fatal flood events around the world have led to many projects in an attempt to solve some of the prevailing flood control problems (Krzhizhanovskaya et al., 2011). These studies have identified an increase in the frequency of flood events over the years, with climate change being one of the main root causes (Millington et al., 2011; Aronica et al., 2012; Norouzi & Taslimi, 2012; Xie et al., 2012). The increases accompanied by hydrological alteration and rainfall variation may have great effects, not only on dam and bridge designs, but also on future food security production due to reduced yield (Lauer, 2008; Millington et al., 2011; Sauer, 2011; Syaukat, 2011). Floods usually occur with no warning; under future climate conditions, flood frequency is expected to increase even further (Kang et al., 2009). Thus, it is essential for hydrologists and engineers to be able to predict the magnitude and frequency of floods for planning and mitigation (Chetty & Smithers, 2005; Geoscience Australia, 2013).

This study focuses on the Luvuvhu River catchment in the Limpopo Province of South Africa, which has been identified and considered vulnerable to flooding (Muinga, 2004). As much as flood events have been occurring more frequently in the world (Xie et al., 2012), the Luvuvhu River catchment is no exception. The catchment's vulnerability to flooding is said to be caused by tropical depressions and the geographical distribution of river floodplains (Smith, 2001; Muinga, 2004; Wetterhall et al., 2015). This has led to the catchment experiencing extreme flooding events over the past years; washing away some of the crops and thus resulting in crop failure and reduced crop yield.

This study aims to estimate design flood peaks in the Luvuvhu River catchment by simulating run-off using QSWAT 1.3 2016, an interface between the 2012 version of the Soil and Water Assessment Tool (SWAT) model and QGIS 2.6.1 software (Figure 40). The specific objectives are as follows:

- To choose a hydrological model (QSWAT) that will best simulate streamflow using observed climate, land use and soil data.
- To conduct a streamflow simulation from historical climate data using QSWAT.
- To calibrate and validate the model using observed data of Luvuvhu River catchment.
- To conduct a flood frequency analysis and design flood estimation for the Luvuvhu River catchment using simulated data from the SWAT model.

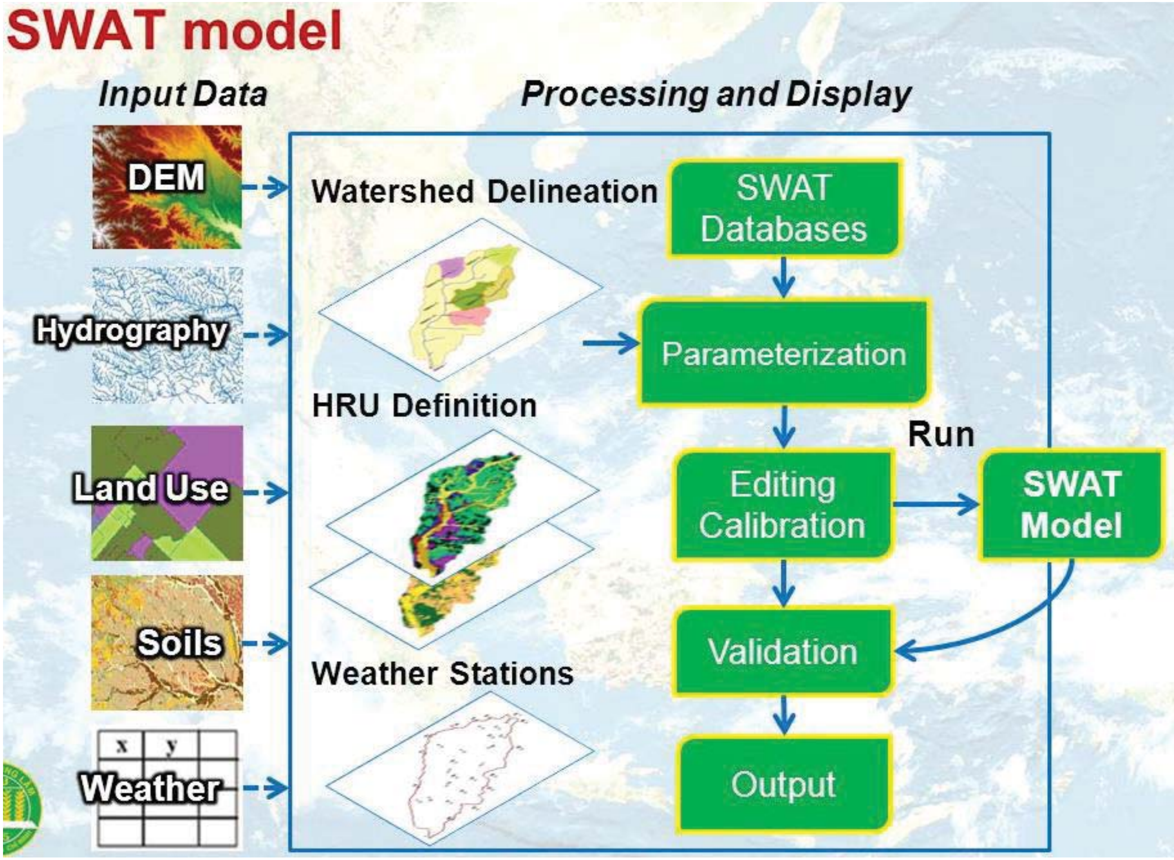

Figure 40: SWAT model (source: Garrison, 2012)

5.2 Data

5.2.1 Climate station data

Climate data for four stations in the Luvuvhu River catchment, which was obtained from the ARC-ISCW, was used for this study. Their locations and station information are shown in Table 30. The weather stations chosen were selected according to the availability of data and position in the catchment, so that there would be proper representation of the whole Luvuvhu River catchment. Stations with fewer years of data were disregarded.

Although acquiring historical data is difficult, be it climatological or hydrological, it is still essential to obtain such data and ensure that it undergoes quality and homogeneity checks using scientifically proven gap-filling techniques (Chen & Liu, 2012). Hydrological simulation models require observed long-term daily climatic data such as daily rainfall, maximum and minimum air temperature, relative humidity, solar radiation and wind speed for modelling purposes (Clemence, 1997; McKague et al., 2003; McKague et al., 2005; Tingem et al., 2007; Safeeq & Fares, 2011).

Table 30: Summary of climate stations

Station	Latitude (º)	Longitude (º)	Altitude (m)	Start date	End date	Years
Levubu	−23.04175	30.1505	880	1983/01/01	2015/06/30	32
Lwamondo	−23.044008	30.37361	648	1978/01/01	2015/06/30	37
Sigonde	−22.3965	30.71308	416	1983/01/01	2015/06/30	32
Tshiombo	−22.80147	30.48145	650	1983/01/01	2015/06/30	32

Rainfall data was patched using an IDW method that is based on the concept of Tobler's law of geography (Chen & Liu, 2012; Moeletsi et al., 2016). The method assigns a value to the missing data using neighbouring stations with known values that are within a certain radius from the weather station to be patched (Chen & Liu, 2012). Three closest weather stations were considered to implement the IDW method using the adjustment of power of two ($\propto = 2$):

$$\hat{R}_p = \sum_{i=1}^{N} w_i R_i \quad (25)$$

$$w_i = \frac{d_i^{-\propto}}{\sum_{i=1}^{N} d_i^{-\propto}} \quad (26)$$

Where

$\hat{R}_p$ is the estimated rainfall data value in mm for the missing value,

R_i is the measured rainfall from the closest rainfall stations in mm,

N is the number of rainfall stations used,

w_i is the weighting of each rainfall station,

d_i is the distance from each rainfall station to that with the missing rainfall, and

$\propto$ is the power or control parameter.

Minimum and maximum air temperatures were patched using the method known as MLR (Moeletsi et al., 2016). The method considers the best correlated stations (Montgomery et al., 2006). In this case, the five best correlated stations were chosen and a linear regression line that best defines the five stations was identified. Thus, the regression equation (Equation 27) obtained from the regression line was then used to estimate the missing air temperature values (Equation 28) (Montgomery et al., 2006):

$$y = \beta_0 + \beta_1 x_1 + \beta_2 x_2 + \varepsilon \ (27)$$

$$y = \sum_{i=1}^{N} \beta_i x_i + \beta_0 \quad (28)$$

Where

y is the estimated value,

β_0 is the intercept of the regression plane,

β_i $(\beta_1, \beta_2 \ldots)$ is the slope coefficient,

x_i $(x_1, x_2 \ldots)$ are the known variables,

N is the number of stations, and

ε is the error term.

Since daily shortwave radiation measurements were not available, daily sunshine hours were used to calculate solar radiation. Solar radiation was calculated using the equation developed by Ångström in 1924 (Equation 29), where solar radiation is related to radiation received at the top of the atmosphere (extra-terrestrial radiation) R_a and the fraction of actual to maximum possible sunshine hours n (Ncube, 2006):

$$R_s = \left[a + b\frac{n}{D}\right] R_a \quad (29)$$

Where

R_s is the daily solar radiation in (MJ·m^{-2}),

a, b are the regression constants for estimation of shortwave radiation from sunshine duration, and

the general values for southern Africa are 0.24 and 0.53 respectively.

The constants vary seasonally, regionally and depend on the time scale (i.e. daily, weekly or monthly):

n is the actual sunshine duration in hours,

D is the day length in hours (*h)*, which varies with latitude and day of year,

R_a is the solar radiation received on a horizontal plane at the top of the atmosphere (i.e. extra-terrestrial solar irradiance in MJ·m^{-2}).

Table 31 summarises the interpolated values for D and R_a obtained from Table 46 and Table 47 in Appendix D by Wilson (1990) (cited by Ncube, 2006). The values together with the sunshine hour time series were used to calculate the solar radiation using the solar radiation equation above. Average daily solar radiation estimated for the four weather stations over the Luvuvhu River catchment depicted high solar radiation over the mountainous region of the catchment (Figure 41).

Table 31: Daily interpolated values for day length and extra-terrestrial solar irradiance for 22 °S

	Jan	Feb	Mar	Apr	May	Jun	Jul	Aug	Sep	Oct	Nov	Dec
D **(h)**	13.35	12.90	12.30	11.65	11.05	10.75	10.85	11.40	12.0	12.65	13.20	13.50
R_a (MJ·m^{-2})	40.79	42.44	34.10	29.72	24.17	22.88	23.30	27.30	33.46	36.98	41.36	41.27

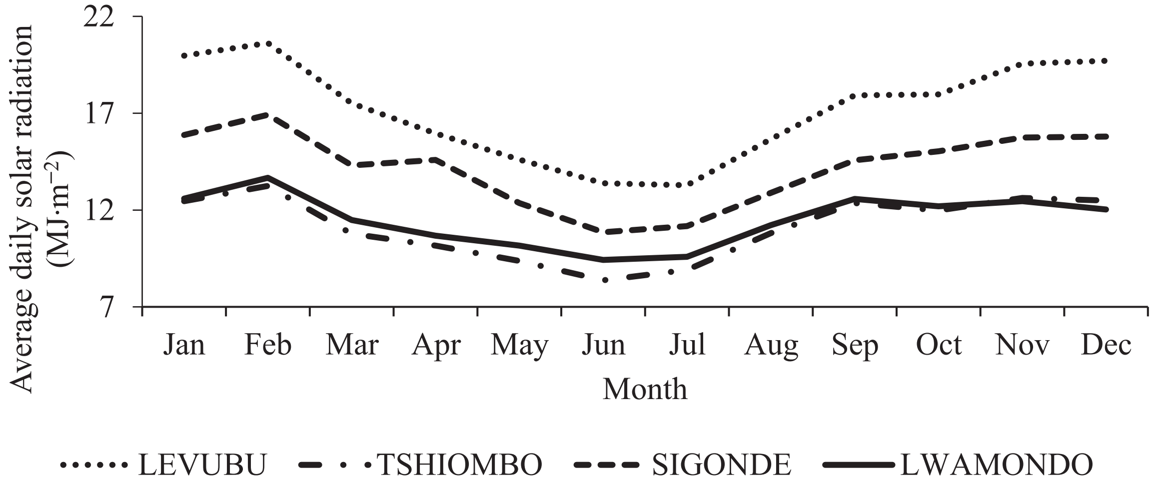

Figure 41: Average daily solar radiation of four selected stations (Luvuvhu River catchment)

Relative humidity (% *RH*) missing values were filled by using a method by Eccel (2012). For this method, estimations of water vapour pressures at the maximum (*Tx*) and minimum (*Tn*) air temperatures were required. This meant that the dew point temperature had to be estimated through the following assumptions (Eccel, 2012):

- The minimum air temperature was assumed to equal the dew point temperature.
- Correction of the first assumption was carried out depending on either the presence or absence of precipitation or the water balance of the previous day.

From the two assumptions, *RH* was estimated using air temperature using the following ratio:

$$RH = \frac{e}{e_s} \times 100 \ (30)$$

Where

e is the actual water vapour pressure (kPa), and

e_s the saturation water vapour pressure (kPa).

The water vapour pressure was calculated using a common exponential function (Allen et al., 1998):

$$e_s(T_n) = 0.61078 \ exp^{17.269 \frac{T}{T+237.3}} \ (31)$$

Where

e_s is the water vapour pressure (kPa) at the daily minimum air temperature (T_n) (°C).

Wind speed gaps were patched with a 2.0 m·s^{-1} value since it is a standard acceptable average wind speed infilling value for most locations (Pasi, 2014).

5.2.2 Streamflow data

Daily flow data from the DWS were used in this study. Stations with 30 years or more of data were selected. Only four stations were chosen from the streamflow weir stations located inside the Luvuvhu catchment: A9H003, A9H006, A9H012 and A9H013 (Table 32). These weir stations were chosen based on the following criteria: availability of data; representation of the catchment (location); and the data set included recent years. The streamflow data was used to calibrate simulated run-off.

5.2.3 GIS data (soil, land use and digital elevation model data)

Shape files were obtained from the ARC-ISCW geographical information system (GIS) data library. The data set contained the catchment delineation shape files of the Luvuvhu River catchment (Luvuvhu secondary, quaternary and river shape files), digital elevation model (DEM), land use map and soils map. Soil and land use data was taken from the national land type and land cover maps respectively; however, a new and rarely researched flow-path improved STRM_90 DEM was used for DEM.

The data was modified according to model requirements. The soil and land use were converted to raster files and together with the DEM were reprojected from WSG 84 to the WSG 84/ Universal Transverse Mercator (UTM) zone 36S projection, which was recommended as an improved projection since the study area has a north-south orientation. The soil, land use and DEM were projected into the same projection so that they would be accepted by the model.

Table 32: Summary of the weir stations

Station no.	Location	Catchment area (km²)	Latitude (°)	Longitude (°)	Data available	Years
A9H003	Tshinane River in haTshivhase	62	−22.89828	30.52391	1931-09-02 2015-04-15	84
A9H006	Livhungwa River in Barotta	16	−23.03577	30.27752	1961-11-13 2014-08-28	53
A9H012	Luvuvhu River in haMhinga	1758	−22.7705	30.88672	1987-11-04 2015-03-03	28
A9H013	Mutale River in Kruger National Park	1776	−22.43775	31.07832	1988-11-02 2013-02-14	25

5.3 Data Processing and Preparation

The processing tools used were:

- Microsoft Excel™ using pivot tables.
- pcpSTAT (Liersch, 2003) for precipitation data manipulation.
- QGIS Desktop 2.6.1 for all GIS data.

All maps generated were projected in the same projection (see Table 33).

Table 33: UTM for the Luvuvhu River catchment

Parameters	WSG 84/UTM zone 36S
Projection	Transverse Mercator
Spheroid	WGS_1984
Datum	D_WGS_1984
Zone	36
Central meridian	33
Reference latitude	0
Northing (m)	10000000
Easting (m)	500000
Scale factor	0.9996

5.3.1 DEM preparation

A DEM is required to facilitate the delineation of the catchment into multiple hydrologically connected sub-catchments (Dile et al., 2015). As mentioned previously, a flow-path improved 90 m DEM from the Shuttle Radar Topography Mission (STRM) was used. Although the 90 m resolution is considered to be inadequate, the study area catchment is large and using a less detailed DEM was advisable. The created DEM for the study area is depicted in Figure 42.

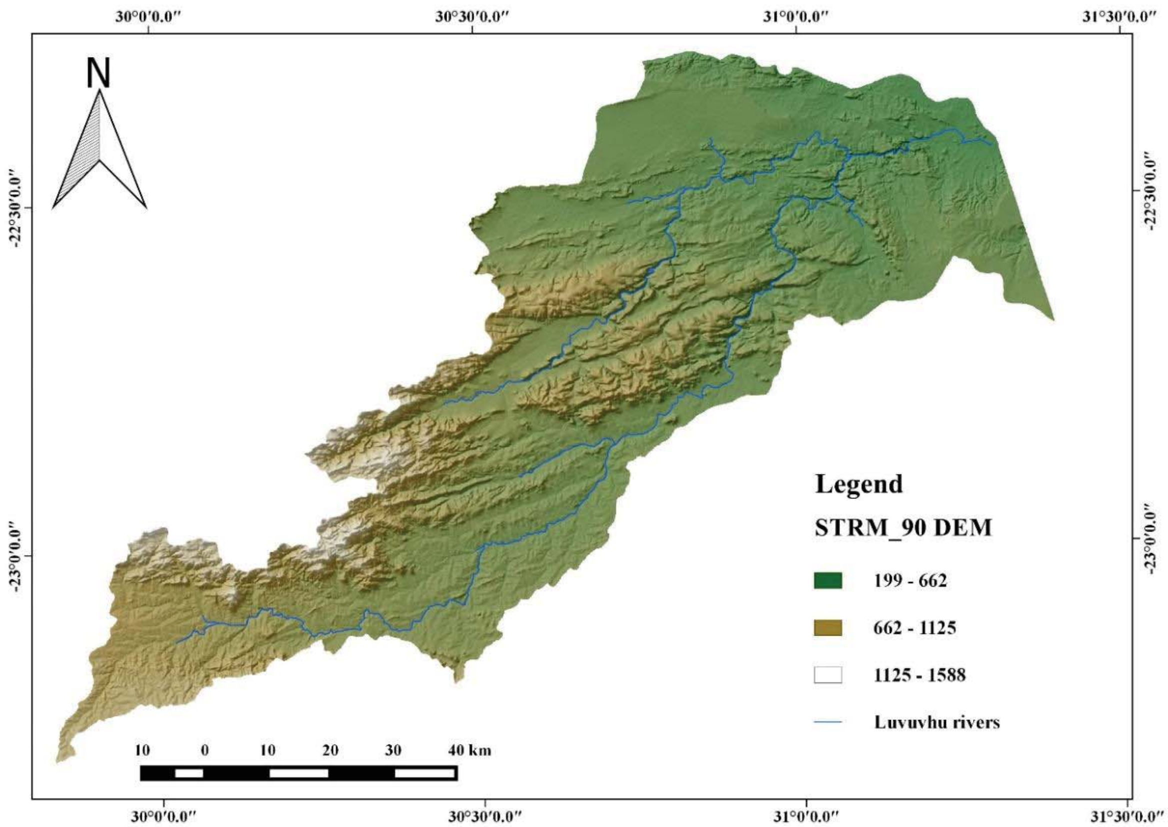

Figure 42: DEM for the study area (flow-path improved STRM_90m)

5.3.2 Land use and soil data preparation

Land use and soil data is important for determining soil and land use hydrologic parameters for the creation of hydrological response units (HRUs) (Ncube, 2006; Golmohammadi et al., 2014). The land use and soil shapefile maps, which were obtained from the ARC-ISCW, were clipped to fit the Luvuvhu River catchment.

The model requires that a table be created for land use and soil maps. The prepared tables should be copied to either the QSWAT project database, which is created when SWAT Editor software is installed, or the project database, which is created for every new project. In the case of the former, the tables are copied into every new project database created. For the latter, the tables are only for the particular project. For this study, the prepared tables were copied to the QSWAT project database.

5.3.2.1 Soils

In the case of the soil map, the table needs to have the string *soil* in its name to allow the table to be recognised by the model and be offered as an option for soil table on the drop-down menu. The table should contain the soil identity and the soil name. All the soil names used should also be available on the *usersoil* table found in the SWAT reference database. The soil map created is depicted in Figure 43 while the table created is depicted in Table 48 in Appendix D.

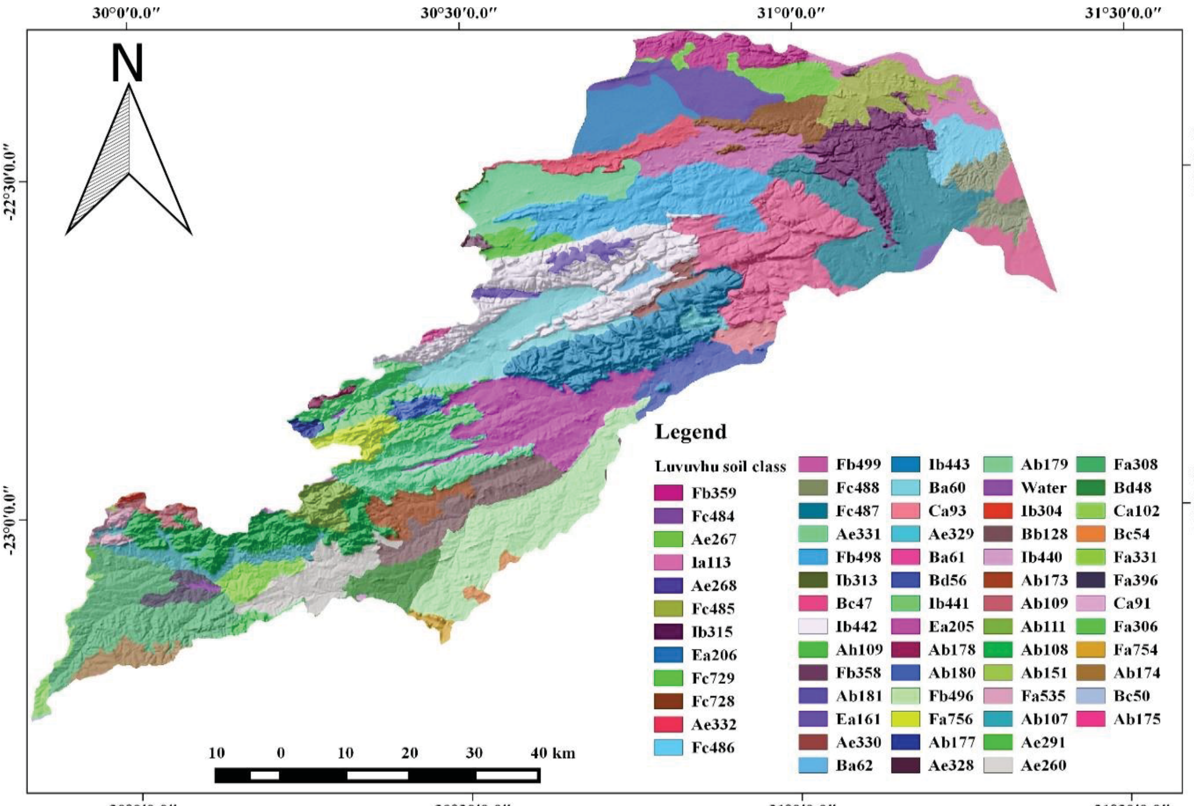

Figure 43: Soil map for the Luvuvhu River catchment

The SWAT model requires soil physical properties for simulation purposes (Table 34). Since there were no available data for different soil layers, it was assumed that there was only one layer. One of the soil physical properties required is soil hydrologic group. The different groups are defined by grouping soils with the same infiltration rates, soil depths, and drainage capacity and run-off potential under storm and cover conditions (Ponce & Hawkins, 1996). The soil hydrologic group was assigned to each soil class in the catchment according to the information obtained from the soil map and soil inventory data sets from the ARC-ISCW (Table 48). A default soil albedo of 0.1 was used.

Table 34: Soil physical properties required by SWAT model

Parameter	Definition
HYDGRP	Soil hydrologic group (**A**, **B**, **C** and **D**).
SOL_ZMX	Maximum rooting depth of soil profile.
ANION_EXCL	Fraction of porosity (void space) from which anions are excluded.
SOL_CRK	Crack volume potential of soil.
TEXTURE	Texture of soil layer.
SOL_Z	Depth from soil surface to bottom of layer.
SOL_BD	Moist bulk density.
SOL_AWC	Available water capacity of the soil layer.
SOL_K	Saturated hydraulic conductivity.
SOL_CBN	Organic carbon content.
CLAY	Clay content.
SILT	Silt content.
SAND	Sand content.
ROCK	Rock fragment content.
SOL_ALB	Moist soil albedo.

The available water capacity (θ_a) parameter was attained by taking the difference between field capacity (θ_{fc}) and permanent wilting point (θ_{pwp}). Field capacity is the index of the water content that can be held against the force of gravity, thus corresponding to the pressure head of −3.4 m. The permanent wilting point is calculated as the soil water content corresponding to −150 m since plants cannot exert suctions stronger than −150 m (Karkanis, 1983; Muthuwatta, 2004). These parameters are thus computed as follows:

Field capacity (θ_{fc}):

$$\theta_{fc} = \emptyset(\frac{\varphi_{ae}}{340})^{1/b} \quad (32)$$

Permanent wilting point (θ_{pwp}):

$$\theta_{pwp} = \emptyset(\frac{\varphi_{ae}}{15000})^{1/b} \quad (33)$$

and therefore:

$$\theta_a = \theta_{fc} - \theta_{pwp} \quad (34)$$

Where

$\emptyset$ is the porosity,

φ_{ae} is the air entry water content in m, and

b the exponent describing the soil water characteristic relationship.

Values for the different variables above are expressed in Table 35, including the saturated hydraulic conductivity (K_h) values. Other soil parameters required by the SWAT model such as bulk density and organic carbon are expressed in Appendix D.

Table 35: Parameters for estimating the available water capacity in different soils (Muthuwatta, 2004)

Soil texture	ϕ	K_h (m·s^{-1})	φ_{ae} (m)	b
Sand	0.395	1.76×10^{-4}	121	4.05
Loamy sand	0.410	1.56×10^{-4}	90	4.38
Sandy loam	0.435	3.47×10^{-5}	218	4.90
Silt loam	0.485	7.20×10^{-6}	786	5.30
Loam	0.451	6.95×10^{-6}	478	5.39
Sandy clay loam	0.420	6.30×10^{-6}	299	7.12
Silty clay loam	0.477	1.70×10^{-6}	356	7.75
Clay loam	0.476	2.45×10^{-6}	630	8.52
Sandy clay	0.426	2.17×10^{-6}	153	10.40
Silty clay	0.492	1.03×10^{-6}	490	10.40
Clay	0.482	1.28×10^{-6}	405	11.40

5.3.2.2 Land use

In the case of preparing a land use table, there should be a string named *landuse* in the file name so that it would be recognised by the model and be offered as an option for the land use table on the drop-down menu. The land use table should contain at least columns named *land use ID* and *SWAT* code, where the SWAT code strings are four letters and should be found in the *crop* table contained in the SWAT reference database. The created land use table is depicted in Table 36 while the map is depicted in Figure 44.

Table 36: SWAT land use name convention

Land use	SWAT code	Physical name
1	WATR	Water
2	FRST	Forest – mixed
3	SAVA	Savana
4	CRWO	Cropland/woodland mosaic
5	GRAS	Grassland
6	SHRB	Shrubland
7	ORCD	Orchard
8	MIXC	Mixed dryland/irrigated crop
9	FRSE	Forest – evergreen

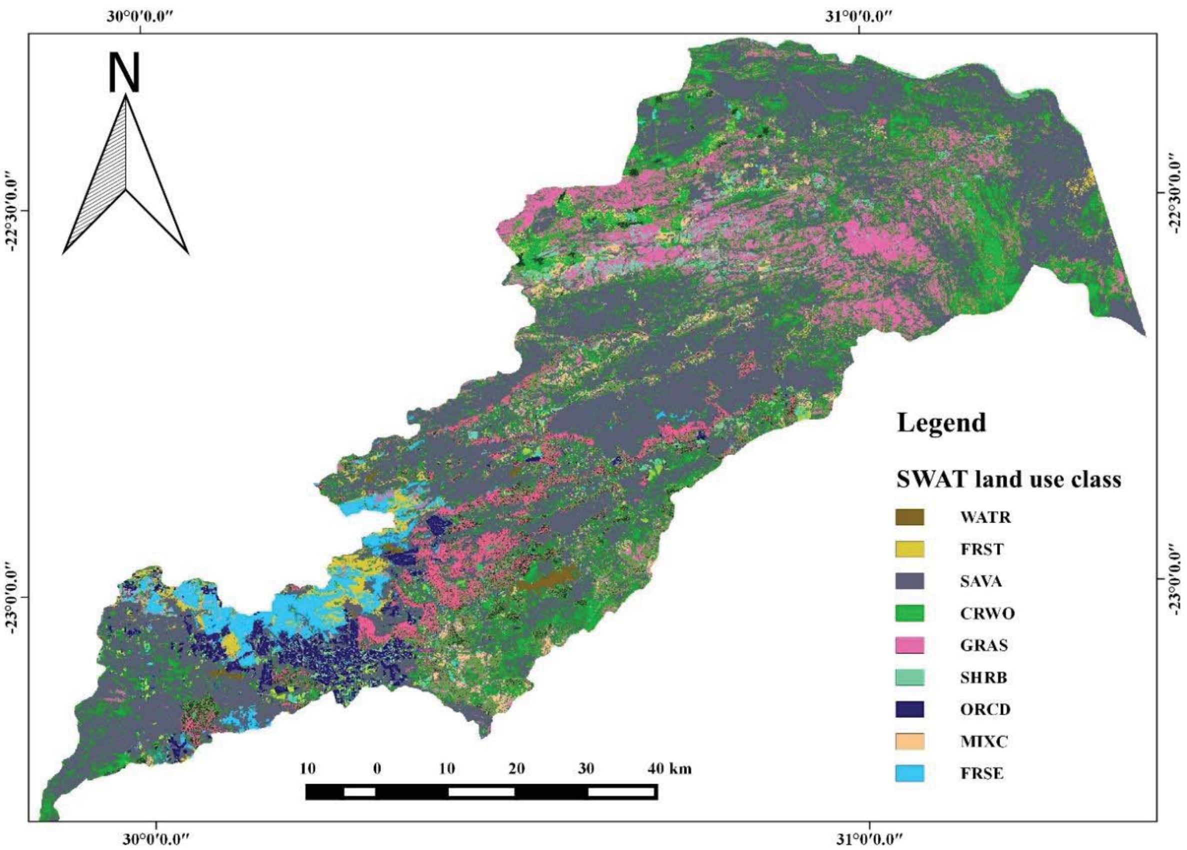

Figure 44: Land use map for the Luvuvhu River catchment

5.4 Methods

5.4.1 Climate data preparation

The model requires that the station information of all climate variables available be prepared before it can be implemented. The information needed includes station ID, station name, latitude, longitude and elevation. Missing values in the data were replaced with −99. The data format of all climate variables [i.e. solar radiation ($MJ \cdot m^{-2}$), wind speed ($m \cdot s^{-1}$), relative humidity (decimal fraction) and precipitation (mm)] was the same, while the difference was when preparing minimum and maximum air temperature, where the minimum and maximum air temperature had to be separated by a comma.

5.4.2 Weather generation and preparation

The SWAT model requires observed long-term daily climatic data such as daily rainfall, air temperature, relative humidity, solar radiation and wind speed for it to run or be applied (Clemence, 1997; McKague et al., 2003; McKague et al., 2005; Tingem et al., 2007; Safeeq & Fares, 2011). If there are no measured data available, the SWAT model uses data that is simulated by a weather generator model WXGEN. The WXGEN model generates precipitation data for the day and is thus able to generate data for other parameters (minimum/maximum air temperature, solar radiation and relative humidity) based on the availability of daily rainfall (Muthuwatta, 2004).

SWAT was able to generate rainfall using the WXGEN model based on historical statistics of weather elements such as precipitation. The estimated parameters expressed in Table 37 were tabulated in a weather generator table required by SWAT. The weather generator table contained parameters for all the weather stations where each weather station was represented by one line in the table. The weather generator table was created using statistical parameter data of daily precipitation obtained from the precipitation statistics (pcpSTAT) software, while other parameters such as air temperature, relative humidity, solar radiation and wind speed were obtained using the Excel™ pivot tables. The created weather generator table was added to the QSWAT reference database starting with a string *WGEN* so that whenever a new project is created, the table would be available. The SWAT Editor allocates the nearest weather generation from the selected table to each sub-catchment. Figure 45 depicts a snapshot of the window that appears in SWAT Editor when selecting the appropriate weather generator table.

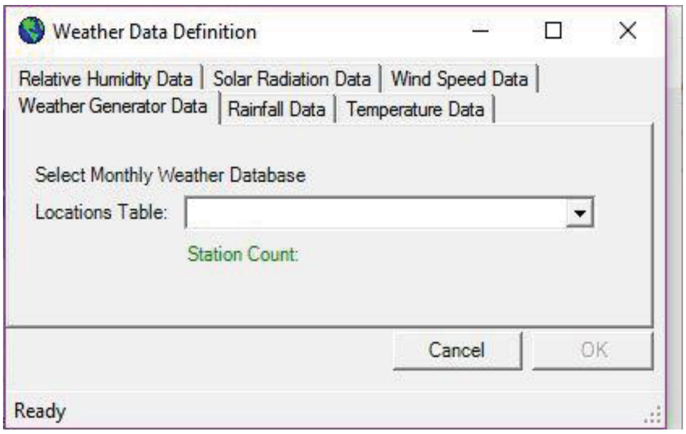

Figure 45: Weather data definition menu in the QSWAT program

Table 37: Climate & statistical parameters needed by the SWAT model for weather generator table

Parameter	Min_	Max_	Default	Units	Definition
RAIN_YRS	5	100	14	–	The number of years of maximum monthly 0.5 hour rainfall data.
TMPMX	−30	50	0	°C	Average maximum air temperature for month.
TMPMN	−40	40	1	°C	Average minimum air temperature for month.
TMPSTDMX	0.1	100	2	°C	Standard deviation for maximum air temperature in month.
TMPSTDMN	0.1	30	3	°C	Standard deviation for minimum air temperature in month.
PCPMM	0	600	4	$mm \cdot month^{-1}$	Average amount of precipitation falling in month.
PCPSTD	0.1	50	5	$mm \cdot month^{-1}$	Standard deviation for daily precipitation in month.
PCPSKW	−50	20	6	–	Skew coefficient for daily precipitation in month.
PR_W1	0	0.95	7	fraction	Probability of a wet day following a dry day in the month.
PR_W2	0	0.95	8	fraction	Probability of a wet day following a wet day in the month.
PCPD	0	31	9	days	Average number of days of precipitation in month.
RAINHHMX	0	125	10	mm	Maximum 0.5 hour rainfall in entire period of record for month.
SOLARAV	0	750	11	$MJ \cdot m^{-2}$	Average daily solar radiation in month.
DEWPT	−50	25	12	°C	Average dew point temperature in month.
WNDAV	0	100	13	$m \cdot s^{-1}$	Average wind speed in month.

5.5 Modelling Using SWAT Hydrological Model

5.5.1 Model set-up

A hydrological simulation was performed with the 2012 version of SWAT model through an interface between the model and QGIS Desktop 2.6.1 software, QSWAT 1.3 2016. The model was set up following the guidelines given in Dile et al. (2015), which describe the use of the QGIS interface of SWAT 2012 known as QSWAT. The process of running the SWAT model on a QGIS interface, QSWAT, is shown in Figure 46. The model was run for a 33-year period from 1983 to 2015, but the first years were used as a warm-up period to mitigate unknown initial conditions and hence were excluded from the analysis.

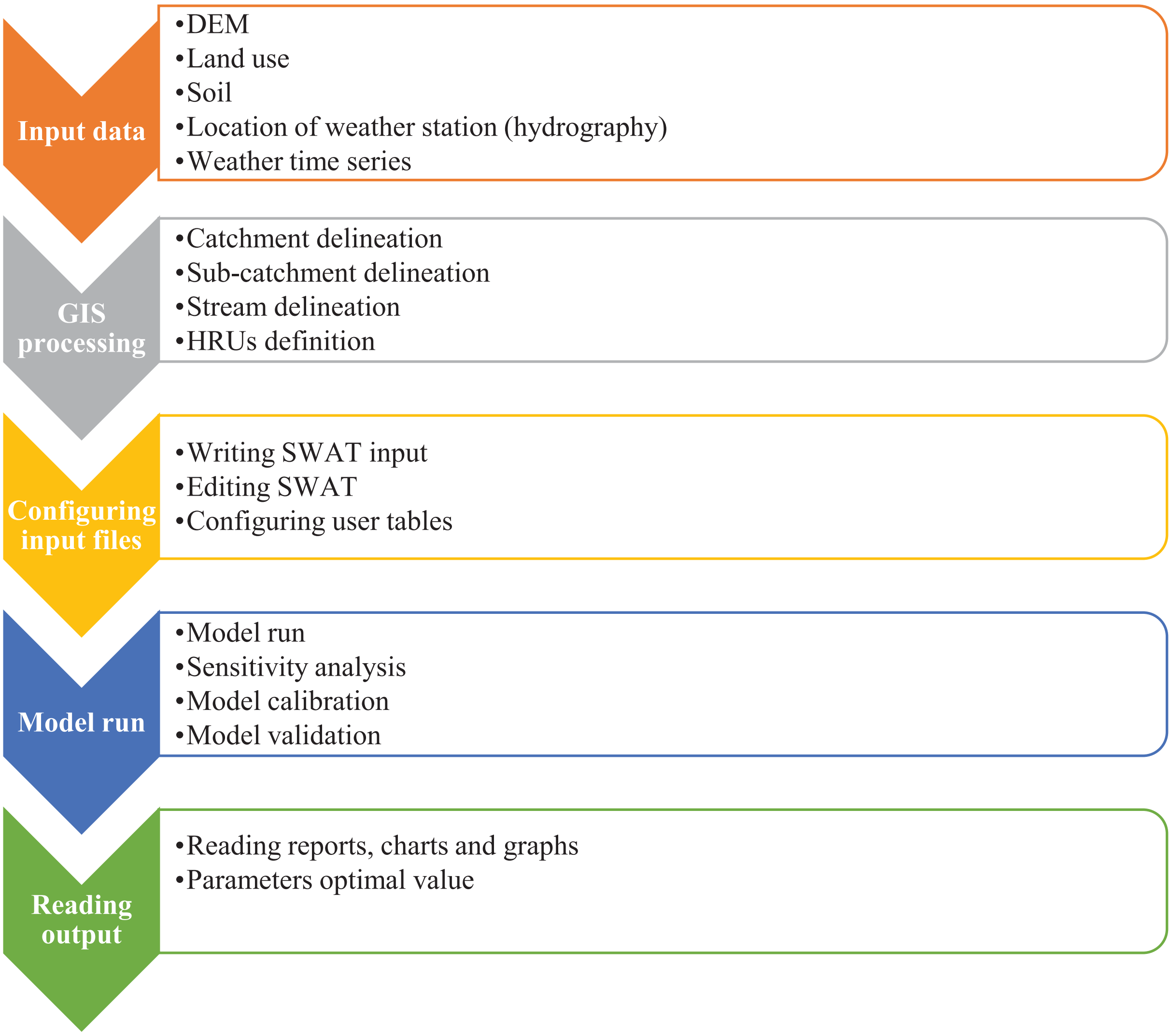

Figure 46: The SWAT model process flow diagram

There are three steps that a user needs to complete before the model can run (Figure 75 and Figure 76 in Appendix E):

1. Delineate the catchment.
2. Create HRUs.
3. Edit inputs and run SWAT.

The following sections will review the different steps detailing the five input parameters required by the model.

1. **Delineate the catchment**

Delineation of the catchment and sub-catchment was done automatically using the SWAT tool whereby the catchment was subdivided into smaller catchments and stream networks generated looking at topography, flow direction and flow accumulation (Figure 47). In delineating the catchment, a flow vector is created by filling the basins in the DEM thus increasing the elevation of basins until they overflow (Fadil et al., 2011). When the overflow has occurred, a flow accumulation grid is then created by numbering the cells flowing into each unit in the grid, meaning the flow accumulation is related to the flowing cells (which are part of the stream network) (Ncube, 2006). Stream networks were created automatically and the catchment outlet was modified to fit the project's requirements by adding the outlet position manually. The watershed was then created and point sources added to each sub-catchment.

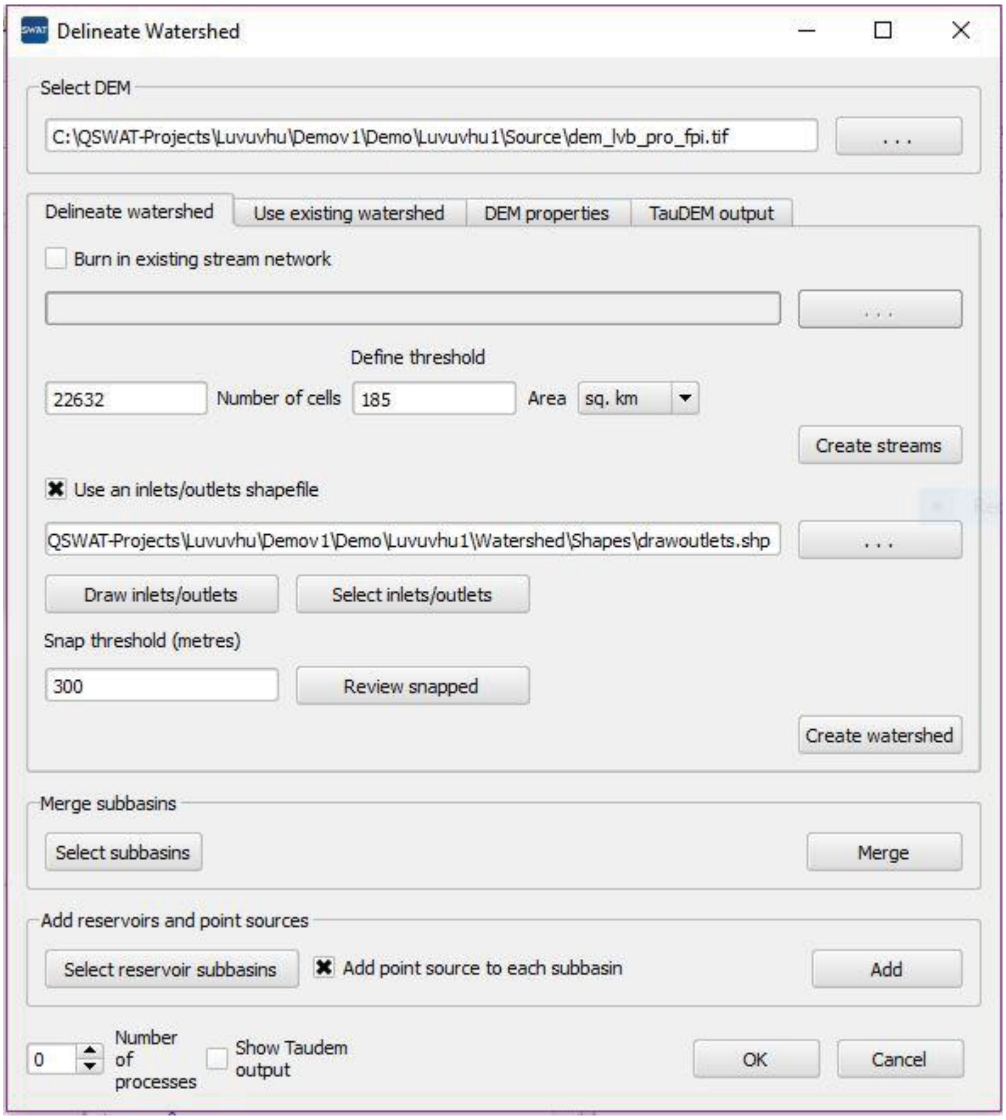

Figure 47: Catchment and sub-catchment delineation

2. Create HRUs

Soil and land use data is very important when it comes to the creation of HRUs. Soil and land use maps were imported into the SWAT model using the procedure given in Dile et al. (2015). The created soil and land use tables were saved in the QSWAT project database in order for them to appear as options in the model drop-down menu (Figure 48).

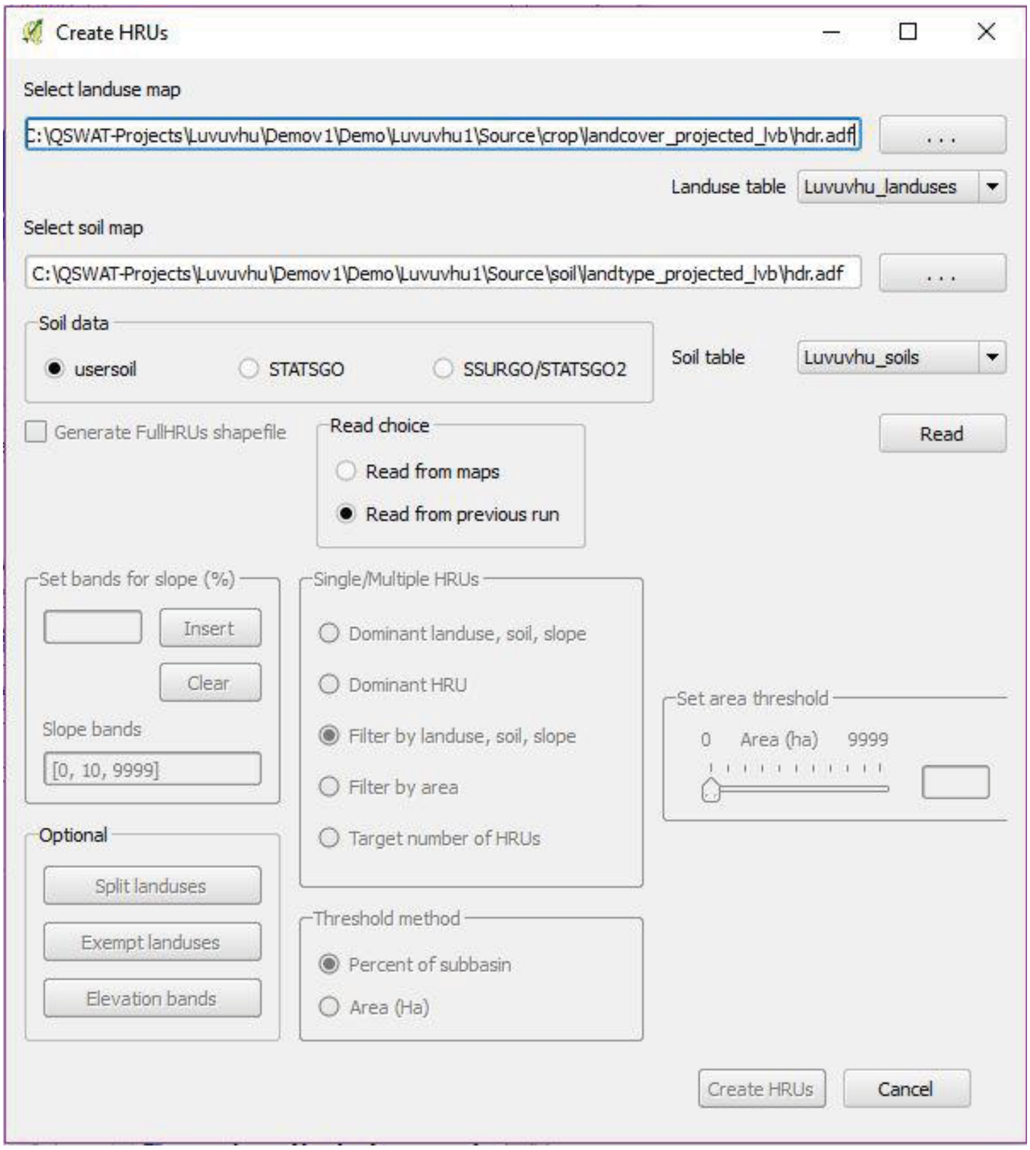

Figure 48: HRUs creation through land use and soil overlay definition

Having divided the catchment into several sub-catchments, the catchments were further divided into smaller units. These are the HRUs that are used by the SWAT model (Figure 48) (Vazquez-Amabile et al., 2006; Jha, 2011).

The SWAT model was able to read the information supplied in the land use and soil tables and HRUs creation through land use and soil overlay definition in the maps and, therefore, able to create the HRUs. The HRUs were created by overlaying analysis of land use, soil and slopes from information obtained from slope range, soil and land use maps and tables (Vazquez-Amabile et al., 2006). A threshold of 10% was recommended and selected for soil, land use and slope to divide the HRUs. This meant that if the percentage of soil and land use was less than the threshold value (10%) of the sub-catchment area, it was considered insignificant and not included in the analysis (Mutenyo et al., 2013). This approach defines the HRUs by creating at least one HRU per sub-catchment given the threshold value for soil and land use (Ncube, 2006). In the process of delineation, QSWAT automatically estimates the number of HRUs and stores the parameters in a SWAT sub-catchment input file.

3. **Edit inputs and run SWAT**

The SWAT Editor was connected to the project database and SWAT reference database, which was then able to activate the *Write* input tables (Figure 49 and Figure 50). Weather generator and climate data is provided through the option of *Weather stations*. For each sub-catchment, the model uses observed climate data from the closest station. If there is no observed station climate data, QSWAT uses simulated data from the weather generator (Golmohammadi et al., 2014).

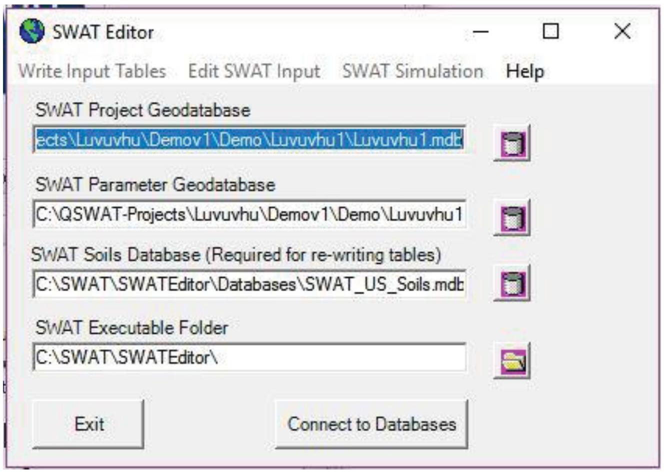

Figure 49: SWAT Editor input database

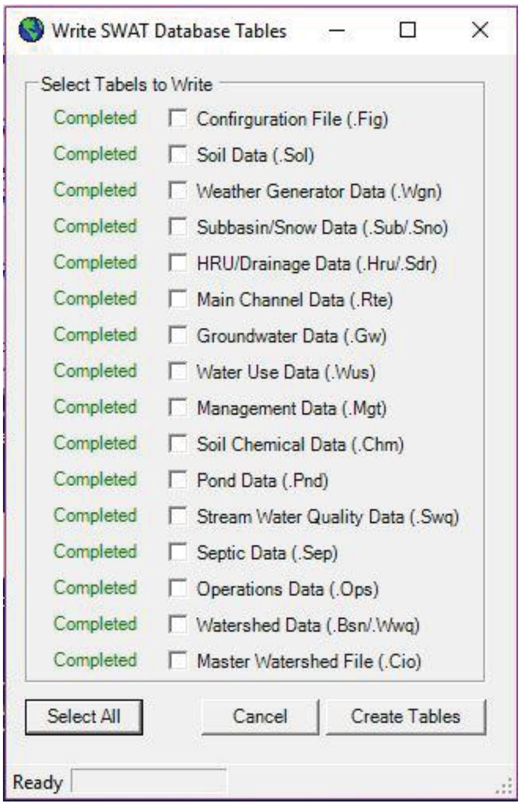

Figure 50: Window of complete written database tables

5.6 Sensitivity Analysis, Calibration and Validation

5.6.1 Parameter sensitivity analysis

Before the calibration and validation processes, SWAT requires that a sensitivity analysis of the most sensitive parameters for a given catchment be conducted (Mutenyo et al., 2013). Several parameter inputs influence the catchment processes (Gyamfi et al., 2016). Hence, it is essential to perform a sensitivity analysis test. A sensitivity analysis was conducted using the sequential uncertainty fitting (SUFI-2) algorithm to categorise main parameters that have more effect on streamflow. To determine the most sensitive parameters, the global sensitivity analysis approach was chosen. This considers the sensitivity of one parameter in relation to other parameters under consideration (Arnold et al., 2012). The global sensitivity of surface run-off parameters was calculated using Latin hypercube regression analyses. The minimum and maximum ranges of parameters were then fitted for calibration using the SUFI-2 uncertainty technique. The parameters were ranked according to their model sensitivity during calibration. Consistent with literature, these parameters are responsible for model calibration and parameter changes during different iterations. During sensitivity analyses, scatter plots were created and used to display the distribution of simulations in parameter sensitivity analysis by comparing parameter values on the x-axis with the objective functions on the y-axis, coefficient of determination with a threshold of 0.5.

The level of significance between data sets was established by applying *t*-test and *p*-value sensitivity analyses parameters to identify relative sensitivity of each parameter and to provide the significance of the sensitivity respectively. The *t*-test and *p*-value were used to rank the various parameters considered to have more influence on streamflow. The *t*-test gives a measure of the sensitivity of a parameter while the *p*-value gives the significance of the sensitivity of that parameter (Gyamfi et al., 2016). Parameters with high *t*-test values and less *p*-value show greater sensitivity on the streamflow (Jha, 2011).

Table 38 depicts parameters that have been discovered to be sensitive to streamflow according to past studies. A sensitivity analysis was conducted for each sub-catchment as parameters vary from one catchment to another depending on geomorphological characteristics and other processes occurring in the catchment (Arnold et al., 2012). Initially, parameters in Table 38 were considered for sensitivity analyses and final parameters were selected based on the *t*-test and *p*-value. Having accomplished the sensitivity analyses, the model was calibrated using the selected most sensitive parameters.

Table 38: Parameters considered for sensitivity analysis (Gyamfi et al., 2016)

Parameter	Description
CN2	Soil Conservation Service (SCS) run-off curve number.
ESCO	Soil evaporation compensation factor.
GWQMN	Threshold depth of water in the shallow aquifer required for return flow to occur (mm H_2O).

Parameter	Description
SOL_AWC	Soil available water storage capacity (mm H_2O/mm soil).
GW_REVAP	Groundwater re-evaporation (revap) coefficient.
RCHRG_DP	Deep aquifer percolation function.
SOL_Z	Soil depth (mm).
SURLAG	Surface run-off lag coefficient (days).
SOL_K	Soil conductivity ($mm \cdot h^{-1}$).
CH_K2	Effective hydraulic conductivity in the main channel ($mm \cdot h^{-1}$).
ALPHA_BF	Baseflow alpha factor (day).
GW_DELAY	Groundwater delay (day).
ALPHA_BNK	Baseflow alpha factor for bank storage (day).
REVAPMN	Threshold depth of water in the shallow aquifer for revap to occur (mm).

5.6.2 Calibration and validation

It is important to calibrate and validate the model in order to reduce errors (Pasi, 2014; Gyamfi et al., 2016). SUFI-2 was used to calibrate and validate the hydrologic set-up of the model through its interface with the SWAT calibration and uncertainty procedure (SWAT-CUP). The streamflow weir station A9H013 was selected as the outlet point of the catchment due to its location in the catchment and the availability of streamflow data, which makes it applicable for calibration and validation.

A split sample procedure using daily streamflow data from weir stations A9H003, A9H006, A9H012 and A9H013 for the periods 1986-2005 and 2006-2015 was used for calibration and validation respectively. Multiple simulation iterations were executed with a minimum of 300 simulations in each run.

5.6.3 Performance indices

Performance of the model in simulating the observed streamflow was judged against four objective functions. Objective functions are not universally applicable to all situations, hence the choice is dictated by the objective of the particular study (Gyamfi et al., 2016). The goodness-of-fit and efficiency of the model were tested using four main objective functions, namely, coefficient of determination, Nash–Sutcliffe Efficiency (NSE), PBIAS, RMSE observations standard deviation ratio (RSR) and two performance indices, namely, *P*-factor and *R*-factor. The performance of the model was judged according to findings from literature.

The formulae of these efficiency measures are as follows:

$$NSE = 1 - \frac{\sum_{i=1}^{n}(O_i - S_i)^2}{\sum_{i=1}^{n}(O_i - \bar{O})^2} \quad (35)$$

$$R^2 = \left[\frac{\sum_{i=1}^{n}(O_i - S_i)(S_i - \bar{S})}{(\sum_{i=1}^{n}(O_i - \bar{O})^2)^{0.5}(\sum_{i=1}^{n}(S_i - \bar{S})^2)^{0.5}}\right]^2 \quad (36)$$

$$PBIAS = \frac{\sum_{i=1}^{n}(O_i - S_i) \times 100}{\sum_{i=1}^{n} O_i} \quad (37)$$

$$RSR = \frac{\sqrt{\sum_{i=1}^{n}(O_i - S_i)^2}}{\sum_{i=1}^{n}(O_i - \bar{O})^2} \quad (38)$$

Where

O_i is observed variable,

S_i is simulated variable,

$\bar{O}$ is the mean observed variable,

$\bar{S}$ is the mean simulated variable, and

n is the number of observations under consideration.

The model calibration was aimed at achieving a satisfactory model efficiency of concurrently having NSE ≥ 0.5, PBIAS ±25% and RSR < 0.7 (Mutenyo et al., 2013).

SUFI-2 assumes large parameter uncertainty and decreases this uncertainty through *P*-factor and *R*-factor performance statistics. The *P*-factor was used to quantify all the uncertainties associated with the SWAT model by bracketing an amount of measured data containing all uncertainties. The SUFI-2 algorithm was used to reduce uncertainty by placing most of the observed streamflow data in the 95% band. These model uncertainties can be accounted for due to some errors in data input sources, data preparation and parameterisation. Other sources of uncertainty may be the result of human and instrumental errors during data processing. Rainfall in the Luvuvhu catchment is not equally distributed due to topography variation and thus may contribute to some of the uncertainties in the model because of insufficient data availability.

5.6.4 Flood frequency and risk analysis

Following calibration and validation, SWAT was run to simulate 30 years to compute flood annual exceedance probability. Flood frequency analyses were performed for all four sub-catchments for the simulated peaks. The log-normal probability distribution was used to fit the maximum annual peak data to estimate the flood frequencies. The flood magnitudes were estimated at seven different return periods of 2, 5, 10, 25, 50, 100 and 200 years. A 30-year period of data from 1986 to 2015 was used to attain the flood frequencies. The data was sorted from highest to lowest so that a reoccurrence interval could be calculated. The reoccurrence interval was calculated using:

$$RI = \frac{n+1}{m} \quad (39)$$

Where

n is the number of years in the set, and

m is the rank of discharge.

The exceedance probability of the critical value was presented in plots for the whole catchment and the other three sub-catchments.

5.7 Results and Discussion

5.7.1 Initial model run analysis

Once the SWAT model was set up, reports retrieved from the model indicated elevation ranging from 199 m to 1588 m with mean of 625.21 m and standard deviation of 235.72 m. The model was initially run for four sub-catchments, namely, 6, 10, 15 and 17, which were produced during the delineation process (Figure 51). Simulations from the four sub-catchments were compared with the observed daily flows from four weir stations chosen for the study (Figure 52).

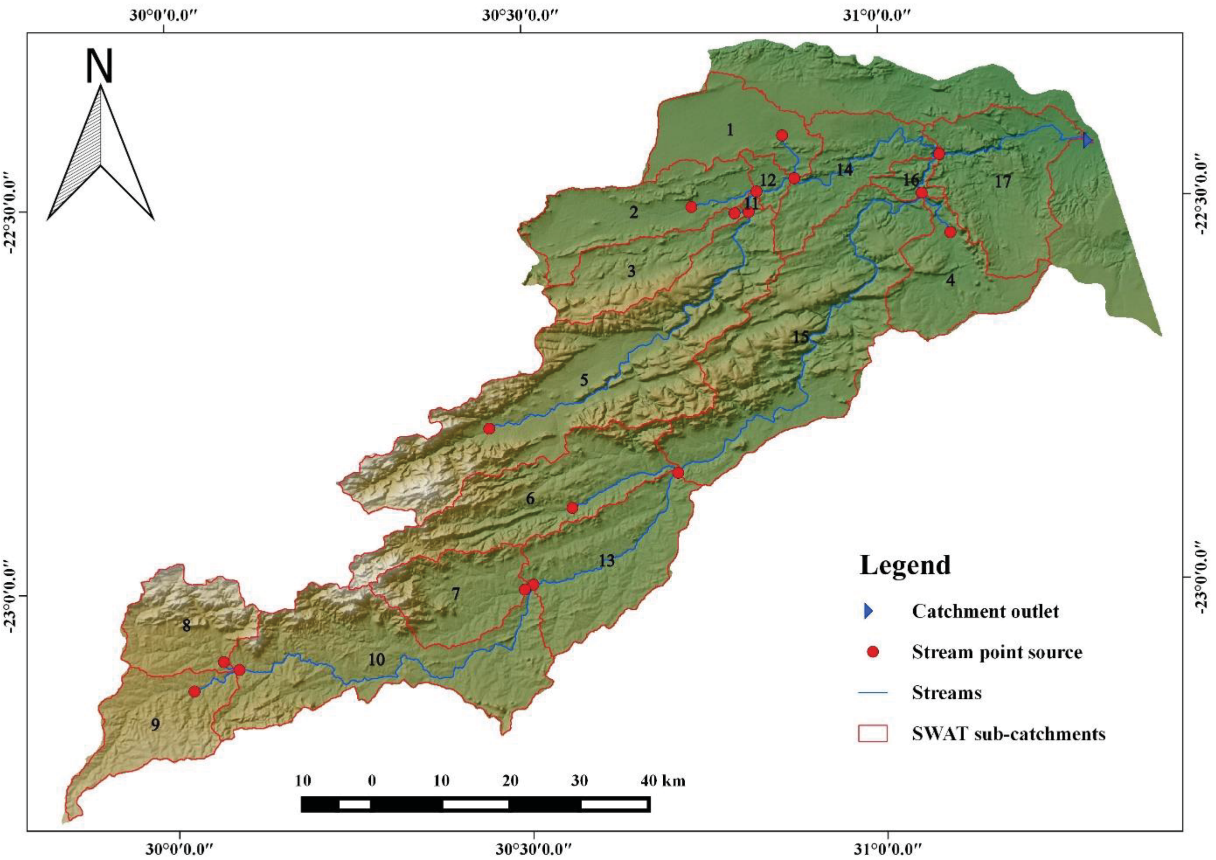

Figure 51: Sub-catchments delineation through QSWAT

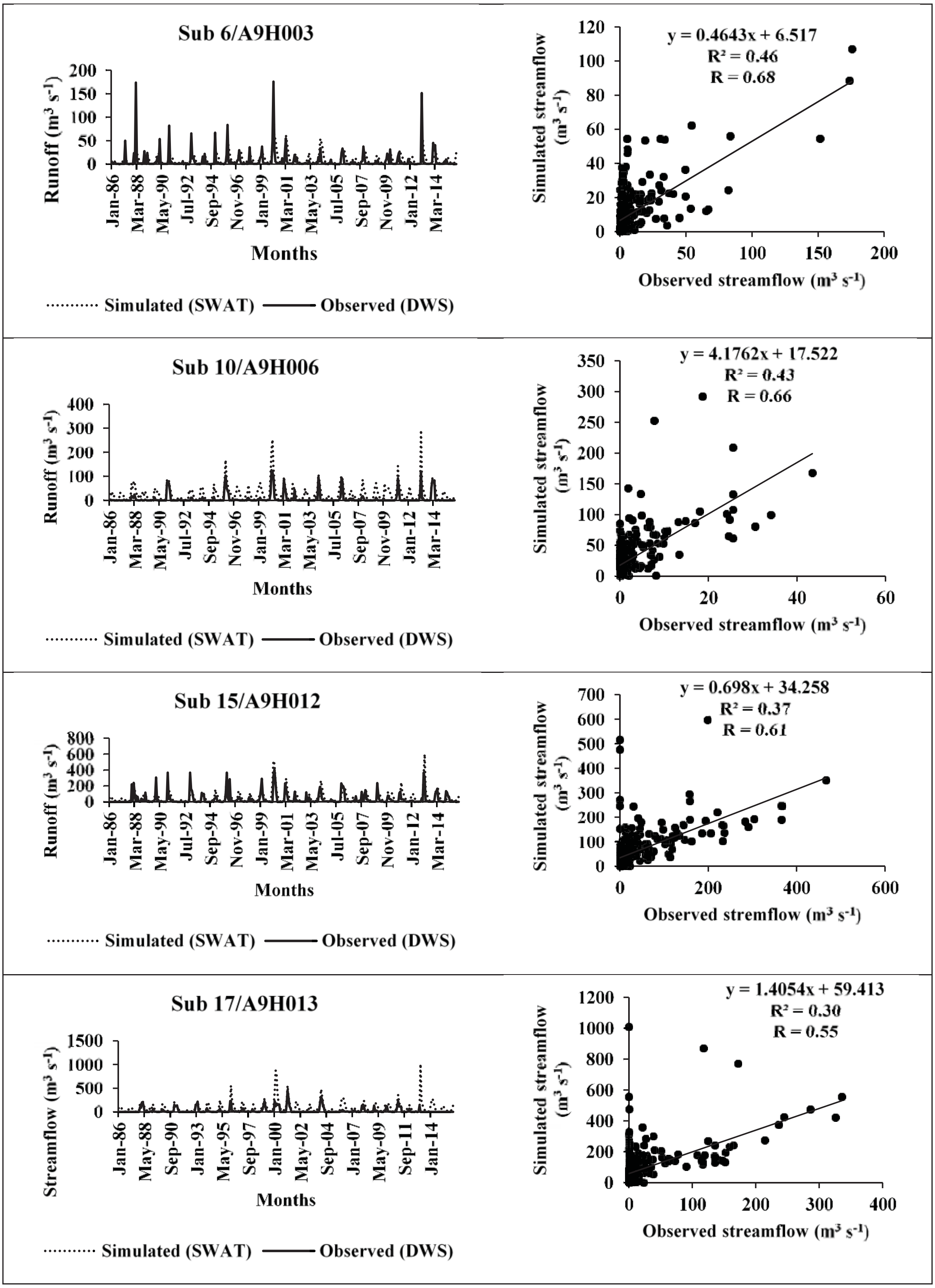

Figure 52: Comparison of simulated and observed daily discharge through hydrographs and regression graphs for the period 1986-2015 at weir stations A9H003, A9H006, A9H012 and A9H013

The water balance components of the catchment were calculated using the water balance equation of the SWAT model and the computed results were analysed in the SWAT check tool (Table 39). The average curve number was computed to be 49.96, which meant that the hydrological condition of the Luvuvhu River catchment ranged from fair to poor and therefore prone to run-off and ultimately flooding (Pitt, 2002).

Table 39: Simulation details of the SWAT model set-up

General details	Values
Simulation length (years)	33
Warm-up (years)	3
Hydrological response units	214
Sub-basins	17
Output time-step	Daily
Precipitation method	Measured
Watershed area (km^2)	5273.1
Hydrology (water balance ratio)	
Streamflow/precipitation	0.61
Baseflow/total flow	0.68
Surface run-off/total flow	0.32
Percolation/precipitation	0.42
Deep recharge/precipitation	0.02
Evapotranspiration/precipitation	0.34
Hydrological parameters	
Average curve number	49.96
Evapotranspiration and transpiration (mm)	268.4
Precipitation (mm)	780.3
PET (mm)	946.4
Surface run-off (mm)	153.18
Lateral flow (mm)	33.18
Return flow (mm)	293.45
Percolation to shallow aquifer (mm)	325.04
Recharge to deep aquifer (mm)	16.25
Re-evaporation from shallow aquifer (mm)	16.53

To evaluate the performance of the model before calibration, the correlation coefficient (R), coefficient of determination (R^2), MAE, mean bias error (MBE), RMSE and NSE index were used. Results reveal a significant correlation in all the sub-catchments 6, 10, 15 and 17 with R of 0.68, 0.66, 0.61 and 0.55 respectively. However, the R^2 results for sub-catchments 6, 10, 15 and 17 reveal that in all of them, one cannot be certain when predicting using the model because of the R^2 of 0.46, 0.43, 0.37 and 0.30 respectively.

Table 40: Statistical evaluation of simulated versus observed streamflow data before calibration

Sub-catchments	MAE*	MBE**	RMSE***	R^2	R	NSE****
6	7.68	3.01	9.41	0.46	0.68	0.54
10	23.87	23.82	25.93	0.43	0.66	−11.05
15	36.14	25.57	58.01	0.37	0.61	0.11
17	66.51	66.06	98.80	0.30	0.55	-3.04

*MAE = Mean absolute error ($m^3 \cdot s^{-1}$) **MBE = Mean bias error ($m^3 \cdot s^{-1}$) ***RMSE = Root mean square error ($m^3 \cdot s^{-1}$) ****NSE = Nash–Sutcliffe efficiency

The regression line does not represent the data well as the strength between the observed and simulated variables was not strong. Only less than 46% of the simulated variation can be explained by the linear relationship between observed and simulated while more than 54% remains unexplained. The RMSE implies unacceptable model results since there is larger variation than bias while the positive MBE shows that the model overestimates the observed data.

There is not much difference between MAE and RMSE for sub-catchments 6 and 10 hence there was less variance in the individual errors in the sample. However, sub-catchments 15 and 17 revealed a greater difference between MAE and RMSE, which implies greater variance in the individual errors in the sample. The NSE index indicated a good model performance in sub-catchments 6 and 15 showing an NSE index of 0.54 and 0.11 respectively. Conversely, sub-catchments 10 and 17 revealed an NSE index less than zero, which suggests that the observed mean was a better predictor than the model. Judging the initial model run by the above efficiency measures, it is evident that a calibration and validation procedure should be done for each of the sub-catchments to attain improved parameter estimation for improved model simulation.

5.7.2 Model calibration

SUFI-2 was applied for model sensitivity, calibration and uncertainty analysis. The model was calibrated using 12 parameters that, based on previous studies, were recorded to be the most sensitive parameters for streamflow. Over 300 simulations in five iterations were run to achieve the best model efficiency between the observed and simulated flows.

The global sensitivity analysis based on surface run-off showed that the most sensitive parameters in SWAT hydrological modelling for the Luvuvhu River catchment are baseflow alpha factor (ALPHA_BF), initial SCS run-off curve number for moisture condition II (CN2), groundwater delay time (GW_DELAY), and saturated hydraulic conductivity (SOL_K) with $p < 0.05$ (Figure 53 and Table 41). This result confirms similar studies done by Fadil et al. (2011), Mamo and Jain (2013), and Gyamfi et al. (2016) where these parameters were shown to be most sensitive to streamflow.

The remaining parameters were found to have no significant effect on streamflow simulations and caused no significant changes in the model surface run-off output with $p > 0.05$. This agreed with literature, with Jha (2011) confirming that there is great sensitivity on streamflow when there is a high *t*-test value and lower *p*-value.

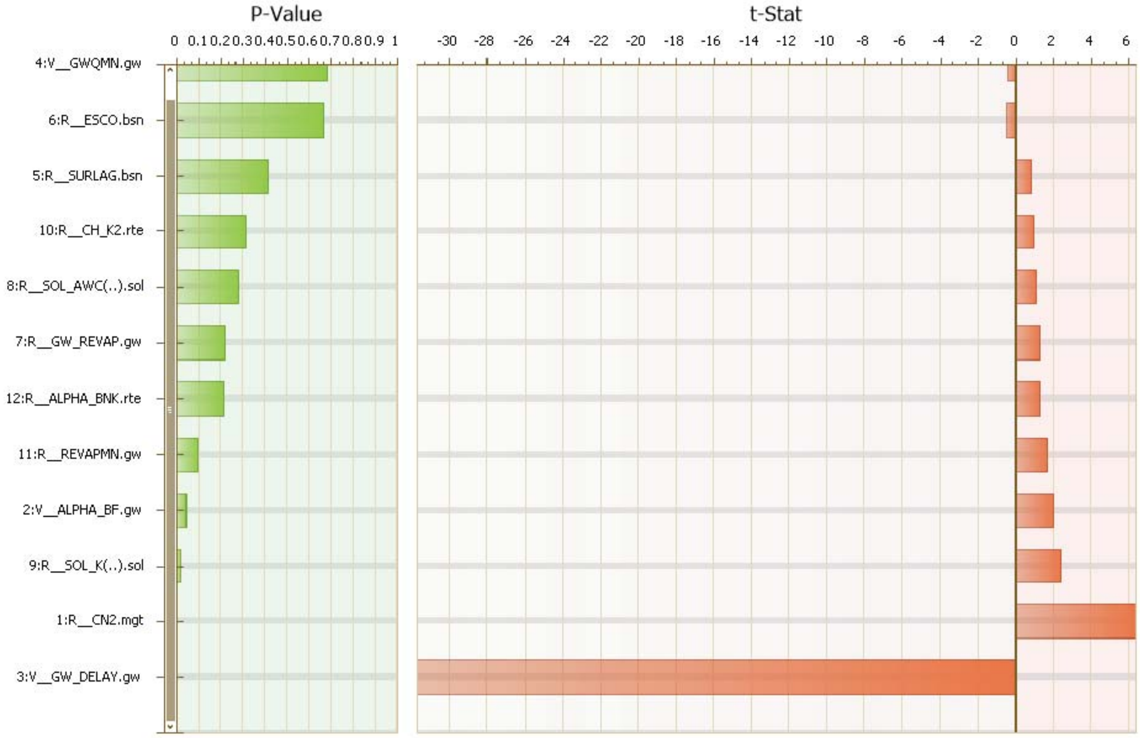

Figure 53: Global sensitivity analysis and ranking of SWAT parameters

Looking at the scatter plots created during calibration, significant variation/distribution parameter values were observed in most of the parameters (Figure 77, Appendix F). However, parameters (ALPHA_BF, CN2, GW_DELAY and SOL_K) were more distinguishable, showing more variance than other parameters, which indicate that they are the primary source of streamflow uncertainty in the Luvuvhu River catchment.

The ALPHA_BF parameter forms part of the baseflow, which contributes to channel run-off and thus delay may have an effect on streamflow discharge and run-off. SOL_K is important for groundwater seepage to streamflow, while GW_DELAY is as important in knowing the amount time the percolated water will take to eventually reach the streams (Van Liew et al., 2007; Chapuis, 2012).

The *P*-factors during calibration were 0.64, 0.52, 0.67 and 0.45 for sub-catchments 6, 10, 15 and 17 respectively. The model produced *R*-factors of 0.59, 1.81, 0.68 and 0.91 for sub-catchments 6, 10, 15 and 17 respectively, showing good calibration results.

Table 41: Sensitivity ranking of SWAT parameters in the Luvuvhu River catchment with high sensitivity ranking in italics

Parameter	Parameter definition	Ranking	*t*-Stat	*p*-value	Min.	Max.	Fitted values
r__CN2.mgt	Initial SCS run-off curve no. for moisture condition II	**2**	**6.420**	**0.000**	**−0.018**	**0.345**	**0.082**
r__ALPHA_BF.gw	Baseflow alpha factor (days)	**4**	**2.050**	**0.040**	**0.499**	**1.498**	**0.943**
r__GW_DELAY.gw	Groundwater delay time (days)	**1**	**-31.740**	**0.000**	**−17.162**	**24.294**	**0.319**
r__GWQMN.gw	Threshold depth of water in the shallow aquifer required for return flow to occur (mm)	12	−0.410	0.690	−2388.583	2538.583	1873.416
r__GW_REVAP.gw	Groundwater revap coefficient	7	1.230	0.220	0.091	0.234	0.167
r__ESCO.hru	Soil evaporation compensation factor	11	−0.440	0.660	−0.123	0.626	0.108
r__CH_K2.rte	Effective hydraulic conductivity in main channel alluvium	9	1.010	0.310	54.592	163.908	159.718
r__ALPHA_BNK.rte	Baseflow alpha factor for bank storage	6	1.250	0.210	0.127	0.709	0.658
r__SOL_K.sol	Saturated hydraulic conductivity	**3**	**2.440**	**0.020**	**−137.606**	**154.218**	**7.819**
r__SOL_AWC.sol	Available water capacity of the soil layer	8	1.090	0.270	0.484	1.453	0.889
r__SURLAG.bsn	Surface run-off lag coefficient (days)	10	0.820	0.410	−0.853	15.722	2.379
r__REVAPMN.gw	Threshold depth of water in the shallow aquifer for revap to occur (mm)	5	1.670	0.100	153.640	461.360	454.692

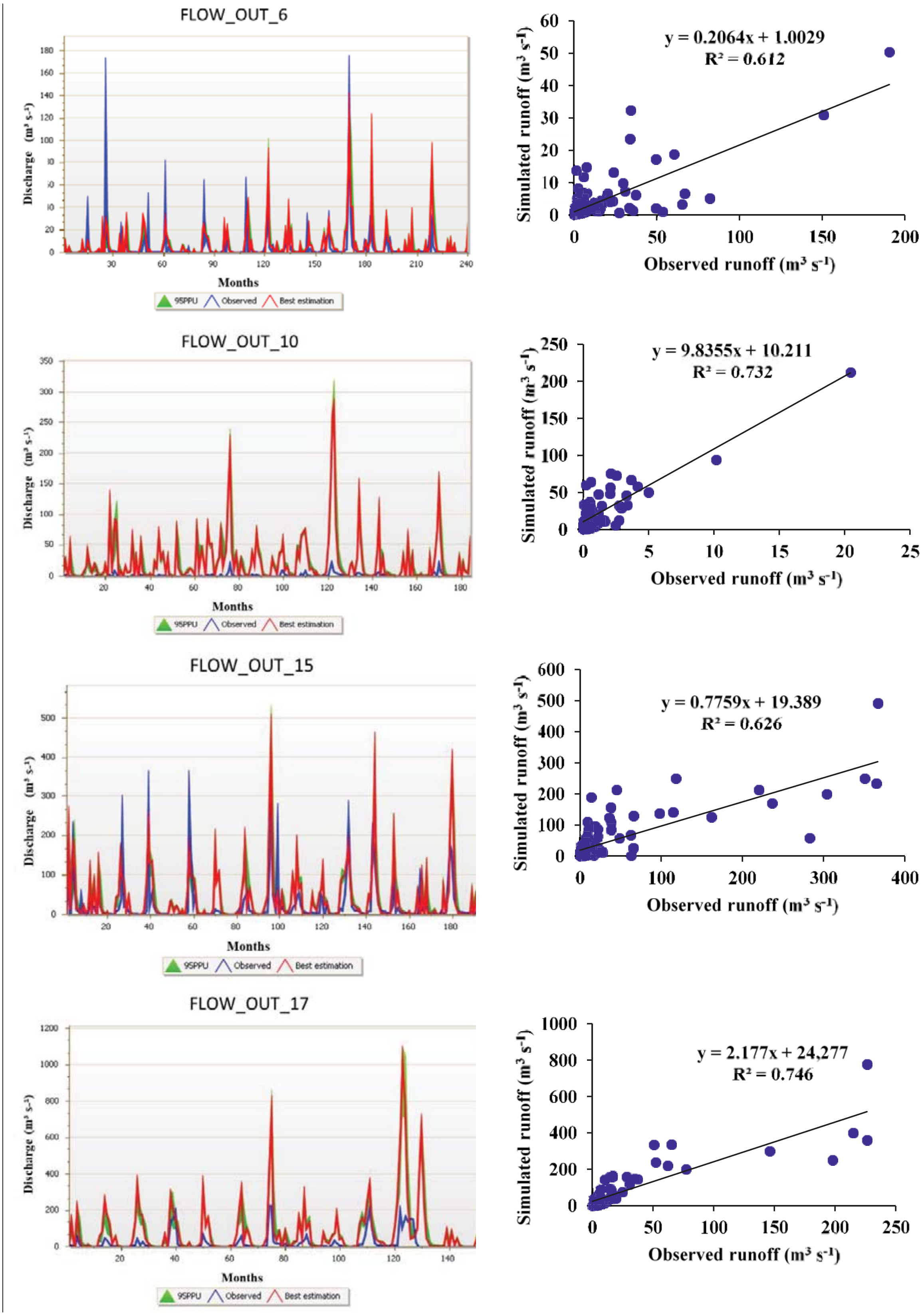

Figure 54: Comparison of observed and simulated streamflow for the calibration period (1986-2005) for sub-catchments 6, 10, 15 and 17

Performance indices results obtained (Figure 54 and Table 42) for sub-catchments 6, 10, 15 and 17 proved to have satisfactory simulation results with R^2 values of 0.61, 0.73, 0.63 and 0.75 respectively. Results further indicated NSE indices of 0.35 and 0.66 for sub-catchments 6 and 15 respectively, which meant acceptable results, while sub-catchments 10 and 17 revealed unsatisfactory results of −16.46 and −0.36 respectively. The model revealed acceptable RSR results of 0.62, 0.56 and 0.71 for sub-catchments 6, 15 and 17 respectively, while sub-catchment 10 showed unsatisfactory results of 3.23. Sub-catchments 6 and 15 showed positive PBIAS of 1.18 and 16.3 respectively, while sub-catchments 10 and 17 gave a negative PBIAS of −7.60 and −2.40 respectively.

Table 42: Performance indices of the SWAT model during calibration

Index	*P*-factor	*R*-factor	R^2	NSE	RSR	PBIAS
FLOW_OUT_ 6	0.64	0.59	0.61	0.35	0.62	1.18
FLOW_OUT_10	0.52	1.81	0.73	−16.46	3.23	−7.60
FLOW_OUT_15	0.67	0.68	0.63	0.66	0.56	16.30
FLOW_OUT_17	0.45	0.91	0.75	−0.36	0.71	−2.10

5.7.3 Model validation

During the period 2006-2015, the *P*-factors obtained were 0.59, 0.34, 0.69 and 0.41 for sub-catchments 6, 10, 15 and 17 respectively, while the *R*-factors obtained were 0.46, 2.67, 0.53 and 0.75 for the same sub-catchments respectively. The percentage of observed data grouped together by 95PPU during validation was 59, 34, and 69 and 41 for sub-catchments 6, 10, 15 and 17 respectively, which indicates the strength of the model calibration to be satisfactory and thus satisfactory model performance.

Objective function results obtained (Figure 55 and Table 43) revealed an R^2 of 0.63, 0.52 and 0.62 for sub-catchments 10, 15 and 17 respectively, which showed satisfactory results while sub-catchment 6 still showed unsatisfactory results with an R^2 of 0.34. NSE in sub-catchments 6, 15 and 17 gave acceptable results of 0.35, 0.48 and 0.31 respectively while sub-catchment 10 still gave unsatisfactory results of −0.45. Sub-catchment 15 showed acceptable RSR result of 0.72 while sub-catchments 6, 10 and 17 showed unacceptable RSR results of 0.86, 1.14 and 2.10 respectively. Sub-catchments 6 and 15 gave positive PBIAS of 65.0 and 19.90 respectively and negative PBIAS values of −12.30 and −14.60 were observed in sub-catchments 10 and 17 respectively.

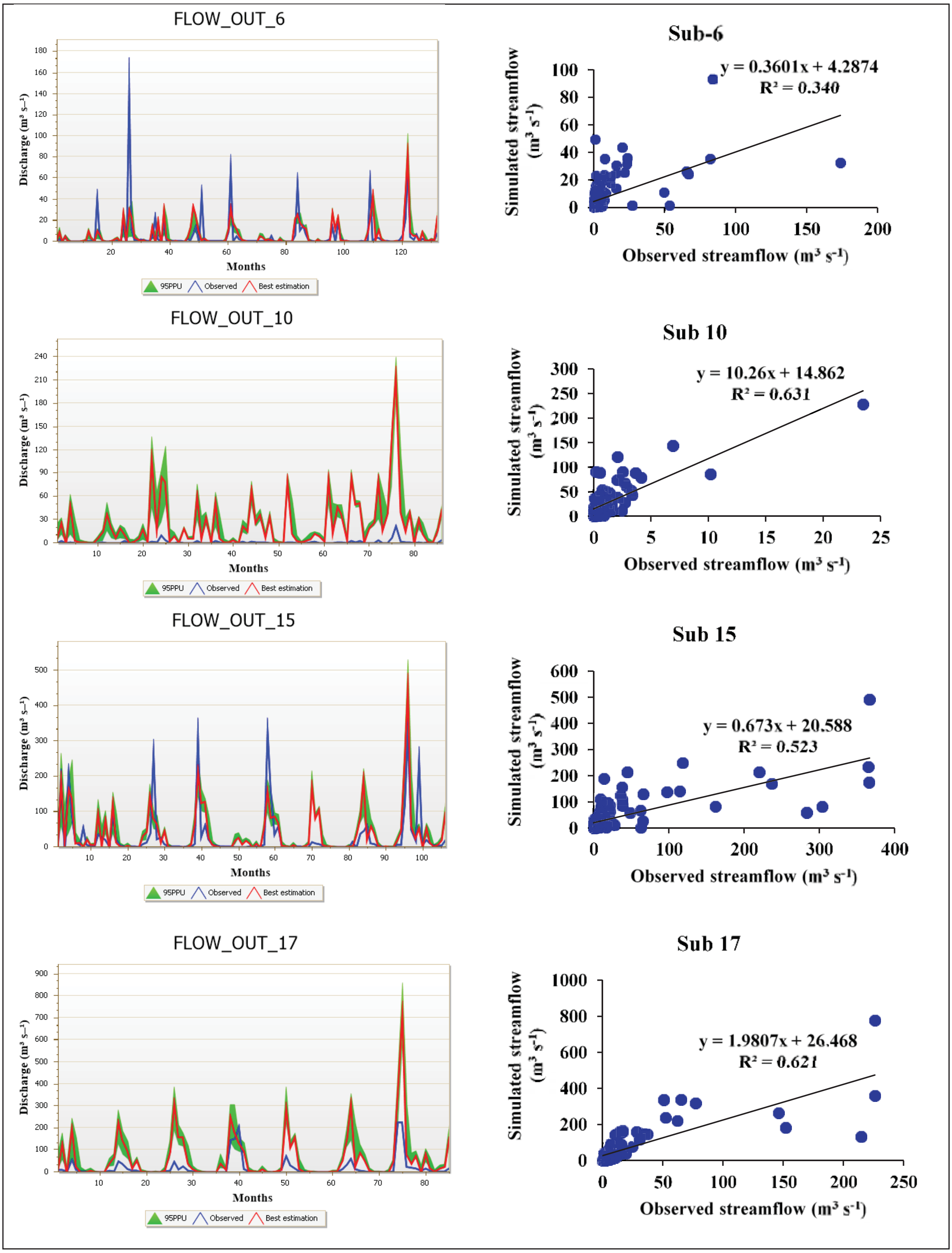

Figure 55: Comparison of observed and simulated streamflow for the validation period (2006-2015) for sub-catchments 6, 10, 15 and 17

Table 43: Performance indices of the SWAT model during validation

Index	*P*-factor	*R*-factor	R^2	NSE	RSR	PBIAS
FLOW_OUT_ 6	0.59	0.46	0.34	0.35	0.86	65.00
FLOW_OUT_10	0.34	2.67	0.63	−0.45	1.14	−12.30
FLOW_OUT_15	0.69	0.53	0.52	0.48	0.72	19.90
FLOW_OUT_17	0.41	0.75	0.62	0.31	2.10	−14.60

5.7.4 Flood frequency analysis and design flood estimation

Flood return periods were plotted against the flood discharges in order to estimate 100- and 200-year floods (Figure 56). Sub-catchment 6 received very low flood discharges compared with sub-catchment 17, which was expected since sub-catchment 6 had a smaller catchment area than sub-catchment 17. A 30-year flood data period was used, thus the 5% and 95% confidence bound showed considerable scatter. Using the equations created from the plots for each sub-catchment, flood magnitudes for different return periods were established (Table 44). At the outlet of sub-catchment 17, the 50-, 100- and 200-year flood magnitudes of 960.70 $m^3 \cdot s^{-1}$, 1121.02 $m^3 \cdot s^{-1}$ and 1281.35 $m^3 \cdot s^{-1}$ occur respectively.

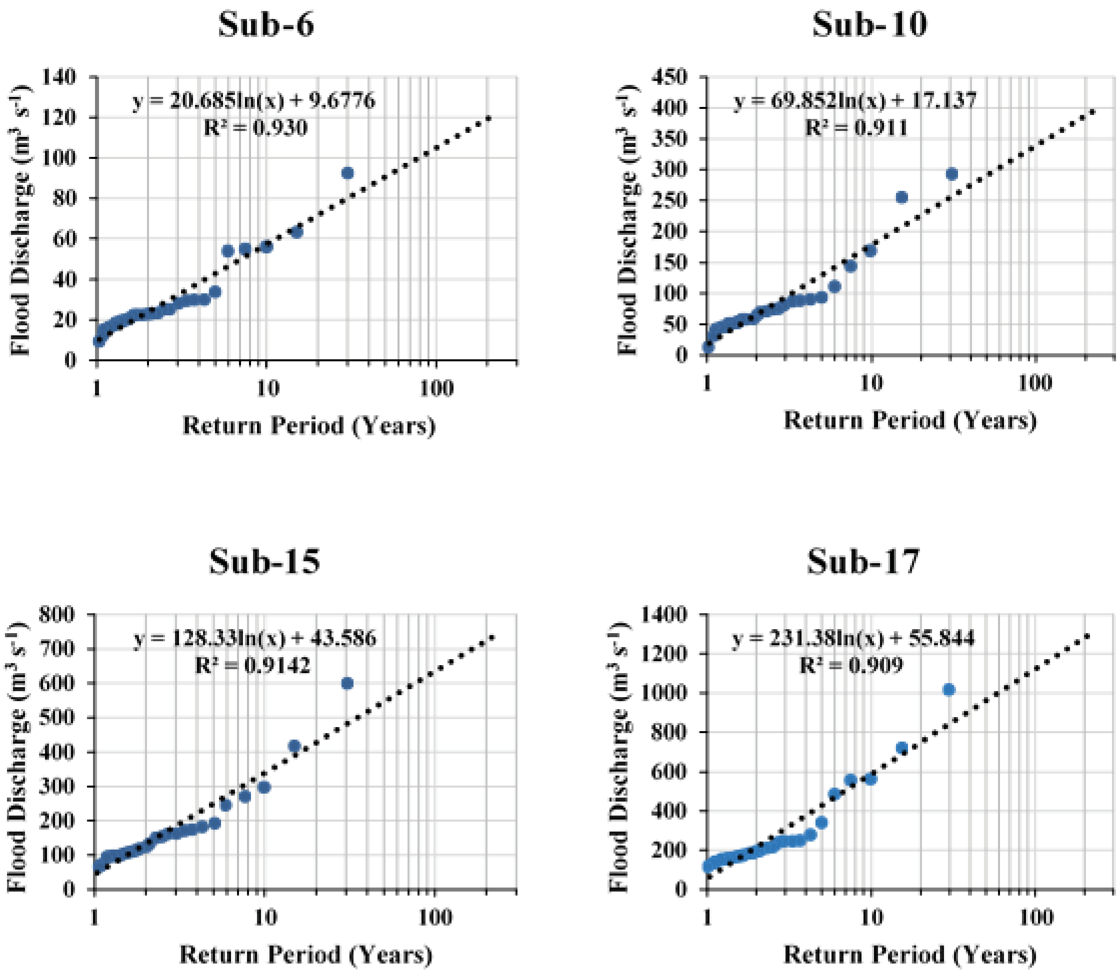

Figure 56: Flood return periods and magnitudes for a 30-year period

Table 44: Sub-catchment return periods and estimated flood magnitudes

Return period (years)	Probability of exceedance (%)	Probability of non-exceedance (%)	Estimated flood magnitude ($m^3 \cdot s^{-1}$)			
			Sub-catchment 6 405.2 km^2	Sub-catchment 10 1068 km^2	Sub-catchment 15 2800 km^2	Sub-catchment 17 5273 km^2
2	50	50	24.02	65.56	132.54	216.17
5	20	80	42.97	129.56	250.13	428.11
10	10	90	57.31	177.98	339.08	588.43
25	4	96	76.26	241.98	456.66	800.37
50	2	98	90.60	290.40	545.62	960.70
100	1	99	104.94	338.82	634.57	1121.02
200	0.5	99.5	119.27	387.24	723.52	1281.35

The cumulative frequency distribution indicates that there is a 99.5% chance of non-exceedance for such a 200-year flood of 1281.35 $m^3 \cdot s^{-1}$ in the catchment, which means that there is only a 0.5% chance for this flood magnitude to equalled or exceeded (Figure 57). The cumulative probability graphs indicate the non-exceedance probability for all possible flood magnitudes in the catchment. A 100-year flood of magnitude 1121.02 $m^3 \cdot s^{-1}$ has a 99% chance of non-exceedance, while 50-, 25-, 10-, five-, and two-year floods respectively indicate a 98%, 96%, 90%, 80% and 50% chance of them not being exceeded.

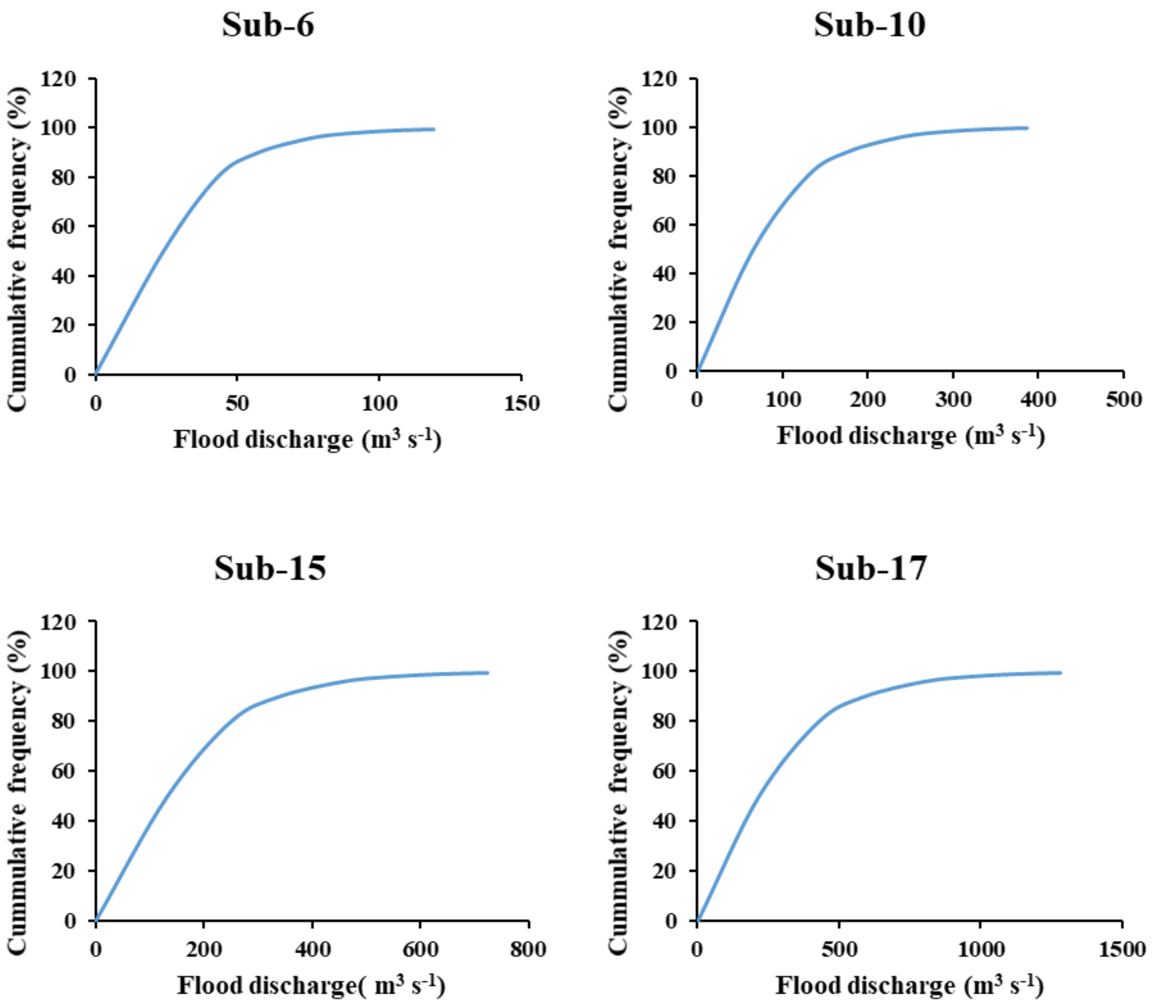

Figure 57: Cumulative frequency distribution for sub-catchments 6, 10, 15 and 17

5.7.5 Discussion

Simulating streamflow is a challenging process due to the numerous uncertainties in the form of input parameter inaccuracies, processes unaccounted for by the model, and processes occurring in the catchment that are unknown to the modeller. The lack of continuous high quality data is another challenge that hydrologists face when modelling streamflow. The process of modelling streamflow becomes even more difficult in catchments where irregular rainfall distribution occurs, such as the Luvuvhu River catchment. Despite this, modelling efforts involving the SWAT model have been conducted in various catchment types such as agricultural land and mountainous catchments by Jha (2011) and Mutenyo et al. (2013)

respectively. The studies proved that the SWAT model is capable of simulating run-off with satisfactory results for these conditions.

Initially, the model was unable to capture run-off discharge flows well. It is commonly experienced when simulating streamflow using SWAT because the model is executed through numerous parameters that interact and thus affect various processes. It is therefore a challenge to determine which parameter or parameter combination may be reducing the model's performance.

Initial simulation values were generated by SWAT, based on the general land use, soil and slope, where the peak flows were drastically overestimated. This meant that the water balance within the catchment may have been incorrect, thus contributing to the overestimation of the peak flows. Initial sensitivity analysis resulted in the choice of 12 parameters, which were used for calibration and validation. The twelves parameters were discovered to be more sensitive to streamflow output based on the large *t*-stat values and low *p*-values (< 0.05). After careful parameter adjustments based on SUFI-2 minimum and maximum parameter output values, parameters ALPHA_BF, CN2, GW_DELAY and SOL_K showed to be more sensitive to streamflow output. Ultimately, the model was able to simulate both peak and low flows well for both calibration and validation.

The use of SUFI-2 in SWAT-CUP to calibrate assisted in enabling adequate modelling since it incorporates almost all forms of uncertainties in the modelling processes. The model produced reasonable results of the *P*-factor during calibration and validation and the small indication of uncertainties could be due to inputs driving variables such as rainfall. An *R*-factor of less than 1 generally indicates good calibration results (Rostamian et al., 2008), which was the case for all sub-catchments 6, 10, 15 and 17 during both calibration and validation. However, the *P*-factor values for sub-catchments 10 and 17 were just lower than the acceptable value of 60%. According to Rostamian et al. (2008) this indicates that the actual uncertainty is higher than that shown, and could be improved by a higher *R*-factor value. The remainder of the sub-catchments' results indicated that most of the observed values were bracketed and were within the 95PPU boundary.

Overall, parameter ranges of the *P*-factor and *R*-factor reached desired limits, indicating substantial parameter uncertainties results, which were acceptable. Moreover, model uncertainties were falling within the permissible limits. Hence, SUFI-2 is capable of capturing the model's behaviour, with *P*-factor results indicating good model calibration strength and desirable levels of *R*-factor. For this reason, results obtained in this study demonstrate good model performance and acceptable accuracy of the model in run-off simulation. It can be concluded that the SWAT simulation results were satisfactory for the simulation of run-off in the Luvuvhu River catchment.

Observation functions coefficient of determination, NSE, RSR and PBIAS were analysed according to the limits placed by Moriasi et al. (2007) and Mutenyo et al. (2013) with objective functions reaching model efficiency of concurrently having an NSE index greater than 0.5, a PBIAS of ±25% and an RSR < 0.7. According to this standard, the model performed well during both calibration and validation. For sub-catchments that were unable to reach these limits, such as sub-catchments 10 and 17, this could be due to the choice of objective function influencing the results (Abbaspour, 2015).

To achieve the run-off simulation, a careful and time-intensive effort of calibrating SWAT parameters to better represent the catchment area was made. Once the parameters were set within a sufficient and acceptable calibration range, the model's results demonstrated the capability of the model to provide reasonable simulation of run-off.

One of the limitations of the model is the high number of parameters, which complicates the model's parameterisation and calibration process, which is therefore considered the SWAT model's weakness. Parameterisation continues to be of importance as highlighted in previous studies conducted. For parameterisation to be more efficient and sustainable, long period quality data is needed, which is a major obstacle in hydrological modelling. Despite results from this study being generally acceptable, the lack of data sets hinders better results and increases prediction uncertainties. Good quality data of climate and observed streamflow would improve the ability of run-off modelling to accurately simulate flow and improve the parameterisation and calibration process.

Following calibration and validation, a 30-year period of simulated flood discharge from 1986 to 2015 was used to analyse flood frequencies and estimate design flood. The data was sorted from highest to lowest and a reoccurrence interval was estimated. Through the sorting of simulated data it was evident that the highest flood flows were experienced in the years 1987/88, 2000/01, 2010/11 and 2013/14; these are years that correspond with the years Luvuvhu catchment received great flooding. The increase in flood peak frequency may be attributed to the changing land uses over the years.

Four probability plot graphs were created for the four sub-catchments using log-normal probability distribution. Sub-catchment 17, which is the outlet catchment, produced the highest flood magnitudes compared with the other catchments as it covered the whole Luvuvhu catchment in area. The 100- and 200-year floods revealed flood magnitudes of 1121.02 $m^3 \cdot s^{-1}$ and 1281.35 $m^3 \cdot s^{-1}$ respectively. This means that, for example, in 100 years a flood of 1121.02 $m^3 \cdot s^{-1}$ will occur in any given year. This flood magnitude may occur several times in that 100-year period and may occur in two or more years consecutively. This is also the case for a 200-year flood.

From the results, it is evident that the low-lying areas received more flooding during the 2000 and 2013 flood events while the mountainous areas received less flooding. This was unusual since naturally the Luvuvhu River catchment receives high rainfall in the mountainous areas. However, literature confirms that low-lying areas are more prone to flooding than mountainous areas. Furthermore, the floods were caused by tropical cyclones from Mozambique, hence results obtained can be justified.

The 2000 floods had more impact on the Limpopo Province and Mozambique due to tropical cyclone Eline (Reason & Keibel, 2004). The cyclone occurred from February to March 2000, causing intense flooding, which was later recorded as the worst flood event in 50 years, thus making it a 50-year flood (Smithers & Schulze, 2001). The 2013 floods started as a tropical low over Mozambique in January 2013. Later, tropical cyclone Hellen met the tropical low, causing extreme rainfall and flooding in South Africa.

The 10- and 50-year floods are regarded as high-risk floods since they occur more frequently. Knowing such magnitude will help to better prepare the community and disaster management groups in the catchment. Looking at upstream (sub-catchment 10) and downstream (sub-catchment 17) sub-catchments, the log-normal distribution showed a 10-year return period with estimated flood magnitude of 177.98 $m^3 \cdot s^{-1}$ upstream and 588.43 $m^3 \cdot s^{-1}$ downstream while a 50-year flood had an estimated flood of 290.40 $m^3 \cdot s^{-1}$ upstream and 960.70 $m^3 \cdot s^{-1}$ downstream.

Cumulative frequency distribution indicates that there is a 0.5% chance for a 200-year flood to occur, which means that there is a 0.5% chance for the event to be equalled or exceeded. The log-normal distribution model showed high peak events that can be used as estimating limiting values for design purposes. Furthermore, the distribution performed well enough to be considered as a distribution of choice in terms of flood frequency analysis and planning in the Luvuvhu River catchment.

Results obtained in this study were based on daily data that was available. However, a study undertaken by Lee et al. (2017) indicated that a shorter time increment might be suitable in producing an improved estimation. Therefore, it is suggested that use of hourly data can be useful in producing approximate estimations. However, this can be impractical in our study site since there is no shorter time increment data available. Nevertheless, it can still be recommended that future data collection may be done in hourly time increments for more accurate results.

The 2000 and 2013 flood disasters caught the Luvuvhu community unaware because people were not prepared for such disasters. The effects of the disasters could have been avoided through proper planning and investment management strategies. Therefore, results obtained from this study can be used for such planning to mitigate and adapt during future flooding events. It is further recommended that there be improved transfer of knowledge to the community and farmers of weather forecast and warnings of possible heavy rains that may lead to flooding so that people may be better prepared for such events. In planning, it is of utmost importance that planners be advised and reminded that hydrological models are guides and results are not certain. The floods may or may not occur as modelled as there are probabilities with various uncertainties involved.

5.8 Conclusions

This study aimed to assess the SWAT model in simulating run-off in the Luvuvhu River catchment. The catchment lies in an area vulnerable to flooding due to tropical depressions and the geographical distribution of river floodplains. This has led to catchments experiencing extreme flooding events over the past years, destroying crops and thus resulting in crop failure and reduced crop yield. A 2012 version of SWAT model was run through an interface with a QGIS Desktop 2.6.1 software, QSWAT 1.3 2016. The model was chosen because it is physically based, deterministic and semi-distributed, thus capturing many physical processes occurring in the catchment.

The SWAT model's initial run was implemented successfully. The model successfully simulated streamflow and proved to be capable of capturing streamflow trends despite the sub-catchment's characteristics and location. However, initial results indicated an overestimation of observed flows in parts of the catchment, revealing unacceptable correlation coefficient results in three of the sub-catchments (6, 15 and 17) while sub-catchment 10 displayed a good correlation. The evaluation of the model using the six statistical parameters (R, R^2, MAE, MBE, RMSE and NSE index) revealed model results that were unsatisfactory. From the initial results, it was evident that calibration and validation of the model needed to be conducted before attempting further analyses.

Calibration was conducted using 12 parameters which, based on previous studies, were recorded to be the most sensitive parameters for streamflow. Global sensitivity analyses found ALPHA_BF, CN2, GW_DELAY and SOL_K to be more distinguishable with $p < 0.05$. Performance indices results indicated that most of the observations with different parameters were grouped together by the 95PPU boundary, which signified the capability of SUFI-2 to capture the SWAT model behaviour. Following calibration and validation, SWAT simulation revealed satisfactory results for the prediction of run-off and the final parameter ranges were considered acceptable for the Luvuvhu River catchment. The percentage of observed data being grouped together by 95PPU during calibration indicated the strength of the model calibration to be satisfactory, with 60% of the data bracketed. *R*-factor results showed acceptable model calibration. Objective functions R^2, NSE index, RSR and PBIAS used to quantify the model's calibration result showed satisfactory results for both calibration and validation. It can be concluded that the SWAT model performed well in simulating run-off in the Luvuvhu River catchment after calibration and validation.

Flood frequency analyses were done, and a design flood estimation completed. This was accomplished using a 30-year period of simulated flood discharge from the SWAT model. Flood frequency analyses indicated increasing floods at greater probability of exceedance for all return periods. Focusing on sub-catchment 17, the Luvuvhu River catchment outlet, 50-, 100- and 200-year floods revealed flood magnitudes of 960.70 $m^3 \cdot s^{-1}$, 1121.02 $m^3 \cdot s^{-1}$ and 1281.35 $m^3 \cdot s^{-1}$ respectively. This meant that in 50 years, a flood of 960.70 $m^3 \cdot s^{-1}$ would occur in any given year. The flood may occur several times in the 50 years and may occur in two or more years consecutively. This is also the case for 100- and 200-year floods.

Cumulative frequency distribution indicates that there is a 0.5% chance for a 200-year flood to occur, which means that there is a 0.5% chance for the event to be equalled or exceeded. The log-normal distribution model produced good results that can be used to support planning and decision-making about development, flood mitigation and adaptation during the flooding season. Hence, it can be considered as a distribution model of choice among other probability distribution models for flood frequency analysis at any point in the Luvuvhu River catchment. It is of utmost importance that planners remember that hydrological models are guides and results are not certain. The floods may or may not happen because these are probabilities with various uncertainties involved.

6 DECISION SUPPORT TOOL FRAMEWORK

6.1 Introduction

Human beings are faced with making decisions every second and decision-making is normally based on a combination of experience, empirical data, and analysis of the situation. According to Nguyen et al. (2007), a decision support system (DSS) is a computer-based program that is either quantitative or qualitative and that assists in the decision-making process. A DSS is mostly designed to help users in making effective decisions by leading them through the step-by-step clear decision stages and with the likelihood of various outcomes resulting from different options (Rose et al., 2016).

In the agricultural sector, decision support tools (DST) are supposed to help farmers and their advisers in making better decisions helping them to alter their production systems accordingly for optimum production as well as reducing production costs (Newman et al., 1999; Lynch, 2002). During the worst times, the system should be able to assist the farmer by minimising losses. DST or tools developed for agricultural production are mostly built on raw input data like rainfall, soil water content and temperature.

DST can be helpful aids for sustainable natural resource management and deployment of these tools depends on their usability, appropriateness and simplicity. In this chapter, we present the framework for developing a DSS for the Luvuvhu River catchment. The Luvuvhu Agroclimatological Risk Tool (LART) was developed to provide agroclimatological risk information important to the production of rain-fed maize in the catchment. The tool is intended for use by farmers, extension officers, policymakers and agricultural risk advisers. Table 45 shows the potential users of the tool and their intended purposes.

The LART has two main components: climatological risk and forecasting. The climatological risk part enables the user to obtain drought stress risk, frost risk and flood risk for different maize crop varieties for a planting window starting in October to January. The best planting dates based on the risk associated with the onset and cessation of both rains and frost can be determined. Using climate forecasts obtained from the national forecasting centres, drought index can be predicted for different planting dates, thus giving the farmer valuable information when planning for the coming season. The tool also has a functionality of predicting onset of rains using weather and climate forecasts.

Table 45: Target groups and the possible use of LART decision support tool

Group	Purpose
Farmers	• To determine drought risk associated with planting maize near their location on different planting dates. • To determine flood risk at their locations. • To determine the rainy season characteristics (onset, cessation and duration of rainy season) of their locations based on climatology data to help in planning of major agricultural activities such as planting dates. • To help in planning the activities for the forthcoming season using forecast start of rains and agricultural drought risk depending on the planting dates.

Group	Purpose
Extension officers	• As an educational tool for the climate risk affecting crops in their designated area to equip them with climate information that will contribute in their decision-making towards ensuring natural resource protection and productivity of farms. • To help in their formulation of advisories to farmers before the start of the agricultural season on the cultivar choice using risk forecasting of drought and onsets of rain.
Government agricultural risk officers	• To help in issuing advisories related to climate risks associated with dryland maize production across the province.
Agricultural disaster managers	• To help in formulating policies that aim at adaptation to the climate risks affecting maize production in the province as well as in the policies that aim at mitigating the effects of climate risks in agriculture.
Agricultural insurance officers	• To assist in kinds of insurance that are applicable for different localities depending on the degree of the climate hazards normally encountered in the past.

6.2 User Interface

The user interface (Figure 58) was designed in a user-friendly manner to enable ease of manipulation of the information.

Figure 58: The LART decision support tool user interface

6.3 Functionality

The flow chart shown in Figure 59 illustrates the options available in the framework for the Luvuvhu decision support tool. The different multi-layered architecture used in the development of the decision support tool is shown in Figure 60 with the corresponding programming languages.

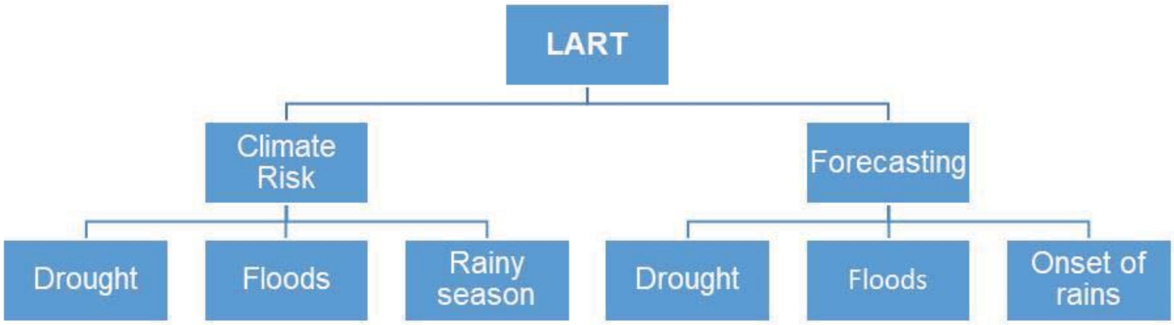

Figure 59: Flow chart for the model options of the decision support tool for dryland maize production in the Luvuvhu River catchment

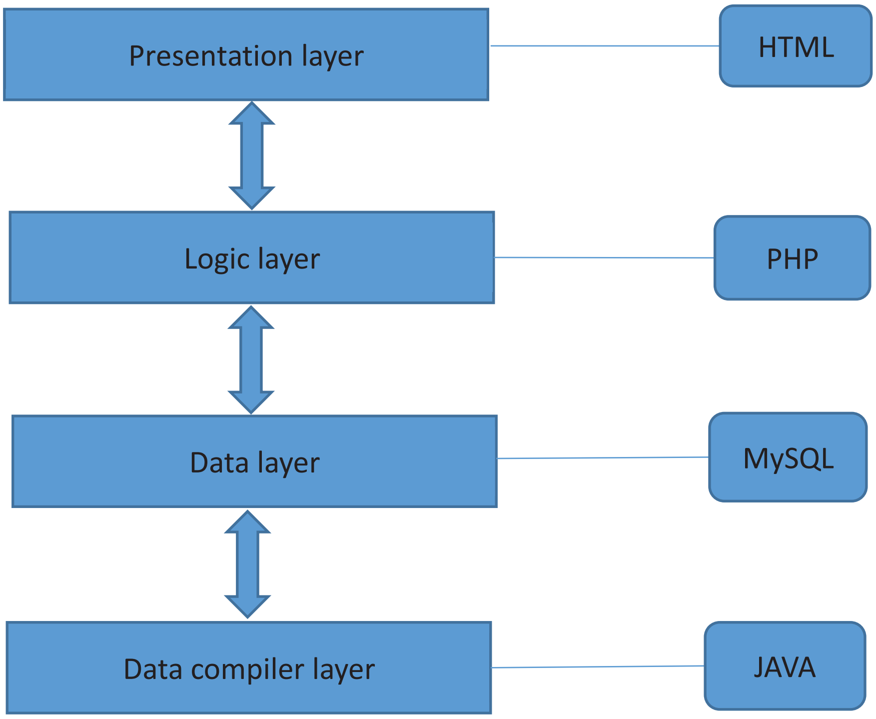

Figure 60: Luvuvhu agroclimatic DSS architecture

6.3.1 Seasonal weather forecasting

Every month, updates of the seasonal forecast generated by SAWS are uploaded into the DSS with implications of the forecast on the farming community of the Luvuvhu River catchment (Figure 61).

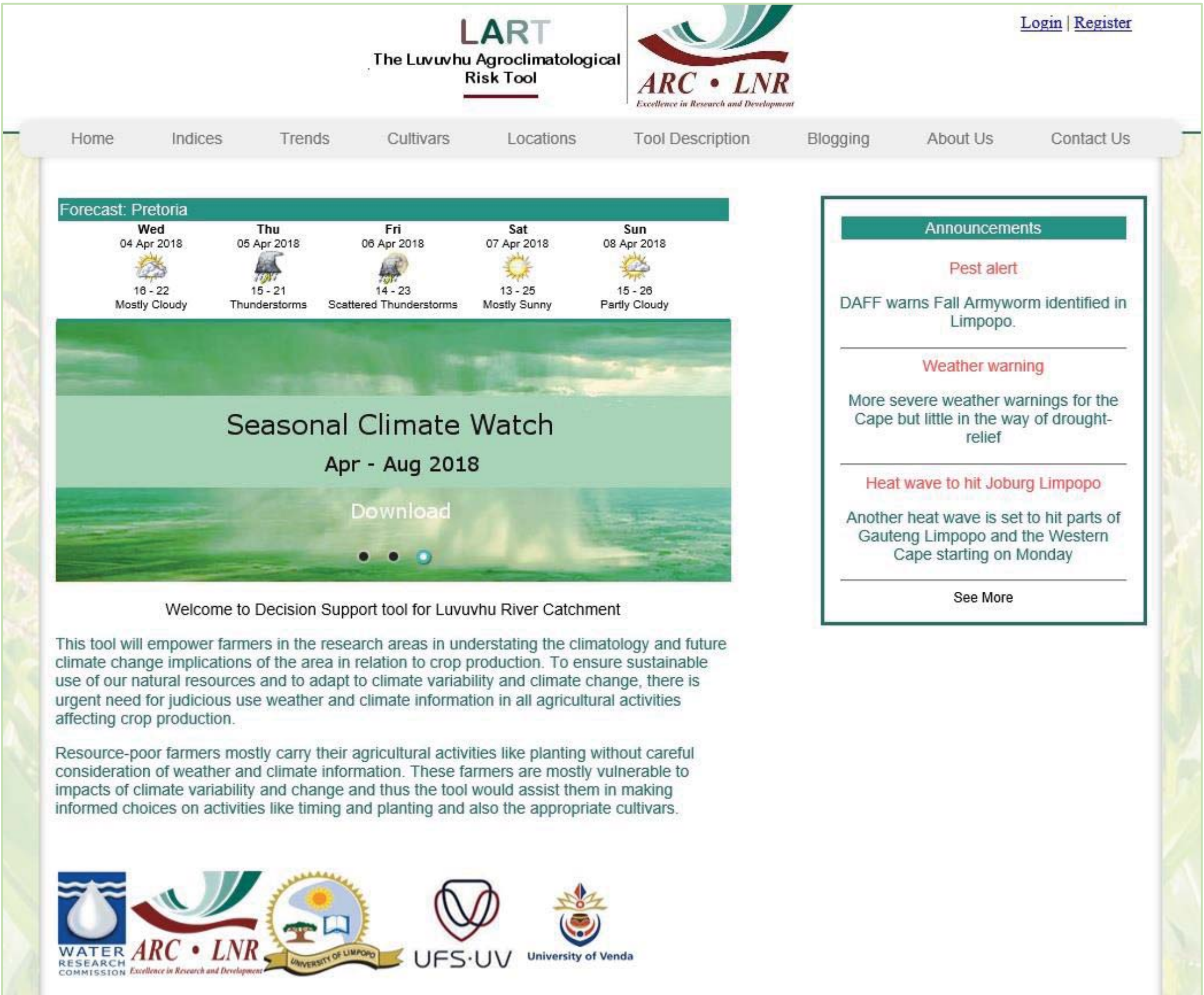

Figure 61: Seasonal climate watch information for end users

6.3.2 Warnings

The tool also updates the climate and agricultural warnings that are relevant to the study area. End users are provided with up-to-date news on what is happening and are given tips on relevant issues. Users also have the ability to comment on those issues. An example is the recurrence of the fall armyworm that was detected during the 2017/18 growing season (Figures 62 and 63).

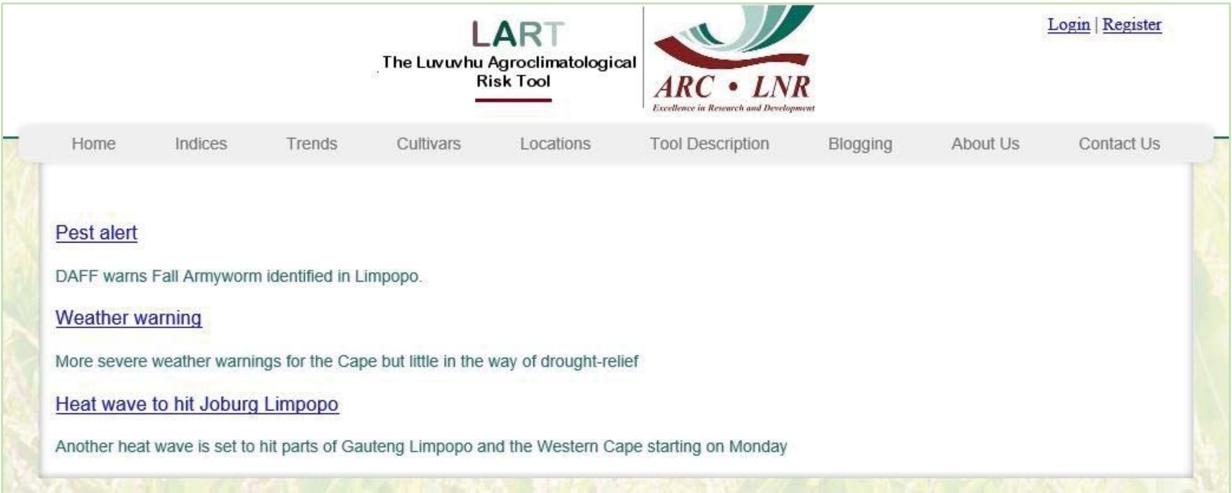

Figure 62: Example of warnings in December 2017

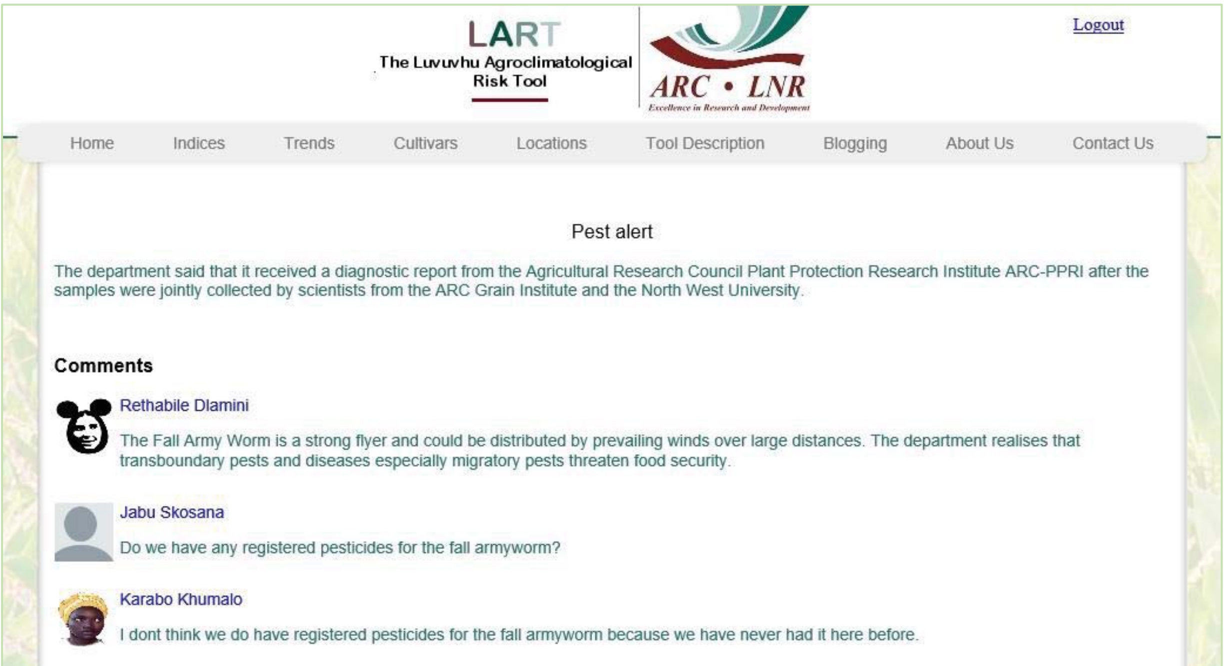

Figure 63: Examples of user comments on fall armyworm warnings in December 2017

6.3.3 Agronomic choices

The user has an option to select the most suitable maize cultivar they are interested in obtaining the climate risks that occur during the growing period of the particular cultivar (Figure 64). Alternatively, they can also key in the growing-degree days of their cultivar if it is not in the list provided.

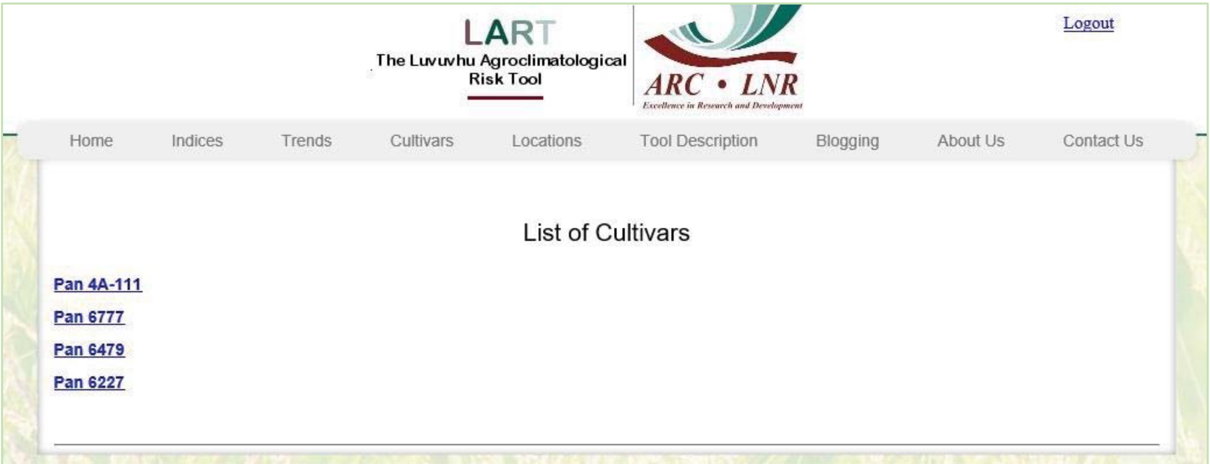

Figure 64: Some of the initial agronomic options that users have in determining climate risk

6.3.4 Area of interest

The major villages in the catchment are in the drop-down menu provided and a user can type in their area of interest. Alternatively, they can enter the coordinates of their farm for accurate estimation of climate information (Figure 65).

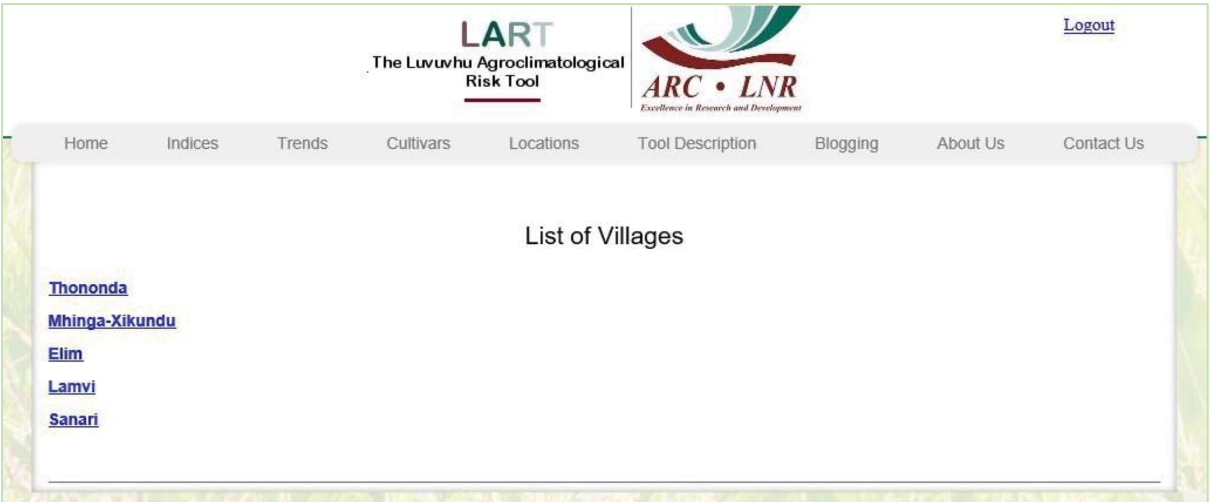

Figure 65: Choice of villages from the list

6.3.5 Rainy season options

Rainy season characteristics for all the locations within the catchment can be assessed by either selecting a village or by entering the coordinates of choice (Figure 66). The tool will interpolate the data stored in the database to provide information needed (Figure 67).

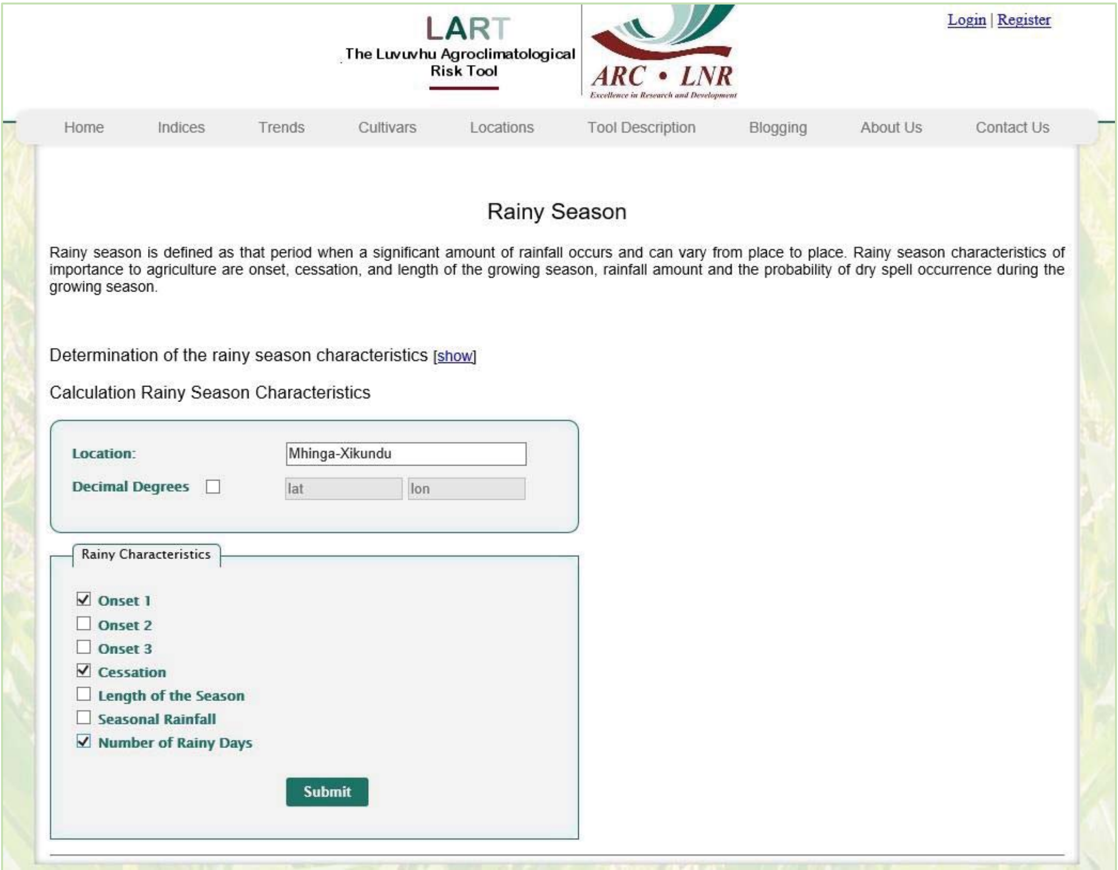

Figure 66: Choices for assessing rainy season characteristics

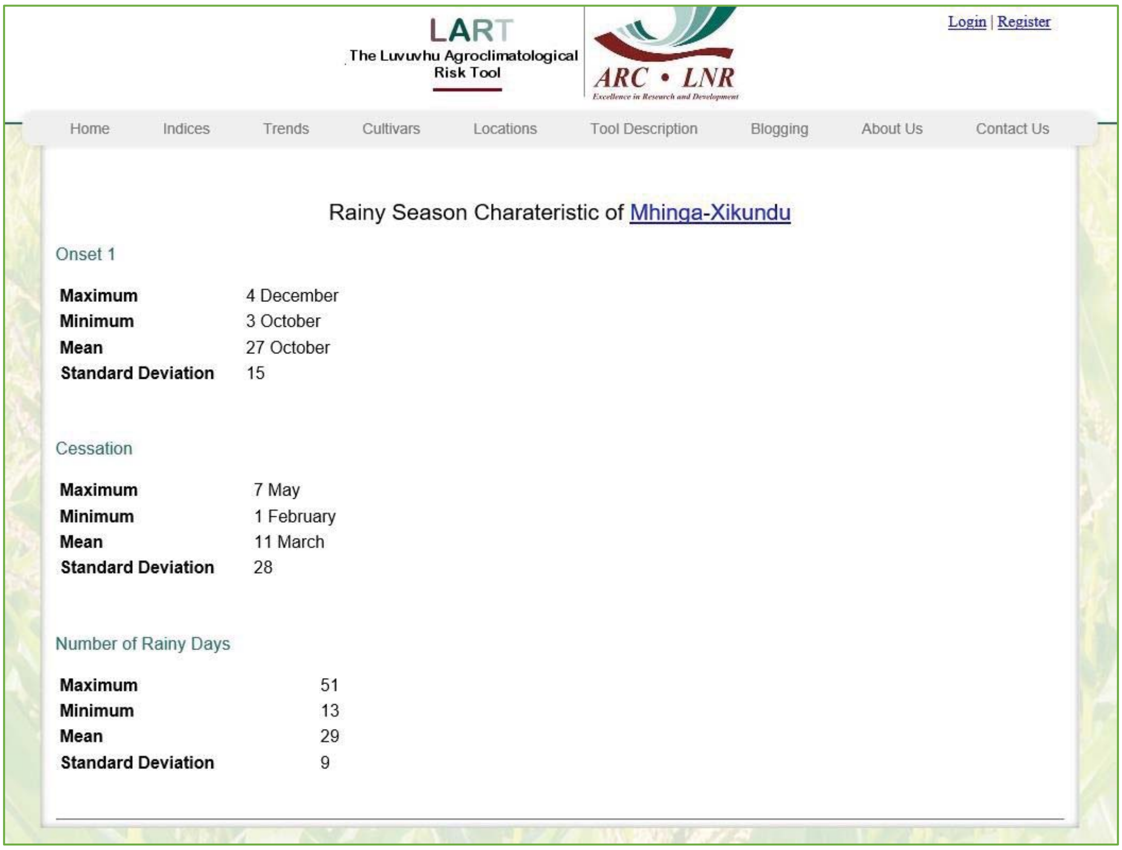

Figure 67: Example of the results of a query on rainy season characteristics

6.3.6 Dry spells options

The probability of dry spells for all the locations within the catchment can be assessed by either selecting the village or by entering the coordinates of choice, and thereafter selecting a cultivar type, planting date and planting stages (Figure 68). The tool interpolates the data stored in the database to provide the information needed (Figure 69). The user can also compare more than one probability distribution results by selecting different villages, cultivars, planting dates and planting stages (Figure 70).

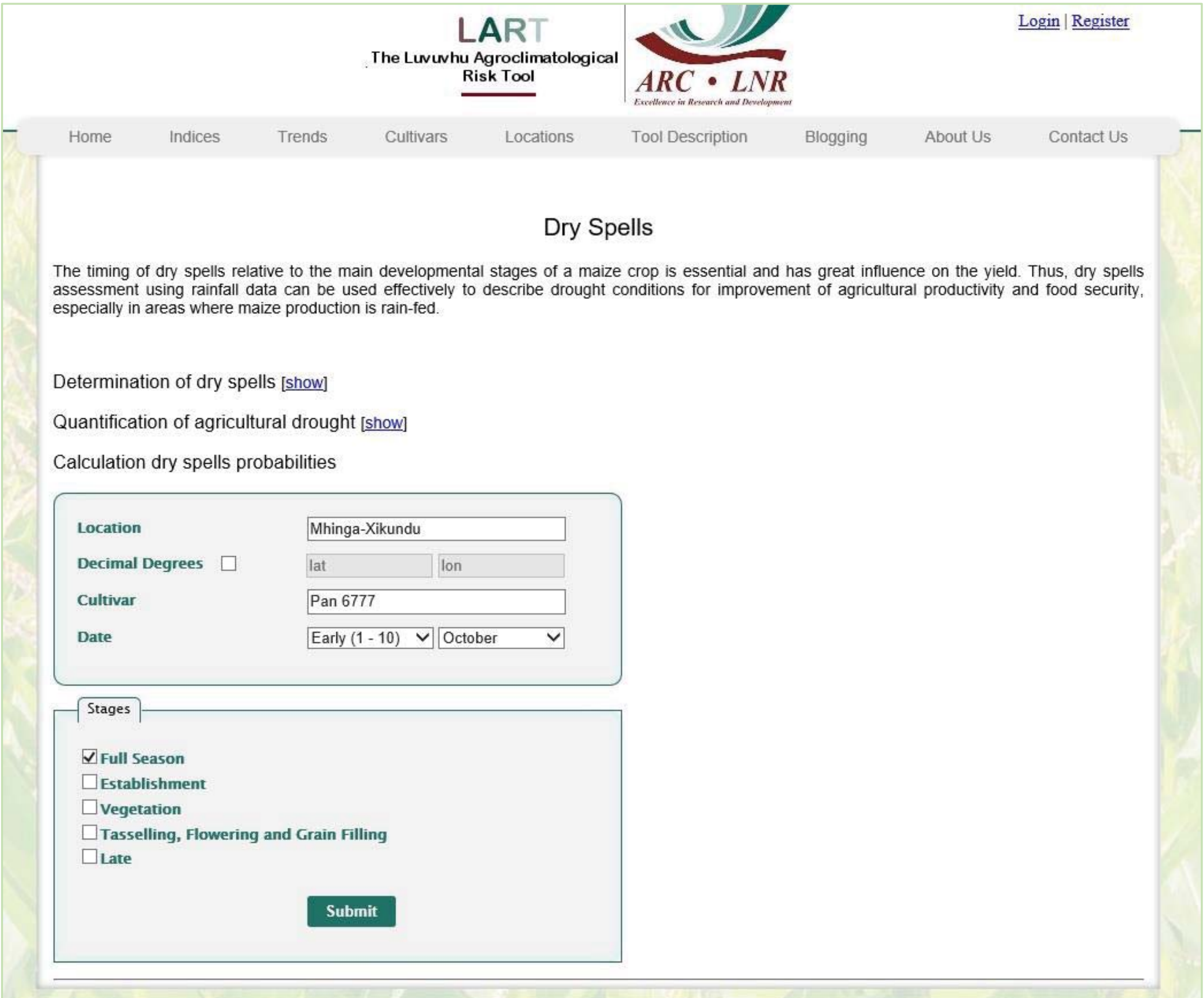

Figure 68: Choices for assessing dry spells

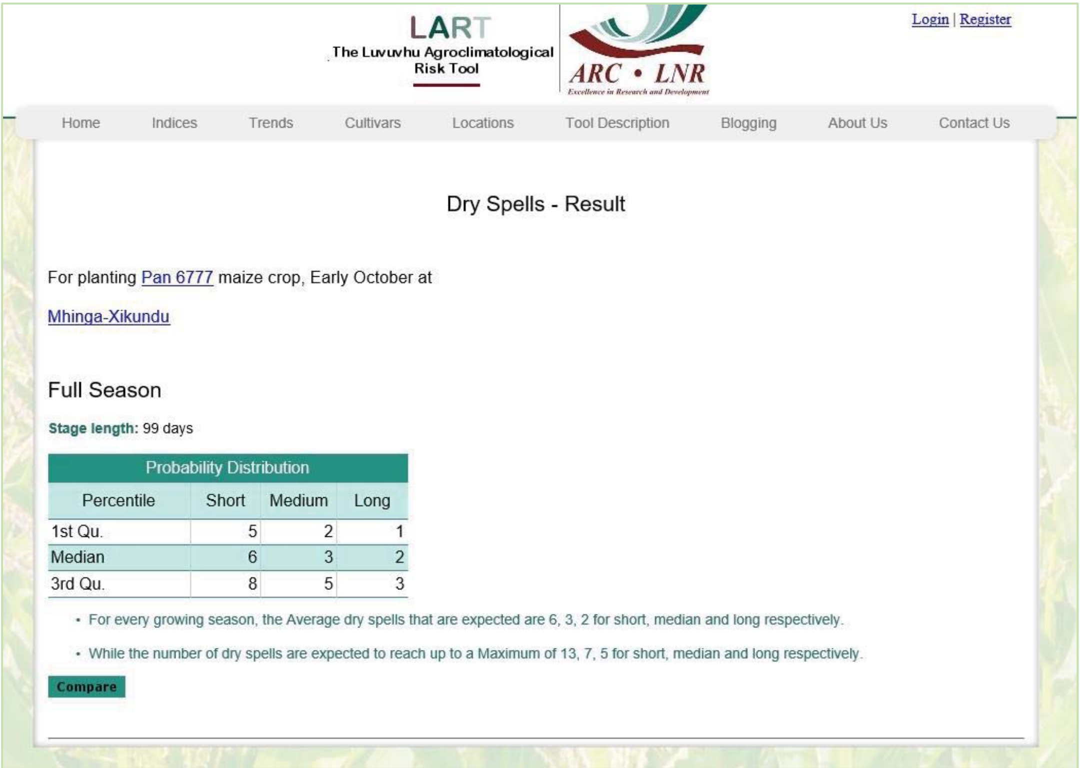

LART
The Luvuvhu Agroclimatological Risk Tool

ARC • LNR
Excellence in Research and Development

Login | Register

Home Indices Trends Cultivars Locations Tool Description Blogging About Us Contact Us

Dry Spells - Result

For planting Pan 6777 maize crop, Early October at

Mhinga-Xikundu

Full Season

Stage length: 99 days

Probability Distribution			
Percentile	Short	Medium	Long
1st Qu.	5	2	1
Median	6	3	2
3rd Qu.	8	5	3

- For every growing season, the Average dry spells that are expected are 6, 3, 2 for short, median and long respectively.
- While the number of dry spells are expected to reach up to a Maximum of 13, 7, 5 for short, median and long respectively.

Compare

Figure 69: Example of the results of a query on probability of dry spells

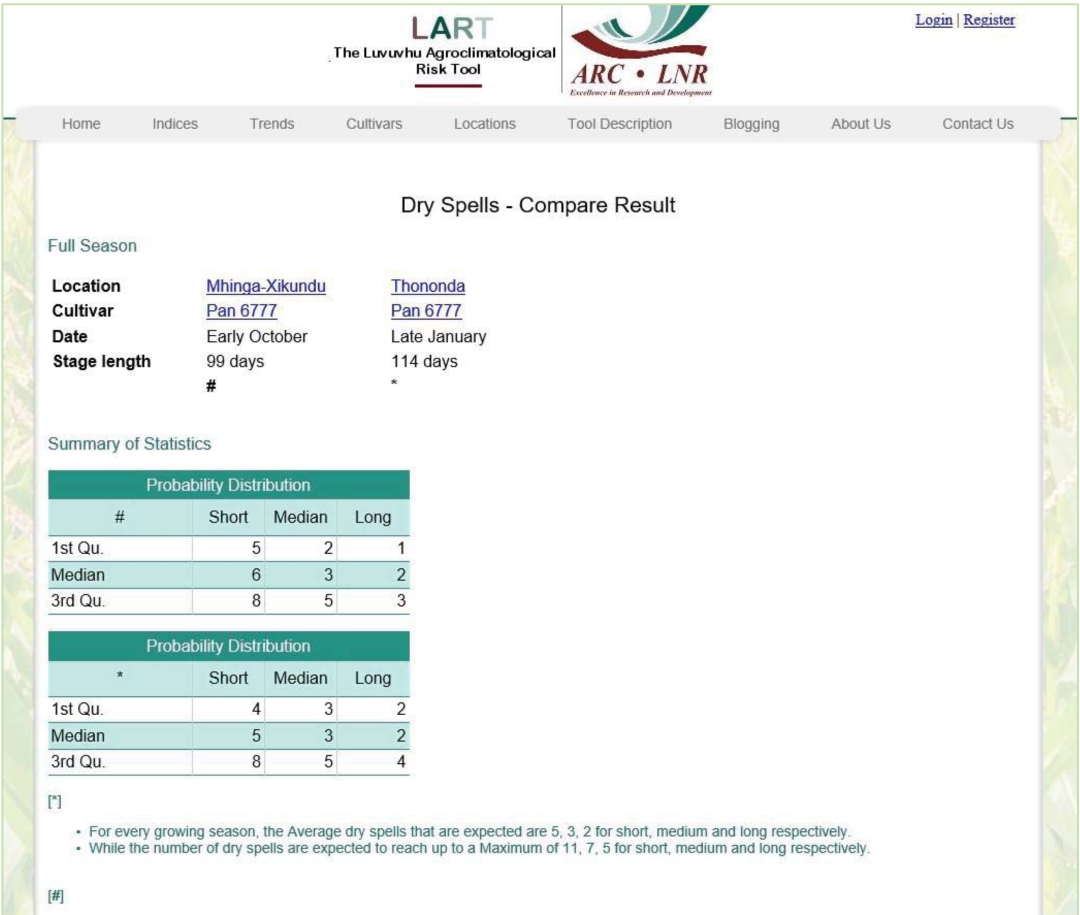

LART
The Luvuvhu Agroclimatological Risk Tool

ARC • LNR
Excellence in Research and Development

Login | Register

Home Indices Trends Cultivars Locations Tool Description Blogging About Us Contact Us

Dry Spells - Compare Result

Full Season

Location	Mhinga-Xikundu	Thononda
Cultivar	Pan 6777	Pan 6777
Date	Early October	Late January
Stage length	99 days	114 days
	#	*

Summary of Statistics

Probability Distribution			
#	Short	Median	Long
1st Qu.	5	2	1
Median	6	3	2
3rd Qu.	8	5	3

Probability Distribution			
*	Short	Median	Long
1st Qu.	4	3	2
Median	5	3	2
3rd Qu.	8	5	4

[*]

- For every growing season, the Average dry spells that are expected are 5, 3, 2 for short, medium and long respectively.
- While the number of dry spells are expected to reach up to a Maximum of 11, 7, 5 for short, medium and long respectively.

[#]

Figure 70: Example of the results of a query on comparison of dry spells

6.3.7 Trends

The tool also provides the user with interactive charts, which are drawn in real time. Users can view annual/agricultural year trends of some weather elements (rainfall or temperature) (Figure 71). In addition they can view one or even compare rainy season characteristics trends such as seasonal rainfall, length of the season or number of rainy days, from one or more villages. Figure 72 shows a comparison of trends of the length of the season between two villages.

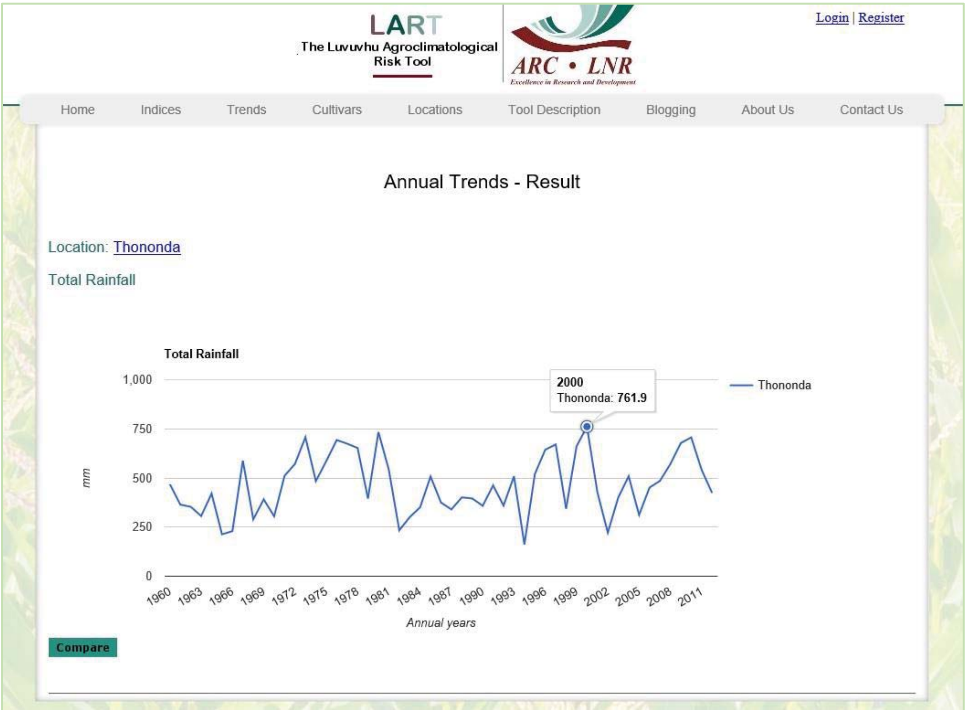

Figure 71: Example of the results of a query on annual rainfall

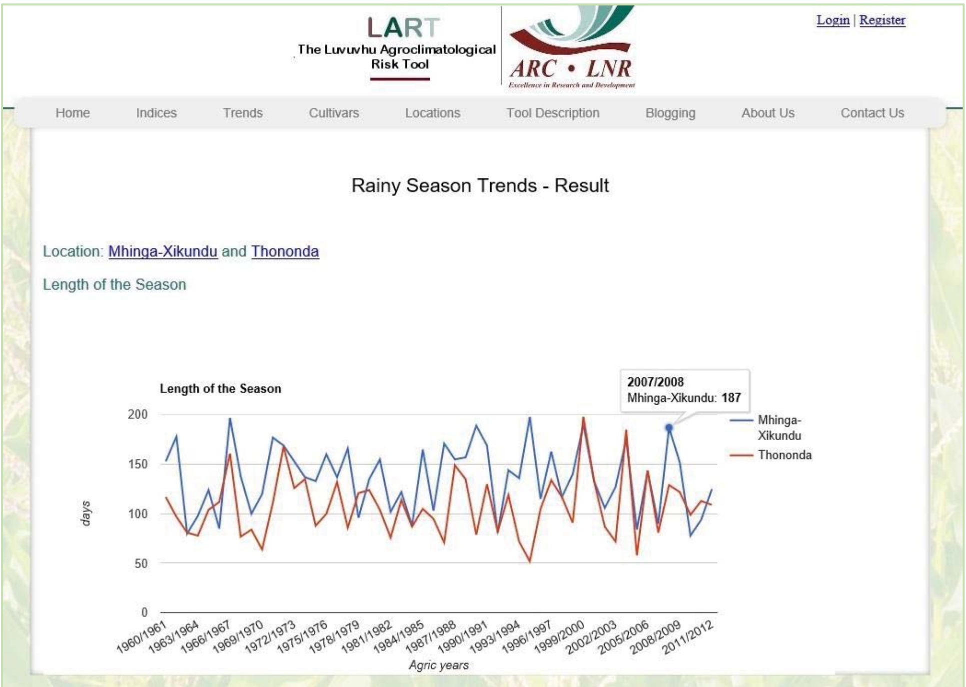

Figure 72: Example of the results of the query on comparison of length of the season

6.3.8 Blogging

The LART decision support tool allows end users to register/log in; thereafter they can view or edit their profiles. End users can share ideas by posting relevant information to the tool, whether it is a farmer giving or asking for advice, or expert raising awareness. Thereafter, other users can comment and have a discussion (Figure 73).

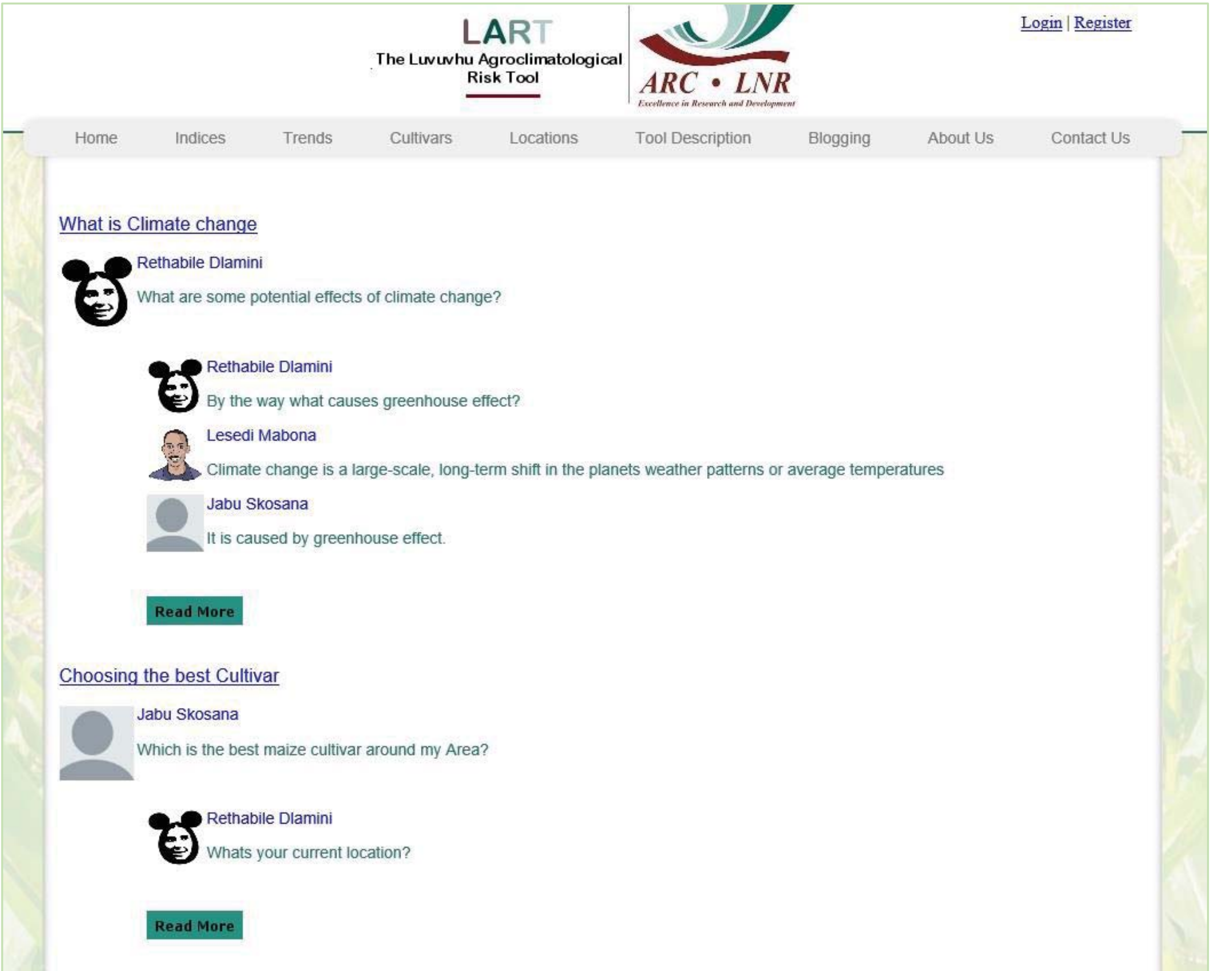

Figure 73: Example of a blogging page

6.4 Conclusions

The LART has significant potential for application in the Limpopo Province. The tool at its operational state will bridge the gap that exist between the scientists and the policymakers with the enhancement of the scientific approaches that are generalised for use by the ordinary people. The tool can be of crucial importance to the entire farming community as a guide to ensure that informed decisions are taken with the consideration of the climatology and weather forecast information for that particular region.

7 CONCLUSIONS AND RECOMMENDATIONS

7.1 Project Conclusions

The project demonstrated the importance of measuring and archiving weather information in the Luvuvhu River catchment. In recent times, the number of stations recording climate information has decreased in the region. There are a number of reasons for the decline in the recording stations but the trend has to be stopped by investing in weather station network. Weather data is used by a number of stakeholders to make decisions in their area of interest. This necessitated the installation of four extra automatic weather stations in areas of need in the Luvuvhu River catchment.

The recorded climate from the weather stations is filled with gaps that arose from a number of reasons. These gaps in the climate data are inconvenient to the decision makers and thus there was a need for the project to develop means of solving the problem. Scientists have developed a number of techniques that can be used to close the gaps that are in the climate data. Most of the techniques use neighbouring station data relationships with the data at the target station. The patching program was then developed incorporating some of the recommended techniques for patching weather data. The tool can be used by meteorologists and agricultural practitioners all over the world to assist scientist in filling missing climate data.

It can be concluded that this project was successful in investigating rainfall characteristics, drought and estimating flood peaks in the Luvuvhu River catchment. Findings show that rainy season characteristics are influenced by spatial rainfall distribution as wet areas of the catchment experience early onset, late cessation, high seasonal rainfall, and a high number of rainy days, low chances of false onset and low chances of dry spells. Dry areas are characterised by late onset, early cessation, short season, low seasonal rainfall, and a low number of rainy days and high chances of dry spells. Compared with wet areas of the catchment, dry areas have a high probability of crop failure if planting is undertaken after the first onset due to a high number of dry spells. Furthermore, all areas had a high probability of both short and medium dry spells in October. With Sigonde, Pafuri, Tshiombo and Folovhodwe still having a high probability of dry spells in November, planting is not advised at these areas in November but rather in December. Therefore, farmers should use the first onset for land preparation and planting following the second onset in November and December as there are fewer dry spells depending on the location. However, if planting is undertaken after the first onset, it should be supplemented with irrigation or harvested rainwater to avoid the negative effects of long dry spells on maize growth. Areas such as Punda Maria, Sigonde, Folovhodwe, Pafuri and Sigonde do not meet maize production requirements in the current climate. On the other hand, they do meet production requirements of other crops such as cowpeas, sorghum and dry beans which can be marketed in place of maize.

Analysis on drought revealed that stations receiving moderate to high annual rainfall were at a higher risk of frequent SPEI values of −1 to −1.99 (moderate to severe drought) during the most critical stage of the crop following planting in December, while the upper catchment experienced more frequent droughts relative to October planting date. Results given by WRSI on the performance of the maize crop subjected to drought conditions revealed a high risk of crop water requirements not being met during critical periods of the growing season, following planting in December at all stations. Generally, Spearman's rank correlation test revealed that there was a regularity in the behaviour of drought and that the area did not become drier or wetter over time. Overall features of drought conditions in the future as projected under the RCP 4.5 scenario showed a tendency to intensify during the far-future as relative to the base. This was statistically significant at all stations, based on the WRSI, while SPEI results revealed this change at two stations. Overall drought conditions in the future showed a propensity to intensify during the near-future and far-future climates relative to the base.

The work on hydrology assessed the flood frequency analysis over the catchment. Since hydrological systems are very complex and not easily understood, therefore, hydrological models are used to simulate flows. For this study, initial simulation results indicated an over-estimation of low flows, which necessitated the calibration and validation of the SWAT model. Flood frequency analyses indicated increasing floods at greater probability of exceedance for all return periods. Focusing on sub-catchment 17 being the Luvuvhu River catchment outlet, 50-, 100- and 200-year floods revealed flood magnitudes of 960.70 $m^{3\cdot}s^{-1}$, 1121.02 $m^{3\cdot}s^{-1}$ and 1281.35 $m^{3\cdot}s^{-1}$ respectively.

Moreover, essential communication between meteorological scientists, decision makers and the farmers can help in planning and decision-making ahead of the upcoming agricultural season and during the season. It is crucial to package all the agroclimatic risks affecting crops into a decision support tool. The proposed LART aims at assisting the farming community in the region in making decisive deductions such as appropriate planting dates and frequency of droughts during different planting windows.

7.2 Recommendations and Future Research

Recommendations based on the key findings of the report can be given as follows:

- In dry years, semi-arid areas of the catchment experience a short season as sufficient rainfall only occurs in December and then starts to decrease again in January, implying that in four out of five years there would not be any planting of maize as there would not be sufficient rainfall for farmers to begin planting and sustain the crop through its growing cycle. For sub-humid and humid areas of the catchments such as Levubu, Thathe and Entabeni, rainfall is sufficient for all years to permit maize production (dry, normal and wet years). However, farmers are advised to plant drought-tolerant cultivars and crops in years with below-normal rainfall but planting can commence as early as October.
- In wet years planting can begin as early as October for all areas of the catchments. In wet years, farmers should plant larger areas so that they can store maize for dry years, meaning that farmers should also invest in proper storage facilities for maize. Production of maize at favourable areas such as Entabeni, Levubu, Thathe, Lwamondo, Vreemedeling and Tshiombo should be maximised so that there is sufficient maize to supply all areas of the catchment. Proper storage facilities for maize should be built to store surplus in high rainfall seasons.

- Farmers can be advised to invest in rainwater harvesting technologies or a proper irrigation system and reduce plant population density. For farms located next to rivers, farmers can purchase generators to pump water during irregular rains and long periods of dry spells.
- Analysis on previous droughts led to a recommendation of using October-November as the optimum planting date in the catchment. In order to minimise the risk of damaging drought conditions on maize, planting in October can be recommended at stations Levubu, Lwamondo, Thohoyandou and Tshiombo, however, planting too early (1st dekad of October) might place crops grown in these areas under drought stress.
- It can also be advised for farmers located near the stations Punda Maria, Sigonde and Pafuri to plant in November. However, these three regions have shown (by the WRSI results) to be unsuitable for rain-fed maize production, with the number of seasons subjected to extreme drought conditions being >50% out of all the analysed seasons.
- It is evident that the vast majority of farmers in the Luvuvhu River catchment can expect to prepare for more intense drought conditions during the future climate periods. In order to mitigate the possible effects of droughts under climate change, farmers should consider planting drought-tolerant and short maturing crop varieties. This will increase the probability of meeting crop water requirements during the sensitive stages of crop growth.
- Sustainable water management measures such as conservation agriculture (intercropping, mulching, rainwater harvesting, crop rotation, among others) should be applied to mitigate the possible drought effects under climate change. Apart from farm level, strategies can also be adopted on a national level for effective mitigation and adaptation.

Future research at the catchment could investigate the following:

- The availability and accessibility of drought-tolerant and early-maturing maize cultivars for the smallholder farmers in rural areas.
- The introduction of other crops requiring less rainfall such as sorghum, millet, cow peas and beans as well as their economic value for areas not meeting rain-fed maize production requirements.
- The introduction of water management strategies for semi-arid and sub-humid regions of the catchment to increase maize yield.
- Crop suitability taking into account all production requirements of the crops including soil, water, air temperature, solar radiation, and pH.
- Assessments on adapting to climate change on different staple crops as well as suitability studies can also be considered in the area.
- In addition, for a more comprehensive assessment of climate change, future studies may also consider using emission scenarios provided by the IPCC's latest assessment report.
- Future work could consider using crop modelling to estimate maize yields, considering different management practices, crop varieties and seasonal variations of climate.
- There are many future research areas involving the SWAT model that need attention. Due to the size of the catchment study area, a lower resolution DEM was used, which also contributed to the lack of accuracy of the results obtained. The accuracy of results would increase if a study were undertaken on a smaller, more specific sub-catchment using a much higher DEM resolution.

- Using more than one weather generation model could improve the quality of generated climate data and reveal some inconsistencies that may have existed with the SWAT model. The SWAT model simulation results in the catchment may be compared with another hydrological model simulation results in order to quantify the calibration process, which may be a possible future study.
- SWAT model interaction with other hydrological models may also be a good tool for future catchment planning and management purposes. The model can be used to simulate sediment loading and land use management practices, which due to the scope of the study was not undertaken.

REFERENCES

Abbaspour KC. 2015. SWAT-CUP 2012: SWAT Calibration and Uncertainty Programs: A User Manual, Switzerland: Eawag Aquatic Research.

Abdullah MA, AL-Mazroui MA. 1998. A climatological study of the southwestern region of Saudi Arabia. I. Rainfall analysis. Climate Research. 9: 213-223.

Abramowitz M, Stegun, IA. 1965. Handbook of Mathematical Functions With Formulas, Graphs, and Mathematical Tables, National Bureau of Standards: Applied Mathematics Series No. 55, pp. 446-452.

Agricultural Disaster Management Policy. 2011. South Africa: Agricultural disaster management policy: Limpopo Provincial Government, 16 pp. Available at: http://www.lda.gov.za/downloads/disaster_management_policy/agric_disaster_management.pdf (Accessed on 15 November 2015).

Alexakis DD, Hadjimitsis DG, Agapiou A. 2012. Estimating flash flood discharge in a catchment area with the use of hydraulic model and terrestrial laser scanner. In: CG Helmis, PT Nastos (Eds.). Advances in Meteorology, Climatology and Atmospheric Physics, Springer Atmospheric Sciences. DOI 10.1007/978-3-642-29/72-2_2.

Allan RJ. 2000. ENSO and climate variability in the past 150 years. In: HF Diaz and V Markgraf (Eds.), El Niño and the Southern Oscillation: Multiscale Variability and Global and Regional Impacts. New York, NY: Cambridge University Press. pp. 3-55.

Allen RG, Pereira LS, Raes D, Smith M. 1998. Crop evapotranspiration: Guidelines for computing crop water requirements. Irrigation and drainage FAO Paper (56). Rome, Italy, 300(9).

Ambrosino C, Chandler RE, Todd MC. 2014. Rainfall-derived growing season characteristics for agricultural impacts assessment in South Africa. Theoretical and Applied Climatology 115: 411-426.

ARC-ISCW. 2016. Agroclimatology Database. Agricultural Research Council: Institute for Soil, Climate and Water, Pretoria, South Africa.

Arnold JG et al. 2012. SWAT: Model use, calibration and validation. American Society of Agricultural and Biological Engineers 55: 1491-1508.

Aronica GT, Candela A, Fabio P, Santoro M. 2012. Estimation of flood inundation probabilities using global hazard indexes based on hydrodynamic variables. Physics and Chemistry of the Earth 42: 119-129.

Aslam M, Zamir MSI, Afzai I, Yaseen M, Mubeen M, Shoaib A. 2013. Drought stress, its effect on maize production and development of drought tolerance through potassium application. Agronomical Research in Moldavia 2(154): 99-114.

Ati OF, Stigter CJ, Oladipo EO. 2002. A comparison of methods used to determine the onset of growing season in Northern Nigeria. Journal of Climatology 22: 731-742.

Austin WD. 2008. Drought in South Africa: Lessons lost and/or learnt from 1990 to 2005. M.Sc. thesis, University of the Witwatersrand, Johannesburg, 161 pp.

Aviad Y, Kutiel H, Lavee H. 2004. Analysis of beginning, end, and length of the rainy season along with a Mediterranean arid climate transect for geomorphic purposes. Journal of Arid Environments 59: 189-204.

Ayoade JO. 2004. Introduction to Climatology for the Tropics, 2nd ed. Ibadan: Spectrum Books.

Barron J, Rockström J, Gichuki F, Hatibu N. 2003. Dry spell analysis and maize yields for two semi-arid locations in east Africa. Agricultural and Forest Meteorology 117: 23- 37.

Bergueria S, Vicente-Serrano SM. 2013. Calculation of the Standardized Precipitation Evapotranspiration Index. R package version 1. Available at: https://cran.r-project.org/web/packages/SPEI/SPEI.pdf (Accessed on 23 June 2016).

Bjørnæs C. 2013. A guide to representative concentration pathways. Center for International Climate and Environmental Research. Available at: https://www.sei-international.org/mediamanager/documents/A-guide-to-RCPs.pdf (Accessed on 1 June 2017).

Brouwer C, Heibloem M. 1986. Irrigation water management: Irrigation water needs. FAO, Training manual no. 3, Rome, Italy.

Canadian Food Inspection Agency. 2014. The biology of Zea mays (L.) (Maize). Biology document no. BIO1994-11. Available at: http://www.inspection.gc.ca/plants/plants-with-novel-traits/applicants/directive-94-08/biology-documents/zea-mays-l-/eng/1330985739405/1330985818367 (Accessed on 15 November 2015).

Chabane N. 2002. An evaluation of the influences on price and production in the maize market following liberalisation. TIPS Forum, 21 pp.

Chapuis RP. 2012. Predicting the saturated hydraulic conductivity of soils: A review. Bulletin of Engineering Geology and the Environment 71: 401-434.

Chen FW, Liu CW. 2012. Estimation of the spatial rainfall distribution using inverse distance weighting (IDW) in the middle of Taiwan. Paddy Water Environment 10: 209-222.

Chetty K, Smithers J. 2005. Continuous simulation modelling for design flood estimation in South Africa: Preliminary investigations in the Thukela catchment. Physics and Chemistry of the Earth 30: 634-638.

Chikodzi D, Simba FM, Murwendo T. 2012. Perceptions, vulnerability and adaptation to climatic change and variability in Masvingo Province. Greener Journal of Political and Social Sciences 2(5):156-165.

Clemence BSE. 1997. A brief assessment of a weather data generator (CLIMGEN) at Southern African Sites. Water SA 23: 271-274.

Dai A. 2011. Drought under global warming: A review. WIREs Climatic Change 2: 45-65.

Daniel WW. 1999. Biostatistics: A Foundation for Analysis in the Health Sciences. New York, NY: John Wiley and Sons.

Das HP. 2012. Agrometeorology in Extreme Events and Natural Disasters. Hyderabad, India: BS Publications, India, 600 pp.

Davis C, Joubert A. 2011. Southern Africa's climate: Current state and recent historical changes. In: C Davis (Ed.), Climate Risk and Vulnerability: A Handbook for Southern Africa. Stellenbosch: CSIR, pp. 7-20.

DePue M. 2010. Flood types and characteristics. In: Annual Georgia Association of Floodplain Management Conference, 23 March, Lake Lanier Islands, Georgia, pp. 1-27.

De Silva RPD, Dayawansa NDK, Ratnasiri MD. 2007. A comparison of methods used in estimating missing rainfall data. The Journal of Agricultural Sciences 3(2):101-108.

Dile Y, Srinivasan R, George C. 2015. QGIS interface for SWAT (QSWAT): User manual for QSWAT version 1.4.

Dlamini, L. 2013. Modelling of standardized precipitation index using remote sensing for improved drought monitoring. M.Sc. thesis, University of Witwatersrand, Johannesburg, p.8-82.

Droogers P, Allen RG. 2002. Estimating reference evapotranspiration under inaccurate data conditions. Irrigation and Drainage System 16: 33-45.

DWAF. 2004. Luvuvhu/Letaba water management area: Internal strategic perspective. Report no. 02/000/00/0304, 166 pp. Department of Water Affairs and Forestry, Pretoria.

DWAF. 2012. Development of a reconciliation strategy for the Luvuvhu and Letaba water supply system: Inception report. Report no. P WMA 02/B810/00/1412/1, 73 pp. Department of Water Affairs and Forestry, Pretoria.

Dyson LL. 2009. Heavy daily-rainfall characteristics over the Gauteng Province. Water SA 35: 627-638.

Eccel E. 2012. Estimating air humidity from temperature and precipitation measures for modelling applications. Meteorological Applications 19: 118-128.

Engelbrecht F et al. 2015. Projections of rapidly rising surface temperatures over Africa under low mitigation. Environmental Research Letters 10: 8.

Etuonovbe AK. 2011. The devastating effect of flooding in Nigeria. FIG working week, 18-22 May, Mairakech, Morocco, pp. 1-15.

Ezemonye MN, Emeribe CN. 2011. Flood characteristics and management adaptation in parts of the IMO river system. Ethiopian Journal of Environmental Studies and Management 4: 56-64.

Fadil A, Rhinane H, Kaoukaya A, Kharchaf Y, Bachir OA. 2011. Hydrologic modelling of the Bouregreg watershed (Morocco) using GIS and SWAT model. Journal of Geographic Information System 3: 279-289.

FAO. 1986. Early agrometeorological crop yield assessment. In: Plant Production and Protection Paper No. 73. Food and Agriculture Organization of the United Nations, Rome, Italy, 158 pp.

FAO. 2004. Drought impact mitigation and prevention in the Limpopo River Basin: A situation analysis. In: Land and Water Discussion Paper No. 4. Food and Agriculture Organization of the United Nations, Rome, Italy, 149 pp.

FAO. 2005. New local climate estimator. Food and Agriculture Organization of the United Nations, Rome, Italy. Available at: http://www.fao.org/nr/climpag/pub/en3_051002_en.asp (Accessed on 04 November 2015).

Friesland H, Lopmeier FJ. 2006. The activities of the German Weather Service (DWD) in the field of agroclimatology. Meteorological Applications (Supplement) 13: 61–67.

Garrison E. 2012. Asia geospatial forum: Introduction study area methodology expectation related issues primary results. In: 11th Annual Asian Conference and Exhibition on Geospatial Technologies and its Applications, 17-19 September, Asia Geospatial Forum.

Gaur A. 2013. Climate change impact on flood hazard in the Grand River basin, Ontario, Canada. M.Sc. Eng. dissertation, University of Western Ontario, Canada.

Gauthier TD. 2001. Detecting trends using Spearman's rank correlation coefficient. Environmental Forensics 2: 359-362.

Geoscience Australia, 2013. Where do floods occur? Available at: http://www.ga.gov.au/hazards/flood/flood-basics/where.html (Accessed on 06 May 2014).

Gichere SK et al. 2013. Effects of drought and floods on crop and animal losses and socio-economic status of households in the Lake Victoria Basin of Kenya. Journal of Emerging Trends in Economics and Management Sciences 4: 31-41.

Gitau W. 2011. Diagnosis and predictability of intraseasonal characteristics of wet and dry spells over equatorial east Africa. Ph.D dissertation. University of Nairobi, Kenya and Université de Bourgogne, France, 260 pp.

Gocic M, Trajkovic S. 2014. Spatiotemporal characteristics of drought in Serbia. Journal of Hydrology 510: 110-123.

Golmohammadi G, Prasher S, Madani A, Rudra R. 2014. Evaluating three hydrological distributed watershed models: MIKE-SHE, APEX, SWAT. Hydrology 1: 20-39.

Griscom HR, Miller SN, Gyedu-Ababio T, Sivanpillai R. 2009. Mapping land cover change of the Luvuvhu catchment, South Africa for environmental modelling. GeoJournal 75: 163-173.

Gyamfi C, Ndamuka JM, Salim RW. 2016. Application of SWAT model to the Olifants basin: Calibration, validation and uncertainty analysis. Journal of Water Resource and Protection 8: 397-410.

Hachigonta S, Reason CJC, Tadross M. 2008. An analysis of onset date and rainy season duration over Zambia. Theoretical and Applied Climatology 91: 229-243.

Hao Z, Aghakouchak A. 2013. Multivariate standardized drought index: A parametric multi-index model. Advances in Water Resources 57: 12-18.

Hargreaves GH. 1994. Simplified coefficients for estimating monthly solar radiation in North America and Europe. Departmental Paper, Department of Biological and Irrigation Engineering, Utah State University, Logan, Utah.

Hargreaves GH, Allen RG. 2003. History and evaluation of Hargreaves evapotranspiration equation. Journal of Irrigation and Drainage Engineering 129: 53-63.

Hargreaves GH, Samani ZA. 1982. Estimating potential evapotranspiration. Journal of Irrigation and Drainage Division 108(3): 225-230.

Hargreaves GH, Samani ZA. 1985. Reference crop evapotranspiration from temperature. Applied Engineering in Agriculture 1: 96-99.

Hart NCG, Reason CJC, Fauchereau N. 2013. Cloud bands over southern Africa: Seasonality, contribution to rainfall variability and modulation by the MJO. Climate Dynamics 41: 1199-1212.

Harvest Choice. 2010. Rainfall variability and crop yield potential. International Food Policy Research Institute, University of Minnesota, WA. http://harvestchoice.org/node/2240. (Accessed on 10 June 2016).

Hassan MN, Stern RD. 1988. A simple method for analysing daily rainfall data: A case study for Kota Bharu. Pertanika 11: 101-106.

Heim Jr RR. 2002. A review of twentieth-century drought indices used in the United States. National Climatic Data Center Report No. NC 28801-5001, pp. 1149-1165.

Hewitson BC, Tadross M, Jack C. 2005. Historical precipitation trends over southern Africa: A climatology perspective. In: RE Schulze (Ed.), Climate Change and Water Resources in Southern Africa: Studies on Scenarios, Impacts, Vulnerabilities and Adaptation. Pretoria: Water Research Commission, pp. 319-324.

Hirschboeck KK, Ely LL, Maddox RA. 2000. Hydroclimatology of meteorological floods. In: EE Wohl (Ed.), Inland Flood Hazard: Human, Riparian, and Aquatic Communities. New York, NY: Cambridge University Press, pp. 39-68.

Holloway A et al. 2012. Eden & Central Karoo Drought disaster 2009-2011: The scramble for water. Report, Disaster Mitigation for Sustainable Livelihoods Programme, University of Stellenbosch, Stellenbosch, 132 pp.

Igwenagu CM. 2015. Trends analysis of rainfall pattern in Enugu state Nigeria. European Journal of Statistics and Probability 3(3): 12-18.

IPCC. 2007a. Climate change 2007: Working Group II: Impacts, adaptation and vulnerability. ML Parry, OF Canziani, JP Palutikof, PJ Van Der Linden, CE Hanson (Eds.). Intergovernmental Panel on Climate Change, Cambridge and New York, 976 pp.

IPCC. 2007b. Climate change 2007: Synthesis report. Contribution of Working Groups I, II and III to the fourth assessment report of the Intergovernmental Panel on Climate Change. RK Pachauri, A Reisinger (Eds.). Intergovernmental Panel on Climate Change, Geneva, Switzerland.

Jalota SK, Prihar SS. 1990. Bare soil evaporation in relation to tillage. Advances in Soil Sciences 12: 187-216.

Jayanthi H, Husak G. 2013. A probabilistic approach to assess agricultural drought risk. Background paper prepared for GAR 2013. Geneva, Switzerland, 22 pp.

Jewitt GPW, Garratt JA, Calder IR, Fuller L. 2004. Water resources planning and modelling tools for the assessment of land use change in the Luvuvhu catchment, South Africa. Physics and Chemistry of the Earth 29: 1233-1241.

Jha MK. 2011. Evaluating hydrologic response of an agricultural watershed for watershed analysis. Water 3: 604-617.

Kane RP. 2009. Periodicities, ENSO effects and trends of some South African rainfall series: An update. South African Journal of Science 105: 199-207.

Kang Y, Khan S, Ma X. 2009. Climate change impacts on crop yield, crop water productivity and food security: A review. Progress in Natural Science 19: 1665-1674.

Karkanis PG. 1983. Determining field capacity and wilting point using soil saturation by capillary rise. Canadian Agricultural Engineering 25: 19-21.

Khandlhela M, May J. 2006. Poverty, vulnerability and the impact of flooding in the Limpopo Province, South Africa. Natural Hazards 39(2): 275-287.

Kozlovac JP. 1995. Adventures in flood control: The Johnstown, Pennsylvania story. In: Urban Areas as Environment, 19 April.

Kraemer, EM. 2015. Irrigation Water Requirements under Climate Change and Drought Events in Saskatchewan. Ph.D. thesis, University of Regina, Canada.

Kruger AC. 2006. Observed trends in daily precipitation indices in South Africa: 1910-2004. International Journal of Climatology 26: 2275-2285.

Kruger AC, Shongwe S. 2004. Temperature trends in South Africa: 1960–2003. International Journal of Climatology 24(15): 1929-1945.

Krzhizhanovskaya VV et al. 2011. Flood early warning system: Design, implementation and computational modules. Procedia Computer and Science 4: 106-115.

Lauer J. 2008. Flooding impacts on corn growth and yield. Field Crops 28: 49-56.

Lee JE, Heo JH, Lee J, Kim NW. 2017. Assessment of flood frequency alteration by dam construction via SWAT simulation. Water 9: 264-282.

Legesse G. 2010. Agricultural drought assessment using remote sensing and GIS techniques. M.Sc. thesis. Addis Ababa University, Ethiopia, pp. 1-56.

Li Y, Ye W, Wang M, Yan X. 2009. Climate change and drought: A risk assessment of crop-yield impacts. Climate Research 39: 31-46.

Liersch S. 2003. The program pcpSTAT-SWAT user manual. Berlin.

Lobell DB, Gourdji SM. 2012. The influence of climate change on global crop productivity. Plant Physiology 160(4): 1686-1697.

Lynch, TA. 2002. Intelligent support systems in agriculture: A study of their adoption and use. Ph.D. dissertation, Central Queensland University, Australia.

Makhuvha T, Pegram G, Sparks R, Zucchini W. 1997. Patching rainfall data using regression methods: 1. Best subset selection, EM and pseudo-EM methods: Theory. Journal of Hydrology 198(1-4), 289-307.

Mamo KHM, Jain MK. 2013. Runoff and sediment modeling using SWAT in Gumera catchment, Ethiopia. Open Journal of Modern Hydrology 3: 196-205.

Maponya P. 2010. Climate change and agricultural production in Limpopo Province, South Africa: Impact and adaptation options. Ph.D. thesis, University of South Africa, Pretoria.

Masereka EM, Otieno FAO, Ochieng GM, Snyman J. 2015. Best fit and selection of probability distribution models for frequency analysis of extreme mean annual rainfall events. International Journal of Engineering Research and Development 11: 34-53.

Masupha TE, Moeletsi ME, Tsubo M. 2016. Dry spells assessment with reference to the maize crop in the Luvuvhu River catchment of South Africa. Physics and Chemistry of the Earth 92: 99-111.

McKague K, Rudra R, Ogilvie J. 2003. ClimGen: A convenient weather generation tool for Canadian climate stations. In: Proceeedings CSAE/SCGR Meeting, 6-9 July, Montreal, Quebec. pp. 3-118.

McKague K, Rudra R, Ogilvie J, Ahmed I, Gharabaghi B. 2005. Evaluation of weather generator ClimGen for southern Ontario. Canadian Water Resources Journal 30: 315-330.

McKee TBN, Doesken J, Kleist J. 1993. The relationship of drought frequency and duration to time scales. In: Proceedings of the 8th Conference on Applied Climatology, Boston, MA: American Meteorological Society, pp. 179-184.

Meyer SJ, Hubbard KG, Wilhite DA. 1993. A crop-specific drought index for corn: I. Model development and validation. Agronomy Journal 85(2): 388-395.

Millington N, Das S, Simonovic SP. 2011. The Comparison of GEV, Log-Pearson Type 3 and Gumbel distributions in the Upper Thames River Watershed under global climate models. Water Resource Research Report No. 077. Canada: Water Resource Research.

Mniki S. 2009. Socio-economic impact of drought induced disasters on farm owners of Nkonkobe Local Municipality. M.Sc. thesis, University of the Free State, Bloemfontein, pp. 9-92.

Moeletsi ME, Moopisa SG, Walker S, Tsubo M. 2013. Development of an agroclimatological risk tool for dryland maize production in the Free State Province of South Africa. Computers and Electronics in Agriculture 95: 108-121.

Moeletsi ME, Shabalala ZP, De Nysschen G, Walker S. 2016. Evaluation of an inverse distance weighting method for patching daily and dekadal rainfall over the Free State Province, South Africa. Water SA 42: 466-474.

Moeletsi ME, Walker S. 2011. Assessment of agricultural drought using a simple water balance model in the Free State Province of South Africa. Theoretical and Applied Climatology 108: 425-450.

Moeletsi ME, Walker S. 2012. Rainy season characteristics of the Free State Province of South Africa with reference to rain-fed maize production. Water SA 38(5): 775-782.

Moeletsi ME, Walker S, Landman WA. 2011. ENSO and implications on rainfall characteristics with reference to maize production in the Free State Province of South Africa. Physics and Chemistry of the Earth 36: 715-726.

Montgomery DC, Peck EA, Vining G. 2006. Introduction to Linear Regression Analysis (4th edn). Hoboken, New Jersey: John Wiley and Sons.

Moodley K. 2014. Ethical concerns in disaster research: A South African perspective. In: DP O'Mathuna, B Gordijn, M Clarke (Eds.), Disaster Bioethics: Normative Issues When Nothing is Normal. Dordretcht: Springer Science, pp. 191-208.

Moriasi DN, Arnold JG, Van Liew MW, Bingner RL, Harmel RD, Veith TL. 2007. Model evaluation guidelines for systematic quantification of accuracy in watershed simulations. American Society of Agricultural and Biological Engineers 50: 885-900.

Mubvuma MT. 2013 Climate change: Matching growing season length with maize crop varietal life cycles in semi-arid regions of Zimbabwe. Greener Journal of Agricultural Sciences 3(12): 809-816.

Mugulavai EM, Kipkorir EC, Raes D, Rao MS. 2008. Analysis of rainfall onset, cessation and length of growing season for western Kenya. Agriculture and Forest Meteorology 148: 1123-1135.

Muinga MG. 2004. Flood assessment and zonation in the lower Limpopo, Mozambique. M.Sc. dissertation. Institute for Geo-Information Science and Earth Observation, Enschede, Netherlands.

Munodowafa A. 2011. The effect of rainfall characterisation and tillage on sheet erosion and maize grain yield in semi-arid conditions of granitic sandy soils of Zimbabwe. Applied and Environmental Sciences 1-8.

Mupangwa W, Walker S, Twomlow S. 2011. Start, end and dry spells of the growing season in semi-arid southern Zimbabwe. Journal of Arid Environments 75: 1097-1104.

Mutenyo I, Nejadhashemi AP, Woznicki SA, Giri S. 2013. Evaluation of SWAT perfomance on a mountainous watershed in tropical Africa. Hydrology Current Research S14: 001. DOI:10.4172/2157-7589.S14-001

Muthuwatta LP. 2004. Long term rainfall-runoff lake level modelling of the Lake Naivasha basin, Kenya. M.Sc. dissertation, University of the Netherlands, Netherlands.

Mzezewa J, Misi T, Van Rensburg LD. 2010. Characterisation of rainfall at a semi-arid ecotope in the Limpopo Province (South Africa) and its implications for sustainable crop production. Water SA 36: 19-26.

Ncube M. 2006. The impact of land cover and land use on the hydrologic response in the Olifants, Johannesburg. M.Sc. dissertation, University of the Witwatersrand, Johannesburg.

Newman S, Lynch T, Plummer AA. 1999. Success and failure of decision support systems: Learning as we go. Proceedings of the American Society of Animal Science, 1999, 12 pp.

Nguyen N, Wegener M, Russell I. 2007. Decision support systems in Australian agriculture: State of the art and future development. Australasian Farm Business Management Journal 4: 14-21.

Nicholson SE, Selato JC. 2000. The influence of La Nina on African rainfall. International Journal of Climatology 20(14):1761-1776.

Nkuna TR, Odiyo JO. 2011. Filling of missing rainfall data in Luvuvhu River catchment using artificial neural networks. Physics and Chemistry of the Earth 36: 830-835.

Norouzi G, Taslimi M. 2012. The impact of flood damages on production of Iran's agricultural sector. Middle-East Journal of Scientific Research 12: 921-926.

Nyabeze WR. 2004. Estimating and interpreting hydrological droughts on selected catchments in Zimbabwe. Physics and Chemistry of the Earth 29: 1173-1180.

O'Connell EO, Ewen J, O'Donnell G, Quinn P. 2007. Is there a link between agricultural land-use management and flooding? Hydrology and Earth System Sciences 11: 96-107.

Omotosho JB, Balogun AA, Ogunjobi K. 2000. Predicting monthly and seasonal rainfall, onset and cessation of the rainy season in West Africa using only surface data. International Journal of Climatology 20: 865-888.

Orang MN, Grismer ME, Ashktorab H. 1995. New equations to estimate evapotranspiration in Delta. California Agriculture, May-June, CA.

Pasi JM. 2014. Modelling the impacts of increased air temperature on maize yields in selected area of the South African highveld using the Cropsyst model. M.Sc. dissertation, University of KwaZulu-Natal, Durban.

Pitt R. 2002. Regional rainfall conditions and site hydrology for construction site erosion evaluations. Available at: http://rpitt.eng.ua.edu/Workshop/WSErorionControl/Module4/Module4.htm (Accessed on 16 November 2016).

Ponce VM, Hawkins RH. 1996. Runoff curve number: Has it reached maturity? Journal of Hydrologic Engineering 1: 11-19.

Prasad PVV, Staggenborg SA, Ristic Z. 2008. Impacts of drought and/or heat stress on physiological, developmental, growth and yield processes of crop plants. In: LH Ahuja, L Ma, S Saseendran (Eds.), Response of Crops to Limited Water: Understanding and Modeling Water Stress Effects on Plant Growth Processes. Advances in Agricultural Systems Modeling Series 1. Madison, WI: ASA-CSSA, pp. 301-355.

Pretorius CJ, Smal MM. 1992. Notes on the macro-economic effects of the drought. South African Reserve Bank Quarterly Bulletin 184: 31-38.

Prucha B et al. 2016. MIKE-SHE integrated groundwater and surface water model used to simulate scenario hydrology for input to DRIFT-ARID: The Mokolo River case study. Water SA 42, 384–398.

Radi NFA, Zakaria R, Azman MAZ. 2015. Estimation of missing rainfall data using spatial interpolation and imputation methods. In: The 2nd ISM International Statistical Conference 2014 (ISM-II): Empowering the Applications of Statistical and Mathematical Sciences (Vol. 1643, pp. 42-48). AIP Publishing.

Raes D, Sithole A, Makaru A, Millford J. 2004. Evaluation of first planting dates recommended by criteria currently used in Zimbabwe. Agriculture and Forest Meteorology 125: 177-185.

Reason CJC, Hachigonta S, Phaladi RF. 2005. Interannual variability in rainy season characteristics over the Limpopo region of southern Africa. International Journal of Climatology 25: 1835-1853.

Reason CJC, Keibel A. 2004. Tropical cyclone Eline and its unusual penetration and impacts over the southern African mainland. Weather Forecasting 19(5): 789-805.

Rockstrom J et al. 2010. Managing water in rain-fed agriculture: The need for paradigm shift. Agricultural Water Management 97: 543-550.

Rose DC et al. 2016. Decision support tools for agriculture: Towards effective design and delivery. Agricultural Systems, 149, 165–174.

Rostamian R et al. 2008. Application of a SWAT model for estimating runoff and sediment in two mountainous basins in central Iran. Hydrological Sciences Journal, 53: 977-988.

Safeeq M, Fares A. 2011. Accuracy evaluation of ClimGen weather generator and daily to hourly disaggregation methods in tropical conditions. Theoretical and Applied Climatology 106: 321-341.

Sauer J. 2011. Natural disasters and agriculture: Individual risk preferences towards flooding. In: The EAAE 2011 Congress Change and Uncertainty, 30 August-2 September, Zurich, Switzerland. pp. 1-15.

Senay GB, Verdin JP. 2002. Evaluating the performance of a crop water balance model in estimating regional crop production. In: Proceedings of the Pecora Symposium 15/Land Satellite Information IV/ ISPRS Commission I/FIEOS. Denver, CO, 8 pp.

Shabalala ZP, Moeletsi ME. 2015. Climate data patching program. Agricultural Research Council: Institute for Soil, Climate and Water, Pretoria.

Sharma MA, Singh MA. 2010. Use of probability distribution in rainfall analysis. New York Science Journal 3(9): 40-49.

Sheffield J, Woods EF, Roderick ML. 2012. Little change in global drought over the past 60 years. Nature 491: 435-438.

Singo LR, Kundu PM, Odiyo JO, Mathivha FI, Nkuna TR. 2012. Flood frequency analysis of annual maximum stream flows for Luvuvhu River catchment, Limpopo Province, South Africa. In: 16th SANCIAHS National Hydrology Symposium, University of Pretoria, 1-3 October. Session 2C.

Sithole A. 2010. Agroclimatic characterisation of the growing season for improved rain-fed maize productivity in Zimbabwe. In: J Masaka (Ed.), Midlands State University Journal of Science, Agriculture and Technology 2: 1-11.

Smith K. 2001. Environmental Hazards: Assessing Risk and Reducing Disaster (3rd edn). London/New York: Routledge Physical Environment Series.

Smith IN, Wilson L, Suppiah R. 2008. Characteristics of the northern Australian rainy season. Journal of Climate 21: 4298-4311.

Smithers JC, Schulze RE. 2001. Design rainfall estimation: A review with reference to practices in South Africa. In: Proceedings 10th South African National Hydrology Symposium, 26-28 September, School of BEEH, University of KwaZulu-Natal, Pietermaritzburg.

Sonmez FK, Komuscu AU, Erkan A, Turgu E. 2005. An analysis of spatial and temporal dimension of drought vulnerability in Turkey using the standardized precipitation index. Natural Hazards 35: 243-264.

Srikanthan R, McMahon TA. 2001. Stochastic generation of annual, monthly and daily climate data: a review. Hydrology and Earth System Sciences 5(4):653–670

Stephens MA. 1974. EDF statistics of the goodness of fit and some comparisons. Journal of the American Statistical Association 69: 730-737.

Stern RD, Coe R. 1984. A model fitting analysis of daily rainfall data. Journal of the Royal Statistical Society: Series A 147(1): 1-34.

Syaukat Y. 2011. The impact of climate change on food production and security and its adaptation programs in Indonesia. Journal of the International Society for Southeast Asian Agricultural Science 17: 40-51.

Tadross M et al. 2007. Changes in growing-season rainfall characteristics and downscaled scenarios of change over southern Africa: Implications for growing maize. Regional Expert Meeting Report, pp. 193-204. Available at: www.csag.uct.ac.za/~mtadross

Tadross MA, Hewiston BC, Usman MT. 2003. Interannual variability of the onset of the maize growing season over South Africa and Zimbabwe. Journal of Climate 18: 3356-3372.

Tait A, Zheng X. 2003. Mapping frost occurrence using satellite data. Journal of Applied Meteorology 42: 193-203.

Tang WY, Kassim AHM, Abubakar SH. 1996. Comparative studies of various missing data treatment methods: Malaysian experience. Atmospheric Research 42(1-4): 247-262.

Tennant WJ, Hewitson BC. 2002. Intra-seasonal rainfall characteristics and their importance to the seasonal prediction problem. International Journal of Climatology 22: 1033-1048.

Thomas RJ. 2008. Opportunities to reduce the vulnerability of dryland farmers in Central and West Asia and North Africa to climate change. Agriculture, Ecosystems & Environment 126: 36-45.

Tilahun MK. 2006. The characterisation of rainfall in the arid and semi-arid regions of Ethiopia. Water SA 32(3): 429-436.

Tingem M, Rivington M, Azam-Ali S, Colls J. 2007. Assessment of the ClimGen stochastic weather generator at Cameroon sites. African Journal of Environmental Science and Technology 1: 86-92.

Tongwane MI, Moeletsi ME. 2014. Intra-seasonal rainfall variability during maize growing season in the northern lowlands of Lesotho. Theoretical and Applied Climatology 120: 575-585.

Törnros T, Menzel L. 2014. Addressing drought conditions under current and future climates in the Jordan River region. Hydrology and Earth System Sciences 18(1): 305-318.

Trambauer P, Maskey S, Werner M, Pappenberger F, Van Beek LHP, Uhlenbrook S. 2014. Identification and simulation of space-time variability of past hydrological drought events in the Limpopo River basin, southern Africa. Hydrology and Earth System Sciences 18: 2925-2942.

Trenberth KE. 2011. Changes in precipitation with climate change. Climate Research 47: 123-138.

Tshikolomo K, Walker S, Nesamvuni A. 2013. Prospect for developing water storage through analysis of runoff and storage capacity of Limpopo and Luvuvhu-Letaba Water Management Areas of South Africa. International Journal of Applied Science and Technology 3: 70-79.

Tyson, PD, Preston-Whyte, RA. 2000. The Weather and Climate of Southern Africa. Cape Town: Oxford University Press, 396 pp.

Ujeneza EL. 2014. Simulating the characteristics of droughts in Southern Africa. M.Sc. thesis, University of Cape Town, Cape Town, 80 pp.

UNEP. 1992. World Atlas of Desertification. United Nations Environment Programme. London: Edward Arnold.

Van Liew MW, Veith TL, Bosch DD, Arnold JG. 2007. Sustainability of SWAT for the conservation effects assessment project: Comparison on USDA agricultural research service watersheds. Journal of Hydrologic Engineering 12: 173-189.

Vazquez-Amabile G, Engel BA, Flanagan DC. 2006. Modeling and risk analysis of nonpoint-source pollution caused by Atrazine using SWAT. American Society of Agricultural and Biological Engineers 49: 667-678.

Vicente-Serrano, SM. 2006. Spatial and temporal analysis of droughts in the Iberian Peninsula (1910-2000), Hydrological Science Journal 51:83-97.

Vicente-Serrano SM, Beguería S, López-Moreno JI. 2010. A multi-scalar drought index sensitive to global warming: The Standardized Precipitation Evapotranspiration Index – SPEI. Journal of Climate 23: 1696-1718.

Vicente-Serrano SM, Sergio M, National Center for Atmospheric Research Staff. 2015. The climate data guide: Standardized Precipitation Evapotranspiration Index (SPEI). Available at: https://climatedataguide.ucar.edu/climatedata/standardizedprecipitation evapotranspiration-index-spei (Accessed on 15 April 2016).

Vilazón MF, Willems P. 2010. Filling gaps and daily disaccumulation of precipitation data for rainfall-runoff model. BALWOIS 2010, Ohrid, Republic of Macedonia, 25-29 May 2010.

Vogel, C, Laing, M, Monnik, K. 2000. Drought in South Africa, with spatial reference to the 1980-94 period, pp. 348-366. In DA Wilhite (Ed), Drought: A Global Assessment. Abingdon: Routledge.

Walter MW. 1967. Length of the rainy season in Nigeria. Niger. Geography Journal 10: 123-128.

Wani SP, Pathak P, Sreedevi TK, Singh HP, Singh P. 2003. Efficient management of rainwater for increased crop productivity and ground water recharge in Asia. In: JN Kijne, R Barker, D Molden (Eds.), Water Productivity in Agriculture: Limits and Opportunities for Improvement. Wallingford, UK and Colombo: CABI Publishing and International Water Management Institute.

Warburton ML, Schulze RE, Jewitt GPW. 2010. Confirmation of ACRU model results for applications in land use and climate change studies. Hydrology and Earth System Science 14: 2399-2414.

Wetterhall F, Winsenius HC, Dutra E, Werner M, Pappenberger E. 2015. Seasonal predictions of agro-meteorological drought indicators for the Limpopo basin. Hydrology and Earth System Sciences 19: 2577-2586.

Whitmore, JS. 2000. Drought Management on Farmland. Vol. 35. Kluwer, Netherlands: Springer 360 pp.

Wilhite DA, Glantz MH. 1987. Understanding the drought phenomena: The role of definitions. In: DA Wilhite, WE Easterling (Eds.), Planning for Drought: Towards a Reduction of Societal Vulnerability, Boulder, CO: Westview Press, pp. 111-120.

Wilhite DA, Svoboda MD. 2000. Drought early warning systems in the context of drought preparedness and mitigation. In: DA Wilhite, MVK Sivakumar, DA Wood (Eds.), Early Warning Systems for Drought Preparedness and Drought Management. WMO/TD No. 1037. Geneva, Switzerland: World Meteorological Organization, pp. 1-21.

WMO. 2015. Global climate observation system. Available at: https://www.wmo.int/pages/prog/wcp/index_en.html (Accessed on 22 November 2015).

Woltering L. 2005. Estimating the influence of on-farm conservation practices on the water balance: Case of the Mzinyathini catchment in Zimbabwe. M.Sc. thesis. Delft University of Technology, Netherlands.

WRC. 2001. State of rivers report: Letaba and Luvuvhu river systems: 2001. Report no. TT165/01. Water Research Commission, Pretoria.

Wright CY, Engelbrecht, F, Sweijd N. 2015. The three culprits behind South Africa's weird weather patterns. Available at: http://mg.co.za/article/2015-11-18-the-three-culprits-behind-south-africas-weird-weather-patterns (Accessed on 12 September 2016).

Wu H, Hubbard KG, Wilhite DA. 2004. An agricultural drought risk-assessment model for corn and soybeans. International Journal of Climatology 24: 723-741.

Xia Y, Fabian P, Winterhalter M, Stohl A. 1999. Forest climatology: Estimation of missing values for Bavaria, Germany. Agricultural and Forest Meteorology 96(1-3): 131-144.

Xie X, Gu W, Wang B, Yang Q. 2012. Risk assessement of rainstorm and flood disaster based on multi-index. Communications in Information Science and Management Engineering 2: 10-16.

Yengoh GT, Armah FA, Onumah EE, Odoi JO. 2010. Trends in agriculturally-relevant rainfall characteristics for small-scale agriculture in Northern Ghana. Journal of Agricultural Science 2(3): 3.

Zuma BM, Luyt CD, Chirenda T, Tandlich R. 2012. Flood disaster management in South Africa: Legislative framework and current challenges. In: Proceedings from the 2012 International Conference on Applied Life Sciences (ICALS2012), 10-12 September, Konya, Turkey. pp. 127-132.

Page left blank intentionally

APPENDIX A: CAPACITY BUILDING OF POSTGRADUATE STUDENTS

Six students (four M.Sc. and one B.Sc. Hons.) were attached to this project as a form of capacity building in the scarce skills area of climate change and variability in agriculture. The students involved in the project as well as the status of their degrees (completed, submitted or in progress) are listed below.

Name:	**Fhulufhelo Phillis Tshililo**
Degree:	M.Sc. Agriculture (Agrometeorology)
Title:	Rainy season characteristics with reference to maize production for the Luvuvhu River catchment, Limpopo Province, South Africa
University:	University of KwaZulu-Natal
Supervisors:	MJ Savage and ME Moeletsi
Status:	Completed
Reference:	Tshililo, F.P. (2017). Rainy season characteristics with reference to maize production for the Luvuvhu River catchment, Limpopo Province, South Africa. M.Sc. thesis. University of KwaZulu-Natal, South Africa, 112 pp.

Name:	**Elisa Teboho Masupha**
Degree:	M.Sc. Agriculture
Title:	Drought analysis with reference to rain-fed maize for past and future climate conditions over the Luvuvhu River catchment in South Africa
University:	University of South Africa
Supervisor:	ME Moeletsi
Status:	Completed
Reference:	Masupha, E.T. (2017). Drought analysis with reference to rain-fed maize for past and future climate conditions over the Luvuvhu River catchment in South Africa. M.Sc. thesis. University of South Africa, 114 pp. http://hdl.handle.net/10500/23197

Name:	**Mulalo Precious Thavhana**
Degree:	M.Sc. Agriculture (Agrometeorology)
Title:	Runoff simulation using the SWAT model for flood frequency analysis and design flood estimations in the Luvuvhu River catchment, South Africa
University:	University of KwaZulu-Natal
Supervisors:	MJ Savage and ME Moeletsi
Status:	Completed
Reference:	Thavhana, M.P. (2018). Runoff simulation using the SWAT model for flood frequency analysis and design flood estimations in the Luvuvhu River catchment, South Africa. M.Sc. thesis. University of KwaZulu-Natal, South Africa, 123 pp.

Name:	**Sabelo Marvin Mazibuko**
Degree:	M.Sc. Geography
Title:	Spatio-temporal assessment of drought and floods in the Luvuvhu River catchment
University:	University of the Free State
Supervisor:	G Mukwada
Status:	To be submitted in 2018

Name:	**Zakhele Phumlani Shabalala**
Degree:	B.Sc. Hons
University:	University of South Africa
Supervisor:	ME Moeletsi
Status:	In progress

Rainy season characteristics with reference to maize production for the Luvuvhu River Catchment, Limpopo Province, South Africa

by

Fhulufhelo Phillis Tshililo

Submitted in fulfillment of the academic requirements of

Master of Science in Agriculture

in Agrometeorology

Soil-Plant-Atmosphere-Continuum Research Unit

School of Agricultural, Earth and Environmental Sciences

College of Agriculture, Engineering and Science

University of KwaZulu-Natal

Pietermaritzburg

South Africa

August 2017

ABSTRACT

In arid and semi-arid regions, crop yields are mainly dependent on the amount and spatio-temporal distribution of rainfall. For most smallholder farmers in rural areas of southern Africa, rainfall is a critical input to agricultural production of most staple crops such as maize. To effectively plan for agricultural development, it is of utmost importance that the spatial distribution and temporal variation of rainfall is understood as it govern the type of farming systems that can be practiced in any region. Therefore, a detailed understanding of rainfall is necessary before any farming activities can commence. The study investigated rainy season characteristics with reference to maize production in the Luvuvhu River Catchment. Rainy season characteristics assessed included aridity index, onset, cessation, length of the season, false onset, dry spells, seasonal rainfall, number of rainy days and monthly rainfall. Historical daily rainfall and minimum and maximum air temperature data (1923-2015) were obtained from the Agricultural Research Council. Twelve meteorological stations that were evenly distributed and represented different climatic regions within the catchment were chosen.

An aridity index for different areas of the catchment was calculated using the United Nations Environment Programme equation. Evapotranspiration was calculated using the Hargreaves and Samani equation. Annual rainfall was calculated by summing daily rainfall from 1st January to 31st December. The Instat+ v 3.36 statistical programme was utilized to calculate onset, cessation, and length of the season, the number of rainy days, dry spells, seasonal rainfall and monthly rainfall. The Statistica software was used to generate descriptive statistics as well as to calculate probability of exceedance and non-exceedance for the rainy season characteristics. The Anderson–Darling goodness-of-fit test was performed to determine the distribution model that best represents the data. The resultant probabilities of exceedance were then computed from the distribution models that best fit the data. A non-parametric Spearman rank correlation coefficient test was used to analyze data for trends in rainy season characteristics as well as monthly rainfall.

The results from the study showed that monthly rainfall at the Luvuvhu River Catchment during the rainy season varies temporally and spatially. In the high rainfall areas of the catchment, the rainy season commences early from the third week of October and ends the first week of April the following year. For dry areas of the catchment, the rainy season commences in the second week of November and ends early in the third week of February. The results further show a decrease in length of the rainy season, the number of rainy days, and seasonal rainfall further away from wet to dry areas of the catchment. There was no significant change on the onset of the rainy season on the catchment for the past 27-90 years. There is a high risk of both short and medium dry spells at most stations during the month of October, with, Folovhodwe, Pafuri and Sigonde being at highest risk. Farmers are therefore advised to use the first onset for land preparation and plant after the second onset in November and December to avoid the high risk of dry spells and false onset in October and November, depending on the location at the catchment. Folovhodwe, Mampakuil, Pafuri and Sigonde have a mean length of rainy season of less than 120 days and seasonal rainfall of less than 500 mm per rainy season. Hence, these areas are not suitable for rain-fed maize in the current climate. However, they are suitable for the production of other crops which may be sold in order to purchase maize. The most favourable sites for maize production within the catchment are Entabeni, Levubu, Lwamondo, Thathe, Tshiombo, and Vreemedeling. Therefore, production should be maximized at these areas so that there is sufficient maize for the whole catchment.

In dry years, stations situated in the low-lying areas in the north-eastern and eastern parts of the catchments receive less rainfall which does not permit planting of maize. In normal and wet years, rainfall is sufficient for the production of various crops. However, in semi-arid areas of the catchment, plans should be made for supplementary water due to high evapotranspiration rates in order to maximize maize production. Stations in the middle/south-western parts of the catchment can receive significant rainfall in both dry, normal and wet years. Trend analysis for long-term rainfall data did not show any significant changes in monthly rainfall except for Lwamondo and Levubu where an increasing trend is notable in January rainfall. In December, the rainfall trend was significant at Entabeni, Folovhodwe and Lwamondo. An increase in rainfall is notable at Lwamondo and a decrease in rainfall at Entabeni and Folovhodwe.

Keywords: Cessation, dry spells, length of the rainy season, onset, rainy days, and seasonal rainfall.

Drought analysis with reference to rain-fed maize for past and future climate conditions over the Luvuvhu River catchment in South Africa

by

ELISA TEBOHO MASUPHA

submitted in accordance with the requirements

for the degree of

MASTER OF SCIENCE

in the subject

AGRICULTURE

at the

UNIVERSITY OF SOUTH AFRICA

SUPERVISOR: DR M E MOELETSI

FEBRUARY 2017

ABSTRACT

Recurring drought conditions have always been an endemic feature of climate in South Africa, limiting maize development and production. However, recent projections of the future climate by the Intergovernmental Panel on Climate Change suggest that due to an increase of atmospheric greenhouse gases, the frequency and severity of droughts will increase in drought-prone areas, mostly in subtropical climates. This has raised major concern for the agricultural sector, particularly the vulnerable small-scale farmers who merely rely on rain for crop production. Farmers in the Luvuvhu River catchment are not an exception, as this area is considered economically poor, whereby a significant number of people are dependent on rain-fed farming for subsistence. This study was therefore conducted in order to improve agricultural productivity in the area and thus help in the development of measures to secure livelihoods of those vulnerable small-scale farmers.

Two drought indices viz. Standardized Precipitation Evapotranspiration Index (SPEI) and Water Requirement Satisfaction Index (WRSI) were used to quantify drought. A 120-day maturing maize crop was considered and three consecutive planting dates were staggered based on the average start of the rainy season. Frequencies and probabilities during each growing stage of maize were calculated based on the results of the two indices. Temporal variations of drought severity from 1975 to 2015 were evaluated and trends were analyzed using the non-parametric Spearman's Rank Correlation test at α (0.05) significance level. For assessing climate change impact on droughts, SPEI and WRSI were computed using an output from downscaled projections of CSIRO Mark3.5 under the SRES A2 emission scenario for the period 1980/81 – 2099/100. The frequency of drought was calculated and the difference of SPEI and WRSI means between future climate periods and the base period were assessed using the independent t-test at α (0.10) significance level in STATISTICA software.

The study revealed that planting a 120-day maturing maize crop in December would pose a high risk of frequent severe-extreme droughts during the flowering to the grain-filling stage at Levubu, Lwamondo, Thohoyandou, and Tshiombo; while planting in October could place crops at a lower risk of reduced yield and even total crop failure. In contrast, stations located in the low-lying plains of the catchment (Punda Maria, Sigonde, and Pafuri) were exposed to frequent moderate droughts following planting in October, with favourable conditions noted following the December planting date. Further analysis on the performance of the crop under various drought conditions revealed that WRSI values corresponding to more intense drought conditions were detected during the December planting date for all stations. Moreover, at Punda Maria, Sigonde and Pafuri, it was observed that extreme drought (WRSI <50) occurred once in five seasons, regardless of the planting date.

Temporal analysis on historical droughts in the area indicated that there had been eight agricultural seasons subjected to extreme widespread droughts resulting in total crop failure i.e. 1983/84, 1988/89, 1991/92, 1993/94, 2001/02, 2002/03, 2004/05 and 2014/15. Results of Spearman's rank correlation test revealed weak increasing drought trends at Thohoyandou (ρ = of 0.5 for WRSI) and at Levubu and Lwamondo (ρ = of 0.4 for SPEI), with no significant trends at the other stations. The study further revealed that climate change would enhance the severity of drought across the catchment. This was statistically significant (at 0.10%

significance level) for the near-future and intermediate-future climates, relative to the base period.

Drought remains a threat to rain-fed maize production in the Luvuvhu River catchment area of South Africa. In order to mitigate the possible effects of droughts under climate change, optimal planting dates were recommended for each region. The use of seasonal forecasts during drought seasons would also be useful for local rain-fed maize growers especially in regions where moisture is available for a short period during the growing season. It was further recommended that the Government ensure proper support such as effective early warning systems and inputs to the farmers. Moreover, essential communication between scientists, decision makers, and the farmers can help in planning and decision-making ahead of and during the occurrence of droughts.

Keywords: Climate change, crop water requirements, drought trends, Hargreaves method, maize growing period, planting dates, probability distributions, relative drought frequency, small-scale farming, water balance.

Runoff simulation using the SWAT model for flood frequency analysis and design flood estimations in the Luvuvhu River catchment, South Africa

by

Mulalo Precious Thavhana

submitted in fulfilment of the academic requirements of the degree of

Master of Science in Agriculture

in Agrometeorology

Soil-Plant-Atmosphere-Continuum Research Unit

School of Agricultural, Earth and Environmental Sciences

College of Agriculture, Engineering and Science

University of KwaZulu-Natal

Pietermaritzburg

South Africa

Supervisor: Professor MJ Savage

Co-supervisor: Dr ME Moeletsi

March 2018

ABSTRACT

Fatal flood events around the world have led to the execution of many projects in an attempt to solve some of the prevailing flood control problems. These studies have identified an increase in the frequency of flood events over the years. The increases accompanied by hydrological alteration and rainfall variation may have great effects on future flood design and planning. This study focuses on the Luvuvhu River catchment in the Limpopo Province of South Africa, which has been identified and considered vulnerable to flooding.

The soil and water assessment tool (SWAT) was used to simulate daily streamflows (runoff) of the Luvuvhu River catchment. The model was executed through an interface between SWAT and QGIS desktop 2.6.1 software, QSWAT 1.3 2016. The model was run for a 33-year period of 1983 to 2015. Having compared observed streamflow data with the simulated data, the initial streamflow evaluation was unsatisfactory and the model needed to be calibrated and validated.

Sensitivity analysis, calibration and validation were conducted using the SUFI-2 algorithm through its interface with SWAT calibration and uncertainty procedure (SWAT-CUP). The calibration process was conducted for the period 1986 to 2005 while the validation process was from 2006 to 2015 inclusive. A minimum of 300 simulations were performed for each run. The model performance to simulate runoff was based on four objective functions coefficient of determination (R^2), Nash–Sutcliffe efficiency (NSE) index, root mean square error (RMSE)-observations standard deviation ratio (RSR) and percent bias (PBIAS) and two performance indices probability (*P*)-factor and correlation coefficient (*R*)-factor.

During the calibration period, the model produced a *P*-factor of 0.64, 0.52, 0.67, and 0.45 and an *R*-factor of 0.59, 1.81, 0.68 and 0.91 for the four sub-catchments. The objective function results revealed an R^2 of 0.61, 0.73, 0.63 and 0.75, an NSE index of 0.35, -16.46, 0.66 and -0.36, an RSR of 0.62, 3.23, 0.56 and 0.71 and a PBIAS of 1.18, -7.60, 16.30 and -2.10 for the sub-catchments. During the validation period, the model produced a *P*-factor of 0.59, 0.34, 0.69 and 0.41 and an *R*-factor of 0.46, 2.67, 0.53 and 0.75 for the sub-catchments. The objective function results revealed an R^2 of 0.34, 0.63, 0.52 and 0.62, an NSE index of 0.35, -0.45, 0.48 and 0.31, an RSR of 0.86, 1.14, 0.72 and 2.10 and a PBIAS of 65.0, -12.30, 19.90 and -14.60 for the sub-catchments.

Predominantly, parameter ranges of the *P*-factor and *R*-factor reached desired limits indicating considerable parameter uncertainties results, which were acceptable. Moreover, model uncertainties were falling within the permissible limits, which signified the capability of SUFI-2 to capture the model's behaviour. Objective functions analyzed performed well during both calibration and validation. For this reason, results obtained in this study demonstrated acceptable model performance and acceptable accuracy of the model in runoff simulation. It can be concluded that SWAT simulation results were satisfactory for runoff simulation in the Luvuvhu River catchment.

Flood frequency analysis and design flood estimation were completed following model validation. This was accomplished using a 30-year period of simulated flood discharge from the SWAT model. A log-normal probability distribution was used to fit the maximum annual peak data to estimate flood frequencies. Focusing on a sub-catchment, the Luvuvhu River catchment outlet, 50, 100 and 200-year floods revealed flood magnitudes of 960.70, 1121.02 and 1281.35 $m^3\ s^{-1}$ respectively. The results obtained from the frequency analysis would assist in the planning and designing purposes of the catchment, to mitigate and adapt during flooding season.

Keywords: Design flood estimation, flood frequency analysis, hydrological modelling, probability of exceedance, QSWAT, return interval, runoff simulation, SUFI-2, SWAT-CUP.

APPENDIX B: CAPACITY BUILDING AT COMMUNITY LEVEL

Workshops

Stakeholder involvement was conducted in a form of various workshops as shown below:

Date	Workshop	Venue
04 December 2014	Inception	University of Limpopo
02 July 2015	Farmers	Department of Agriculture (Vhembe)
11 February 2016	Scientific	Naledzi Lodge, Shayandima
30 January 2018	Scientific	2Ten Hotel, Sibasa

Seasonal forecast forums

Agrometeorology team members visited various sites in the Luvuvhu River catchment area in November 2015, 2016 and 2017.

The main aim of the visits was to present the seasonal forecast released in November by the SAWS in preparation for the agricultural season ahead.

The training sessions were conducted using the local language and began with a discussion reflecting on the previous season. Farmers were made aware of the weather conditions to be expected for the upcoming season. The presentations focused on providing potential benefits as well as the possible negative effects provided by the forecast. Recommendations and preplanting training were then given accordingly.

Figure 74: Agrometeorology team members at various sites in the Luvuvhu River catchment area

APPENDIX C: CAPACITY BUILDING AT ORGANIZATION LEVEL

The findings of the project were communicated with researchers, farmers and other stakeholders through presentations at conferences, scientific publications, workshops and organization of farmers' information days that empowered farmers in the research areas in understanding the climatology and future climate change implications of the area in relation to crop production.

Presentations at conferences

15th WaterNet/WARFSA/GWP-SA Symposium, Lilongwe, Malawi, 29-31 Oct 2014

- Masupha, T.E., Franke, A.C. and Moeletsi, M.E. (2014). Dry spells assessment with reference to the maize crop in the Luvuvhu River catchment area in South Africa.

16th WaterNet/WARFSA/GWP-SA Symposium, Pointe Aux Piments, Mauritius, 28-30 Oct 2015

- Masupha, T.E. and Moeletsi, M.E. (2015). Drought assessment during the growing season of maize in the Luvuvhu River catchment of South Africa.

17th WaterNet/WARFSA/GWP-SA Symposium, Gaborone, Botswana, 26-28 Oct 2016

- Masupha, T.E. and Moeletsi, M.E. (2016). Using crop water balance model to assess drought on maize in the Luvuvhu River catchment, South Africa.
- Tshililo, F.P., Savage, M.J. and Moeletsi, M.E. (2016). Investigating rainy season characteristics with reference to maize production at the Luvuvhu River catchment of South Africa.
- Thavhana, M.P, Savage M.J. and Moeletsi M.E. (2016). Simulation of runoff for the Luvuvhu catchment of South Africa using the SWAT model (poster presentation).

32nd Annual Conference of South African Society for Atmospheric Sciences, Cape Town, South Africa, 30 Oct – 1 Nov 2016

- Masupha, T.E. and Moeletsi, M.E. (2016). Temporal evolution of agricultural drought in the Luvuvhu River catchment of South Africa.

2nd World Irrigation Forum (WIF2) 2016, Chiang Mai, Thailand, 6-8 Nov 2016

- Masupha, T.E., Moeletsi, M.E. and Mpandeli, S. (2016). Drought analysis on maize in the Luvuvhu River catchment, South Africa.

33rd Annual Conference of South African Society for Atmospheric Sciences. Limpopo, South Africa, 21-22 September 2017

- Masupha, T.E. and Moeletsi, M.E. (2017). Observed extreme widespread drought during the growing season of maize in the Luvuvhu River catchment of South Africa.
- Masupha, T.E. and Moeletsi, M.E. (2017). Assessing potential future agricultural droughts limiting maize production in the Luvuvhu River catchment of South Africa (poster presentation).
- Tshililo, F.P., Savage, M.J. and Moeletsi, M.E. (2017). Rainfall variability over the Luvuvhu River catchment during the growing season.

- Thavhana, M.P. Savage, M.J. and Moeletsi, M.E. (2017). Runoff simulation using the SWAT model for flood frequency analysis and design flood estimations in the Luvuvhu River catchment, South Africa.
- Mazibuko S, Mukwada, G. and Moeletsi, M. (2017). Spatio-temporal assessment of agricultural drought and floods in the Luvuvhu River catchment.

Weather & Climate Decision Tools for Farmers, Ranchers & Land Managers Conference, Gainesville, FL, 5-7 December 2016

- Moeletsi, M.E., Shabala, Z., Masupha, T.E., Tshililo, P.F. and Tsubo, M. (2016). Framework for developing an agrometeorological risk tool for dryland maize production in the Luvuvhu River catchment, South Africa.

Scientific publications

- Masupha T.E, Moeletsi M.E. and Tsubo M. (2016). Dry spells assessment with reference to the maize crop in the Luvuvhu River catchment of South Africa. Physics and Chemistry of the Earth, Parts A/B/C, 92, 99-111. http://dx.doi.org/10.1016/j.pce.2015.10.014
- Masupha, T.E. and Moeletsi, M.E. (2017). Use of standardized precipitation evapotranspiration index to investigate drought relative to maize, in the Luvuvhu River catchment area, South Africa, Physics and Chemistry of the Earth. http://dx.doi.org/10.1016/j.pce.2017.08.002
- Masupha, T.E. and Moeletsi, M.E. (2017). The use of Water Requirement Satisfaction Index for assessing agricultural drought on rain-fed maize, in the Luvuvhu River catchment, South Africa. Theoretical and Applied Climatology (under review).
- Masupha, T.E. and Moeletsi, M.E. (2017). Analysis of potential future droughts limiting maize production, in the Luvuvhu River catchment area, South Africa. Physics and Chemistry of the Earth (accepted).
- Thavhana, M.P. Savage, M.J. and Moeletsi, M.E. (2017). SWAT model uncertainty analysis, calibration and validation for runoff simulation in the Luvuvhu River catchment (accepted).
- Thavhana, M.P. Savage, M.J. and Moeletsi, M.E. (2017). Flood frequency analysis and design flood estimation in the Luvuvhu River catchment (in preparation).
- Tshililo, F.P., Savage, M.J. and Moeletsi, M.E. (2017). Investigating rainy season characteristics with reference to maize production at the Luvuvhu River catchment of South Africa (submitted), Theoretical and Applied Climatology Journal.
- Tshililo, F.P., Savage, M.J. and Moeletsi, M.E. Rainy season characteristics over the Luvuvhu River Catchment, Limpopo Province, South Africa (in preparation).
- Mazibuko S.M., Mukwada G. and Moeletsi M.E. Spatiotemporal assessment of agricultural drought in the Luvuvhu river catchment area, Limpopo province (in preparation).
- Masupha, T.E. et al. A review on drought and its impact on agriculture (in preparation).

APPENDIX D: CALCULATION TABLES

Tables used to calculate solar radiation

Table 46: Angot's values of daily shortwave radiation flux R_A at the outer limit of the atmosphere in g·cal·cm^{-2}* as a function of the month of the year and the latitude (Source: adapted from Ncube, 2006)

Latitude (degree)	Jan	Feb	Mar	Apr	May	Jun	Jul	Aug	Sep	Oct	Nov	Dec
N 90	0	0	55	518	903	1077	944	605	136	0	0	0
80	0	3	143	518	875	1060	930	600	219	17	0	0
60	86	234	424	687	866	983	892	714	494	258	113	55
40	358	538	663	847	930	1001	941	843	719	528	397	318
20	631	795	821	914	912	947	912	887	856	740	666	599
Equator	844	963	878	876	803	803	792	820	891	866	873	829
20	970	1020	832	737	608	580	588	680	820	892	986	978
40	998	963	686	515	358	308	333	453	648	817	994	1033
60	947	802	459	240	95	50	77	187	403	648	920	1013
80	981	649	181	9	0	0	0	0	113	459	917	1094
S 90	995	656	92	0	0	0	0	0	30	447	932	1110

*** 1 g·cal·m^{-2} = 0.0419 MJ·m^{-2}**

Table 47: Mean daylength (h) for different months and latitudes (Source: Ncube, 2006)

Latitude (° south)	Jul	Aug	Sep	Oct	Nov	Dec	Jan	Feb	Mar	Apr	May	Jun
50	8.5	10.1	11.8	13.8	15.4	16.3	15.9	14.5	12.7	10.8	9.1	8.1
48	8.8	10.2	11.8	13.6	15.2	16.0	15.6	14.3	12.6	10.9	9.3	8.3
46	9.1	10.4	11.9	13.5	14.9	15.7	15.4	14.2	12.6	10.9	9.5	8.7
44	9.3	10.5	11.9	13.4	14.7	15.4	15.2	14.0	12.6	11.0	9.7	8.9
42	9.4	10.6	11.9	13.4	14.6	15.2	14.9	13.9	12.5	11.1	9.8	9.1
40	9.6	10.7	11.9	13.3	14.4	15.0	14.7	13.7	12.5	11.2	10.0	9.3
35	10.1	11.0	11.9	13.1	14.0	14.5	14.3	13.5	12.4	11.3	10.3	9.8
30	10.4	11.1	12.0	12.9	13.6	14.0	13.9	13.2	12.4	11.5	10.6	10.2
25	10.7	11.3	12.0	12.7	13.3	13.7	13.5	13.0	12.3	11.6	10.9	10.6
20	11.0	11.5	12.0	12.6	13.1	13.3	13.2	12.8	12.3	11.7	11.2	10.9
15	11.3	11.6	12.0	12.5	12.8	13.0	12.9	12.6	12.2	11.8	11.4	11.2
10	11.6	11.8	12.0	12.3	13.6	12.7	12.6	12.4	12.1	11.8	11.6	11.5
5	11.8	11.9	12.0	12.2	12.3	12.4	12.3	12.3	12.1	12.0	11.9	11.8
0	12.1	12.1	12.1	12.1	12.1	12.1	12.1	12.1	12.1	12.1	12.1	12.1

Soil and land use tables created for SWAT model

Table 48: Soil properties and classification for Luvuvhu River catchment

SNAM	HYDGRP	TEXTURE	SOL_BD1	SOL_AWC1	SOL_K1	SOL_CBN1
Fb359	A	LS	1.24	0.013327	0.0156	0.61
Fc484	A	LS	1.24	0.013327	0.0156	0.61
Ae267	A	LS	1.24	0.013327	0.0156	0.61
Ia113	A	S	1.25	0.017587	0.0176	0.71
Ae268	A	LS	1.24	0.013327	0.0156	0.61
Fc485	A	SL	1.19	0.03343	0.00347	0.71
Ib315	A	LS	1.24	0.013327	0.0156	0.61
Ea206	C	SCL	1.3	0.041541	0.00063	0.19
Fc729	A	LS	1.24	0.013327	0.0156	0.61
Fc728	A	SL	1.19	0.03343	0.00347	0.71
Ae332	A	LS	1.24	0.013327	0.0156	0.61
Fc486	A	SL	1.19	0.03343	0.00347	0.71
Fb499	A	SL	1.19	0.03343	0.00347	0.71
Fc488	A	SL	1.19	0.03343	0.00347	0.71
Fc487	A	SL	1.19	0.03343	0.00347	0.71
Ae331	A	LS	1.24	0.013327	0.0156	0.61
Fb498	A	LS	1.24	0.013327	0.0156	0.61
Ib313	A	LS	1.24	0.013327	0.0156	0.61
Ac164	A	LS	1.24	0.013327	0.0156	0.61
Bc47	A	LS	1.24	0.013327	0.0156	0.61
Ib442	A	SL	1.19	0.03343	0.00347	0.71
Ah109	A	LS	1.24	0.013327	0.0156	0.61
Fb358	A	LS	1.24	0.013327	0.0156	0.61
Ab181	A	LS	1.24	0.013327	0.0156	0.61
Ea161	C	SCL	1.3	0.041541	0.00063	0.19
Ae330	A	SL	1.19	0.03343	0.00347	0.71
Ba62	A	SL	1.19	0.03343	0.00347	0.71
Ib443	A	SL	1.19	0.03343	0.00347	0.71
Dc51	C	SCL	1.3	0.041541	0.00063	0.19
Ba60	A	LS	1.24	0.013327	0.0156	0.61
Ca93	A	SL	1.19	0.03343	0.00347	0.71
Ae329	A	SL	1.19	0.03343	0.00347	0.71
Ba61	A	LS	1.24	0.013327	0.0156	0.61
Bd56	A	SL	1.19	0.03343	0.00347	0.71
Ib441	A	SL	1.19	0.03343	0.00347	0.71
Ea205	A	SL	1.19	0.03343	0.00347	0.71
Ab178	A	SL	1.19	0.03343	0.00347	0.71
Ab180	C	SCL	1.3	0.041541	0.00063	0.19
Fb496	A	SL	1.19	0.03343	0.00347	0.71
Fa756	A	SL	1.19	0.03343	0.00347	0.71

SNAM	HYDGRP	TEXTURE	SOL_BD1	SOL_AWC1	SOL_K1	SOL_CBN1
Ab177	D	SC	1.3	0.020626	0.000217	0.38
Ae328	A	SL	1.19	0.03343	0.00347	0.71
Ab179	A	SL	1.19	0.03343	0.00347	0.71
Water	D	C	0	0	260	0
Ib304	A	LS	1.24	0.013327	0.0156	0.61
Bb128	A	LS	1.24	0.013327	0.0156	0.61
Ib440	A	LS	1.24	0.013327	0.0156	0.61
Ab173	D	SC	1.3	0.020626	0.000217	0.38
Ab109	C	SCL	1.3	0.041541	0.00063	0.19
Ab111	C	SCL	1.3	0.041541	0.00063	0.19
Ab108	C	SCL	1.3	0.041541	0.00063	0.19
Ab151	A	SL	1.19	0.03343	0.00347	0.71
Fa535	A	SL	1.19	0.03343	0.00347	0.71
Ab107	C	SCL	1.3	0.041541	0.00063	0.19
Ae291	C	SCL	1.3	0.041541	0.00063	0.19
Ae260	C	SCL	1.3	0.041541	0.00063	0.19
Fa308	A	SL	1.19	0.03343	0.00347	0.71
Bd48	A	LS	1.24	0.013327	0.0156	0.61
Ca102	A	SL	1.19	0.03343	0.00347	0.71
Bc48	A	LS	1.24	0.013327	0.0156	0.61
Bc54	A	SL	1.19	0.03343	0.00347	0.71
Fa331	A	SL	1.19	0.03343	0.00347	0.71
Fa396	A	LS	1.24	0.013327	0.0156	0.61
Ca91	A	SL	1.19	0.03343	0.00347	0.71
Fa306	A	LS	1.24	0.013327	0.0156	0.61
Fa754	A	SL	1.19	0.03343	0.00347	0.71
Ab174	C	SCL	1.3	0.041541	0.00063	0.19
Ab175	C	SCL	1.3	0.041541	0.00063	0.19
Bc50	A	LS	1.24	0.013327	0.0156	0.61

APPENDIX E: SWAT MODEL SET-UP AND PROCESS

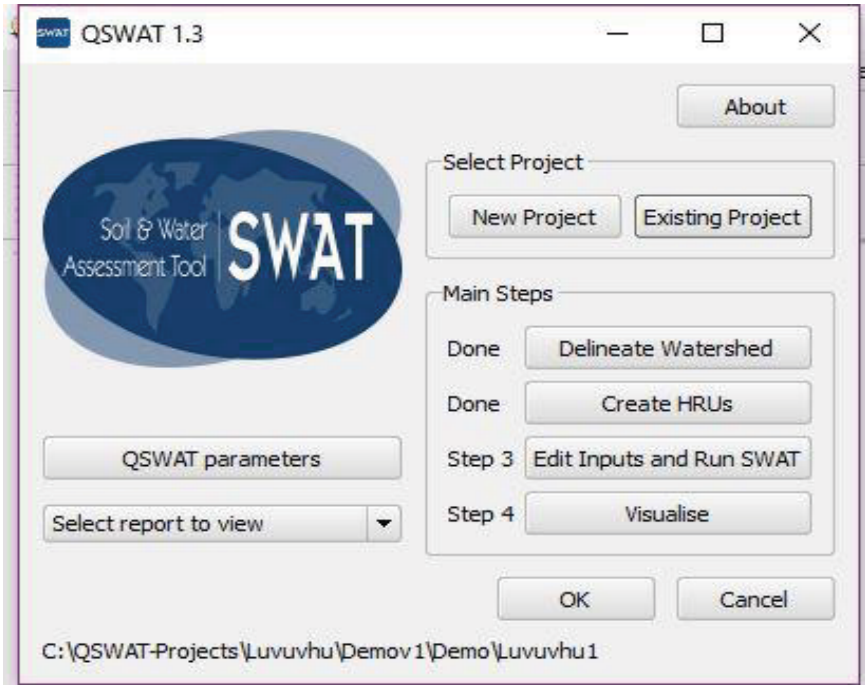

Figure 75: Model set-up interface window in the QSWAT program

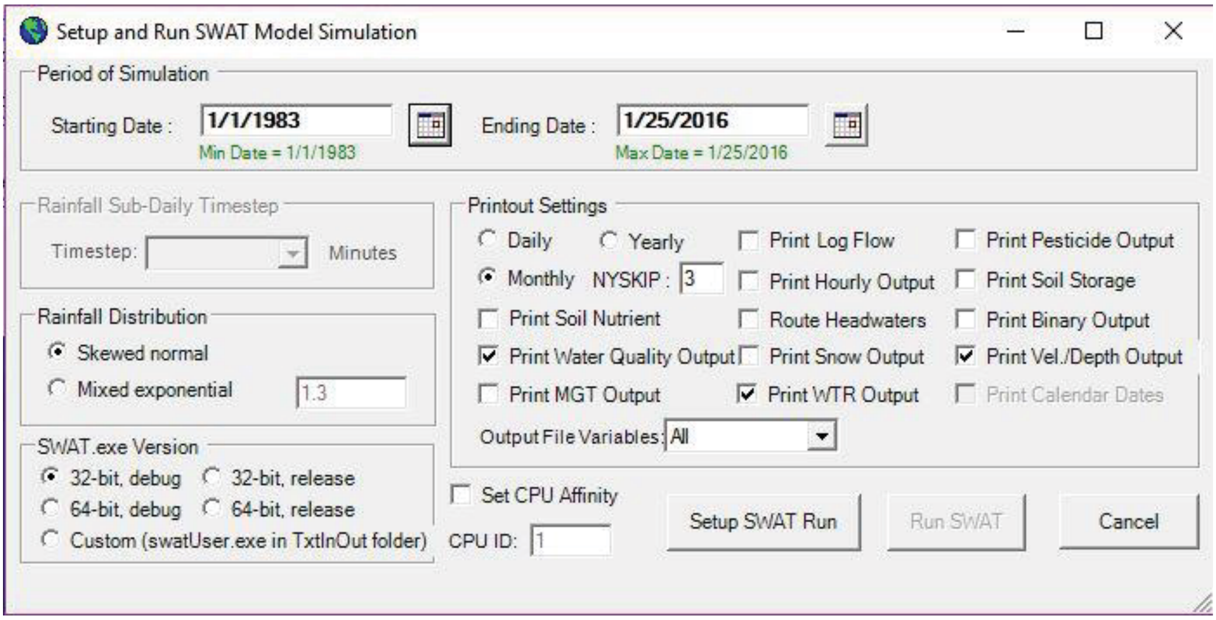

Figure 76: SWAT model simulation and run window

APPENDIX F: SELECTION OF CURVE NUMBER AND CHARACTERISATION, AND SENSITIVITY ANALYSIS

Table 49: Representative curve number values for pasture, grassland and woods

Cover description		Curve numbers for hydrologic soil group			
Cover type	Hydrologic condition	A	B	C	D
Pasture, grassland, or range—continuous forage for grazing. [2]	Poor	68	79	86	89
	Fair	49	69	79	84
	Good	39	61	74	80
Meadow—continuous grass, protected from grazing and generally mowed for hay.	—	30	58	71	78
Brush—brush-weed-grass mixture with brush the major element. [3]	Poor	48	67	77	83
	Fair	35	56	70	77
	Good	30 [4]	48	65	73
Woods—grass combination (orchard or tree farm). [5]	Poor	57	73	82	86
	Fair	43	65	76	82
	Good	32	58	72	79
Woods. [6]	Poor	45	66	77	83
	Fair	36	60	73	79
	Good	30 [4]	55	70	77
Farmsteads—buildings, lanes, driveways, and surrounding lots.	—	59	74	82	86

1 Average runoff condition, and $I_a = 0.2S$.
2 *Poor:* <50%) ground cover or heavily grazed with no mulch.
Fair: 50 to 75% ground cover and not heavily grazed.
Good: > 75% ground cover and lightly or only occasionally grazed.
3 *Poor:* <50% ground cover.
Fair: 50 to 75% ground cover.
Good: >75% ground cover.
4 Actual curve number is less than 30; use CN = 30 for runoff computations.
5 CN's shown were computed for areas with 50% woods and 50% grass (pasture) cover. Other combinations of conditions may be computed from the CN's for woods and pasture.
6 *Poor:* Forest litter, small trees, and brush are destroyed by heavy grazing or regular burning.
Fair: Woods are grazed but not burned, and some forest litter covers the soil.
Good: Woods are protected from grazing, and litter and brush adequately cover the soil.

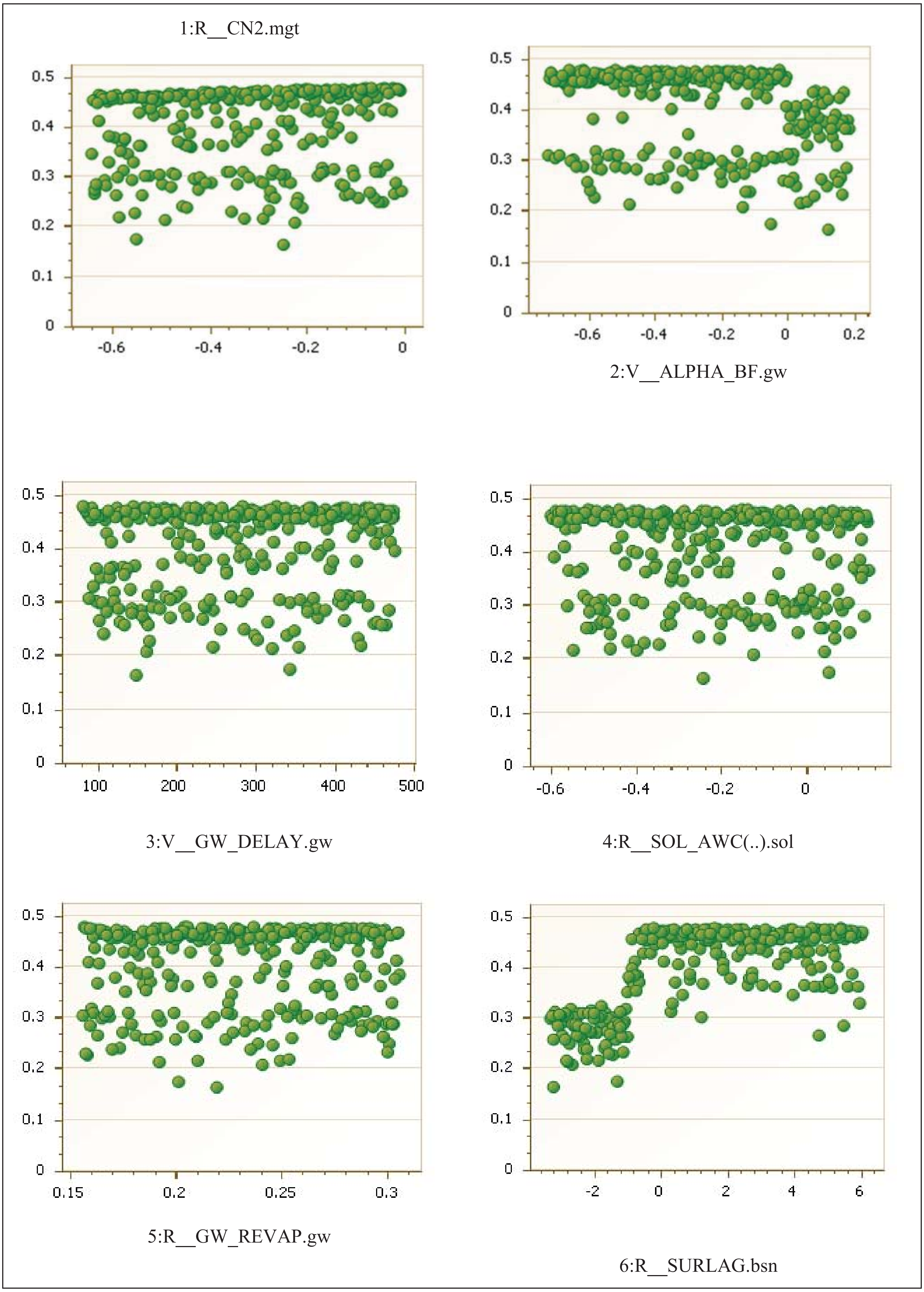

Figure 77: Scatter plots of sensitive parameters showing the sensitivity of model parameters for streamflow discharge

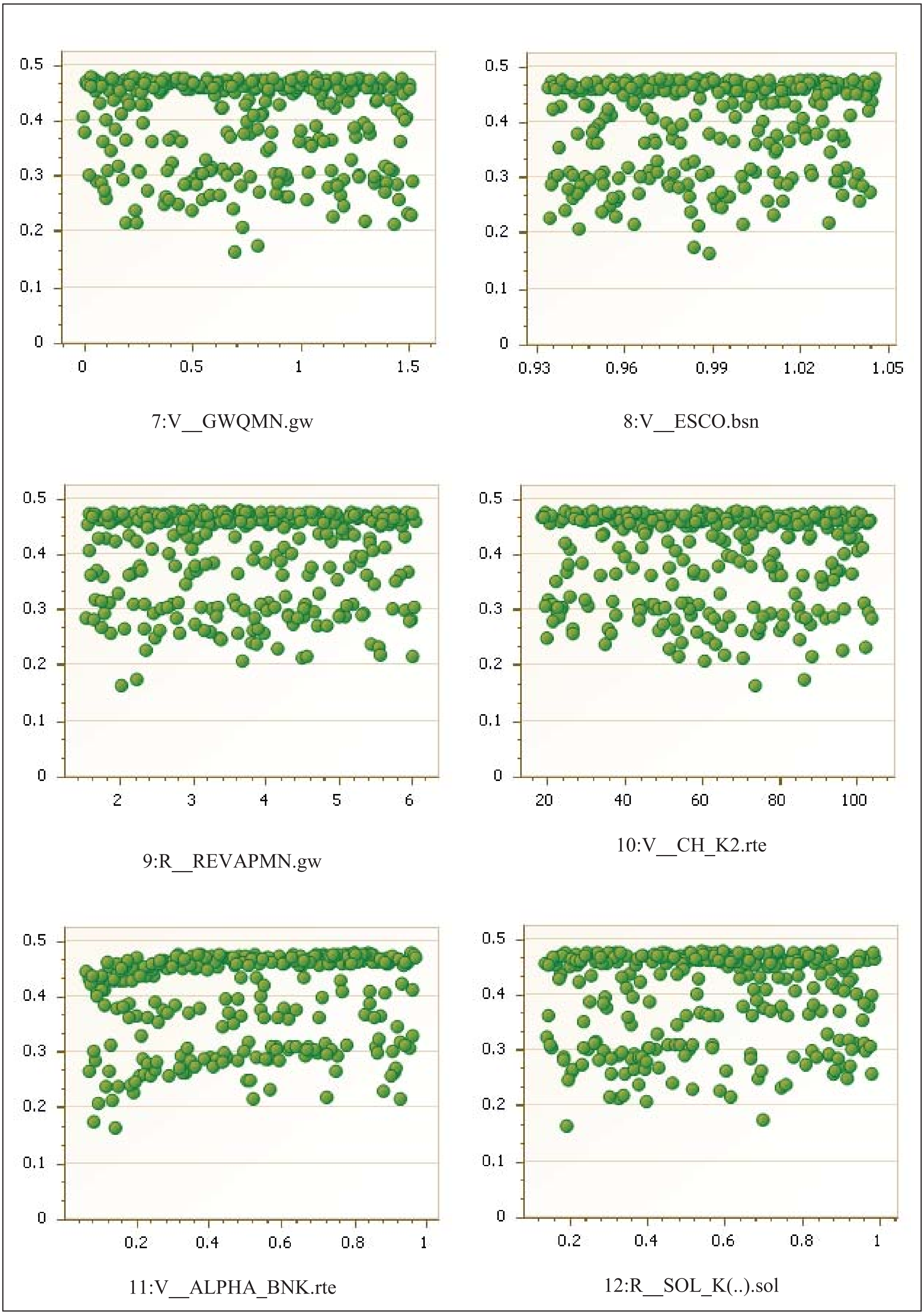

Figure 77 (continued): Scatter plots of sensitive parameters showing the sensitivity of model parameters for streamflow discharge

APPENDIX G: ONSET RESULTS OBTAINED USING TWO DIFFERENT ONSET DEFINITIONS

Appendix G1: Levubu

Years	25 mm in 10 days	25 mm in 10 days and 20 mm in the next 20 days	Difference (days)
1980	110	110	0
1981	94	94	0
1982	101	101	0
1983	107	107	0
1984	107	107	0
1985	101	101	0
1986	112	112	0
1987	95	95	0
1988	102	102	0
1989	101	101	0
1990	98	98	0
1991	136	136	0
1992	122	122	0
1993	93	93	0
1994	106	106	0
1995	120	120	0
1996	114	114	0
1997	100	100	0
1998	94	94	0
1999	142	142	0
2000	103	103	0
2001	99	99	0
2002	99	99	0
2003	110	110	0
2004	103	103	0
2005	97	97	0
2006	110	110	0
2007	94	94	0
2008	116	116	0
2009	118	118	0
2010	127	127	0
2011	110	110	0
2012	103	103	0
2013	110	110	0

Appendix G2: Lwamondo

Years	25 mm in 10 days	25 mm in 10 days and 20 mm in the next 20 days	Difference (days)
1978	108	157	49
1979	131	131	0
1980	134	134	0
1981	142	142	0
1982	102	102	0
1983	99	99	0
1984	95	95	0
1985	120	149	29
1986	94	94	0
1987	129	129	0
1988	104	104	0
1989	112	112	0
1990	95	95	0
1991	104	141	37
1992	100	100	0
1993	93	93	0
1994	120	176	56
1995	99	99	0
1996	96	96	0
1997	93	93	0
1998	100	100	0
1999	112	150	38
2000	111	111	0
2001	108	108	0
2002	113	157	44
2003	122	122	0
2004	143	143	0
2005	110	110	0
2006	161	161	0
2007	187	9999	
2008	126	126	0
2009	138	138	0
2010	128	128	0
2011	95	95	0
2012	104	104	0
2013	111	143	32
2014	102	138	36
2015	137	137	0

Appendix G3: Tshiombo

Years	25 mm in 10 days	25 mm in 10 days and 20 mm in the next 20 days	Difference (days)
1983	105	105	0
1984	107	107	0
1985	123	159	36
1986	112	150	38
1987	150	150	0
1988	103	103	0
1989	101	101	0
1990	138	138	0
1991	137	137	0
1992	125	125	0
1993	98	146	48
1994	146	146	0
1995	111	175	64
1996	104	136	32
1997	107	107	0
1998	100	100	0
1999	116	116	0
2000	117	117	0
2001	131	131	0
2002	121	171	50
2003	110	110	0
2004	161	199	38
2005	128	128	0
2006	110	110	0
2007	96	96	0
2008	117	117	0
2009	139	139	0

Appendix G4: Sigonde

Years	25 mm in 10 days	25 mm in 10 days and 20 mm in the next 20 days	Difference (days)
1984	124	124	0
1985	123	123	0
1986	176	176	0
1987	147	147	0
1988	103	103	0
1989	149	194	45
1990	159	159	0
1991	136	9999	
1992	164	164	0
1993	146	146	0
1994	178	178	0
1995	194	194	0
1996	104	149	45
1997	134	9999	
1998	105	105	0
1999	112	159	47
2000	141	9999	
2001	131	131	0
2002	9999	9999	0
2003	111	111	0
2004	160	9999	
2005	143	143	0
2006	128	183	55
2007	9999	9999	
2008	93	126	33
2009	142	142	0
2010	128	128	0
2011	144	144	0
2012	109	109	0
2013	113	113	0
2014	165	165	0
2015	137	137	0

9999 onset criteria not met

Appendix G5: Pafuri

Years	25 mm in 10 days	25 mm in 10 days and 25 mm in the next 20 days	Difference (days)
1970	127	134	7
1971	100	100	0
1972	140	9999	
1973	172	9999	
1974	132	132	0
1975	172	172	0
1976	122	210	88
1977	152	152	0
1978	102	102	0
1980	106	106	0
1981	110	143	33
1982	147	9999	
1983	9999	9999	
1984	183	9999	
1985	148	148	0
1986	124	9999	
1987	157	195	38
1988	105	158	53
1989	103	103	0
1990	113	113	0
1991	138	138	0
1992	205	9999	
1993	122	122	0
1994	146	146	0
1995	106	177	71
1995	111	173	62
1996	164	164	0
1997	179	9999	
1998	105	141	36
1999	116	116	0
2000	118	9999	
2001	130	9999	
2002	160	160	0
2003	107	107	0

9999 onset criteria not met

Appendix G6: Elim

Years	25 mm in 10 days	25 mm in 10 days and 20 mm in the next 20 days	Difference (days)
1945	105	105	0
1946	9999	9999	0
1947	141	179	38
1948	110	110	0
1949	140	140	0
1950	158	158	0
1951	103	103	0
1952	110	110	0
1953	126	126	0
1954	146	146	0
1955	117	117	0
1956	120	120	0
1957	95	162	67
1958	155	155	0
1959	135	209	74
1960	116	116	0
1961	128	128	0
1962	138	138	0
1963	105	105	0
1964	114	114	0
1965	160	160	0
1966	171	171	0
1967	136	136	0
1968	120	120	0
1969	153	153	0
1970	101	101	0
1971	99	99	0
1972	94	94	0
1973	108	147	39
1974	133	133	0
1975	170	170	0
1976	123	123	0
1977	172	172	0
1978	107	107	0
1979	111	147	36
1980	142	142	0
1981	144	182	38
1982	104	156	52
1983	130	130	0
1984	121	199	78
1985	121	121	0
1986	116	150	34
1987	144	144	0
1988	102	102	0
1989	138	138	0

Years	25 mm in 10 days	25 mm in 10 days and 20 mm in the next 20 days	Difference (days)
1990	98	143	45
1991	135	9999	
1992	125	164	39
1993	128	128	0
1994	142	142	0
1995	142	142	0
1996	148	148	0
1997	99	133	34
1998	128	128	0
1999	111	111	0
2000	116	116	0
2001	128	128	0
2002	154	9999	
2003	110	146	36

9999 onset criteria not met

Appendix G7: Mampakuil

Years	25 mm in 10 days	25 mm in 10 days and 20 mm in the next 20 days	Difference (days)
1945	107	107	0
1946	186	186	0
1947	142	142	0
1948	110	110	0
1949	139	139	0
1950	154	154	0
1951	102	102	0
1952	109	109	0
1953	103	103	0
1954	128	159	31
1955	110	110	0
1956	119	147	28
1957	94	94	0
1958	113	150	37
1959	111	111	0
1960	133	133	0
1961	121	121	0
1962	133	133	0
1963	103	154	51
1964	113	113	0
1965	127	127	0
1966	106	171	65
1967	114	114	0
1968	120	120	0
1969	110	110	0
1970	100	100	0
1971	98	98	0
1972	93	93	0
1973	104	145	41
1974	132	132	0
1975	170	170	0
1976	93	117	24
1977	107	152	45
1978	110	110	0
1979	105	106	1
1980	111	142	31
1981	145	9999	
1982	158	158	0
1983	106	106	0
1984	106	106	0
1985	121	121	0
1986	118	146	28
1987	145	145	0
1988	103	9999	
1989	101	101	0

Years	25 mm in 10 days	25 mm in 10 days and 20 mm in the next 20 days	Difference (days)
1990	99	148	49
1991	136	136	0
1992	124	124	0
1993	130	130	0
1994	122	122	0
1995	111	111	0
1996	103	103	0
1997	100	105	5
1998	96	96	0
1999	112	117	5
2000	128	128	0
2001	131	131	0
2002	111	111	0
2003	111	111	0

9999 onset criteria not met

Appendix G8: Thathe

Years	25 mm in 10 days	25 mm in 10 days and 20 mm in the next 20 days	Difference (days)
1963	104	104	0
1964	113	113	0
1965	128	128	0
1966	107	108	1
1967	114	114	0
1968	114	114	0
1969	93	93	0
1970	102	102	0
1971	99	99	0
1972	95	129	34
1973	102	102	0
1974	123	123	0
1975	114	114	0
1976	99	99	0
1977	106	147	41
1978	100	100	0
1980	122	122	0
1981	111	115	4
1982	96	96	0
1983	102	102	0
1984	108	108	0
1985	106	106	0
1986	100	100	0
1987	111	111	0
1988	95	95	0
1989	101	101	0
1990	100	100	0
1991	138	138	0
1992	156	156	0
1993	124	124	0
1994	98	98	0
1995	121	121	0
1995	116	116	0
1996	103	103	0
1997	100	100	0
1998	105	105	0
1999	159	9999	
2000	186	186	0
2001	112	112	0
2002	111	111	0

9999 onset criteria not met

Appendix G9: Entabeni

Years	25 mm in 10 days	25 mm in 10 days and 20 mm in the next 20 days	Difference (days)
1923	134	134	0
1924	93	93	0
1925	98	98	0
1926	126	126	0
1927	106	106	0
1928	109	109	0
1929	96	96	0
1930	137	137	0
1931	101	101	0
1932	113	113	0
1933	108	108	0
1934	107	107	0
1935	95	95	0
1936	102	102	0
1937	97	97	0
1938	93	93	0
1939	110	110	0
1940	93	125	32
1941	108	108	0
1942	93	93	0
1943	113	113	0
1944	105	105	0
1945	99	99	0
1946	93	130	37
1947	108	108	0
1948	110	110	0
1949	113	113	0
1950	124	124	0
1951	102	102	0
1952	94	94	0
1953	103	103	0
1954	107	107	0
1955	109	109	0
1956	119	119	0
1957	94	94	0
1958	104	104	0
1959	111	111	0
1960	131	131	0
1961	120	120	0
1962	137	137	0
1963	102	102	0
1964	113	113	0
1965	104	127	23
1966	106	106	0
1967	114	114	0

Years	25 mm in 10 days	25 mm in 10 days and 20 mm in the next 20 days	Difference (days)
1968	113	113	0
1969	93	93	0
1970	100	100	0
1971	98	98	0
1972	95	95	0
1973	102	102	0
1974	99	99	0
1975	114	114	0
1976	95	95	0
1977	106	106	0
1978	106	106	0
1979	99	99	0
1980	110	110	0
1981	94	94	0
1982	101	101	0
1983	106	106	0
1984	102	102	0
1985	101	101	0
1986	112	112	0
1987	103	103	0
1988	103	103	0
1989	101	101	0
1990	99	99	0
1991	116	116	0
1992	101	101	0
1993	93	98	5
1994	122	122	0
1995	141	141	0
1996	104	104	0
1997	100	100	0
1998	95	95	0
1999	116	116	0
2000	103	103	0
2001	99	99	0
2002	97	97	0
2003	110	110	0
2004	105	105	0
2005	98	98	0
2006	128	128	0
2007	150	150	0
2008	116	116	0
2009	121	121	0
2010	126	126	0
2011	108	108	0
2012	106	106	0

9999 onset criteria not met

Appendix G10: Folovhodwe

Years	25 mm in 10 days	25 mm in 10 days and 20 mm in the next 20 days	Difference (days)
1945	141	141	0
1946	186	9999	
1947	160	160	0
1948	110	110	0
1949	127	127	0
1950	158	158	0
1951	104	104	0
1952	147	147	0
1953	122	122	0
1954	124	175	51
1955	110	9999	
1956	161	161	0
1957	124	186	62
1958	182	182	0
1959	139	9999	
1960	134	134	0
1961	127	127	0
1962	139	9999	
1963	155	155	0
1964	114	115	1
1965	210	210	0
1966	168	172	4
1967	9999	9999	
1968	134	134	0
1969	93	93	0
1970	134	9999	
1971	99	99	0
1972	139	9999	
1973	171	207	36
1974	132	132	0
1975	167	167	0
1976	211	211	0
1977	168	168	0
1978	116	116	0
1979	110	110	0
1980	110	110	0
1981	145	9999	
1982	9999	9999	0
1983	134	9999	
1984	134	134	0
1985	123	9999	9
1986	198	9	
1987	104	153	49

Years	25 mm in 10 days	25 mm in 10 days and 20 mm in the next 20 days	Difference (days)
1988	103	103	0
1989	113	113	0
1990	158	9999	
1991	9999	9999	0
1992	171	171	0
1993	146	146	0
1994	162	162	0
1994	111	194	83
1996	104	144	40
1997	141	9999	
1998	105	105	0
1999	115	210	95
2000	118	118	0
2001	130	130	0
2002	9999	9999	
2003	110	110	0

9999 onset criteria not met

Appendix G11: Vreemedeling

Years	25 mm in 10 days	25 mm in 10 days and 20 mm in the next 20 days	Difference (days)
1945	106	106	0
1946	139	189	50
1947	122	122	0
1948	110	110	0
1949	140	140	0
1950	160	160	0
1951	103	103	0
1952	109	109	0
1953	122	122	0
1954	127	127	0
1955	109	109	0
1956	119	155	36
1957	94	100	6
1958	104	104	0
1959	135	135	0
1960	115	115	0
1961	120	120	0
1962	137	137	0
1963	104	104	0
1964	113	113	0
1965	127	127	0
1966	106	169	63
1967	114	114	0
1968	133	133	0
1969	110	110	0
1970	100	100	0
1971	98	98	0
1972	95	146	51
1973	108	146	38
1974	134	134	0
1975	149	149	0
1976	121	121	0
1977	105	152	47
1978	107	107	0
1979	111	111	0
1980	110	142	32
1981	110	179	69
1982	100	9999	
1983	130	130	0
1984	121	121	0
1985	122	160	38
1986	112	112	0
1987	104	151	47
1988	102	102	0
1989	114	114	0

Years	25 mm in 10 days	25 mm in 10 days and 20 mm in the next 20 days	Difference (days)
1990	138	138	0
1991	147	147	0
1992	123	123	0
1993	94	123	29
1994	105	105	0
1995	111	111	0
1996	139	139	0
1997	102	180	78
1998	95	95	0
1999	113	117	4
2000	113	113	0
2001	132	132	0
2002	123	164	41
2003	111	144	33

9999 onset criteria not met

Appendix G12: Punda Maria

Years	25 mm in 10 days	25 mm in 10 days and 20 mm in the next 20 days	Difference (days)
1945	134	134	0
1946	181	9999	
1947	180	9999	
1948	111	111	0
1949	129	129	0
1950	155	155	0
1951	117	187	70
1952	147	147	0
1953	125	125	0
1954	128	128	0
1955	106	106	0
1956	155	155	0
1957	120	120	0
1958	103	154	51
1959	134	209	75
1960	134	134	0
1961	152	152	0
1962	139	145	6
1963	156	9999	
1964	113	143	30
1965	162	162	0
1966	168	172	4
1967	155	9999	
1968	133	133	0
1969	101	110	9
1970	127	127	0
1971	99	99	0
1972	95	171	76
1973	107	107	0
1974	132	132	0
1975	136	136	0
1976	122	122	0
1977	111	111	0
1978	111	111	0
1979	132	132	0
1980	110	110	0
1981	115	9999	
1982	306	9999	
1983	106	9999	
1984	124	124	0
1985	122	122	0
1986	120	150	30
1987	145	145	0
1988	103	103	0
1989	114	114	0

Years	25 mm in 10 days	25 mm in 10 days and 20 mm in the next 20 days	Difference (days)
1990	138	138	0
1991	136	9999	
1992	125	164	39
1993	126	126	0
1994	106	178	72
1995	174	174	0
1996	162	162	0
1997	136	136	0
1998	105	105	0
1999	116	116	0
2000	118	118	0
2001	131	131	0
2002	122	127	5
2003	111	177	66

9999 onset criteria not met

9780639200521